European Commission

technical steel research

Hot and cold rolling processes

Control of sheet surface defects and deep drawing properties in final strip production steps

A. Fouratier
Arcelor Atlantique et Lorraine
17, avenue des Tilleuls, F-57191 Florange Cedex 1

A. Lucas
CRM
Technologiepark 903, B-9052 Zwijnaarde

J. H. Bianchi, P. Vescovo, F. Dionisi
CSM
Via di Castel Romano 100, I-00128 Rome

P. D. Pütz
VDeh
Sohnstraße 65, Postfach 105145, D-40237 Düsseldorf

Contract No 7210-PR/338
1 July 2002 to 31 December 2005

Final report

Directorate-General for Research

2007 EUR 22566 EN

Europe Direct is a service to help you find answers to your questions about the European Union

Freephone number (*)**:**

00 800 6 7 8 9 10 11

(*) Certain mobile telephone operators do not allow access to 00 800 numbers or these calls may be billed.

A great deal of additional information on the European Union is available on the Internet. It can be accessed through the Europa server (http://europa.eu).

Cataloguing data can be found at the end of this publication.

Luxembourg: Office for Official Publications of the European Communities, 2007

ISBN 92-79-05018-3

ISSN 1018-5593

Printed in Luxembourg

PRINTED ON WHITE CHLORINE-FREE PAPER

FINAL SUMMARY

Summarized objectives of the project

(1) To understand and to get under control sheet surface defects coming from Lüders' bands in finishing lines, so to guarantee the strip quality by optimising process parameters.

(2) To develop and validate industrial procedures to set the optimum temper rolling degree in such a way that plastic bending deformations induced by participating rolls and by bending caused by coiling are compensated.
These procedures should finally create the possibility to set the most favourable and uniform mechanical strip properties along the total strip length and also from coil to coil.

Overall objectives of the project

The first objectives of this research is to understand formation mechanisms of Lüders' bands and to determine product parameters (composition, thickness…) and process parameters (bending and tensile deformation, temperature, speed…) in order to get under control sheet surface defects. So, we will be able to determine the real influence of anti-coil break rolls, levelling with or without tensile stress (pure stretch levelling) on Lüders' bands and to foresee the size and the morphology of Lüders' bands in function of product and type (level) of applied deformation. The understanding of Lüders' formation in finishing lines will help us to define product state after skin pass and strip performance in end-user applications.

Besides strip flatness and strip surface, the mechanical properties of cold rolled strip which is finally passed to subsequent process stages like deep drawing or stretch forming depend to a high degree on the temper rolling conditions set at the cold finishing line.

These subsequent process stages of skin passed strip, e.g. by deep drawing or stretching processes, usually require the use of temper rolled metal sheet, Lüders' free on its full range of deformability. To be able to produce such strip, it is necessary to control the skin passing process in such a way that the total strip deformation will come as close as possible to the optimum skin pass degree.

Rolls and roll systems like deflecting rolls, anti-sticking rolls and coilers which are participating at the temper rolling process, induce bending deformations into the strip, which extend the yield strength of the rolled material and thus lead to additional plastic deformations of the strip. These additional deformations may exceed up to 30% of the pass reduction with the consequence of non-uniform deformation along the strip length. Furthermore, rolls that introduce levelling of the strip (as in the case of AST configuration) produce non-symmetric rolling conditions in the skin-pass and this affects the through thickness strain distribution in the strip. Current industrial setting procedures of optimum temper rolling degree and therefore the resulting mechanical strip properties, do not include the plastic bending.
The most favourable mechanical strip properties however are achieved when the total deformation (bending plus rolling deformation) leads to such a constant minimum deformation along the total strip length which guarantees a complete suppression of the yield point elongation (concerning e.g. LC-DDQ-steels) and a minimum of yield strength including a high strain hardening exponent.

The results of an ECSC finished project **(A,B)** indicated that the final mechanical strip properties depend to a high extent on the global deformation resulting from work roll deformation of the skin pass mill and bending deformation by guiding the strip around roller bodies and by coiling during the temper rolling process. The two types of deformations can be mutually interlinked: rolls producing a bending prior to entry with a degree of levelling of the strip (as in AST plant) introduce non-symmetric rolling conditions in the skin-pass and this alters the contacting arc and consequently the through

thickness strain distribution in the strip. This needs to be corrected by the rollers placed past the skin pass. The most favourable mechanical strip properties are then achieved when the total deformation leads to such a minimum deformation which guarantees a complete suppression of the yield point elongation (elimination of the Lüders' elongation) and a minimum of yield strength including a high strain hardening exponent.

Another objective of the research work is to develop algorithms and validate industrial procedures which allow to set the optimum temper rolling degree in such way that plastic bending deformations induced by rolls and by coiling are compensated. The control strategy must take into account that varying bending radii (e.g. coiler, changing wrap angles of deflecting rolls) along the coil length lead to varying degrees of deformation to be set in the temper mill's roll gap for compensating the different bending deformations. These measures should finally create the possibility to set the most favourable and uniform mechanical strip properties along the strip length and also from coil to coil.

State of the art

A deep knowledge on the Lüders' bands mechanisms and their consequences on subsequent cold forming came from previous study **(B)**. Some numerical simulations with local law have been made in order to find the characteristic behaviour law in presence of Lüders' band in bending and tension deformation mode.

Temper rolling of cold rolled strip is marked by the demand to offer an optimum product to subsequent process stages (deep drawing, stretch forming etc.), e.g. referring to properties such as :

- strip flatness
- surface quality
- deformability

The deformability of the skin passed strip, e.g. in deep drawing, is essentially favoured by a high r-value for anisotropy, a high exponent n of strain hardening, corresponding to a great uniformity of elongation, as well as a minimum yield stress. The two last mentioned nominal values will be set most favourably if the optimum skin pass degree is adjusted on skin passing. This will be the case if the strip is rolled with a degree of deformation corresponding to the minimum of the yield stress curve. Pass reductions below the optimum skin pass degree should absolutely be avoided (under-skin-passed) to eliminate the appearance of Lüders´ lines in subsequent processing stages, e.g. on materials with upper and lower yield point. So, light over-skin-passing, connected with a small increase of the yield strength and a small reduction of uniformity of elongation, will be tolerated.

Processing of steel strip by deep drawing or stretching processes, usually requires the use of skin passed metal sheet, Lüders' free on its full range of deformability. To be able to produce this strip demanded by the market, it is necessary to control the skin passing process in such a way that total strip deformation will come as close as possible to the optimum skin pass degree.

Temper rolling plants are equipped with measuring and control systems to conduct the skin pass rolling process in such a way that the target plastic deformation to be set by the roll adjustment is safely achieved.

Rolls and roll systems like deflecting rolls, anti-sticking rolls and coilers which are integrated into the pass line of temper rolling plants, induce bending deformations into the strip, which can extend the yield strength of the rolled material and thus lead to plastic deformations of the strip. The presence of bending and levelling can introduce non-symmetric rolling conditions that alter the skin-pass contacting arc and therefore the through thickness strain distribution in the strip. When setting the

optimum temper rolling degree and thus the resulting mechanical strip properties, these plastic bending deformations have not been taken into account so far.

Prior trials (A) on an industrial temper mill equipped with an anti-sticking roll showed that for determining the relevant deformation all plastic strip deformations have to be taken into account, that means not only the pass reduction by rolling but also the plastic bending deformation caused by the anti-sticking roll was very relevant. The bending deformation has proved to accept values up to 30% of the target value of the skin pass degree. Comparing the yield stress - curves evaluated for the temper rolling conditions - rolled without and with acting anti-sticking roll – it can be deduced that in case of pre-deformation by bending the setting of the temper rolling degree has to be compensated by the amount of the pre-deformation in order to achieve a standardisation of the optimum skin pass degree.

Recent investigations carried out within the scope of a ECSC project **(B)** dealt with the effect of plastic bending deformations on the mechanical strip properties, namely :

- Stress-strain behaviour
- Yielding behaviour
- Strain hardening behaviour and
- Lüders' behaviour

The trials were carried out with batch annealed low carbon deep drawable strips (LC-DDQ steel). The test results showed, that plastic bending deformations influence mechanical strip properties in a similar degree than skin pass rolling itself.

Regarding the behaviour of yield stress, the minimum of yield strength, especially for thicker strips, is shifted to higher degrees of deformation than compared to temper rolling. The work hardening, which takes place after the minimum of yield stress, is accompanied by a significantly lower gradient of the yield stress curve than the compression strain caused by skin pass rolling. The thinner the strip thickness the stronger the effect.

The dependency of the hardening exponent on the degree of deformation shows the same trend for both bending and rolling deformation.
Independently from being bending or a rolling deformation, the resulting gradients of the work hardening exponent lead to the same values.

From the investigation, it can be concluded that it is necessary to conduct the process of skin pass rolling in such a way that those deformations caused by plastic bending have to be taken into account when the optimum degree of temper rolling is specified. This makes it possible to achieve the most favourable mechanical strip properties.

Skin-pass procedures without bending for strips were developed and validated against plant data in a previous ECSC funded project **(C)**. This research showed the importance of considering the deformation of the rolls as the strip thickness decreases. A simplified set-up model for the control system of the skin pass was derived from this research **(D)** and successfully installed in AST Terni. A new project on improving formability of low carbon steels by controlling the ageing in the finishing line is starting in 2002 **(E).**

Innovative contents

Roll systems introduce bending deformation that can lead to plastic deformation on the strip. In a previous project **(B)**, the effect of plastic bending deformations on the mechanical strip properties was

investigated at the laboratory scale. The use of bending deformations in order to get under control sheet surface defects in finishing lines has been never done before at the industrial scale.

In temper rolling plastic bending deformations have not been taken into consideration so far.

The results obtained in **(A,B)** have demonstrated the necessity that both deformation modes, rolling deformation as well as bending deformation, have to be taken into account when the optimum degree of skin pass rolling as target value is specified.

The algorithms and industrial procedures to be derived for a control strategy of the optimum degree of deformation will take into account for the first time the interacting effects by rolling and bending. Thus these new process strategies will improve the process of skin pass rolling under the aspect of setting most favorable and uniform mechanical strip properties over the strip length and from coil to coil.

Industrial, technical, economic benefits

The realisation of a strategy to conduct the temper rolling process in such a way that the bending deformations induced into the strip are taken into account by setting the optimum temper rolling degree leads to an improvement of quality of the skin passed strip. The mechanical strip properties which are to be set in temper rolling as the final forming stage before subsequent strip processes like deep drawing and stretch forming will thus achieve most favoured values, equalised along the strip length and from coil to coil.

Many European companies are interested by the problem of Luders' lines or coil breaks, either on soft hot strips or on galvanized sheets.

Different aspects should be considered :

- Understanding of the formation of the Luders' lines. (analysing the effects of the steel composition or steel strength, of the strip or sheet thickness, of the processing parameters, of the final texture and microstructure, of the solute C-content, ...).

- Thin hot strips for direct application (eventually with adherent scale or after pickling). In some case, the SKP operation can be omitted. The problem can occur when decoiling by the customers or in finishing lines.

- Galvanized sheets: the defects can be visible in the production line. (at the exit of the galvanization section at ~470 °C) but is probably induced in the reheating / soaking / cooling sections (outside the present scope).

- Appearance of surface defects in service centre due to Lüders' bands for numerous products.

- After tension levelling in pickling lines, temper milled thin hot strips could present the problem.

- Temper milled ferritic stainless steel is sensitive to Lüders' band.

- Dimension of anti-coil break rolls at the entry.

So, getting under control sheet surface defects will reduce scrap wastes at finishing lines. And finally, this project could give us the way to control process to produce some sensitive product. So, the competitiveness of European steel producers in the international market will be increased.

References

A P. D. Pütz, E. Neuschütz, M. Scherer, Investigation of Procedures for Optimizing Skin Pass Rolling, CECA 7210-EA/143, CECA 7210-EA/144, 1998

B IRSID, D. Grandemange, H. Tsukahara, E. Vasseur, CRM, J.- C. Herman, BFI, P.- D. Pütz Control of the yielding and ageing behaviour in temper rolling, (Draft Final Report), CECA 7210-PR/035, 2001

C Lubrano M., Bianchi J.H., Pütz P., Mennicken H., Scherer M. 'Development and testing of procedures for optimising the degree of strip reduction during skin-pass rolling', EUR 18917 EN,1999.

D Lubrano M., Bianchi J.H., ' A simple model for on-line control of skin pass from FEM analysis of rolling deformation',2nd Int. Conference on Modelling of Metal Rolling Processes, The IOM, London, Dec.1996.

E CSM-MAGONA, SOLLAC, CRM, 'Improvement of formability of continuously organic coated coils by controlling ageing of low carbon steel substrates', Proposal4389 (F4) ECSC2001, approved, to start July 2001.

Summaries of activities

Experimental studies : Part 1

In the scope of the research program the aim of this experimental part was to relate the defect appearance to the microstructure and to the mechanical properties (sensitivity study). Two main points have been studies (CRM activities) :

- **The relation between the stress-strain curve and the microstructure,**

- **The relation between the deformation mode (tensile skin pass or bending) and the appearance of surface defects.**

A short literature review has been performed (effect of the grain size, Csol content, alloying elements, temperature and strain rate) and has been followed by the observation of Lüders defects on industrial and laboratory samples.
Then, all these parameters have been tested at the laboratory scale : ELC steels have been annealed following several thermal cycles to produce the aimed microstructures. The evolution of mechanical properties (YS, TEl, YPEl) have been studied. Results observed in the literature study were globally confirmed, even if such an observation is sometimes very sensitive to process conditions and thus not always reproducible :

- A finer grain size will induce the apparition of more numerous Lüders bands,

- A higher C_{sol} content leads to the formation of more numerous but finer Lüders defect,

- At the same grain size, the Lüders strain is reduced by a P addition. The effect of Sn addition on the Lüders strain of low-carbon steel is quite similar to that of phosphorus,

- An increase of the tensile temperature implies a lower YS and a shorter YPEl, whereas a higher tensile strain rate, implies a higher YS and a longer YPEl.

As far as the relation between the deformation mode (tensile, bending, skin pass) and the appearance of surface defects is concerned, it was observed that :

- The SKP deformation is the most efficient mode to remove the YPEl (1% SKP leads to the lowest YS value),

- A bending deformation of more than 1% is necessary to suppress the YPEl (in this case 2.3% ; no trial has been realised between 0.9 and 2.3% of deformation). The optimum deformation degree is certainly between these two values because it can be seen that YS slightly increases for a deformation of 2.3%. It must be noticed that even when the YPEl is suppressed, the YS values remains high (~ 200 MPa) in comparison with SKP deformation,

- The deformation by tensile has only a low influence on the YPEl and YS behaviour,

- Concerning the ageing behaviour, SKP and bending deformation modes do not seem to be affected by a laboratory ageing treatment (1 hour at 100°C) : YS and YPEl remain unchanged. For the tensile deformation mode, it can be noticed that YS slightly increases (about 10 MPa) after ageing while the YPEl values keep the same level.

Experimental studies : Part 2

This experimental part has focused on the influence of combined bending and temper rolling processes on the following parameters (BFI/VDEh activities) :

- Stress-strain behaviour
- Yielding behaviour
- Strain hardening behaviour
- Lüders behaviour.

During temper rolling in addition to the roll bite deformation plastic bending deformations has proved to accept values up to 30% of the target value of the skin pass degree when the strip is passing rolls being integrated into the strip flow inside the mill.

When setting the temper rolling degree and thus the resulting mechanical strip properties, these plastic bending deformations have not been taken into account during industrial rolling so far. In the scope of this project the question has to be clarified if a total degree of deformation, consisting of roll bite and bending deformation, has to be defined for adjusting the most favourable mechanical strip parameters. This question, however, cannot be answered without including the effect of bending deformations upon the generation or non-generation of Lüders defects on carbon steel strips.

In accordance with the process of temper rolling the effect of bending deformations *with applied strip tension* upon the above mentioned properties was determined and compared to conditions obtained by temper rolling. A combination of both deformation modes is investigated using two successive deformation steps beginning with the bending mode and joined by temper rolling.

The practical investigations were carried on low carbon, batch annealed steel strips presenting different thicknesses using a standard width of 300mm. The examination of the bending effects were performed on a a tension bridle with bending unit, which is operating as a laboratory levelling device at industrial scale. For the execution of temper rolling trials an industrial four high temper rolling mill for narrow strips was available, using polished rolls and dry rolling mode.

For each deformation mode investigated different degrees of deformation had to be adjusted. Starting from a deformation degree of about 0.2%, the deformation levels for different strip segments were incremented in small steps up to a total value of about 6.5 %.

For each reduction increment pre-set in the trials, strip segments were cut off at the strip positions. Four test specimens each were cut across the strip width from these strip segments, which were subjected to tensile testing for the determination of the mechanical properties. In addition, selected samples were used for strip surface inspection carried out by roughness measurements.

The results obtained clearly demonstrate that the *mechanical strip characteristics* yield stress, n-value and yield point elongation are influenced in the same way. For all three deformation modes investigated (merely bending, merely temper rolling as well as a combination of both) the typical drop in yield stress (in case of LC-steels) down to a minimum and the subsequent increase by usual hardening has been verified as well as the continuous decrease on the n-value with increasing degree of deformation. The same applies for the steady progress in the suppression of YPEL by growing degrees of deformation. Moreover, for each deformation mode examined, the three material characteristics accept values covering a small range of dispersion, which can be attributed to material non-conformances and test conditions.

A completely different behaviour between bending and temper rolling can be observed in terms of generation of Lüders effects becoming visible as flow figures on the strip surface. In contrast to the compression state in temper rolling the origination and expansion of Lüders bands is not prevented but rather favoured by the "free" strip surface in strip bending processes. The generation of flow figures could already be observed at very small degrees of bending. Once originated they keep visible during bending procedures at higher deformation levels; their appearance anyway changes, indicated by smaller wavelengths in the detected roughness structure of the strip surface.

The investigations concerning the combination of the two deformation modes in terms of bending and additional temper rolling demonstrates, that Lüders structures generated in the preceding bending deformation step can be levelled by subsequent temper rolling accepting a surface structure similar to the initial batch annealed, non-deformed strip surface. It must be pointed out, that this effect was achieved at a total deformation level corresponding to the recommended temper rolling degree of 0,6% in case of industrial rolling; the bending deformation adjusted was 0,29%, the degree of temper rolling was set to 0,3%.

It can be summarized, that bending deformations, which can accept values up to 30% of the target value of the skin pass degree should be compensated by a reduction of the degree of temper rolling to avoid a lack of deformability in further processing (deep drawing, stretching…). This recommendation can be generally applied to steel grades demonstrating a continuous stress-strain-behaviour (Lüders-free). Particular aspects in terms of limitations concerning roughness transfer and strip shape correction have to be considered.

In case of temper rolling LC steels with upper and lower yield strength the Lüders phenomenon additionally has to be taken into account by all means. However, Lüders structures generated by bending deformations can be levelled by subsequent temper rolling. A reduction of the temper rolling degree in favour of inevitable bending deformations has been proved to be possible when temper rolling Lüders-sensitive LC-steel grades. The summed up total deformation consisting of bending and temper rolling deformation should not remain below that degree of deformation, which is required for suppressing the yield point elongation.

FEM simulation studies : part 3 (Skin-Passing process)

This part of the project has been focused on understanding conditions leading to Lüders bands generation in ferritic stainless steels strips during their processing and consequently prevention of their defects on their end-use applications by further metal forming. This work (CSM activities) has been carried out taking as reference an industrial skin pass configuration with gripping rolls. The effect of changes in processing parameters are examined in detail.

The research has been carried along five interlinked ways: standard tensile testing to characterise the strip mechanical properties, physical simulation of skin pass elongation by tension, pilot mill rolling, industrial rolling and numerical simulation of both the strip processing and its subsequent tensile testing. Extensive validation of the predictions against experiments has been carried out. Good agreement in all tensile properties up to uniform strain was obtained using a local LDH model constructed from a single tensile test of the annealed material. The YPEL predicted by this simulation is however over evaluated for the higher strain rates corresponding to the bigger skin pass reductions. An improvement can be obtained from data obtained by a skin pass physical simulation followed by standard tensile testing, and these used to construct model of the LDH type that has shown to perform best.

The most important conclusion of the Project is that YPEL elimination does not depend only on the accumulated strain, but on a combination of this with strain rate. For the 0.6 mm thickness AISI430 strip a threshold strain rate (order 0.13 s^{-1}) was identified, above which YPEL vanishes in subsequent tension earlier than predicted by the continuous testing at the routinely low strain rate of the

characterising test (10^{-3} s^{-1}). This result from a physical simulation by tension, which involves a deformation mode very different than rolling with or without bending and tension, suggests that skin pass is not a requisite to eliminate YPEL and this could be achieved even by purely bending provided that the strain rate is high enough (0.13 s^{-1}). Such value is still reachable in industrial configurations, but not necessarily in lower speed pilot mills, where also maintaining the strip at a steady longitudinal tension differential that is uniformly distributed across width is not as difficult as for the industrial strip width (1200 mm).

FEM simulation studies : part 4 (Bending process)

Regarding this part of the project (ARCELOR RESEARCH SA activities), the main results can be drawn :

A finite element method (FEM) associated to a physically based description of the constitutive behaviour of steel allows to simulate the bending process and to predict either the plastic deformation performed or elongation necessary to suppress the yield point elongation.

Numerical simulations of tensile test and bending test have been designed. In all cases, rather good agreement is found between Lüders bands pattern observed experimentally and simulated numerically.

Regarding tensile test simulations, it is demonstrated that the local constitutive behaviour must present an initial stress drop to simulate satisfyingly the experimental force-displacement response of the steel. This method has been used successfully to identify the local flow behaviour of steels prior to bending process.

Provided the local flow behaviour of the initial (non bended) material is determined, very good agreement between experimental and calculated evolution of YPEL as a function of the bending process elongation is found. It is worth noting that systematically, the bending elongation leading to the minimum yield stress is lower than the one leading to the suppression of the Lüders plateau.

This procedure is found to be relevant to simulate laboratory temper rolling experiments taking into account plastic bending deformations when the strip passes over deflecting rolls occurring in a temper mill pass-line.
It can for instance replace exhaustive experimental work at the laboratory scale in order to determine the skin pass reduction required for suppressing the Lüders plateau while taking into account potential plastic bending deformations occurring over deflecting rolls through the pass-line. Just a tensile test before temper rolling is necessary to determine the local constitutive behaviour to input for the finite element calculations.

This method could also be useful to build master charts giving the critical temper rolling reduction to apply in order to suppress the yield point elongation.

Others potential industrial applications are possible in the field of leveling modeling, pass-lines optimization, tools dimensioning such as anti coil-break rolls system.

Nevertheless, some improvements could be necessary in order to be still more representative of industrial temper rolling conditions. In particular meshing refinement could be an obstacle to accuracy for evident time calculation.

TABLE OF CONTENTS

DESCRIPTION OF ACTIVITIES AND MAIN RESULTS

Experimental studies : Part 1

List of tables and figures :

INTRODUCTION

The main objective is to relate the defect appearance to the microstructure and to the mechanical properties (sensitivity study). Two main points have been studies :

- **The relation between the stress-strain curve and the microstructure**
- **The relation between the deformation mode (tensile skin pass or bending) and the appearance of surface defects.**

1/ LITERATURE STUDY

Firstly, a short literature study concerning the Lüders bands has been performed concerning the effect of the microstructure on the Lüders defects appearance.

a) Effect of the grain size :

The magnitude of Lüders strain is influenced by the grain size **(1)** (linear function of $d^{-1/2}$, where d is the average grain diameter). It means that a finer grain size will induce the apparition of more numerous Lüders bands.

b) Effect of the Csol :

According to a previous ECSC project "Control of the yielding and ageing behaviour in temper rolling" **(2)** it seems that no direct relation exists between the amount of solute carbon and the appearance of Lüders bands.

c) Effect of the alloying elements :

According to the literature **(3)**, at the same grain size, the Lüders strain is reduced by a P addition to the steel. The effect of Sn addition on the Lüders strain of low-carbon steel is quite similar to that of phosphorus.

Solute elements that are strong grain-boundary segregants, such as tin and phosphorus, may effectively increase the density of such grain-boundary sources.
An addition of boron, which is known to increase the ferrite grain size, leads to less numerous Lüders bands.

d) Effect of the temperature and of the strain rate :

The effect of the temperature and the strain rate are known to be in relation **(4-5)**. An increase of the tensile temperature implies a lower YS and a shorter YPEL, whereas a higher tensile strain rate, implies a higher YS and a longer YPEL. It will be studied in this project if the size of the yield point elongation can be related to the apparition of numerous Lüders bands.

e) Observation of Lüders bands :

Only little literature exists concerning the observation of the formation of Lüders bands (the apparition of the yield point elongation has been mainly studied). One article presents several methods to observe the apparition of Lüders bands during tensile test : " Aspect des bandes de Piobert-Lüders sur des éprouvettes en tôle d'acier extra-doux recouvertes de vernis élastique" **(6)**. Among the different proposed methods, the first one using a photo-elastic varnish seems to be the best one to observe easily the formation of Lüders bands but it necessitates having a polariser and an analyser to perform a quantitative observation. A cracking varnish can also be used (the appearance of Lüders bands imply

the formation of cracks on the steel surface). Finally, the observation of surface defects can be carried out on a well-polished sample by using a low-angled light.

The main conclusions of this study are the following ones :

- Lüders bands appear before YS_{upper} is reached on the tensile curve. This value is reached when the first Lüders band has crossed the whole tensile sample.

- The following YS decrease can be attributed to a quick rotation of the band front.

- During the YPEl, the tensile sample is crossed by several Lüders bands. The YPEl irregularities are due to new bands apparition.

- If the imposed strain rate is faster than the Lüders bands displacement, new bands appear on the tensile sample.

- Two different kinds of Lüders bands can be distinguished : transversal and oblique ones. The first ones present an inclination of 50° in the thickness. The second ones form an angle of 50° in the tensile direction .

- By modifying the steel texture and the direction of the tensile sample (in the rolling direction or not), it is possible to make appear mainly the first or the second kind of Lüders bands.

2/ RELATION BETWEEN THE STRESS-STRAIN CURVE AND THE MACROSTRUCTURE

This part is divided in two sections : the observation and characterisation of Lüders defects and the influence of microstructure on the mechanical properties (confirmation or not of the literature results).

a) Observation and characterisation of the Lüders bands :

Lüders bands have been observed and characterised on both industrial and laboratory products. In the first case, two different steels have been studied : the first one is a hot rolled sample (steel composition and mechanical properties presented in **table 1**) and the second one is a tube annealed at 760°C after forming and cooled in two steps down to room temperature (steel composition and mechanical properties presented in **table 2**).

In the first case, a micro-roughness measurement has been performed in order to determine the spacing (average of 0.8 mm) and the depth of the defects (**figure 1**). It can be observed that the roughness presents a positive value for each surface defect. This can be explained by the presence of oxide, which has been formed preferentially on the defects and creates an over-thickness. For this reason, only the spacing of the bands can be considered.

In the second case (tube), it can be seen that the defects present a “negative roughness” (**figure 2**). The spacing is quite similar than for the previous sample (0.7 mm) and the depth of the defects is about 2-6 µm. By comparing with the photo below, it can be observed that on a sample of 16 mm long, about 5 Lüders bands are visible (green signs spaced by 7 mm in average, 0.5 to 1 mm large) and these defects can be found on the roughness figure (corresponding to the largest holes). It appears that two kinds of defects are present: some are eye visible and larger and the others, finer can not be detected by eyes (illustrated by red signs on the graph).

On laboratory samples, the ELC steel has been polished after annealing and the tensile test was carried out afterwards up to a strain from 0.5 to 6%. It was aimed to see if it exists a relation between the YPEl (and other parameters like Csol, Ctotal, grain size …) and the number of Lüders bands. Unfortunately, contrary to industrial samples, it is difficult to observe distinctly the Lüders bands on laboratory steels in order to count them. Two large strained bands are generally observed (beginning near the head of the tensile sample and presenting very fine Lüders defects : **figure 3 and 4**), which merge together when enough strain is applied.

Two roughness measurements have been performed : the first one on the basis polished material (**figure 5**) and the second one on the mat strained band (**figure 6**). In the case of polished sample, the surface presents no defect. When observing the mat surface, fine lines can be observed, spaced of about 0.7 mm and presenting a depth of 1-2 µm in average (less than for the industrial samples).

b) Influence of the C_{sol} content on the mechanical properties :

First experiments have been realised by quenching ELC steel samples from different temperatures (**figure 7**) to modify the C_{sol} content (from 93 to 3 ppm : **figure 8**). The measurement of the amount of solute carbon was carried out by vibran on small rectangular annealed samples.

It is observed that TS and YS both increase with the amount of C_{sol} but due to the rapid cooling (water quenching on 1 mm thickness samples), dislocations have been introduced, especially when quenching from high annealing temperatures) and no conclusions concerning the effect of the C_{sol} on the YPEl could be made : **figure 9**.

An observation of the Lüders bands has been realised after polishing and applying a deformation by tensile test of 2% elongation (**figure 10**).

It can be concluded that a higher C_{sol} content leads to the formation of more numerous but finer Lüders defect.

Then a new cycle with overageing (**figure 11**) has been tested by modifying the holding time at 400°C to vary the C_{sol} content (**figure 12**). In this case, as the quenching temperature was always the same (400°C), the same amount of dislocation was introduced during water cooling. In these conditions, the range of Csol content is smaller (12 – 24 ppm) than previously. It appears that a higher C_{sol} content induces larger YS, TS and also YPEl values (**figure 13**).

c) Influence of the grain size on the mechanical properties :

In order to modify the grain size, different cold rolling reductions have been realised (50-75 and 95%) on a conventional ELC steel grade. Then, the steel has been annealed in salt bath (750°C 1 min, 400°C 4 min, quench).

Only a small variation of grain size has been observed between the 3 samples (8.5 - 9.5 and 10.5 µm), the smallest grain size being obtained with the highest cold rolling reduction.

Figure 14 gives the evolution of YS, TS and YPEl in function of the grain size. It can be seen that these 3 parameters slightly decrease when the grain size increases.

It was not possible to determine the YPEl on the sample cold rolled with 95% because of the background observed on the tensile curve due to the very small thickness (0.2mm).

In this case, no conclusion can be made concerning the formation and morphology of Lüders defects depending of the grain size (**figure 15**).

d) Influence of the total amount of C in steel

Several steel grades with different C levels have been studied (**table 3**) in order to evaluate the influence of this parameter on the mechanical properties.

These steels have been hot and cold rolled, and then annealed following the thermal cycle shown in **figure 16**. **Figure 17** presents the evolution of the solute C (measured by vibran) in function of the total amount of C in steel. Of course, no C_{sol} has been measured in the IF steel (containing Ti). For the lowest amounts of C_{total} (0.01-0.03), C_{sol} reaches a higher value (here 8 ppm) and then decreases down to about 5-6 ppm for higher amounts of C_{total}.

The evolution of mechanical properties (YS, TS, YPEl) can be observed on **figure 18**. It appears that YS and TS both increase with the amount of C_{total}. The YPEl follows the curve of C_{sol} : in the case of IF steel, no yield point elongation is observed. YPEl reaches the highest value (~7 %) for the lowest alloyed steel and then decreases down to less than 6%.

By increasing the amount of total %C in steel, the formation of Lüders defects also appears to follow the evolution of the C_{sol} content (like YPEl) : for the lowest alloyed steel, the amount of C_{sol} is maximum and more defects can be observed (**figure 19**).

e) Influence of an addition of alloying elements (P, B)

The influence of an addition of B or P has been studied on the evolution of the mechanical properties. Steel grades are presented in **table 4**.

After reheating at 1200°C, steels have been hot rolled in 4 passes (30-20-12-7-3.8 mm) and coiled at 740°C. After pickling, a cold rolling down to 1 mm was performed before the final thermal treatment : 750°C during 1 min followed by cooling and holding at 400°C for 4 minutes.
Mechanical properties for the three steels are presented in **table 5**.
In comparison with the reference steel, it appears that an addition of B leads, as expected, increases the ferrite grain size (from 9.5 µm for the reference steel to 18 µm for the B added steel), leading to the suppression of the yield point elongation (only 0.5% remaining).
This grain size increase implies a loss of strength of about 70 MPa.

In the case of a P addition, the yield point elongation is slightly reduced (from 6.7 to 5%) : as explained in the previous literature study, P is a strong grain-boundary segregant which increase the density of such grain-boundary sources. The strength level is increased (+50MPa) thanks to the solid solution strengthening effect of P.

f) Influence of the temperature and of the strain rate

The influence of the temperature and of the strain rate on the mechanical properties (especially YS and YPEl) have been studied. Tensile tests have been performed with a large temperature range (20 - 400°C) and strain rate ($0.1s^{-1}$ - $100s^{-1}$). Results obtained with strain rates of 10 and $100s^{-1}$ can not be exploited (presence of too much background).

Figures 20 and 21 present the evolution of YPEl and YS in function of the tensile temperature and tensile speed. It appears than YS and YPEl increase with the tensile speed and decrease when temperature increases (no yield point elongation is observed at 400°C).

g) Influence of the surface microstructure modification on the appearance of Lüders defects

In order to avoid the formation of Lüders defects, a modification of the surface microstructure has been proposed. Two routes have been investigated : the formation of a thin layer of pearlite or martensite at the surface by using reactive annealing (the skin is enriched in C during soaking to form a second phase during cooling).

In the case of pearlite, the objective was to form a stronger skin, which could avoid the appearance of Lüders defects. With the martensite layer, the aim is to reproduce the same mechanism than for DP where martensitic islands create dislocations in the surrounding ferrite, leading to a stress-strain curve without yield point elongation.

In both cases, the layer of second phase is chosen thin enough to avoid any significant modification of the mechanical properties of the ELC steel grade. Indeed, for such steel composition, the formability should not be affected.

For these trials, a carburazing atmosphere composed of 33%CO, 66%H_2 was used, with a dew point of +12°C. With a soaking performed at 850°C, the carbon activity was around 0.8, leading to a surface layer composed of 0.8 wt%C. A reactive annealing time, from 2 to 10 seconds, was used to form respectively 5 and 10 µm of C enriched steel at the surface.

Table 6 presents the thermal cycles realised on samples of 0.25 mm in order to reach high cooling rates to form martensite. Indeed, despite the high C content, the very low Mn content of 0.2wt% necessitates to use cooling rates of minimum 150°C/s to avoid any transformation before reaching Ms).

The first cycle a corresponds to a conventional ELC annealing cycle (soaking 750°C, slow cooling in two steps and overageing at 400°C) : this experiment will be used as a reference for the ferritic grain size and the mechanical properties.

Cycles b and c are also references for the reactive annealing cycles (soaking at 850°C, two cooling rates 10°C/s and 150°C/s to simulate the formation of respectively pearlite and martensite) but in these cases, no carburazing atmosphere was used.

Finally, cycles d, e, f and g correspond to the reactive annealing thermal treatments : these samples present 10 or 5 µm of second phase at the surface depending on the carburazing time at 850°C. the nature of the second phase, pearlite or martensite, is determined by the applied cooling rate after soaking : 10 or 150°C/s.

The microstructure at the surface has been studied by optical microscopy (the thickness of the martensite / pearlite layer has been checked) and the ferritic microstructure in the middle of the thickness sample has been characterised (grain size, hardness : **table 7**).

The second phase layer is well visible on samples D, E, F and G : the thickness range is between 6 and 10 µm. To better estimate the nature of this second phase, SEM observations have been carried out (**figure 22**). On these figures, it clearly appears that samples D and E presents a martensitic layer whereas it is a pearlite one for samples F and G.

As far as the ferrite grain size in the middle of the sample is concerned, it can be observed that the thermal treatment has a slight effect : the soaking temperature, soaking time and cooling pattern can modify the grain size. However, the range is quite small (from 8.2 to 12.9 µm) and is considered to have no real impact on the appearance of Lüders defects, especially for samples annealed at 850°C : samples B to G). In such conditions, the study of the second phase layer effect can be performed

Then, the mechanical properties of each sample as annealed steels and after ageing (100°C 1 hour) have been measured by tensile tests (YS, TS, TEl, YPEl) : **Table 8, figures 23 to 26**.

It can be observed that :

- Due to the high cooling rate applied to from martensite at the surface, a high amount of solute carbon is present and leads to a very low ductility.

- The presence of martensite and the high C_{sol} level lead to a significant increase of TS and YS.

- A pearlitic layer of 5 or 10 µm thickness also modifies the mechanical properties (slight increase of YS and TS, decrease of ductility) but less than the martensitic one.

- In the case of martensitic layer, the n value (range between 0.20 and 0.23) and the YPEl (range between 4 and 5.5%) do not seem to be affected by such a modification of the thermal treatment.

- In the case of pearlitic layer, the n value (range between 0.22 and 0.24) is also constant whatever the thermal treatment applied. Nevertheless, the YPEl is slightly increased in presence of pearlite.

An ageing treatment of 1hour at 100° :

- is not enough to make all the C_{sol} precipitate in the case of rapid cooling, the elongation remains low.

- Increases the ductility of steels presenting a pearlitic layer.

- Generally increases the YPEl (especially for reactive annealed samples).

3/ RELATION BETWEEN THE DEFORMATION MODE (TENSILE OR BENDING) AND THE APPEARANCE OF SURFACE DEFECTS

The chemical composition is the following one : 0.032%C, 0.22%Mn, 0.069%Al, 0.0038%N.

The mechanical properties of this industrial steel grade (cold rolled down to 0.62 mm, annealed, not skin passed) used for bending tests at BFI are presented in **table 9** :

a) Influence of bending on the apparition of Lüders bands

The experiment matrix concerning bending trials performed on the BFI equipment has been established in agreement with IRSID. **Table 10** presents the bending conditions : the tension to apply has been determined in function of the deformation degree to reach. The line speed was fixed to 2.6 $m.min^{-1}$. **Figure 27** illustrates the bending applied on the steel plate.

Three different parameters were studied :

- the intermesh (4 – 8 mm)

- the elongation obtained by bending (by modifying the strip tension) : (0.4-2.3 %)

- the strip speed (0.6 - 6 $m.min^{-1}$)

During the trials, some coil sticking occurred (characteristic of batch annealing products) and led to the formation of Lüders defects before the bending unit. Decreasing the tension applied during uncoiling has solved this problem.

After bending, the different steel plates have been characterised and compared with the initial material:

- Tensile tests have been carried out to observe the evolution of YS and YPEl in function of the experimental conditions
- An approximation of the bands spacing has been estimated (eye observation on 30 mm)
- Roughness measurements were realised in order to estimate the depth of the defects (annexe 1)

Table 11 presents the experimental conditions, the surface aspect and the mechanical properties obtained on each sample.

According to these results, it appears that :

- Increasing the deformation by bending leads to an increase of the Lüders defects
- Increasing the intermesh also leads to an increase of the number of Lüders defects.
- In the range studied (0.6 - 6 $m.min^{-1}$), the deformation speed does not have any influence of the defects appearance.
- After having suppressed the Yield Point Elongation, Lüders defects are still present (contrary to SKP or tensile deformation) and an increase of does not lead any more to more numerous Lüders defects.
- In **table 11**, an average of the mechanical properties (transverse and rolling direction) is presented. It must be underlined that the YS and YPEl values are higher in the case of samples taken in the transverse direction.

b) Influence of the deformation mode on the mechanical properties

To determine the influence of the deformation mode on the evolution of mechanical properties, several skin pass and tensile deformations have been performed with the same deformation levels than for bending tests (0.5, 1 and 1.5%). It must be noticed that skin pass deformation performed on these steel do not include any tension. Consequently, this deformation mode can be assimilated to compression.

Tensile tests as deformed and after ageing have been carried on the different steels **(tables 12 and 13)** and the mechanical properties have been compared with those obtained by bending deformation (in the case of intermesh = 8 mm, samples 1, 2 and 3) : **figures 28, 29, 30 and 31.**

For this part, all mechanical properties have been compared in the rolling direction.

By comparing the mechanical properties obtained by the three different deformation modes, it appears that :

• The SKP deformation is the most efficient mode to remove the YPEl (1% SKP leads to the lowest YS value).

• A bending deformation of more than 1% is necessary to suppress the YPEl (in this case 2.3% ; no trial has been realised between 0.9 and 2.3% of deformation). The optimum deformation degree is certainly between these two values because it can be seen that YS slightly increases for a deformation of 2.3%. It must be noticed that even when the YPEl is suppressed, the YS values remains high (~ 200 MPa) in comparison with SKP deformation.

• The deformation by tensile has only a low influence on the YPEl and YS behaviour.

• Concerning the ageing behaviour, SKP and bending deformation modes do not seem to be affected by a laboratory ageing treatment (1 hour at 100°C) : YS and YPEl remain unchanged. For the tensile deformation mode, it can be noticed that YS slightly increases (about 10 MPa) after ageing while the YPEl values keep the same level.

CONCLUSIONS

The aim of this research program was to relate the defect appearance to the microstructure and to the mechanical properties (sensitivity study). Two main points have been studied :

• The relation between the stress-strain curve and the microstructure

• The relation between the deformation mode (tensile skin pass or bending) and the appearance of surface defects.

A short literature review has been performed (effect of the grain size, Csol content, alloying elements, temperature and strain rate) and has been followed by the observation of Lüders defects on industrial and laboratory samples.

Then, all these parameters have been tested at the laboratory scale : ELC steels have been annealed following several thermal cycles to produce the aimed microstructures. The evolution of mechanical properties (YS, TEl, YPEl) have been studied. The laboratory observations have shown that Lüders defects are very sensitive to process conditions (preparation of the samples, tensile test conditions…) and lead to no really reproducible results. In that way, it appears very difficult to give conclusions concerning the effect of the microstructure on the appearance of Lüders defects. Nevertheless, results observed in the literature study were globally confirmed :

• A finer grain size will induce the apparition of more numerous Lüders bands.

• A higher C_{sol} content leads to the formation of more numerous but finer Lüders defect.

• At the same grain size, the Lüders strain is reduced by a P addition. The effect of Sn addition on the Lüders strain of low-carbon steel is quite similar to that of phosphorus.

• An increase of the tensile temperature implies a lower YS and a shorter YPEl, whereas a higher tensile strain rate, implies a higher YS and a longer YPEl.

As far as the relation between the deformation mode (tensile, bending, skin pass) and the appearance of surface defects is concerned, it was observed that :

• The SKP deformation is the most efficient mode to remove the YPEl (1% SKP leads to the lowest YS value).

• A bending deformation of more than 1% is necessary to suppress the YPEl (in this case 2.3% ; no trial has been realised between 0.9 and 2.3% of deformation). The optimum deformation degree is certainly between these two values because it can be seen that YS slightly increases for a deformation of 2.3%. It must be noticed that even when the YPEl is suppressed, the YS values remains high (~ 200 MPa) in comparison with SKP deformation.
• The deformation by tensile has only a low influence on the YPEl and YS behaviour.

• Concerning the ageing behaviour, SKP and bending deformation modes do not seem to be affected by a laboratory ageing treatment (1 hour at 100°C) : YS and YPEl remain unchanged. For the tensile deformation mode, it can be noticed that YS slightly increases (about 10 MPa) after ageing while the YPEl values keep the same level.

LIST OF REFERENCES

1 E.O. HALL, "Yield point phenomena in metals and alloys", Plenum Press, New York, NY, 1970, pp 1- 126

2 E. VASSEUR, D. GRANDEMANGE, H. TSUKAHARA, JC. HERMAN, P.D. PUTZ, ECSC steel RTD programme : "Control of the yielding and ageing behaviour in temper rolling", 7210 – PA,B,C/035. 1997- 2000

3 Hsun HU, "Effect of solutes on Lüders strain in low-carbon sheet steels", Metallurgical transactions, vol 14A, January 1983, p 85-91

4 M. SAWADA, H. IBATA, "The effect of deformation temperature on the formation of Lüders band in mild steel (from the viewpoint of coil break)", South East Asia Iron and steel institute, SEAISI 1997Korea conference on "Flat Product Technology" proceedings, vol1 (Malaysia), pp4/1, May 1997.

5 J. MANJOINE, "Influence of rate of strain and temperature on Yield stresses of mild steel", Journal of applied mechanics, december 1944.

6 G. POMEY, M. GRUMBACH, C. ROSSARD, "Aspect des bandes de Piobert-Lüders sur des éprouvettes en tôle d'acier extra-doux recouvertes de vernis élastique", Mémoires scientifiques, rev. Metallurg. N°4, avril 1964.

C	Mn	Si	Al	YS (MPa)	TS (MPa)	TEl (%)	YPEl (%)
0.08	0.29	0.015	0.056	290	370	39	5

Table 1 : Steel composition (wt %) and mechanical properties of industrial hot rolled steel

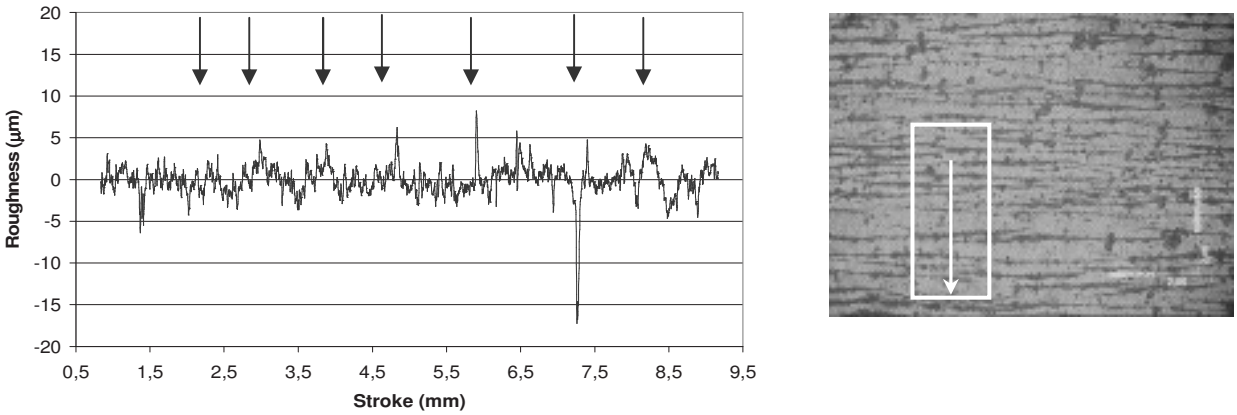

Figure 1 : Micro-roughness on industrial hot rolled material

C	Mn	Si	Al	YS (MPa)	TS (MPa)	TEl (%)	YPEl (%)
0.05	0.29	0.007	0.028	252	338	32	3

Table 2 : Steel composition (wt %) and mechanical properties of the industrial tube

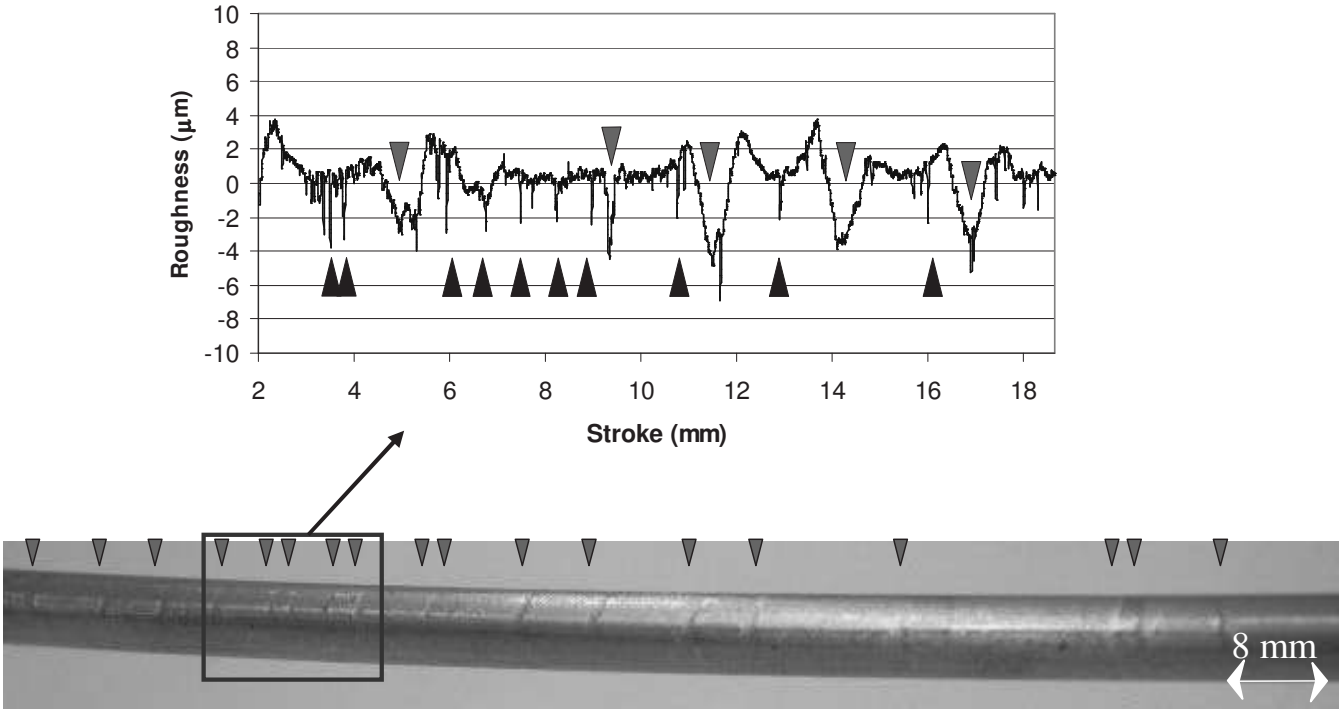

Figure 2 : Micro-roughness on an industrial tube presenting Lüders defects

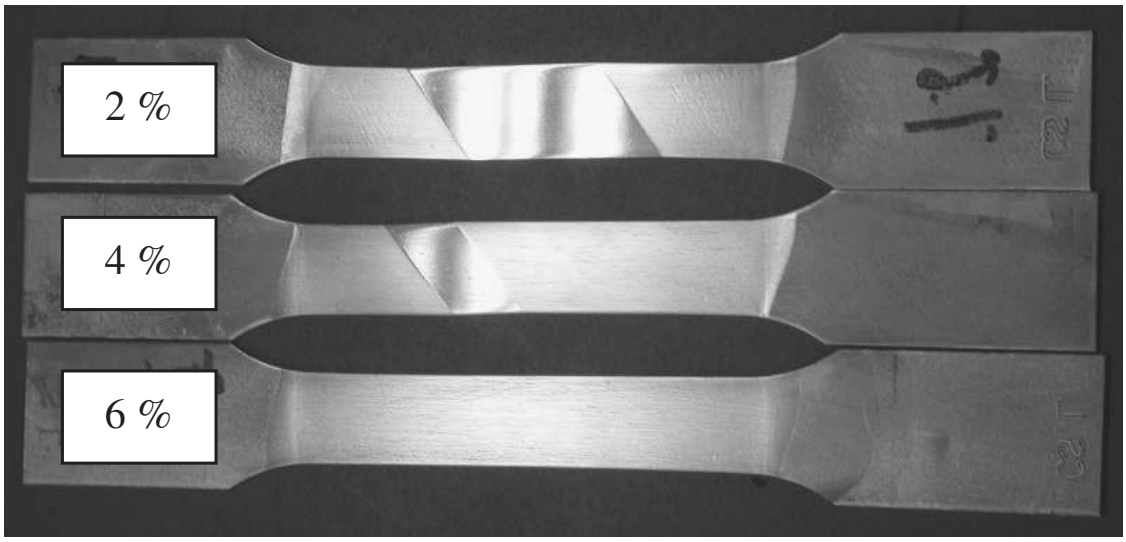

Figure 3 : Observation of Lüders bands on laboratory samples

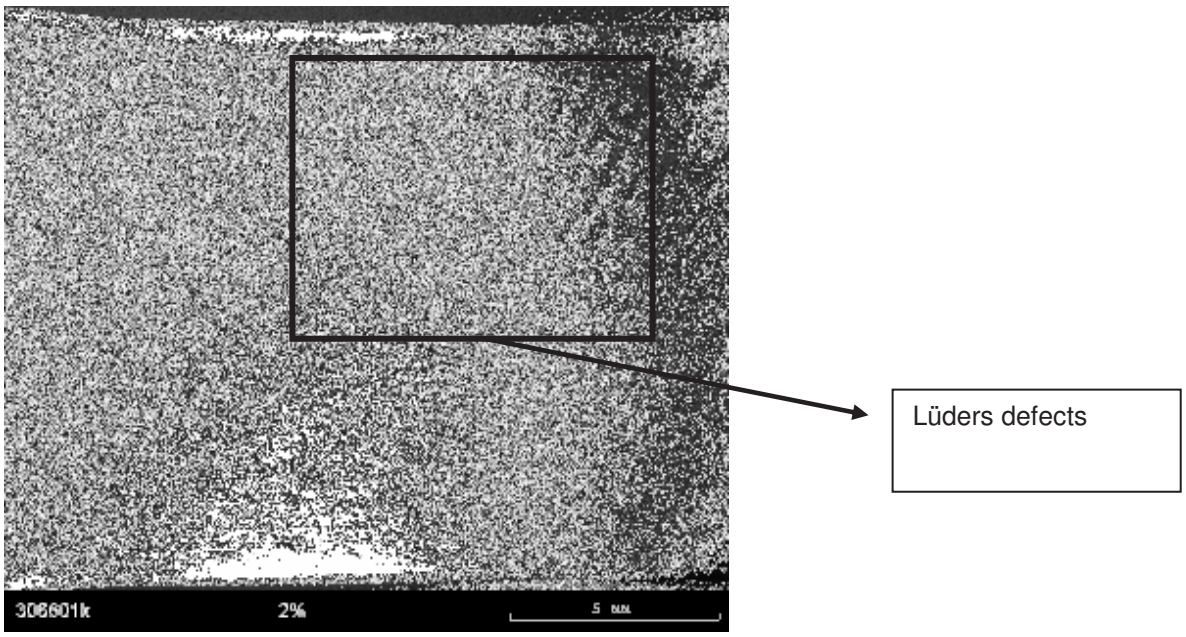

Figure 4 : Observation of Lüders defects on the tensile sample

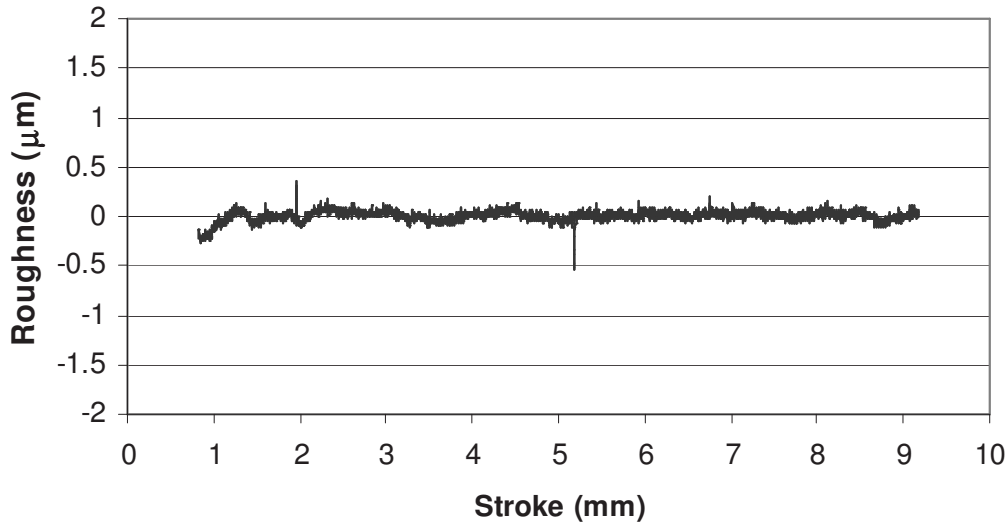

Figure 5 : Micro roughness measurement on the basis polished material

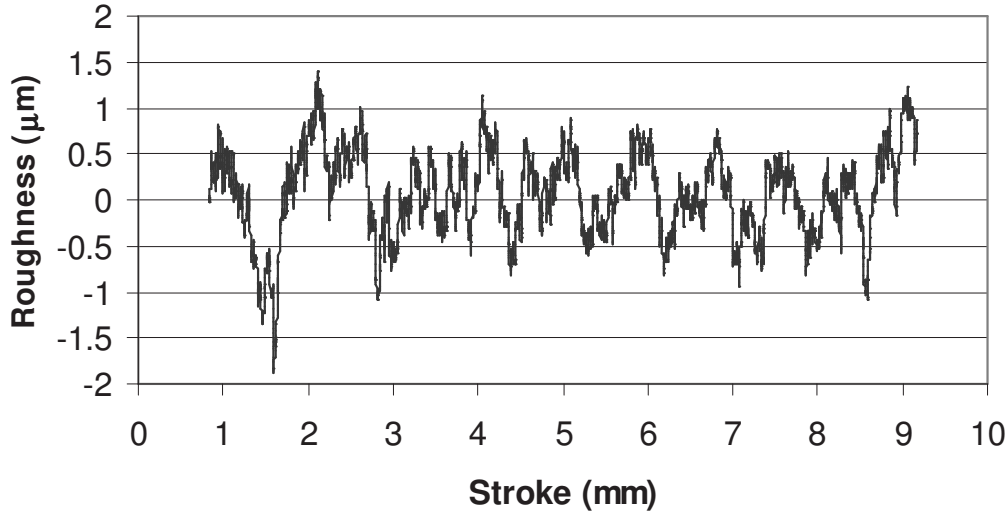

Figure 6 : Micro roughness measurement on the mat strained band

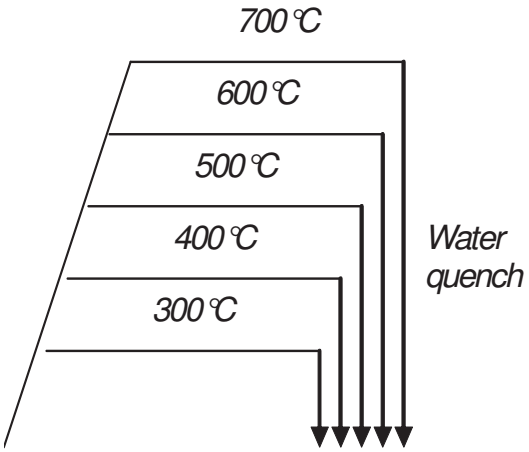

Figure 7 : Cycles performed on ELC steel

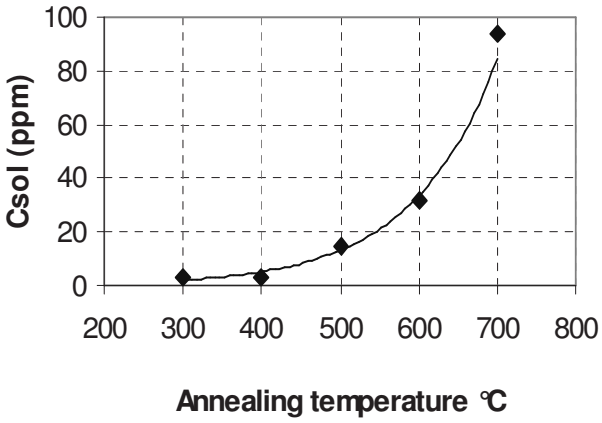

Figure 8 : Evolution of the C_{sol} content in function of the annealing temperature

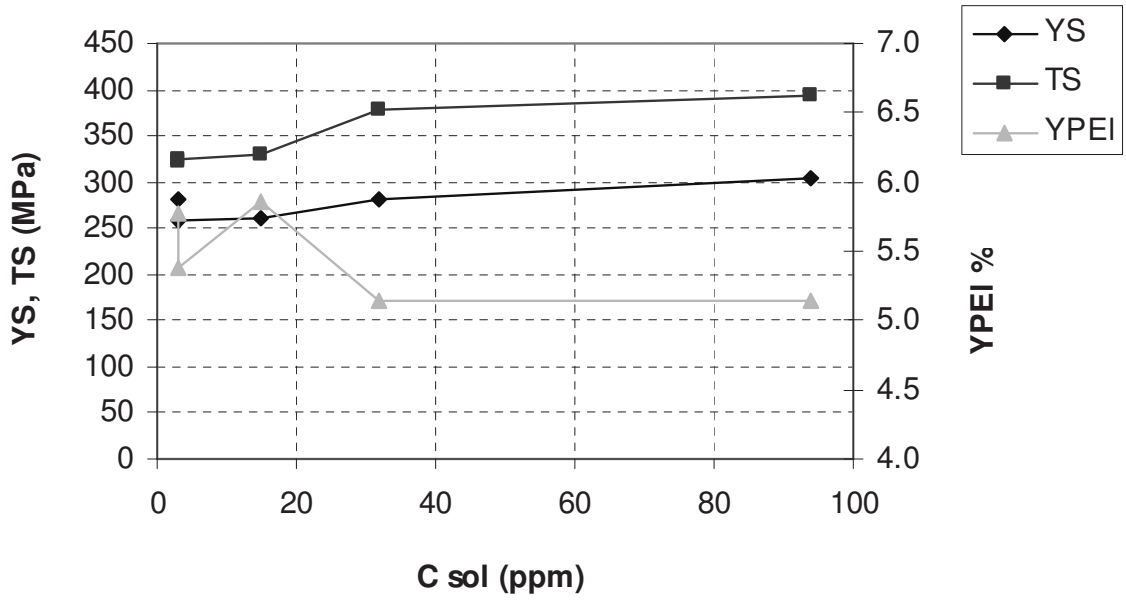

Figure 9 : Evolution of the mechanical properties in function of the C_{sol} content

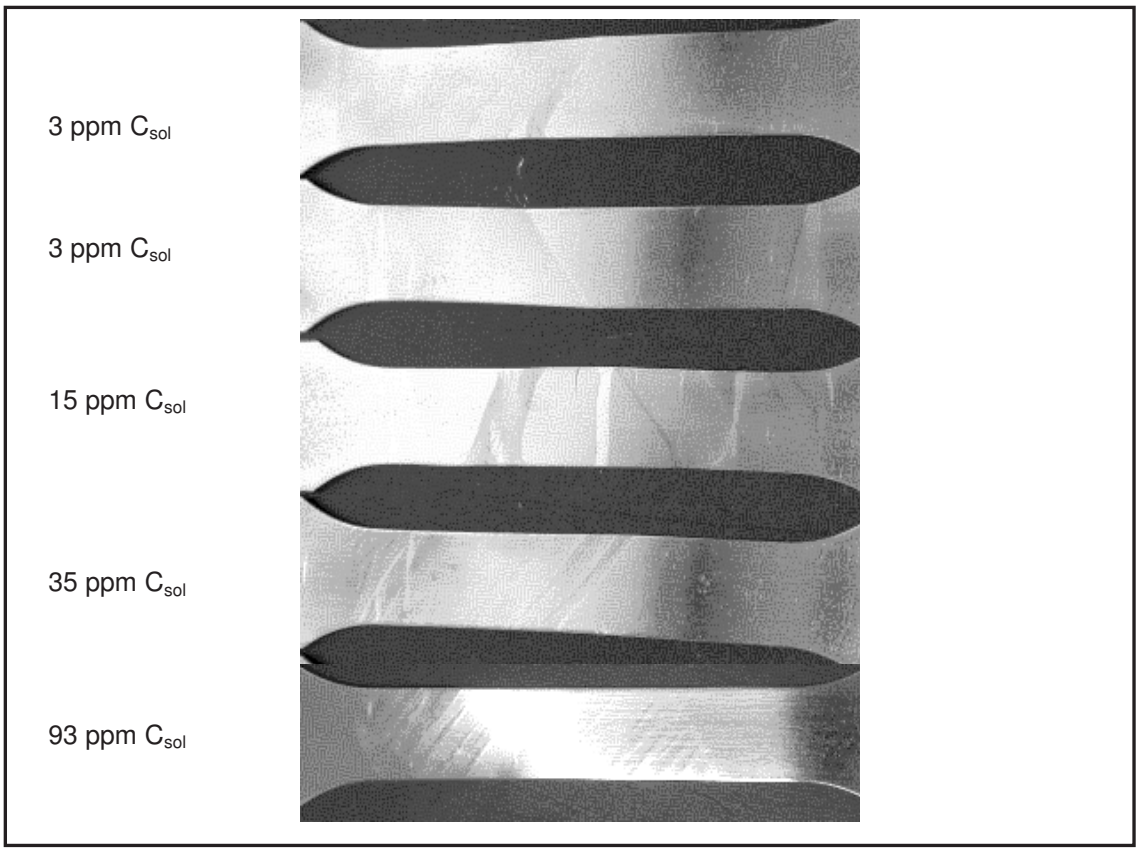

Figure 10 : Lüders defects morphology in function of the amount of solute C.

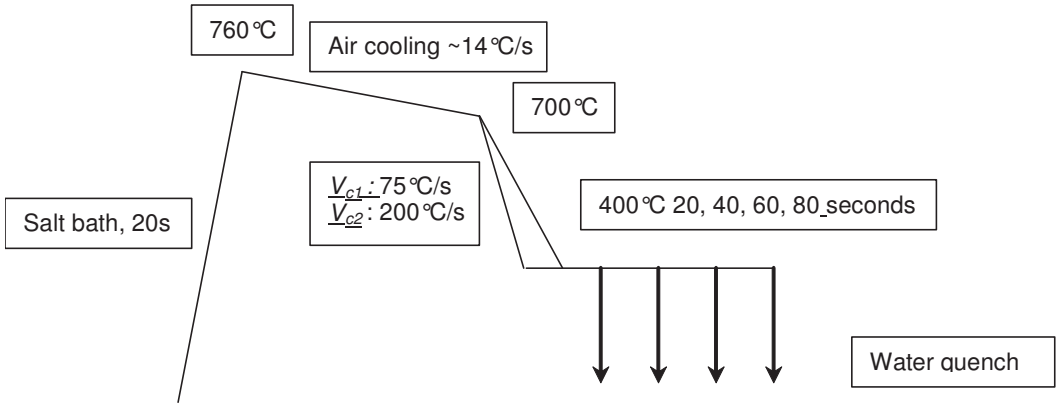

Figure 11 : New cycle with overageing

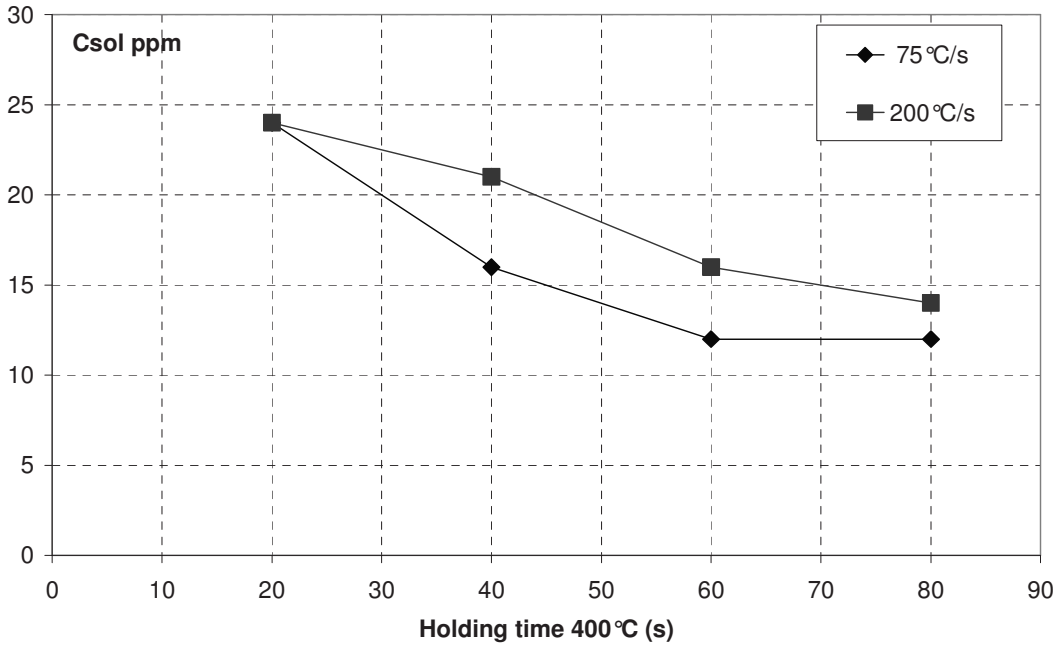

Figure 12 : Evolution of the C_{sol} content in function of the overageing time

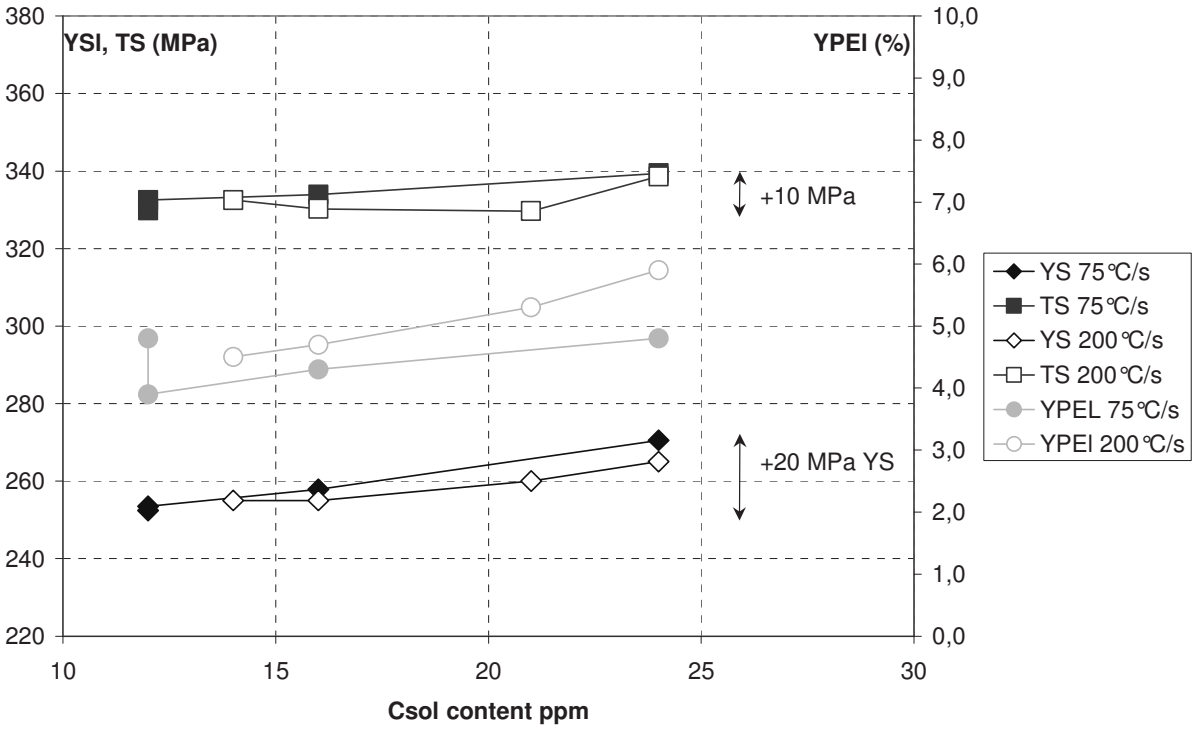

Figure 13 : Evolution of the mechanical properties in function of the C_{sol} content

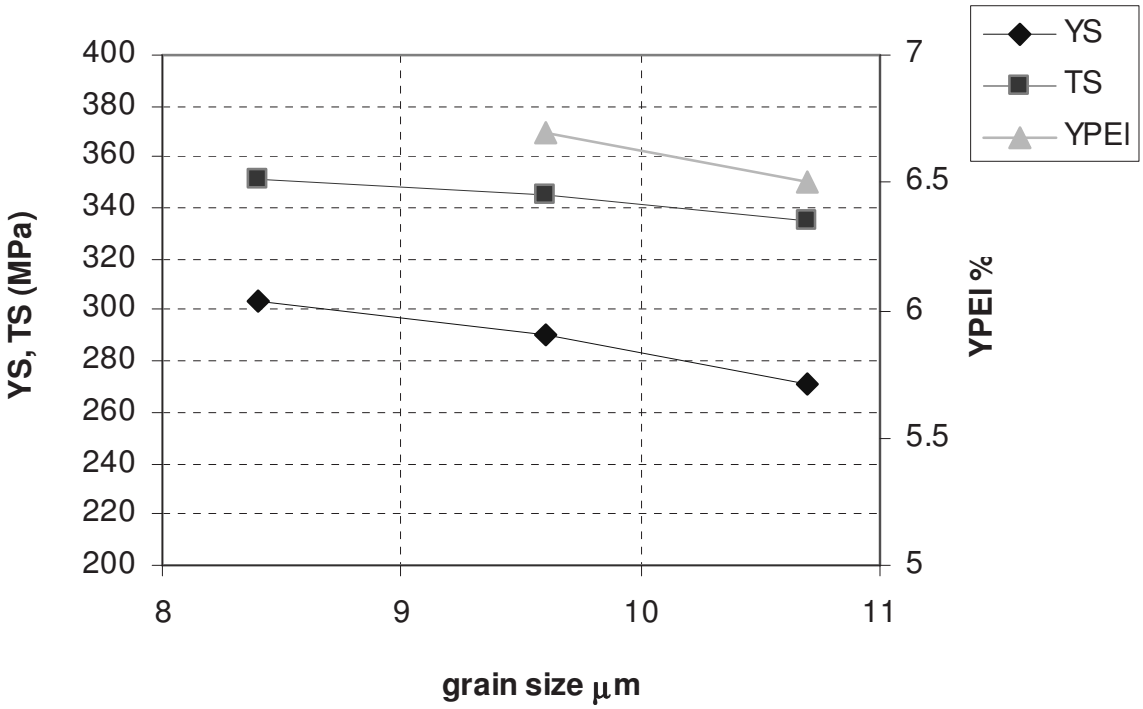

Figure 14 : Influence of the grain size on the mechanical properties

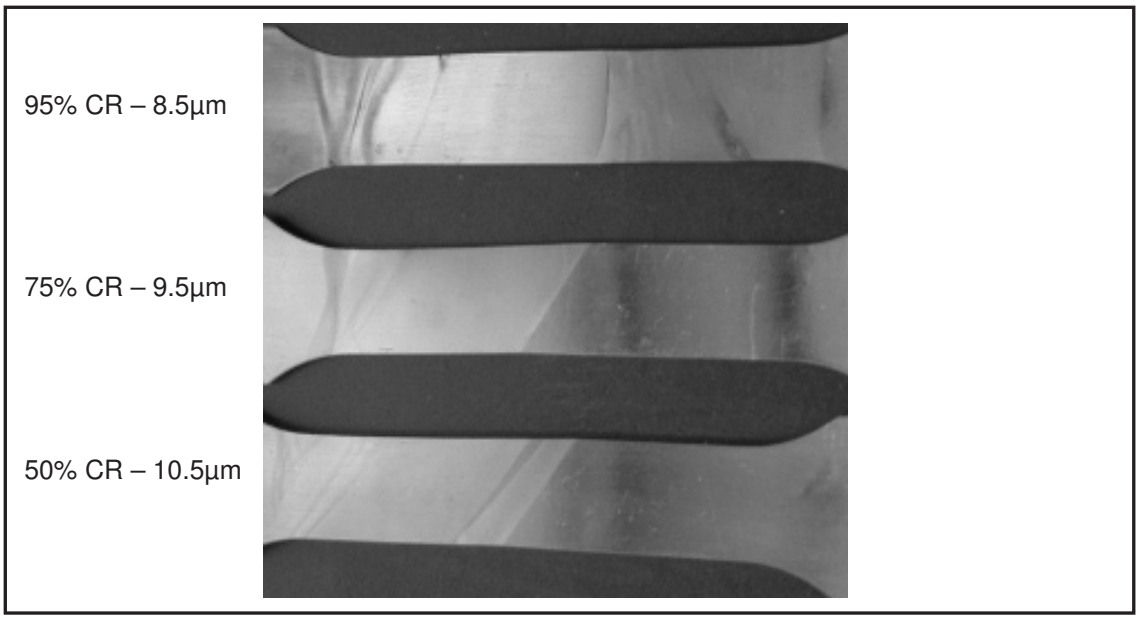

Figure 15 : Lüders defects morphology in function of the grain size

10^{-3}%	C	Mn	Al	N	Ti
IF	3	150	40	3	80
ELC 14	14	190	55	3	-
ELC 40	40	190	40	4	-
ELC 80	80	190	40	4	-

Table 3 : Steel grades with different C contents

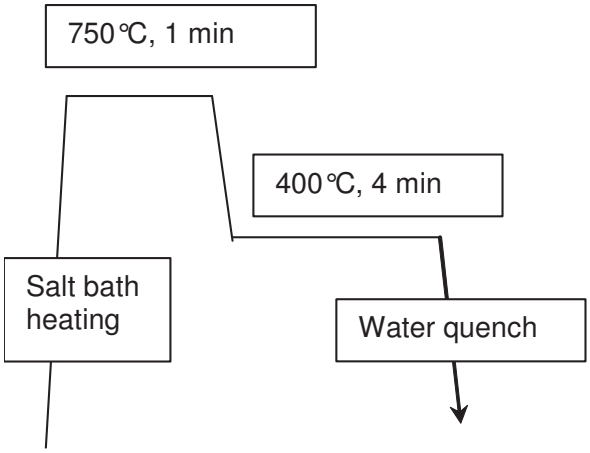

Figure 16 : Thermal treatments performed on the different steel grades

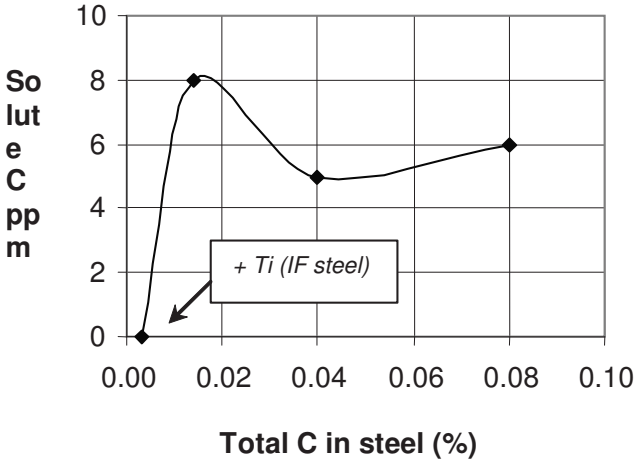

Figure 17 : Evolution of C_{sol} in function of the total amount of C in steel

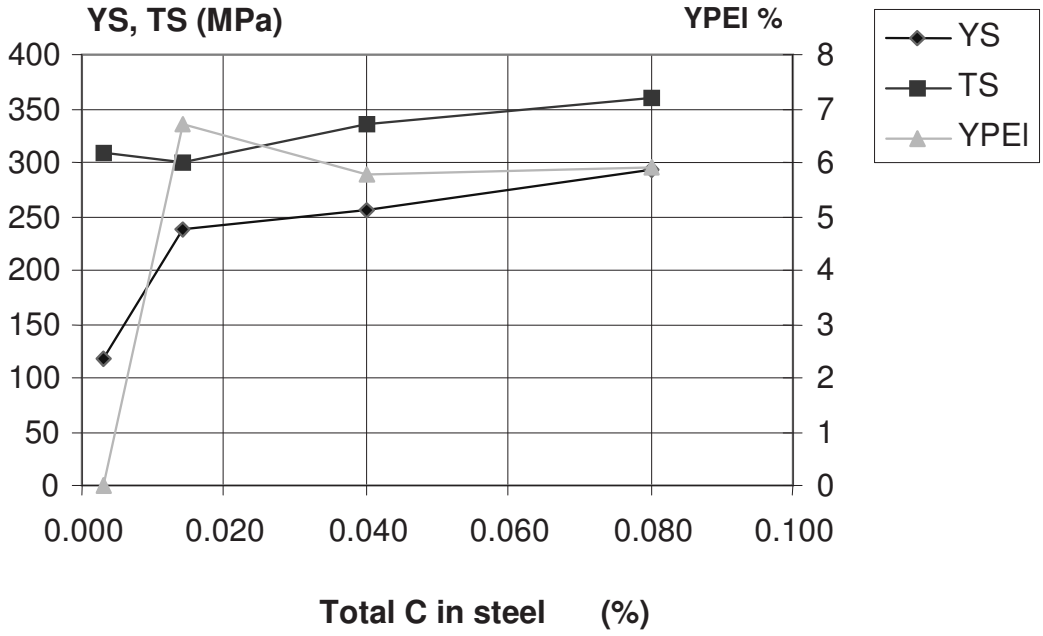

Figure 18 : Evolution of the mechanical properties in function of the total C in steel

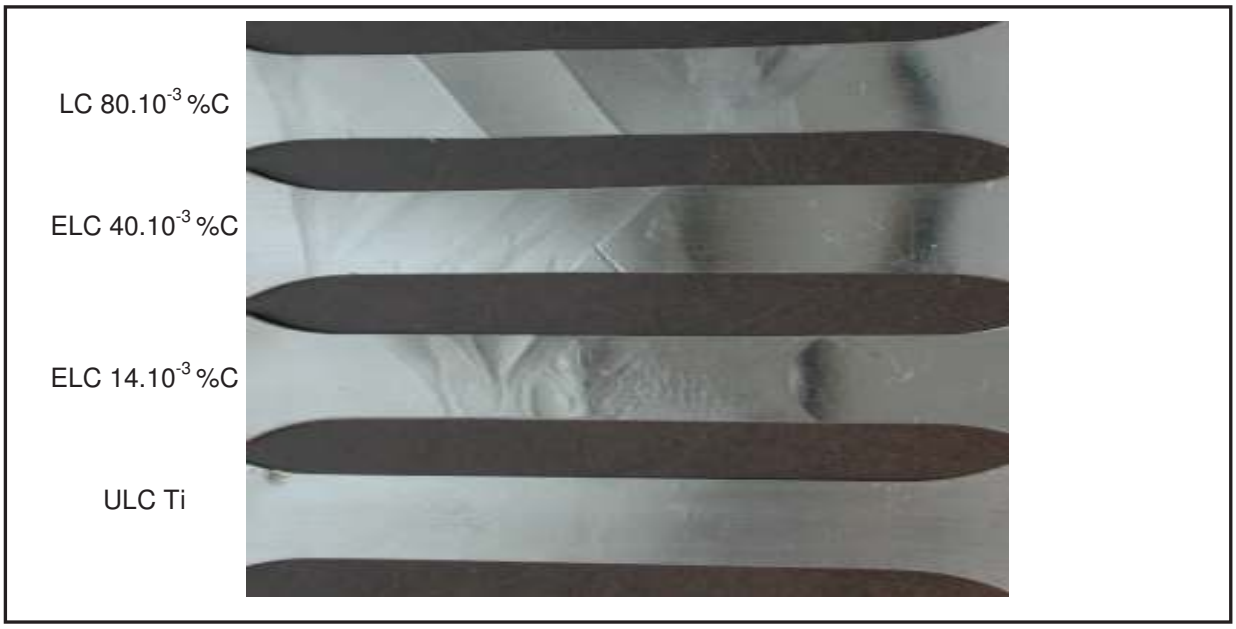

Figure 19 : Lüders defects morphology in function of the total amount of C in steel

10^{-3}%	C	Mn	Al	P	B
Reference steel	40	190	40	-	-
B steel	32	240	44	-	1.8
P steel	39	230	35	0.08	-

Table 4 : Steel grades studied to observe the influence of alloying elements on the evolution of mechanical properties

	YS (MPa)	TS (MPa)	YPEl %	TEl %	GS (µm)
Reference steel	290	345	6.7	41	9.5
B steel	158	287	0.5	47	18
P steel	304	392	5.0	35	-

Table 5 : Steel grades studied to observe the influence of alloying elements on the evolution of mechanical properties

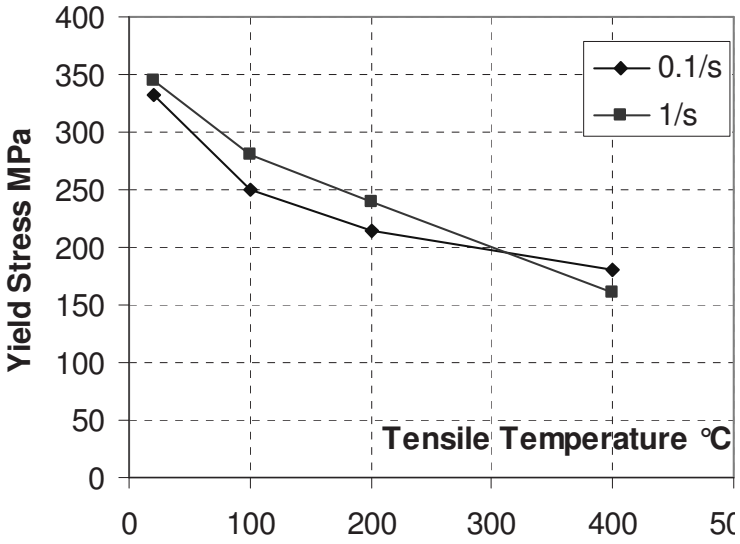

Figure 20 : Evolution of YS in function of tensile T°C

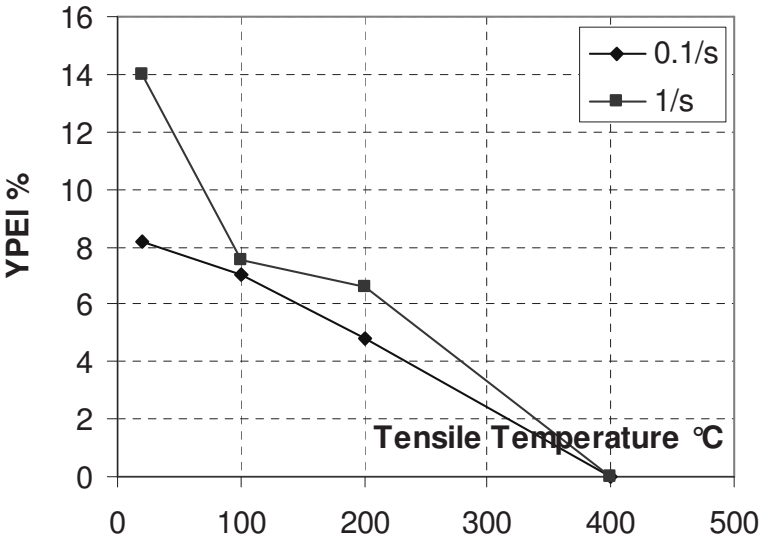

Figure 21 : Evolution of YPEI in function of tensile T°C

	a	*b*	*c*	*d*	*e*	*f*	*g*
Heating rate °C/s	*20*	*20*	*20*	*20*	*20*	*20*	20
Soaking temperature °C	*750*	*850*	*850*	*850*	*850*	*850*	850
Soaking time s	*60*	*60 + 10*	*60 + 10*	*60 + 10*	*68 + 2*	*60 + 10*	68 + 2
Carburization time s	-	-	-	*10*	*2*	*10*	2
Cooling rate 1 -T°C	*10 - 650 °C*	*150*	*10*	*150*	*150*	*10*	10
Cooling rate 2 -T°C	*50 - 400 °C*	-	-	-	-	-	-
Overageing T°C	*400*	-	-	-	-	-	-
Overageing time s	*180*	-	-	-	-	-	-

a : reference with overageing at 400°C
b : reference with accelerated cooling and without overageing
c : reference with low cooling and without overageing
d : 10 µm martensite per face
e : 5 µm martensite per face
f : 10 µm pearlite per face
g : 5 µm pearlite per face

Table 6 : Trials realised on ELC steel grade by reactive annealing with Rhesca equipment

Sample	Surface	Nature of the layer and Thickness (µm)	Centre	Ferritic grain size (µm) Hardness
A	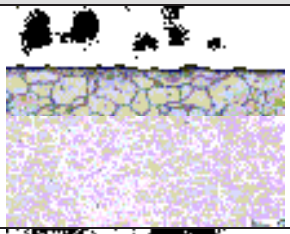	-	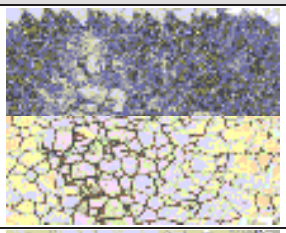	8.2 µm HV_1 = 111
B	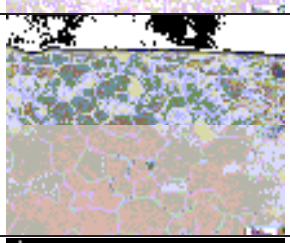	-	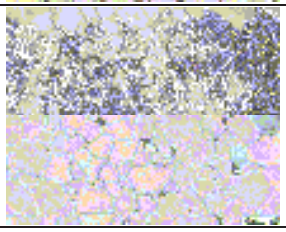	10 µm HV_1 = 127
C	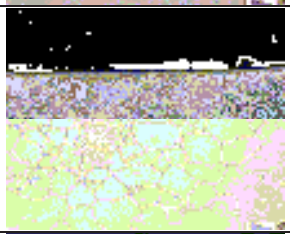	-	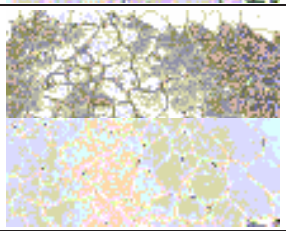	12.9 µm HV_1 = 107
D	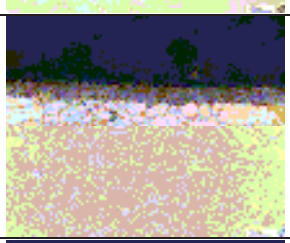	Martensite 10 µm		11.7 µm HV_1 = 130
E	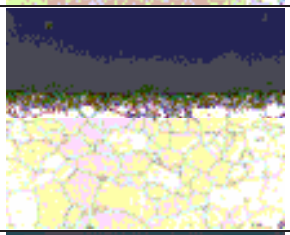	Martensite 6 µm	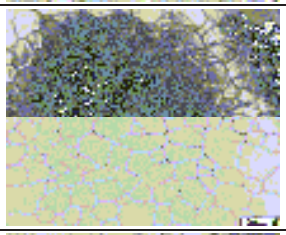	11.9 µm HV_1 = 135
F	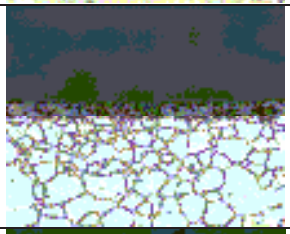	Pearlite 10 µm	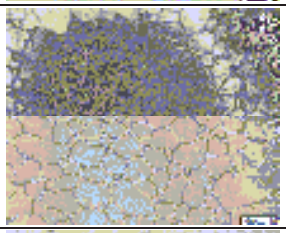	12.1 µm HV_1 = 127
G	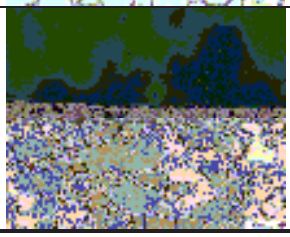	Pearlite 8 µm	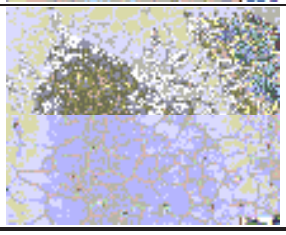	10.9 µm HV_1 = 129

Table 7: Optical microscopy analysis of RHESCA annealed steel sheets

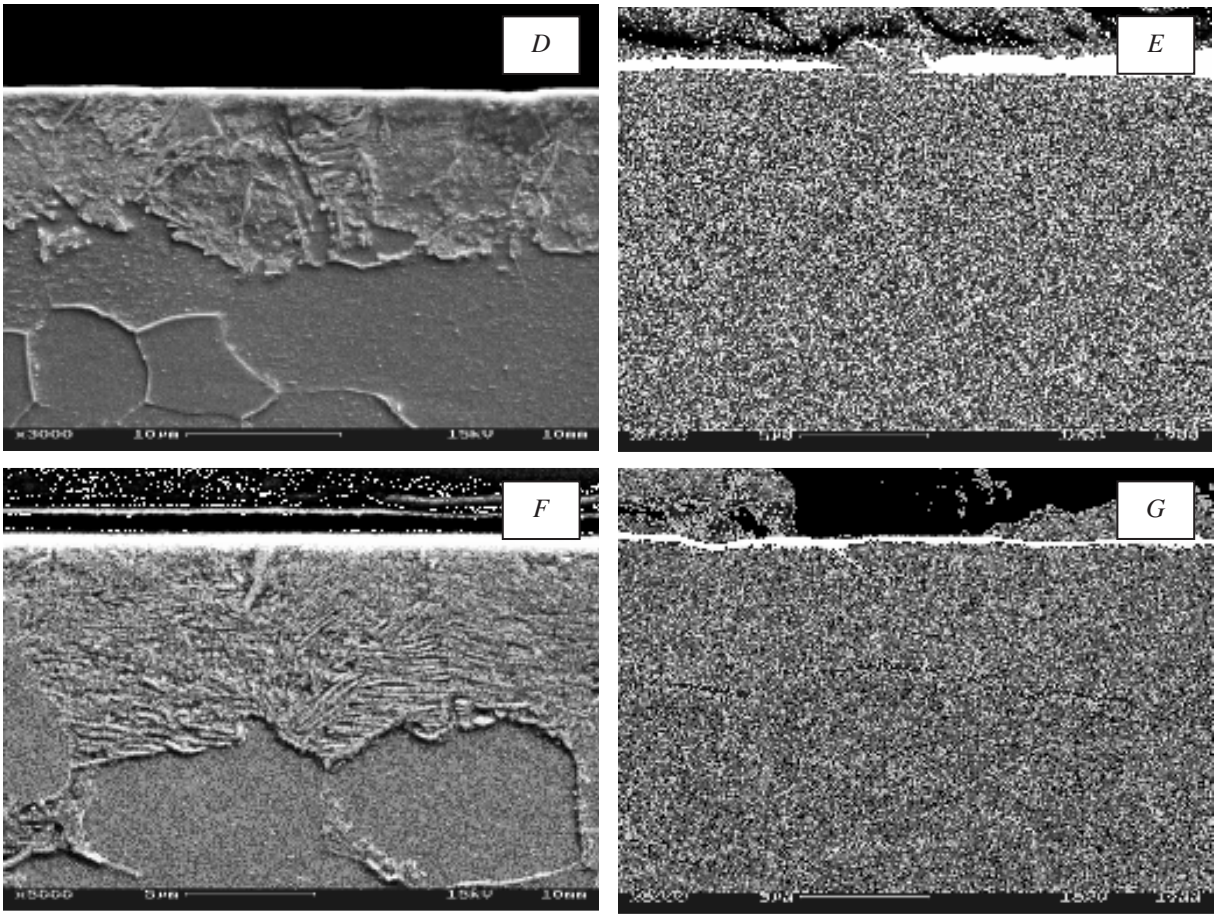

Figure 22 : SEM observations of samples D, E (martensite), F and G (pearlite) for the determination of the nature and thickness of the second phase layer

Sample	Thermal treatment Microstructure	As annealed	Aged
A	Reference with overageing at 400℃	YS : 312 MPa TS : 350 MPa TEl : 31.6 % n : 0.23 YPEl : 5.5 %	YS : 311 MPa TS : 341 MPa TEl : 25.5% n : 0.16 YPEl : 3.7 %
B	Reference with accelerated cooling and without overageing	YS : 357 MPa TS : 408 MPa TEl : 10.8 % n : 0.10 YPEl : 0.9 %	YS : 344 MPa TS : 374 MPa TEl : 7.7 % n : 0.07 YPEl : 0.9 %
C	Reference with low cooling and without overageing	YS : 303 MPa TS : 347 MPa TEl : 31.4 % n : 0.23 YPEl : 6.9 %	YS : 304 MPa TS : 347 MPa TEl :28.2 % n : 0.23 YPEl : 6.2 %
D	Reactive annealing Martensite layer 10 µm	YS : 421 MPa TS : 482 MPa TEl : 12.8 % n : 0.24 YPEl : 4.1 %	YS : 450 MPa TS : 482 MPa TEl : 14.7 % n : 0.18 YPEl : 5.3 %
E	Reactive annealing Martensite layer 6 µm	YS : 424 MPa TS : 484 MPa TEl : 15 % n : 0.20 YPEl : 5.5 %	YS : 442 MPa TS : 462 MPa TEl : 14.4 % n : 0.19 YPEl : 7.7 %
F	Reactive annealing Pearlite layer 10 µm	YS : 341 MPa TS : 397 MPa TEl : 22.9 % n : 0.22 YPEl : 6.3 %	YS : 321 MPa TS : 374 MPa TEl : 25.8 % n : 0.23 YPEl : 7.7 %
G	Reactive annealing Pearlite layer 8 µm	YS : 352 MPa TS : 386 MPa TEl : 24.2 % n : 0.23 YPEl : 7.4 %	YS : 344 MPa TS : 389 MPa TEl : 27.8 % n : 0.22 YPEl : 6.5 %

Table 8: Mechanical properties of RHESCA annealed steel sheets as annealed and aged

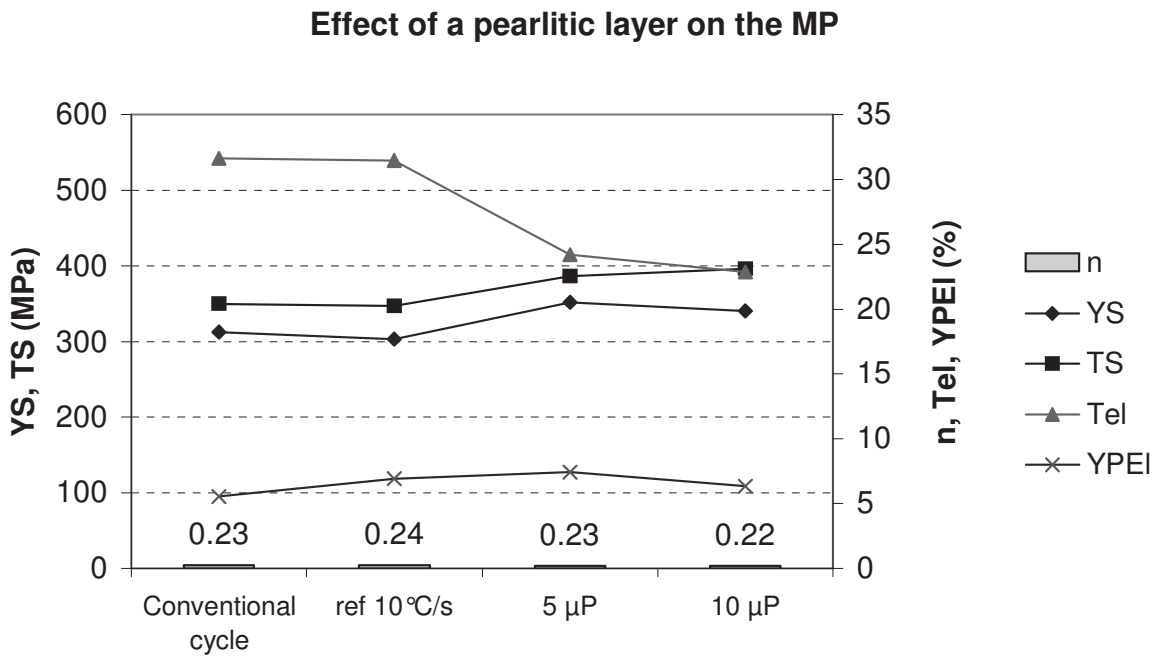

Figure 23 : Effect of a pearlitic layer on the mechanical properties of a ELC steel grade

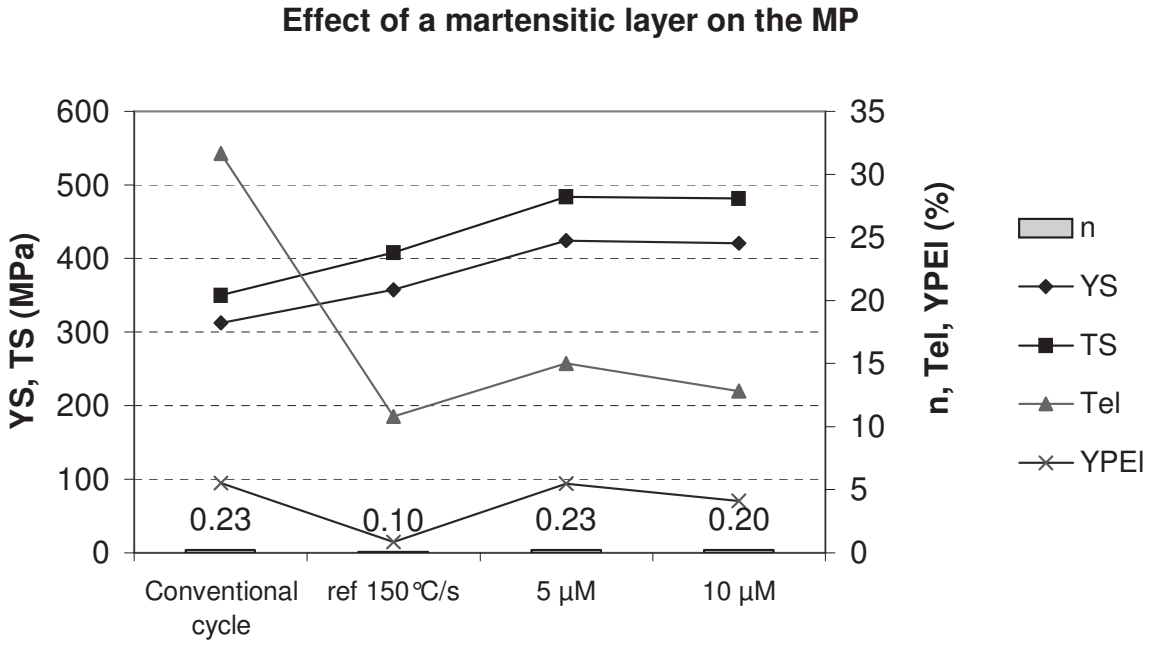

Figure 24 : Effect of a martensitic layer on the mechanical properties of a ELC steel grade

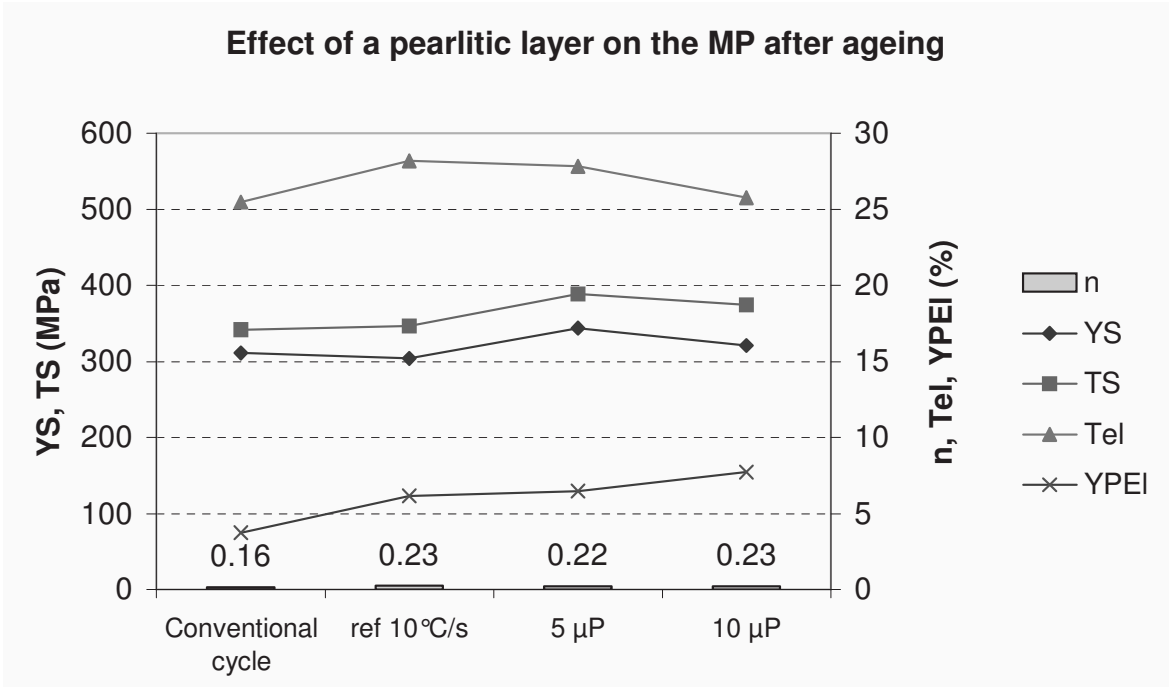

Figure 25 : Effect of a pearlitic layer on the mechanical properties of a ELC steel grade

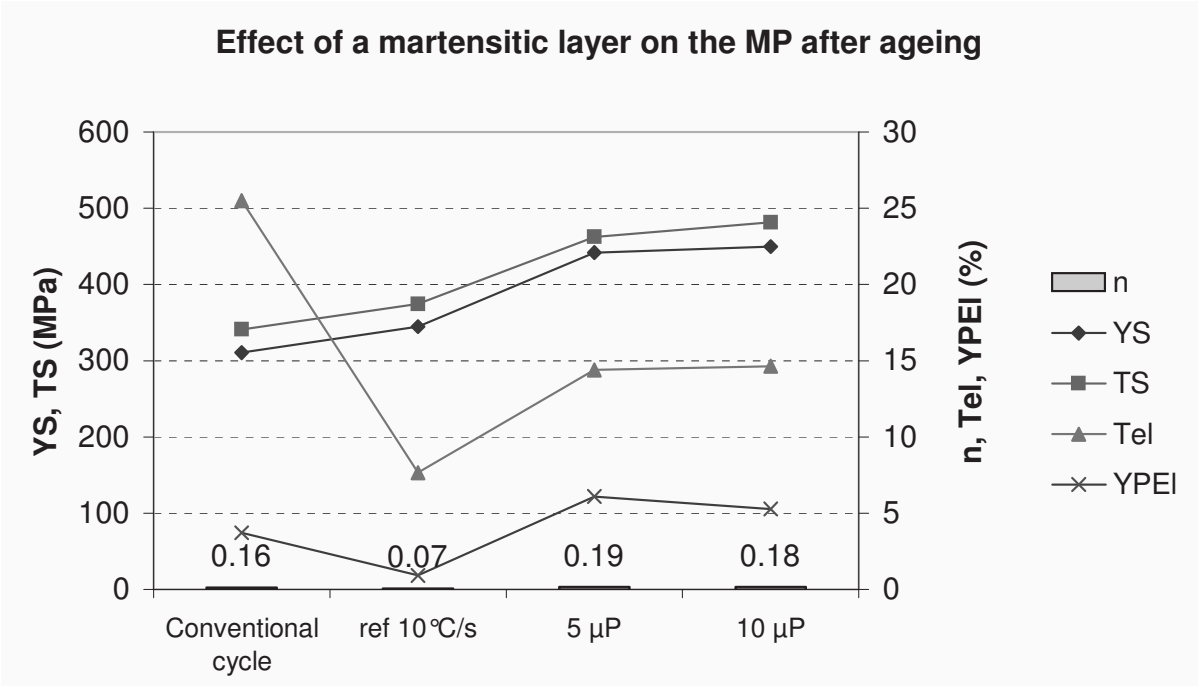

Figure 26 : Effect of a martensitic layer on the mechanical properties of a ELC steel grade

	YS (MPa)	TS (MPa)	TEl (%)	YPEl (%)*
Transverse direction	262	310	46	7
Rolling direction	220	305	46	6
Average (T+R) / 2	240	307	46	6

* The YPEl values are presented with a precision of 1% (due to measurement dispersion)

Table 9 : Mechanical properties of industrial ELC steel used for bending tests

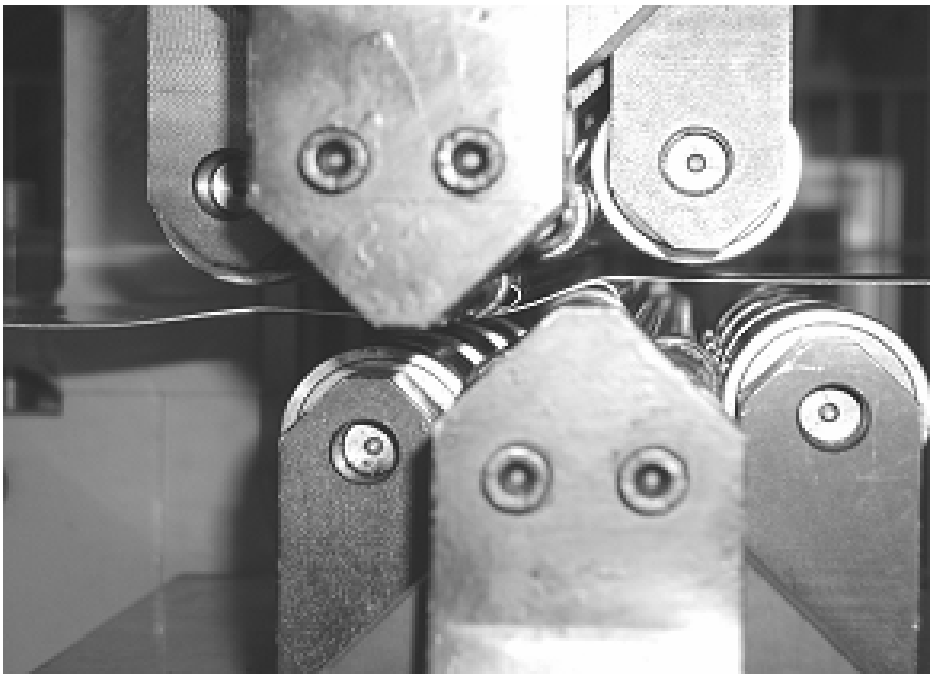

Figure 27 : View of the bending unit during trials

Sample	*intermesh mm*	*v m/min*	*λ %*
1	*8*	*2.6*	*0.90*
2	*8*	*2.6*	*0.60*
3	*8*	*2.6*	*2.30*
5	*4*	*2.6*	*0.80*
6	*4*	*2.6*	*0.40*
7	*4*	*2.6*	*1.10*
8	*8*	*0.6*	*1.00*
9	*8*	*6*	*0.70*

Table 10 : Bending trials matrix

	Speed $m.min^{-1}$	Intermesh mm	λ %	MP*	Surface aspect	nb Lüders bands (30 mm)	Spacing mm
Initial material	-	-	-	YS : 240 TS : 307 YPEl : 6.2 TEl : 46.7	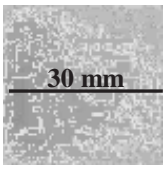	0	-
Sample 1	2.6	8	0.9	YS :215 TS : 308 YPEl : 2.2 TEl : 43.6		18	1.6
Sample 2	2.6	8	0.6	YS : 226 TS : 309 YPEl : 2.8 TEl : 43.8		10	2.7
Sample 3	2.6	8	2.3	YS : 216 TS : 313 YPEl : 0 TEl : 41.3		19	1.5
Sample 5	2.6	4	0.8	YS : 204 TS : 304 YPEl : 2.1 TEl : 43.4		10	2.7

Sample 6	2.6	4	0.4	YS : 210 TS : 306 YPEl : 2.4 TEl : 43.9		8	3.3
Sample 7	2.6	4	1.1	YS : 216 TS : 309 YPEl : 2.5 TEl : 43.2		10	2.7
Sample 8	0.6	8	1	YS : 230 TS : 311 YPEl : 2.7 TEl : 43.3		17	1.7
Sample 9	6	8	0.7	YS : 208 TS : 305 YPEl : 2.4 TEl : 44.1		17	1.7

* Mechanical properties = (MP Rolling direction + MP Transverse direction) / 2

YS, TS (MPa), YPEl, TEl (%)

Table 11 : Results obtained after bending trials (experimental conditions, mechanical properties, surface aspect and spacing of the defects)

SKP	*YS (MPa)*	*TS (MPa)*	*UEl %*	*TEl %*	*YPEl %*
0% SKP	*240*	*305*	*30.0*	*46.0*	*6*
0.5% SKP	*177*	*307*	*26.5*	*43.7*	*0.5*
1% SKP	*167*	*310*	*25.4*	*42.3*	*0*
1.5% SKP	*177*	*310*	*26.5*	*19.5*	*0*
0.5% SKP aged	*172*	*309*	*26.2*	*44.5*	*0.5*
1% SKP aged	*172*	*308*	*27.9*	*43.2*	*0*
1.5%SKP aged	*181*	*312*	*26.5*	*38.5*	*0*

Table 12 : Mechanical properties in function of the skin pass deformation level applied

Tensile test	YS (MPa)	TS (MPa)	UEl %	TEl %	YPEl %
0% strain	240	305	30.0	46.0	6
0.5% strain	231	304	26.8	41.0	6
1% strain	227	304	26.2	41.6	5
1.5% strain	237	305	30.3	39.0	5
2% strain	259	324	22.4	41.2	3.5
0.5% strain aged	240	311	26.3	40.8	5
1% strain aged	235	308	28.1	40.4	6
1.5% strain aged	234	307	29.0	44.0	5
2% strain aged	251	327	19.1	28.2	2.7

Table 13 : Mechanical properties in function of the tensile deformation level

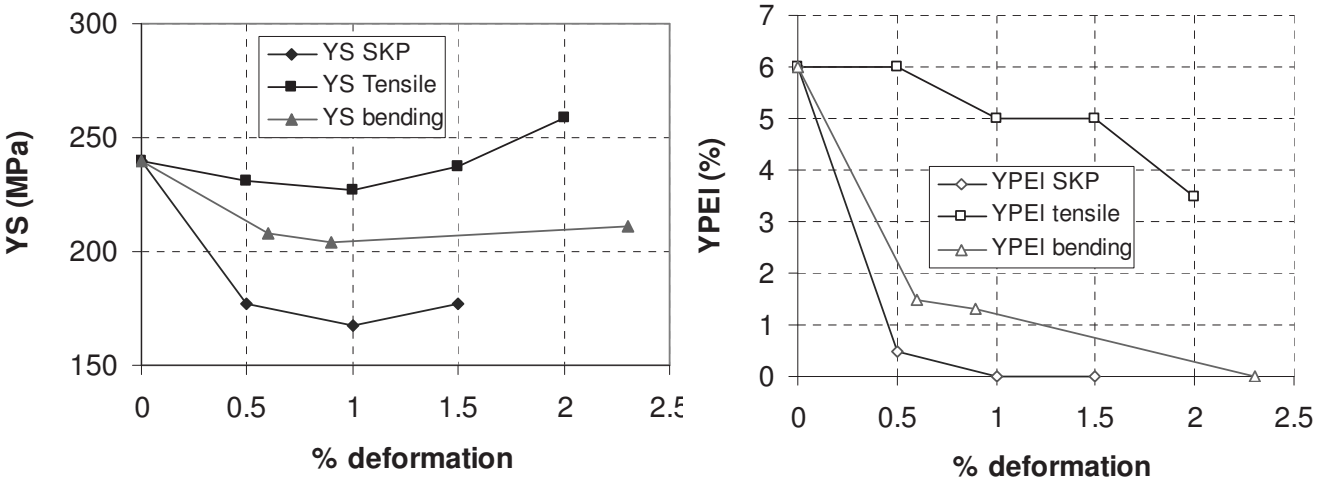

Figure 28 and 29 : Evolution of YS and YPEl in function of the deformation degree applied for the three different deformation modes (tensile, bending, SKP)

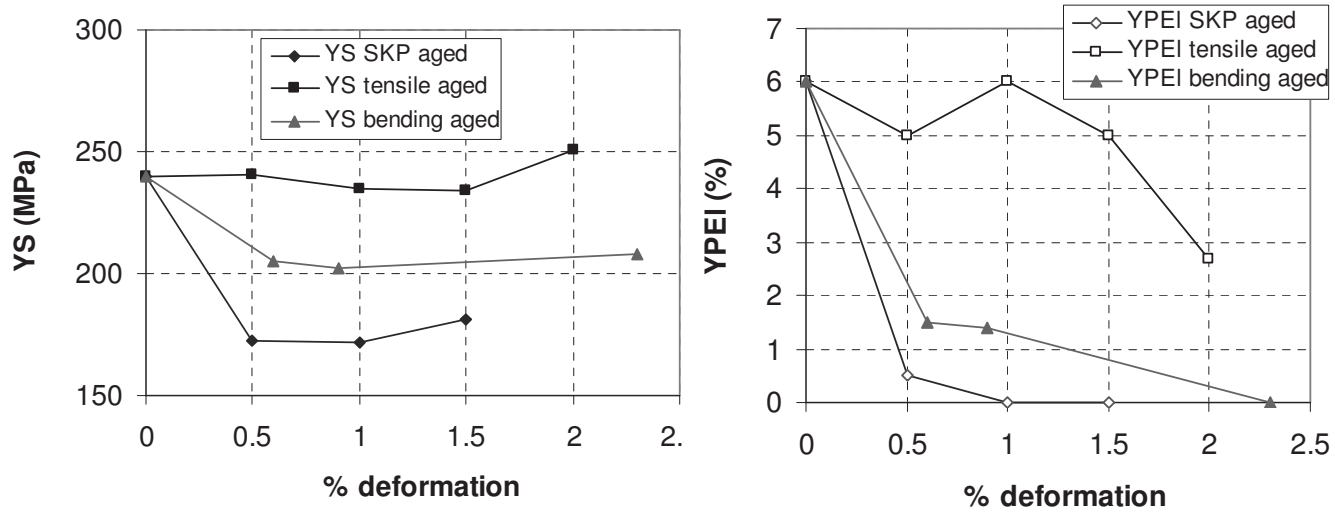

Figure 30 and 31: Evolution of YS and YPEl on the aged material in function of the deformation degree applied for the three different deformation modes (tensile, bending, SKP)

ANNEXES

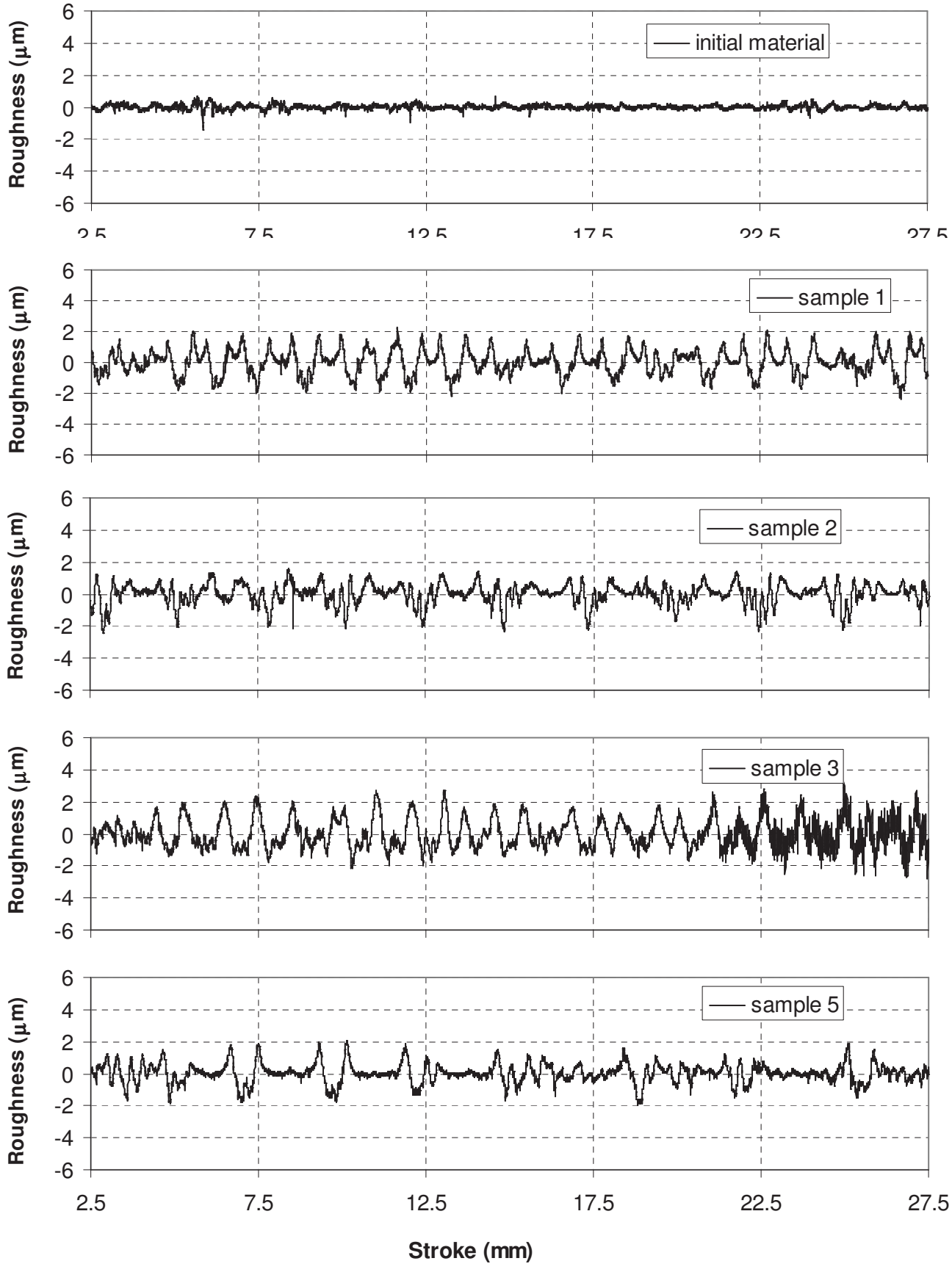

Annexe 1 : Roughness measurements performed on initial material and samples 1, 2, 3 and 5 deformed by bending on the BFI equipment.

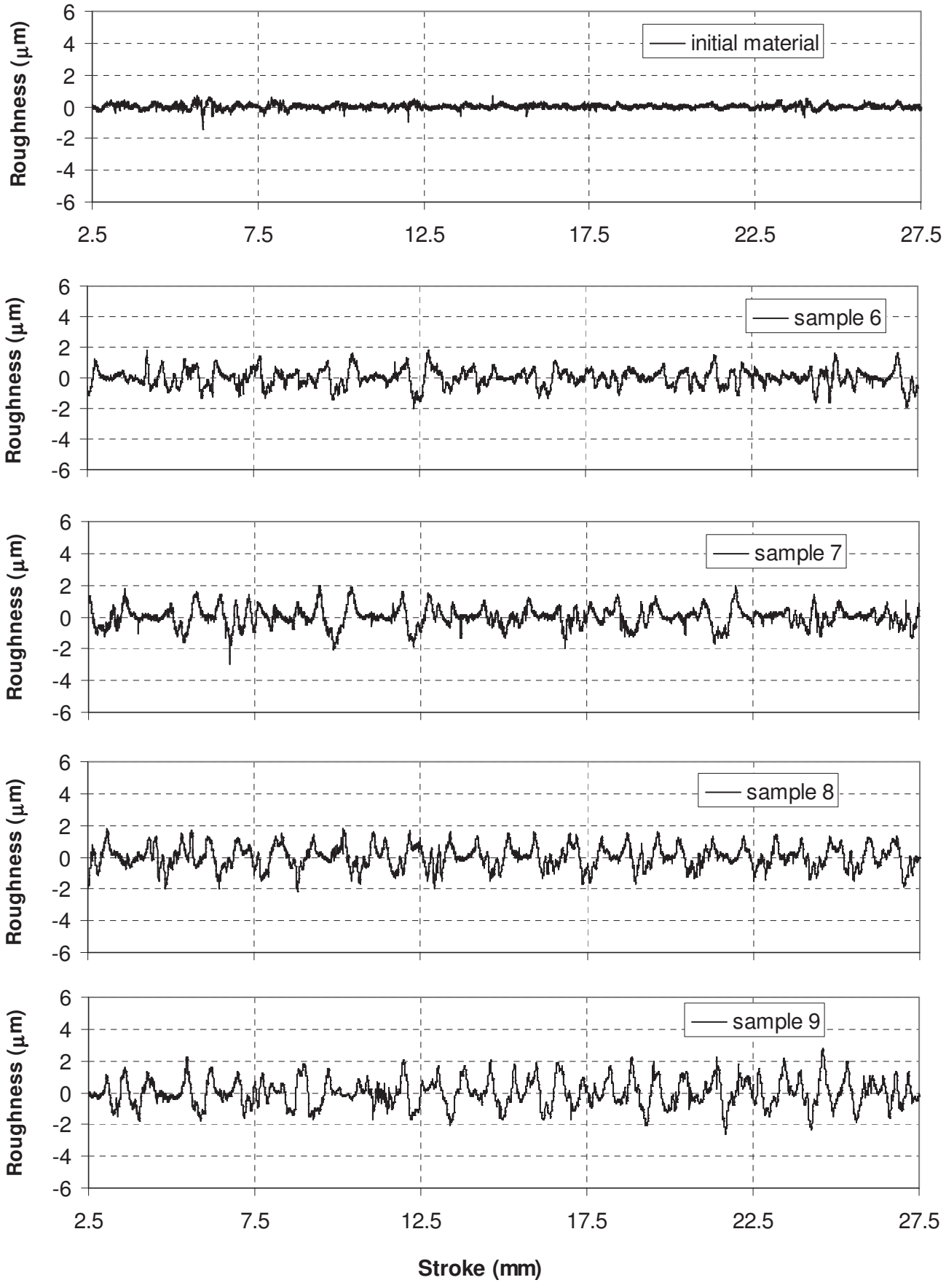

Annexe 2 : Roughness measurements performed on initial material and samples 6, 7, 8 and 9 deformed by bending on the BFI equipment.

Experimental studies : Part 2

List of tables and figures :

1/ INTRODUCTION

Even in the present day of higher strengthened, interstitial-free steels like IF, trip and dual phase steels, which do not suffer from the traditional Lüders lines the temper mill remains a vital part of finishing strip not just to prevent unsightly defects in carbon grade steels. The demands of subsequent processing stages like deep drawing or stretching on the overall product quality of temper rolled cold strips rather require to conduct the temper rolling process in such a way to impact also optimal mechanical properties, superior surface finish or texture as well as proper flatness in both carbon and interstitial free steels.

Carbon grade steels and interstitial free steels differ in their characteristics of stress-strain behaviour and of flow stress respectively. According to their continuous stress-strain characteristics over the whole range of deformation interstitial-free steels demonstrate an increasing work hardening starting from the non-deformed state (values at "0") as shown in **Figure 1**. Carbon grade steels, however, due to their discontinuous stress strain behaviour at low deformation values are characterized by a decrease of yield stress down to a minimum before usual work hardening mechanisms lead to a continuous increase of the yield strength at higher degrees of deformation.

The investigations carried out within the frame of this project are concentrated on carbon steel grades. Consequently two basic strip characteristics, which are influenced by temper rolling had to be taken into account. These are the mechanical strip properties as well as the surface condition in terms of the formation of Lüders bands and their avoidance respectively.

For producing optimal strip conditions concerning further processing, the mechanical strip properties during temper rolling have to be adjusted in such a way that a high deformability is guarantied. The deformability is favored by a high exponent n of strain hardening as well as by a yield stress as low as possible. These parameters would be set most favorably if the optimum temper rolling degree is adjusted. This will be the case if the strip is temper rolled with a deformation degree corresponding to the minimum of the yield stress curve. In terms of achieving a stretcher strains-free surface in subsequent forming stages this nominal value of temper rolling deformation must be selected, which guaranties that Lüders effects no more arise.

The stress-strain characteristics of each steel grade and the hereby derived characteristics of the strain hardening behaviour are the basis for the selection of the optimum degree of deformation in temper rolling, which allows to adjust the optimum mechanical strip properties at simultaneous Lüders-free strip quality. Using the example of a carbon steel grade, **Figure 2** illustrates schematically the correlation between yield strength and degree of temper rolling (temper rolling curve) resulting from stress-strain curvatures, which relate to different degrees of temper rolling deformation. The course of flow stress is characterized by a minimum, which simultaneously corresponds to a deformation ϕ_{opt}, that for the first time leads to an elimination of the yield point elongation indicated as YPEL in the stress-strain curves. This condition of temper rolling deformation is even said to suppress the Lüders mechanisms being responsible for stretcher marks on processed strips.

Consequently the demand for high deformability as well as for a proper strip surface condition in case of strip further processing requires degrees of deformation to be set in temper rolling corresponding to the minimum of the yield stress curve. Pass reductions below this optimum skin-pass degree ϕ_{opt} should absolutely be avoided (under-temper-rolled) to eliminate the appearance of Lüders lines in subsequent processing stages. So, light over-skin-passing, connected with a small increase of the yield stress and a small reduction of uniformity of elongation, will be tolerated.

2/ OBJECTIVES

In temper rolling plants the strip is not only subjected to rolling deformations in the roll gap. Additionally bending deformations are introduced into the skin passed strip by passing rolls and roll

systems like deflection rolls, anti-sticking rolls and coilers, which are integrated into the flow of strip inside the mill. In combination with the strip tension these bending deformations can extend the yield strength of the temper rolled material and thus lead to plastic deformations of the strip. Prior trials **(1)** on an industrial temper rolling mill equipped with an anti-sticking roll had shown that plastic bending deformations has proved to accept values up to 30% of the target value of the skin pass degree.

When setting the temper rolling degree and thus the resulting mechanical strip properties, these plastic bending deformations have not been taken into account during industrial rolling so far. In the scope of this project the question has to be clarified if a total degree of deformation, consisting of roll bite and bending deformation, has to be defined for adjusting the most favorable mechanical strip parameters. This question, however, cannot be answered without including the effect of bending deformations upon the generation or non-generation of Lüders defects on carbon steel strips. Consequently the investigation of the influence of bending deformations has to be concentrated upon the parameters

- Stress-strain behaviour
- Yielding behaviour
- Strain hardening behaviour and
- Lüders behaviour.

In accordance with the process of temper rolling the effect of bending deformations *with applied strip tension* upon the above mentioned properties is determined and compared to conditions obtained by temper rolling. A combination of both deformation modes is investigated using two successive deformation steps beginning with the bending mode, which is afterwards joined by temper rolling steps on an industrial temper rolling mill.

3/ DESCRIPTION OF WORK

The practical investigations were carried on low carbon, batch annealed steel strips presenting different thicknesses and a standard width of 300mm. The bending deformations had been introduced into the strips using a tension bridle with bending unit, which is operating as a laboratory levelling device at industrial scale. An industrial four high temper rolling mill for narrow strips was available for the execution of temper rolling trials. Tensile testing for the determination of the mechanical strip characteristics was executed by the department of material testing of the MPI, Düsseldorf.

3.1 Laboratory tools available

A tension bridle with a bending unit is available at the test laboratory of BFI. **Figure 3** gives a schematic overview of the laboratory plant. The bending-straightening unit is located between the entry and exit sides of the S-roller pairs, within which the pre-adjusted strip tensions are built-up respectively reduced. Measuring rolls are provided at the entry and exit sides of the bending device to determine the strip tensions respectively the shape of the strip.

The degree of deformation obtained by bending is determined by measuring the velocity difference before and after the bending process. For this purpose, high-resolution incremental transducers are provided on the drive shafts of the S-roller pairs at the entry and exit sides. In this way, elongation measurement covers also those bending deformations that are introduced in the strip, throughout the complete tension bridle, namely along the tension rolls, as well as of the strip tension measuring roll installed in front of the bending unit, and the shape meter roll in the excit part of the bending unit.

This illustration also shows a summary of characteristic system features. The plant data make clear that the essential geometrical proportion of this tension leveller is similar to industrial plants.

Figure 4 is an overview of the plant with the bending unit, by which the different bending deformations are introduced into the strips.

3.2 Investigations

The practical investigations for the determination of the effect of the deformation modes bending, temper rolling as well as a superposition of both modes on the strip characteristics has been separated into two basic series. Test series I was focused on the analysis of bending effects on the material strip properties including strip surface formation in terms of Lüders bands. An overall study regarding the bending mode, the temper rolling mode as well as a combination of these types of deformation was subject of the test series II.

3.2.1 General proceeding

For the execution of the test series a common general proceeding was selected. All strips investigated were available as coils with a diameter of about 950mm, corresponding to a strip length between 750m and 1200m according to the actual strip thickness.

The strip was deformed on the above-described S-roller bridle with bending unit at an average longitudinal strip tension on a level of 30% of the initial material yield strength corresponding to the batch annealed non-deformed state. Bending rolls were used with a diameter of 21 mm. The diameter of the correction roll was 40 mm.

In addition to the measurement of the bending deformation by use of incremental transducers a reference measurement of the plastic strip elongation was carried out. For this purpose two marks were scratched in the strip surface with a distance of 1m. The strip elongation throughout the entire bending plant is resulting by a comparison of the distances measured close to the un-coiler and in front of the coiler.

Starting from a deformation degree of about 0.2%, the deformation levels for different strip segments were incremented in small steps up to a total value of about 6.5 %.

For each reduction increment pre-set in the bending trials, strip segments were cut off at the strip positions. Four test specimens each were cut across the strip width from these strip segments, which were subjected to tensile testing for the determination of the mechanical properties.

3.2.2 Test Series I; Influence of bending deformations on the strip characteristics

Test series I included three strips composed out of low carbon deep drawing quality (LC-DDQ), present in a batch annealed condition.

The special initial strip characteristics used in each series are demonstrated in **Table 1**.

The strip was deformed on the S-roller bridle with bending unit according to the description given in chapter 3.2.1 (General proceeding).

3.2.2.1 Results obtained: Yield stress, strain hardening and yield point elongation

The results delivered by the tensile tests of the samples are demonstrated in the **Figures 5÷8**. The initial stress-strain characteristics of the strips examined are displayed in **Figure 5**, starting with strip thickness 0,5mm up to 0,8mm. All three graphs show the typical stress strain behaviour of LC-steels in the non-deformed state, demonstrating a distinctive yield point elongation.

Figure 6 presents the yielding behaviour of the three investigated strips in dependence of the plastic bending deformation adjusted. Independent from the strip thicknesses examined, all strips illustrate a similar flow behaviour compared to the well-known curvatures determined temper rolling deformation.

Starting from a yield strength maximum of the non deformed strip the typical drop in the course of the yield stress take place down to a minimum, which corresponds to deformation degrees of approximately 1,3 %. This decrease in yield strength is due to the fact that at the beginning of plasticity the deformation progresses according the Lüders mechanism. The Lüders behaviour is the result of firstly an increase in yield stress due to the pinning of dislocations and secondly a softening attributed to dislocation unpinning or multiplication. For degrees of deformations above this minimum, usual strain hardening mechanisms contribute to an increase of yield strength.

Figure 7 illustrates the course of the strain hardening exponent n in dependence from the degree of deformation that was set by bending. The decrease over the deformation range investigated shows according the diagrams for all strip thicknesses examined the same behaviour compared to temper rolled strips.

As illustrated in **Figure 8** the evaluation of the stress strain diagrams demonstrates a decrease of the yield point elongation YPEL if the degree of bending deformation increases. At a deformation range between 1,3% and 2% a complete suppression of the YPEL can be observed.
A direct dependence of the mechanical strip characteristics yield stress, n-value and yield point elongation from the strip thickness cannot be derived. However, when regarding the bending process, there is a relationship between thickness and degree of deformation resulting from the bending geometry: On the condition of the same bending geometry, which describes the contact arc between strip and bending roll, the deformation achieved is as higher as the strip thickness is selected.

3.2.2.2 Results obtained: Lüders deformation effects

In contrast to temper rolling, as revealed by a strip surface inspection, a suppression of the YPEL, however, does not prevent the generation of Lüders bands.

For the evaluation of the strip surface, degraded by the generation of Lüders bands, strip surface profiles were measured using strip sections, which had been bended at different degrees of deformation.

The measurements (2D and 3D respectively) of the sheet were carried out using a stationary laboratory instrument with an air-suspended coordinate measuring table (UBM Co.) **(Figure 9).** This system covers a 150 x 150 mm surface area and can be combined with various sensors (mechanical, laser-optical). In the present context a mechanical sensor was used under the following conditions.

- Mechanical stylus; stylus tip radius = 5µm
- Measured area 10 x 10 mm^2
- Resolution 100 points/mm (both measuring directions).

Evaluation was done without filtering. The measurement area was aligned in both directions with a polynome of the 4th order.

The results of the strip-surface-profile-measurements are illustrated in the **Figures 10÷13**. Diagrams a) illustrate an image of the surface on the base of toning down, representing a measuring area of 10x10 mm^2. Diagrams b) demonstrate the course of the measured height distribution for one selected detected track. Additionally diagrams c) show the corresponding stress-strain curves. Each figure relates to a different degree of deformation, starting with a non deformed strip section in **Figure 10** up to a deformation level of 2.9% shown in **Figure 13**.

Starting from the non deformed strip (**Figure 10a,b**), which shows, as expected, a stochastic patterned strip surface, the condition of the strip surface is more and more affected by Lüders deformations if the

degree of bending deformation increases. Whereas the generation of Lüders deformations in the beginning corresponds to a rather stochastic pattern (**Figure 11a**) an oriented extension from local deformations to Lüders bands can be observed according to the **Figures 12a, 13a**. Simultaneously this effect is attended by a degradation of the macro structure of the strip surface, which leads to considerable deviations of the strip surface structure up to 9µm according to the diagrams c) of the **Figures 12 and 13**.

The generation of Lüders deformations cannot be avoided in the range of bending deformations investigated. The suppression of the yield point elongation according to the stress-strain-curves, which had been determined on bended strips [see diagrams c) in **Figures 12-13**], does not, in contrast to the temper rolling mode, indicate Lüders-free strip surface conditions.

3.2.2.3 Consequences

With regard to further processing stages after temper rolling the most favourable strip conditions are then established when the optimum degree of temper rolling, that corresponds to the minimum of the yield strength curve is set in the skin passing process. If plastic bending deformations, which are introduced by rolls (e.g. anti sticking roll) are not taken into account, the strip will be „over temper rolled“ attended by a loss of deformability. This situation is illustrated in **Figure 14a**.
The optimum deformation degree is exceeded by an amount corresponding to the value of bending deformation ϕ_b. Consequently from this effect it must be derived that the temper rolling degree adjusted in the roll gap must be reduced by the bending rate, thus leading to a total degree of deformation ϕ_{total}, which corresponds to the optimum deformation degree ϕ_{opt} (**Figure 14b**).

These corrective measures, however, are only permitted if in addition to the request for an optimum deformability another demand will be accomplished: This is the elimination of the Lüders effect. In the case of pure bending deformation the avoidance of Lüders bands could not be observed in contrast to temper rolling operations leading to a Lüders-free strip if degrees of deformations are selected which correspond to such values that also lead to a suppression of the YPEL..

In consequence one more test series combining both temper rolling and bending deformations should deliver information exactly about the question: To what degree a reduction of the temper rolling deformation is possible in favor of the bending deformation without generation of Lüders bands.

3.2.3 Test Series II: Influence of bending, temper rolling and the combination of both modes on the strip characteristics

In accordance with operating conditions in skin pass rolling practical trials had been carried out from the viewpoint of a combination of the two deformation modes bending and temper rolling. For the assessment of the influence of a combined deformation upon the mechanical strip properties including the Lüders effect, the mechanical strip characteristics resulting separately for each of the two modes should serve as reference status. Thus, starting from a batch annealed coil, three basic test series had been performed. Series II.1 includes the mere bending mode, Series II.2 the merely temper rolling mode whereas the final series II.3 has been concerned with the superimposition of bending and temper rolling.

The trial planning intended that, starting with the bending mode, different segments of a coiled strip should be subjected step by step to various bending deformations. Starting with a deformation of 0,2% the deformation degree was stepwise enlarged in steps of 0,3% up to 5%. This operation was repeated in such a way that the same pattern of deformation was impressed four times to the coil investigated. An overview of the completely selected deforming conditions delivers **Figure 15**. The strip head end including strip section A was not coiled anymore but cut off from the entire strip using the different deformed strip segments (0,2%-5%) for tensile testing. The resulting strip characteristics are representing the reference state for the deformation mode “bending”.

The remaining three coiled strip sections B to D, each including the same sequence of bending deformation from 0,2% to 5% were provided for temper rolling as superimposed deformation stage.

For the sake of creating the reference status for the temper rolling mode the non-deformed strip section E (strip head end of the coiled strip) had been only temper rolled in different deformation steps, starting from 0,3% up to 1,5% in steps of 0,2%.

Starting with the targeted optimum temper rolling degree □□□□ for section B two lower skin pass degrees for the remaining sections C and D were selected, that is □$_{opt}$ minus 0,1% and □$_{opt}$ minus 0,3%.

According to previous investigations as steel grade a low carbon quality was selected, present in batch annealed condition. For the execution of the trials one coil had been divided into two coils, each with a diameter of about 900mm. The initial strip characteristics of the investigated coils and the deformation mode applied are outlined in **table 2**. According to the information given by the strip producer the optimum temper rolling degree is 0,6% in case of industrial temper rolling.

3.2.3.1 Results obtained: Yield stress, strain hardening and yield point elongation

Figure 16 presents the stress-strain graph referring to the initial state (batch annealed, non-deformed) of the strip processed according the specifications for Series II. Both the initial yield strength and the initial yield point elongation are lower compared to the strips used in Series I.

The material characteristics yield stress, n-value and YPEL are illustrated in **Figure 17**, describing the strip behaviour in the case of bending mode and that for deformations in the range of 0% up to 5%. In **Figure 18** these graphs are compared to the results obtained if the initial batch annealed strip is temper rolled. Higher deformation values than 1.8%, although adjusted in the bending trials, are left of in this graphs, as in the case of temper rolling the deformation range was limited to 1,5%. The course of the material characteristics versus the degree of deformation are pointing out that, independent from the deformation mode, yield stress, n-value and yield point elongation not only show the same behaviour but rather lead to almost same values, which cover a range of dispersion conditional on material non conformances and test conditions. According to the suppression of the yield point elongation at a deformation of approximately 0,4% (see YPEL-graph) a yield stress minimum in the upper diagram is indicated for both deformation modes.

Figure 19 illustrates the investigation results in the case of a superimposition of bending and temper rolling deformation. As reference status each diagram includes the curve resulting from merely temper rolling. The upper diagram refers to the yield stress, the lower one to the n-value. Each diagram demonstrates three curves referring to the combination of the deformation modes bending and temper rolling. Each of these curves refer to different values of temper rolling deformation which had been adjusted in the trials, these are 0,3%, 0,5% and 0,6%. Consequently for each point of the diagram the corresponding value of bending deformation results from the difference between the deformation laid off as abscissa and the indicated degree of temper rolling. In the case of the combined deformation mode there are no measuring points existing for deformations smaller than 0,4% due to the selected deformation offsets at the additional temper rolling steps (0,3%, 0,5% and 0,6%). In consequence the yield stress curves describing the superimposed deforming mode are commencing beyond the expected yield stress minimum, that means at deformation values below of which the yield point elongation had already been suppressed. Therefore even a YPEL-diagram makes no sense in the case of the superimposed deformation mode.

From both diagrams presented in **Figure 19** it can be derived that the superimposed deformation mode bending and temper rolling affects the material characteristics yield stress and yield point elongation rather similarly compared to merely temper rolling. All determined values of e.g. yield stress are within a range of dispersion of less than absolutely 10MPa.

3.2.3.2 Results obtained: Lüders deformation effects

Figures 20 to 23 are illustrating roughness measurements of selected states of deformation in terms of the evaluation of the strip surface condition. 2D and 3D measurements had been carried out according to the description in chapter 3.2.2.2. Compared to former measurements the resolution was enlarged from 100P/mm up to 500P/mm in the 2D-graphs. The figures are composed in such a way, that, starting with the initial (batch annealed, non-deformed) strip the roughness distribution for one selected track is demonstrated for a specific deformation state. The measuring directing is rectangular to the strip processing direction. The roughness illustrations are completed with the equivalent stress-strain graphs.

According **Figure 21** the 3D-illustration of the initial, batch annealed strip is demonstrating a basic pattern with a line shape oriented according cold rolling direction prior to batch annealing. The corresponding 2D-record as one selected track in the upper graph of **Figure 20** shows a roughness within a range of ±8µm. if these patterns are measured translatory to their extension.

Using the example of the 3D-illustration (second image of Figure 21) representing a bending deformation of 0,31% the existence of Lüders lines are verified. These flow lines are proceeding transverse to the bending direction. The basic pattern (line shape oriented according to the rolling direction) demonstrating the initial non-deformed state after annealing is still visible as background structure. The corresponding 2D roughness measurement (Figure 20) presents a surface structure with a preferred wavelength of approximately 1mm. The density of this frequency pattern is extending if the deformation proceeds from 0,31% to 0,54% as shown in the last roughness graph.

A suppression of the yield point elongation according the stress strain diagram referring to a bending deformation of 0,54% is, in case of bending deformation, no indicator for a Lüders-free strip surface.

The results of the strip surface examination for the temper rolling mode are summarized in **Figure 22**, starting with a deformation degree of 0,3% and succeeded by a temper rolling degree of 0,5%. Both roughness measurements exhibit, as from eye inspection expected, no preferred wavelength indicating Lüders patterns. The structure belongs to the basic pattern demonstrating a line shape according to the rolling direction.

Figure 23 illustrates the surface conditions if the strip is deformed by a combination of first, bending deformation and secondly, temper rolling deformation. Both surface measurements show a stochastic roughness pattern with no type of wavelength for the indication of Lüders structures. This applies for a bending pre-deformation of 0,15% as well for 0,29%. Compared to a merely bending deformation generating Lüders patterns according Figure 20 it follows from this, that already existing Lüders patterns can be levelled off by subsequent temper rolling. In this demonstrated case the summarized degree of deformation did not exceed the targeted optimum temper rolling degree, which was certified to be 0,6% in case of industrial temper rolling.

4/ DISCUSSION AND EVALUATION

During temper rolling in addition to the deformation inside the roll bite bending deformations are affected when the strip is passing rolls like anti sticking rolls or deflecting rolls. In turn these bending deformations influence as well the mechanical strip properties as, in the case of low carbon steel grades, the generation of Lüders effects. As described, the influence of bending deformations was determined by the investigation of the merely bending mode and the superimposition of bending and temper rolling in comparison to the merely temper rolling mode.

The results obtained clearly demonstrate that the mechanical strip characteristics yield stress, n-value and yield point elongation are influenced in the same way. For all three deformation modes investigated the typical drop in yield stress (in case of LC-steels) down to a minimum and the subsequent increase by usual hardening has been verified as well as the continuous decrease on the n-

value with increasing degree of deformation. The same applies for the steady progress in the suppression of YPEL by growing degrees of deformation. Moreover, for each deformation mode investigated, the three material characteristics accept values covering a small range of dispersion, which can be attributed to material non-conformances and test conditions.

A completely different behaviour between bending and temper rolling can be observed in terms of generation of Lüders effects becoming visible as flow figures on the strip surface. In case of temper rolling the compression state introduced into the rolled strip by the upper and lower work roll prevents the rolled material from the extension of Lüders lines; they are not becoming visible nor detectable by use of the roughness measurements carried out. In consequence, if the Lüders plateau is once suppressed, as indicated by the suppression of yield point elongation in tensile testing, the material has become “Lüders-resistant” for all kinds of subsequent deformation modes.

In contrast to the compression state in temper rolling the origination and expansion of Lüders bands is not prevented but rather favoured by the “free” strip surface in strip bending processes. The generation of flow figures could already be observed at very small degrees of bending. The suppression of yield point elongation, verified in tensile tests both for the temper rolling mode and bending mode, obviously disables the foundation of more Lüders bands if the degree of bending deformation increases. Nevertheless, the once originated Lüders lines keep visible during bending procedures at higher deformation levels; their appearance anyway changes, indicated by smaller wavelengths in the detected roughness structure of the strip surface.

The investigations concerning the combination of the two deformation modes in terms of bending and additional temper rolling demonstrates, that Lüders structures generated in the preceding bending deformation step can be levelled by subsequent temper rolling accepting a surface structure similar to the initial batch annealed, non-deformed strip surface (see Fig. 23). It must be pointed out, that this effect is achieved e.g. by adjusting a degree of temper rolling of 0.3%, which is only half as high as the recommended temper rolling degree of 0,6% in case of industrial rolling. Using the example of 0,29% bending deformation and an additional degree of temper rolling of 0,3% as summed up deformation, it must be emphasized that the total deformation adjusted did not exceed the degree of temper rolling, which should be aimed at in industrial temper rolling.

Taking into account the request for temper rolling Lüders-free and Lüders-resistant strips for subsequent processing stages the investigations in view of a combination of bending and temper rolling result, that a reduction of the temper rolling degree in favor of participating bending deformations is possible in certain ranges. A total degree of deformation, summed up as degree of bending plus degree of temper rolling is, however, not allowed to fall below the value that corresponds to the suppression of the yield point elongation. By applying these corrective measures the operating point in temper rolling is close to the minimum of the yield stress curve, which simultaneously guaranties a high deformability for further processing.

5/ CONCLUSIONS

Plastic bending deformations which occur during temper rolling when the strip passes rolls are influencing the mechanical strip properties yield stress, hardening exponent n and yield point elongation in the same manner like temper rolling itself.

These bending deformations, which can accept values up to 30% of the target value of the skin pass degree should be compensated by a reduction of the degree of temper rolling to avoid a lack of deformability in further processing (deep drawing, stretching…). This recommendation is generally applicable to steel grades demonstrating a continuous stress-strain-behaviour (Lüders-free). Particular aspects in terms of limitations concerning roughness transfer and strip shape correction are to be considered.

In case of temper rolling LC steels with upper and lower yield strength the Lüders phenomenon additionally has to be taken into account by all means. Even though bending deformations suppress the yield point elongation, they are not able to avoid the formations of Lüders related flow figures at lower degrees of deformation. In contrast to the compression-based temper rolling mode, the free-surface-deformation of the bending mode cannot resist the generation of Lüders bands. They keep visible during bending procedures at higher deformations.

However, Lüders structures generated by bending deformations can be leveled by subsequent temper rolling. A reduction of the temper rolling degree in favor of inevitable bending deformations has been proved to be possible when temper rolling Lüders-sensitive LC-steel grades. The summed up total deformation consisting of bending and temper rolling deformation should not remain below that degree of deformation, which is required for suppressing YPEL.

6/ LIST OF REFERENCES

1 D. Pütz, P.-D.; Neuschütz, E.; Scherer M. ; “Investigations of Procedures for Optimizing Skin Pass Rolling” Final Report, ECSC RTD Project – 7210.EA 143/144, Dec. 1998

Strip characteristics	Series I.1	Series I.2	Series I.3
Strip thickness [mm]	0,5	0,6	0,8
Strip width [mm]	300	300	300
Initial yield strength [MPa]	301	261	284
Initial YPEL [%]	9,3	5,4	7,6
Deformation mode	bending	bending	bending

Table 1: Initial strip characteristics and applied deformation mode

Strip characteristics	Series II.1	Series II.2	Series II.3
Strip thickness [mm]	0,5	0,5	0,5
Strip width [mm]	300	300	300
Initial yield strength [MPa]	228	228	228
Initial YPEL [%]	4,7	4,7	4,7
Deformation mode	bending	temper rolling (dry, polished rolls)	bending + temper rolling (dry, polished rolls)

Table 2: Initial strip characteristics and applied deformation modes

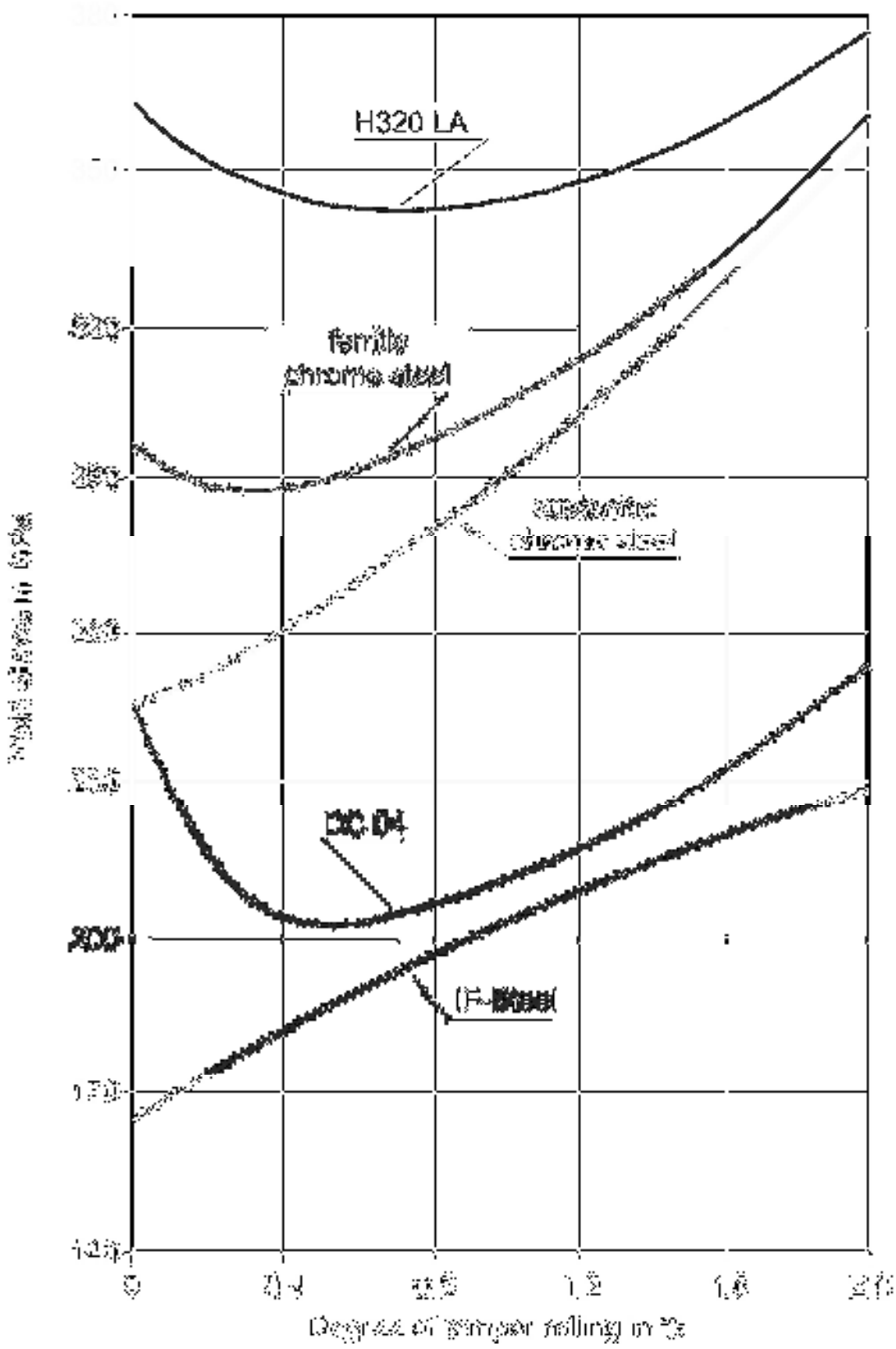

Figure 1: Basic characteristics of flow stress of different steel grades

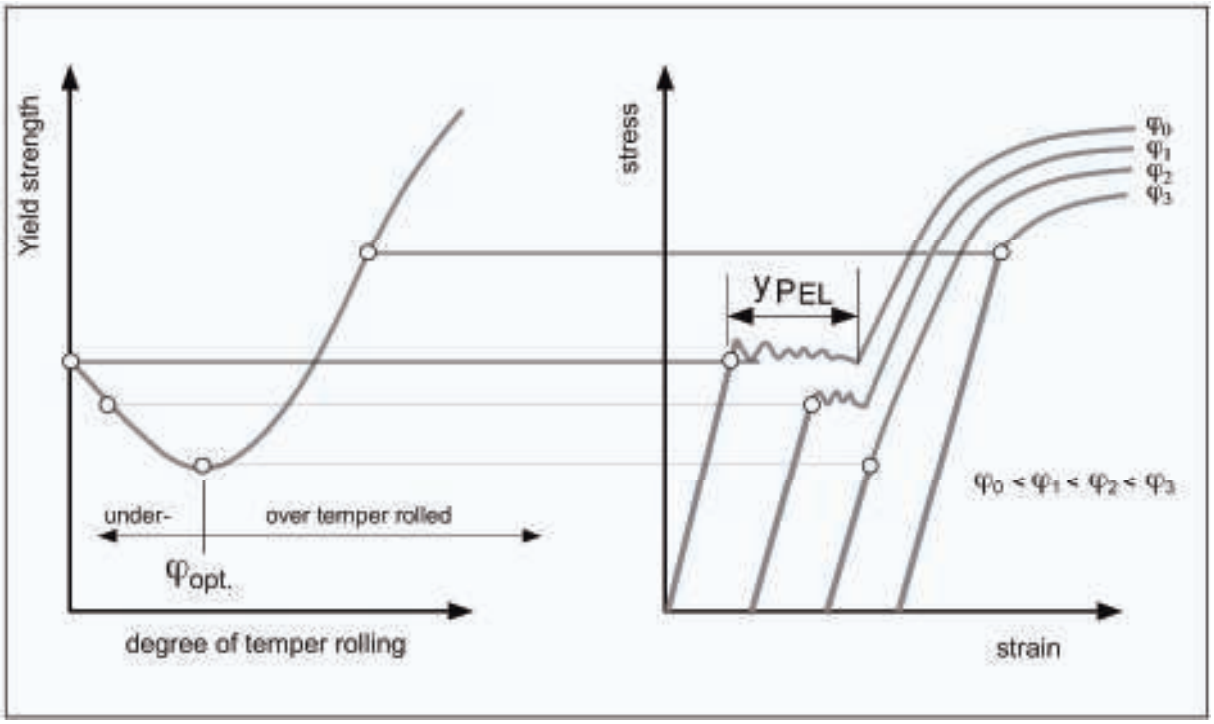

Figure 2: Influence of the temper rolling degree on stress-strain and yielding behaviour of carbon grade steels

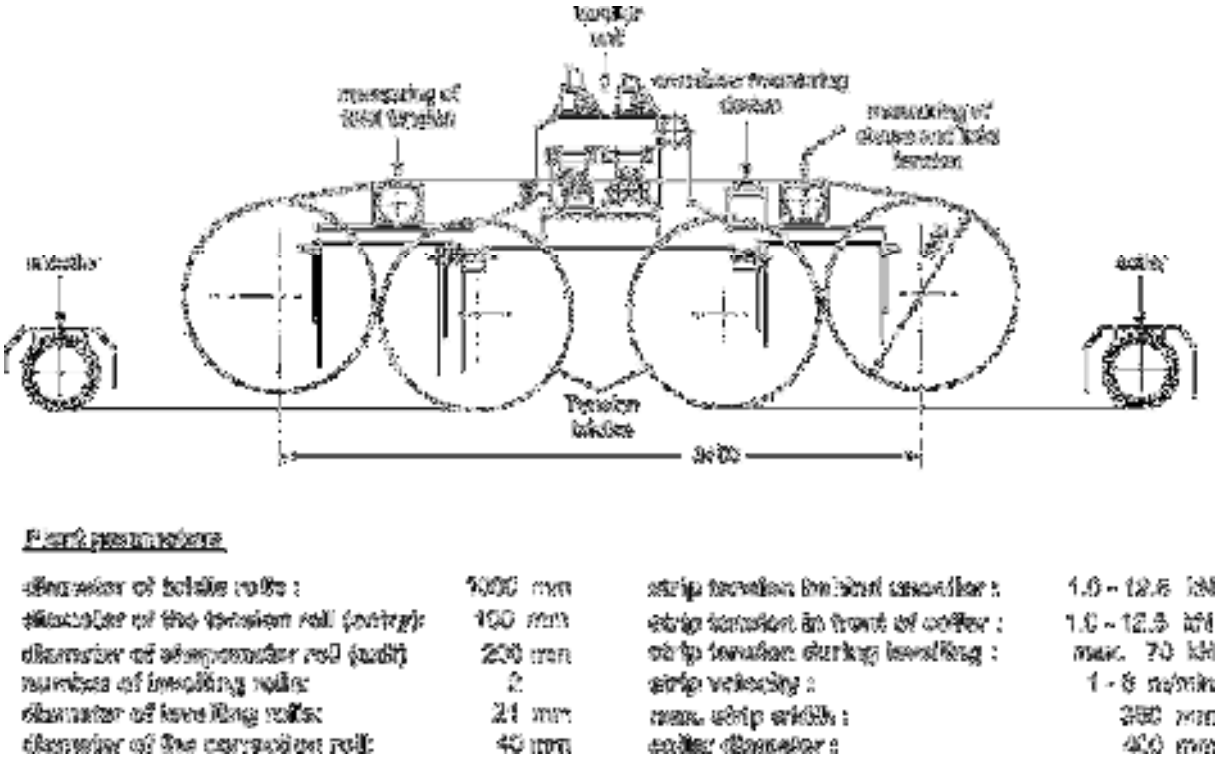

Figure 3: Schematic view of tension roller plant with bending unit

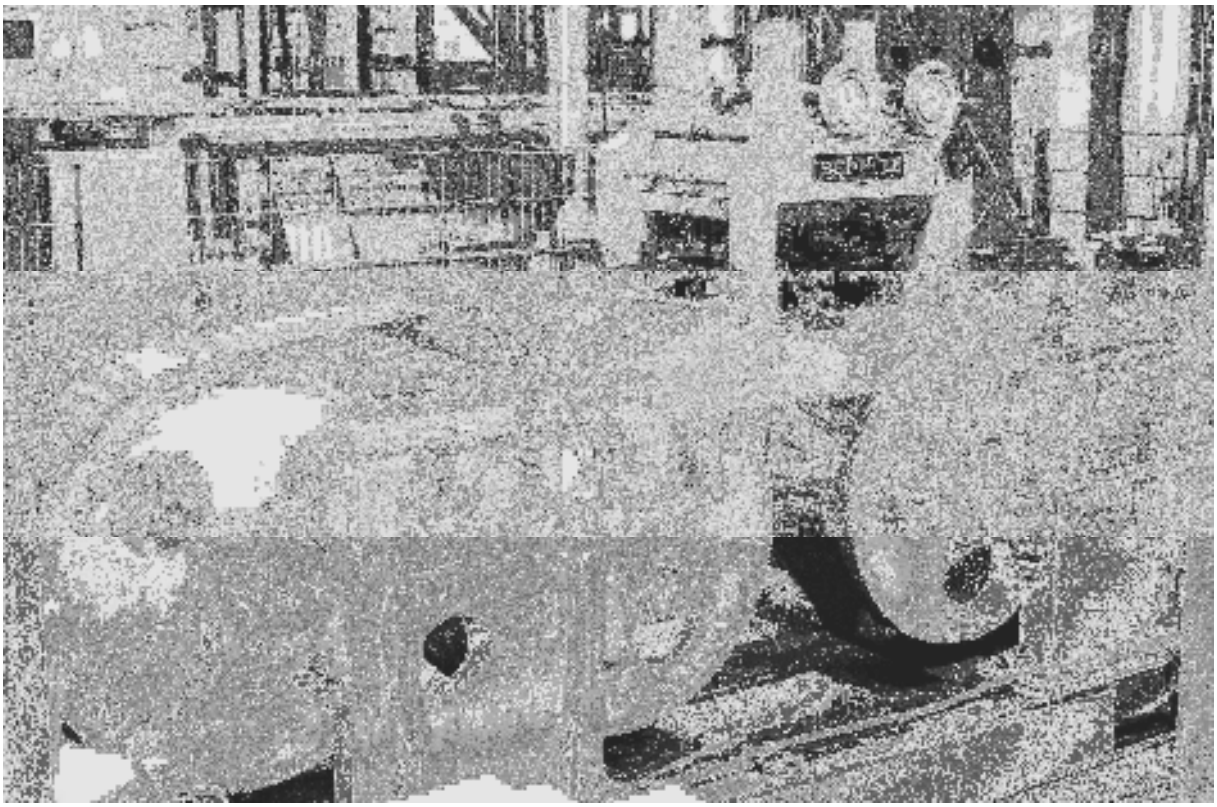

Figure 4: Tension roller plant with bending unit

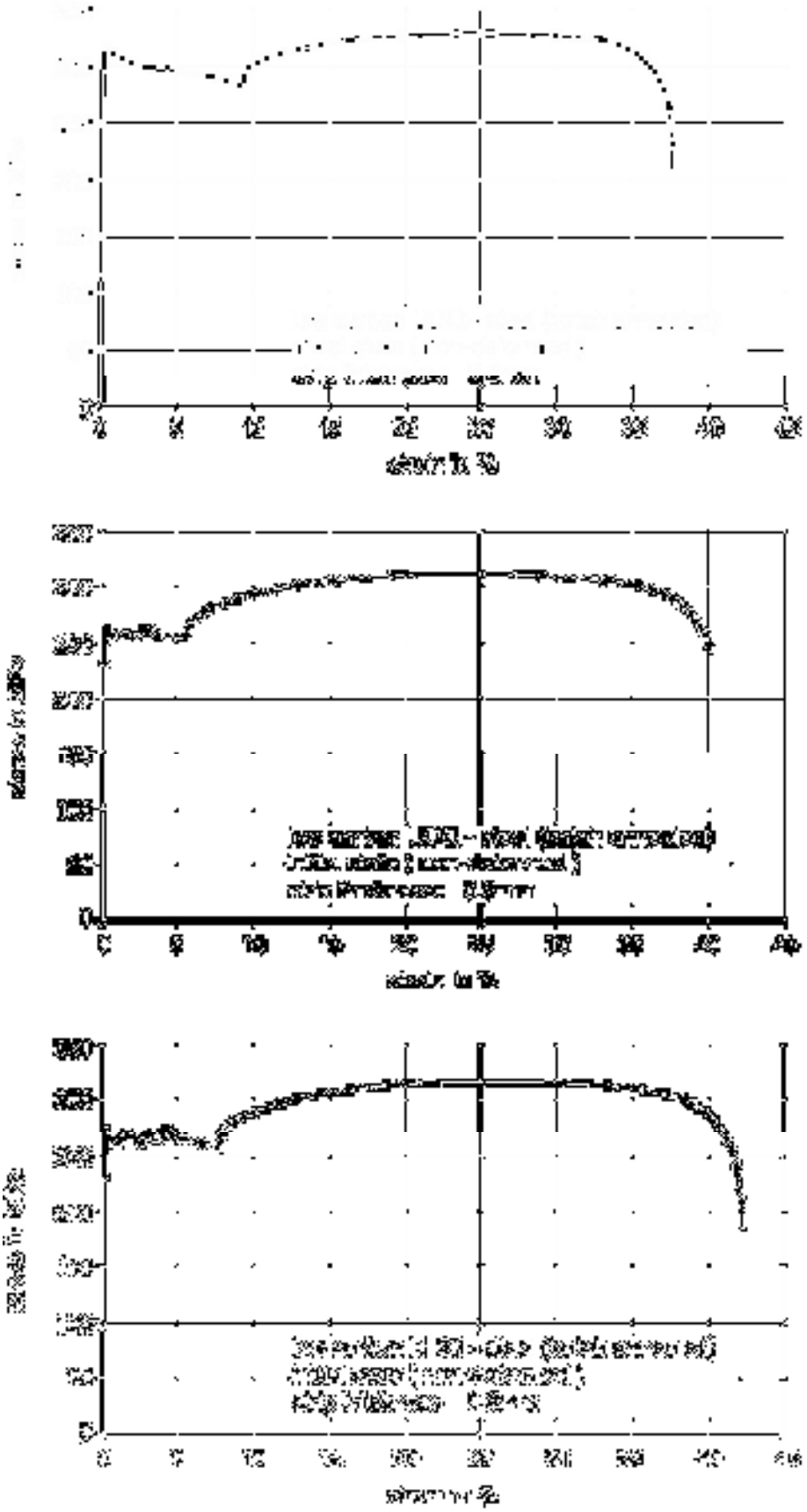

Figure 5: Stress-strain curves of the investigated strips, demonstrating the initial state (batch annealed, non-deformed)

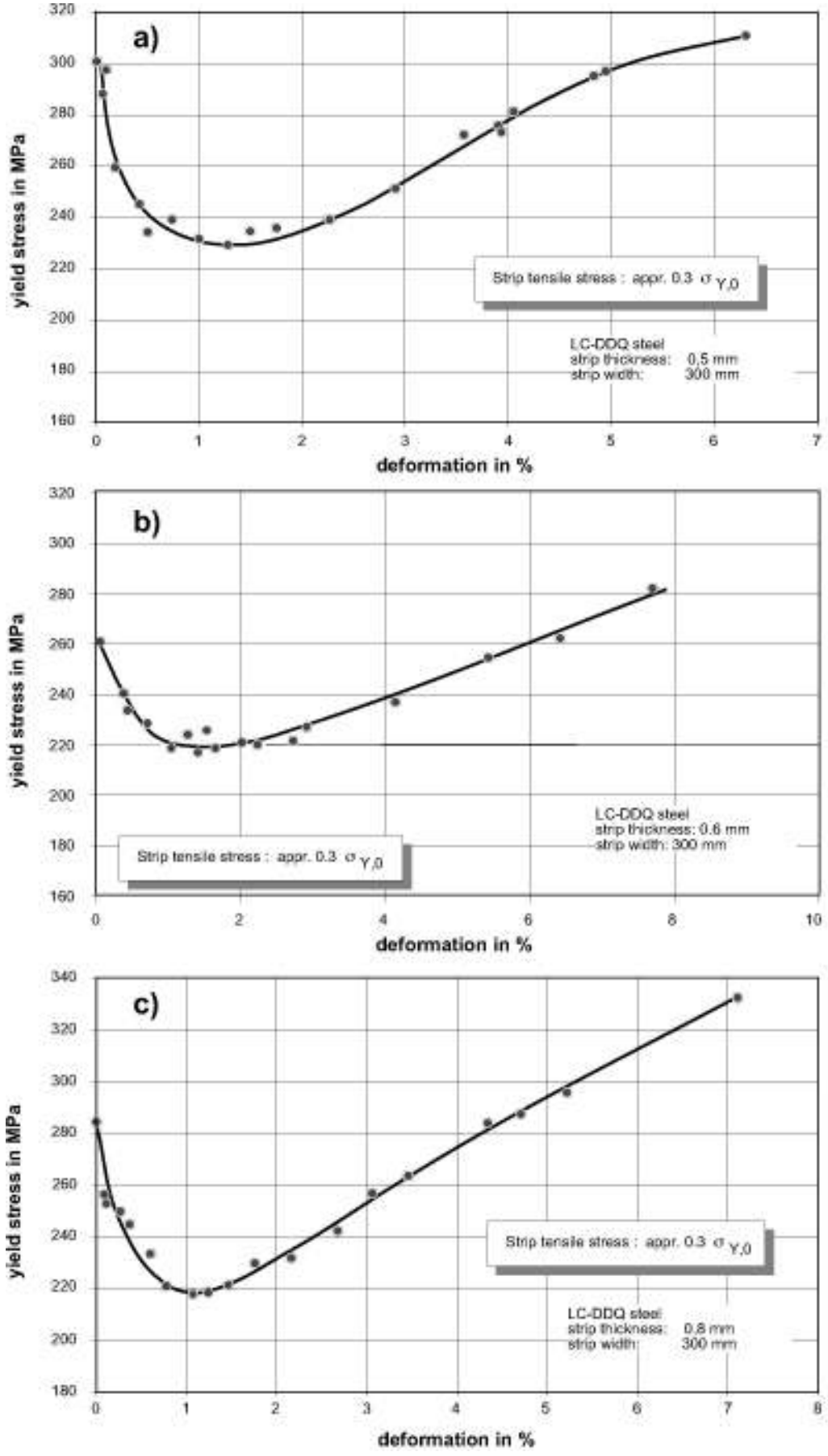

Figure 6: Influence of the bending deformation on the yield stress of a batch annealed LC-steel

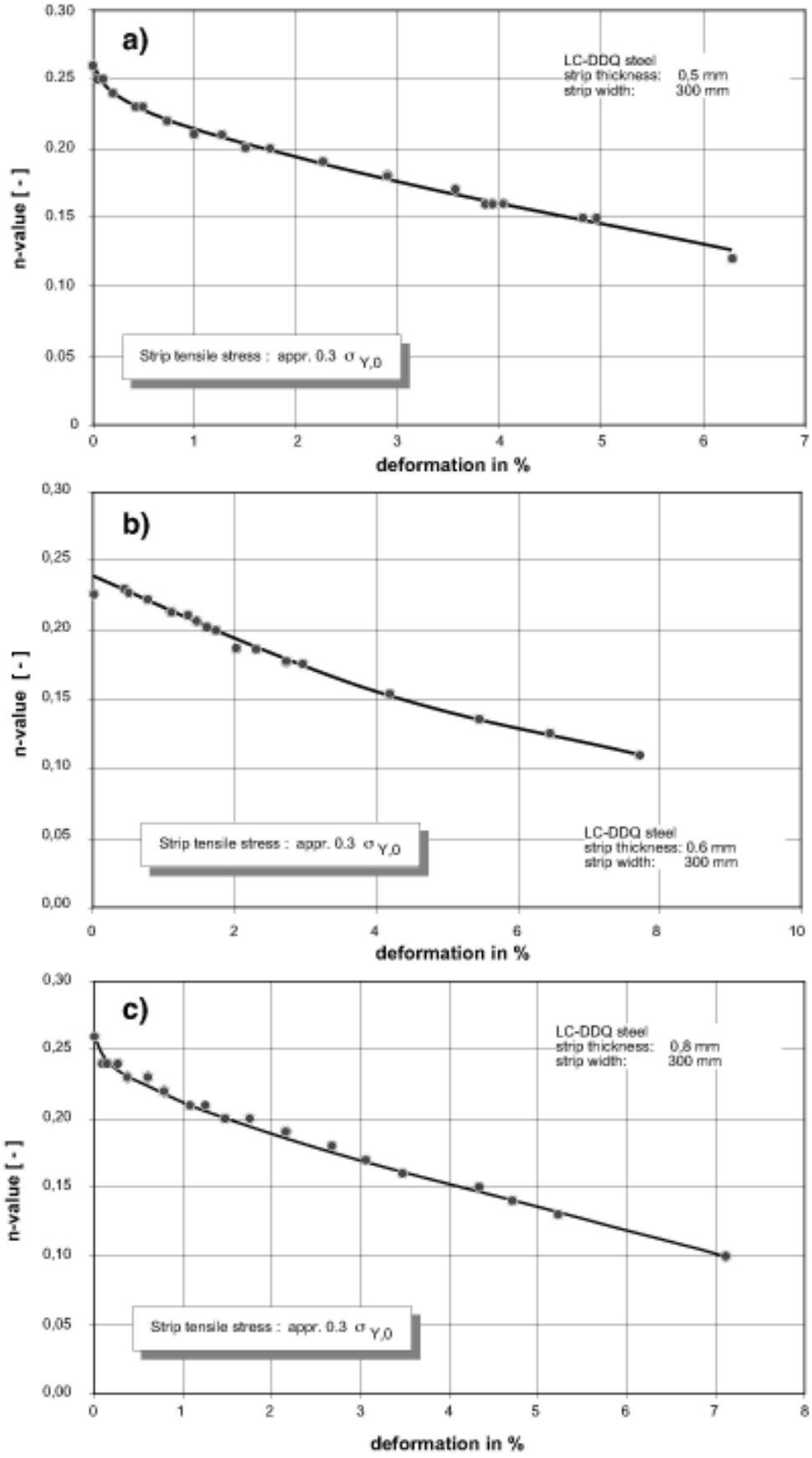

Figure 7: Influence of the bending deformation on the n-value of a batch annealed LC-steel

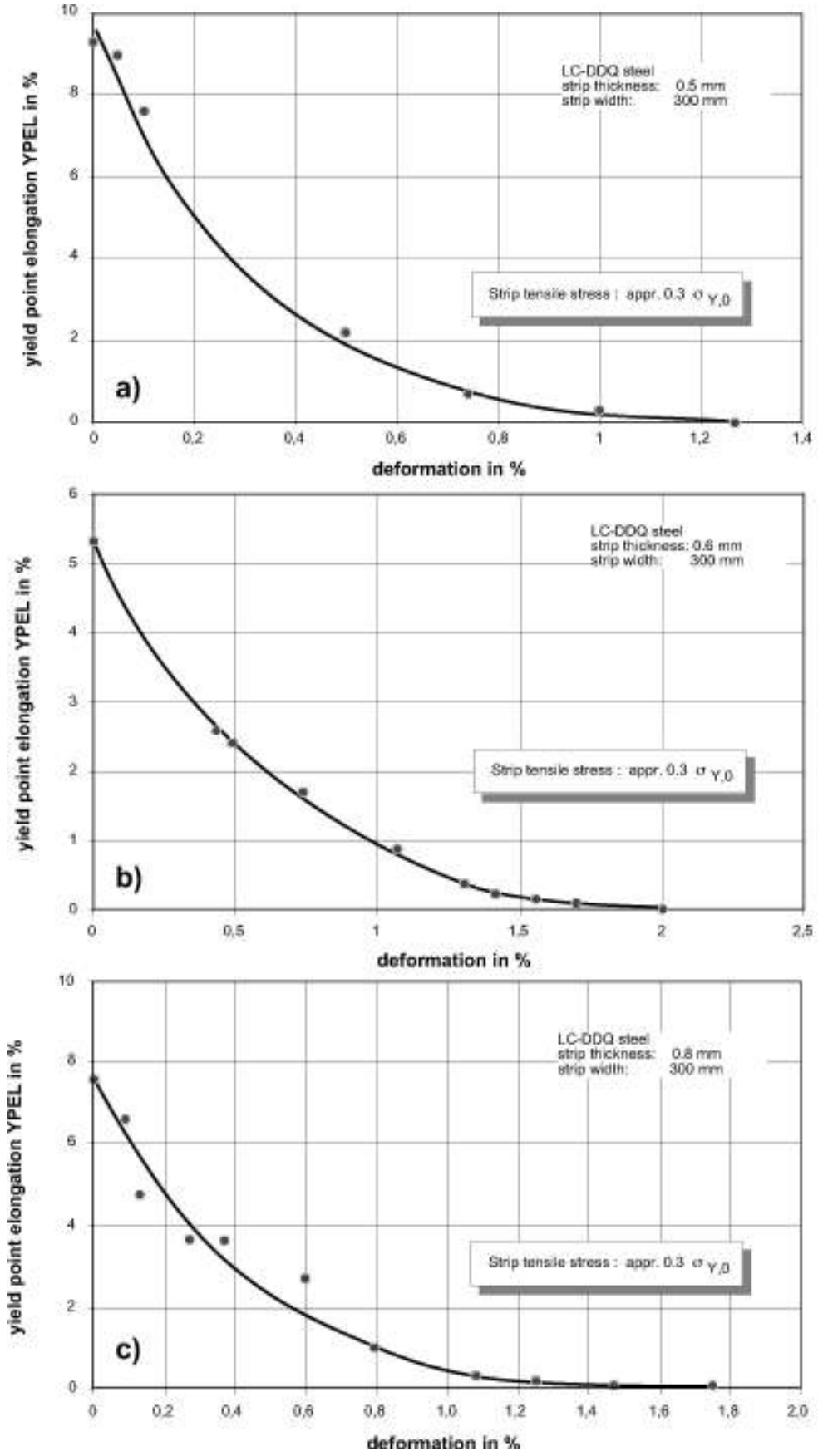

Figure 8: Influence of the bending deformation on the yield point elongation of a batch annealed LC-steel

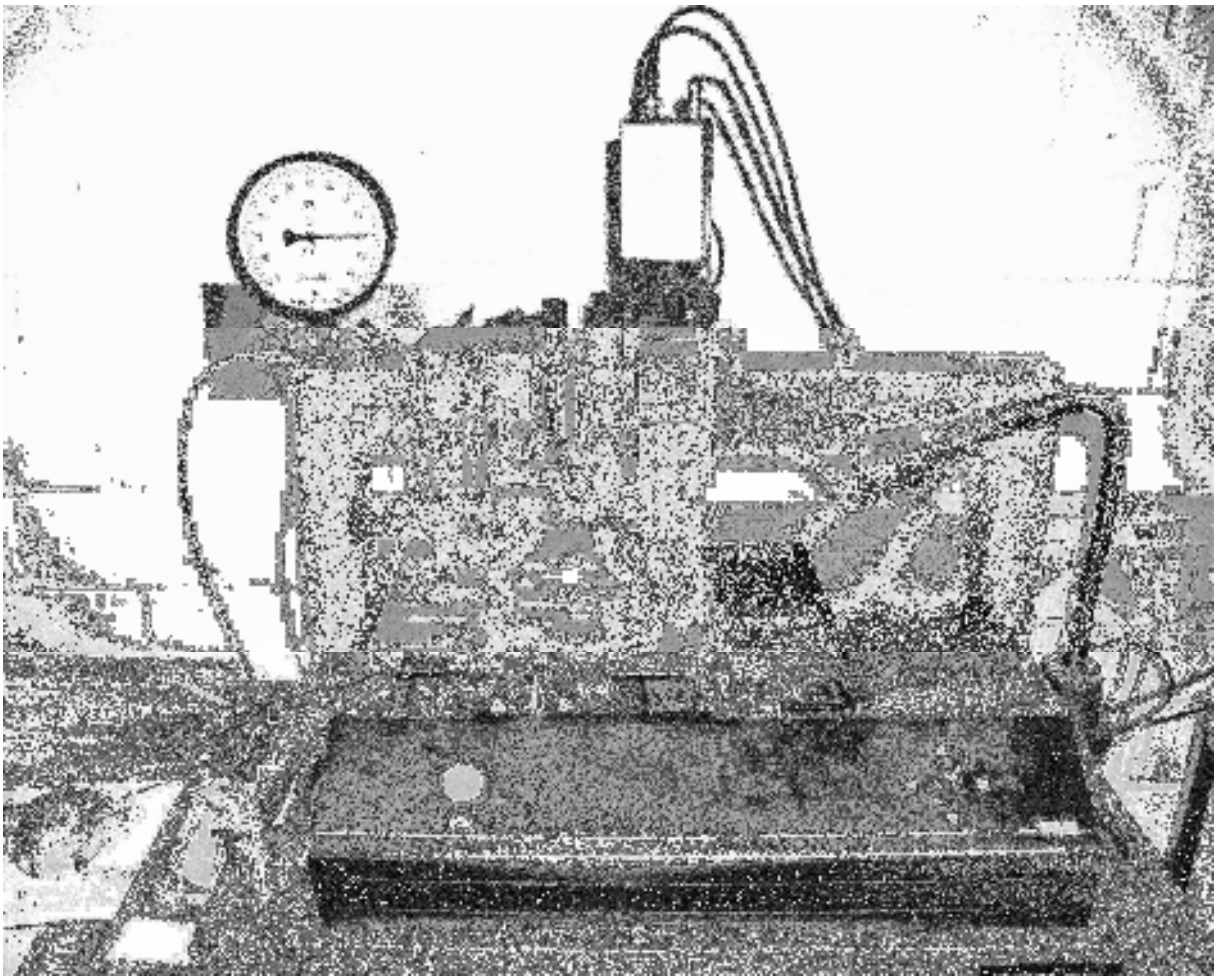

Figure 9: Laboratory measuring system used for strip surface inspection

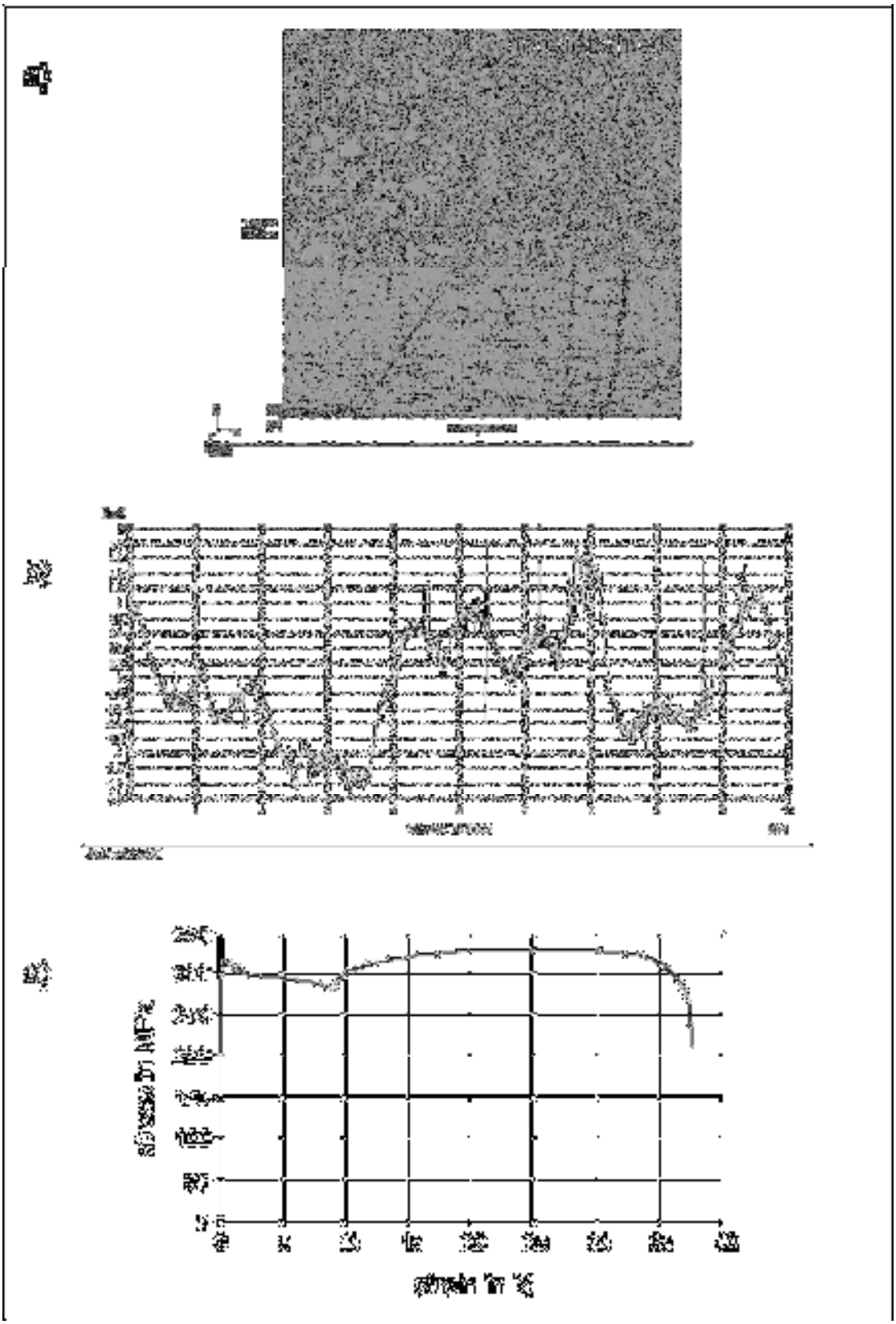

Figure 10: Strip surface topography a) and corresponding height profile b); stress- strain diagram c); (initial state: non-deformed)

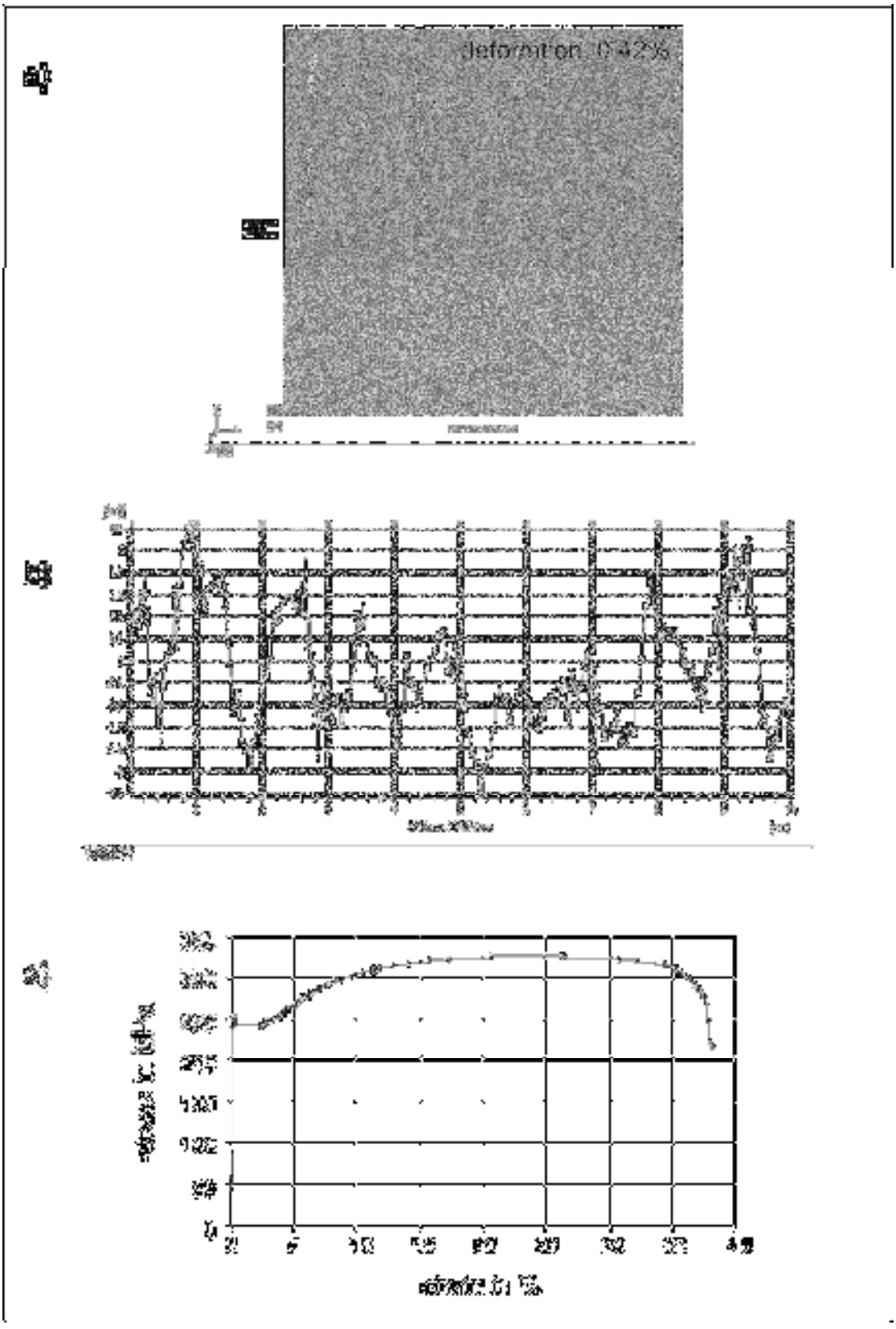

Figure 11: Strip surface topography a) and corresponding height profile b); stress- strain diagram c); (bending deformation: 0,42%)

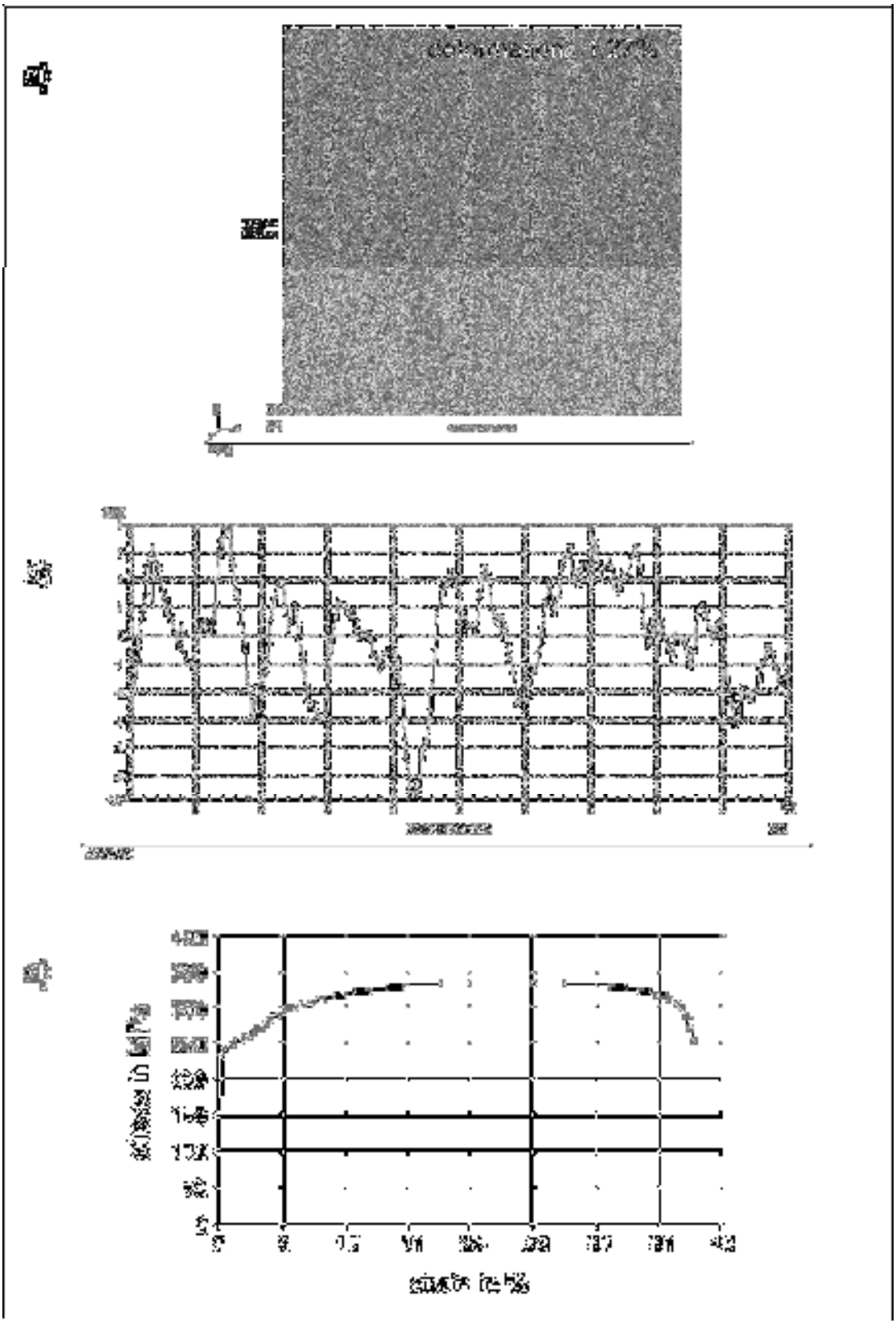

Figure 12: Strip surface topography a) and corresponding height profile b); stress- strain diagram c); (bending deformation: 1,27%)

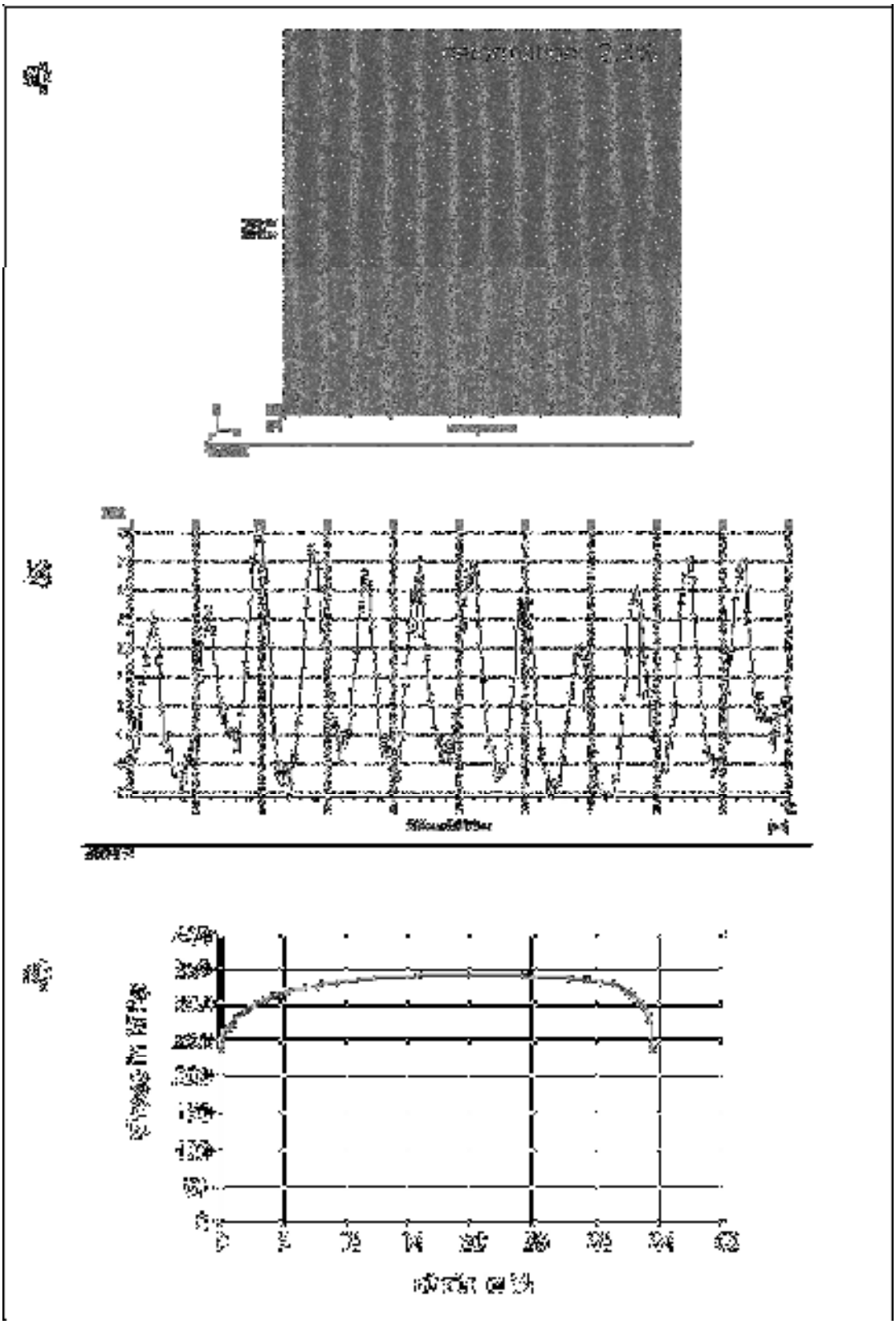

Figure 13: Strip surface topography a) and corresponding height profile b); stress- strain diagram c); (bending deformation: 2,3%)

φ_{TR} - degree of temper rolling

φ_{B} - degree of bending

φ_{total} - degree of temper rolling and bending

$\varphi_{opt.}$ - optimum deformation degree

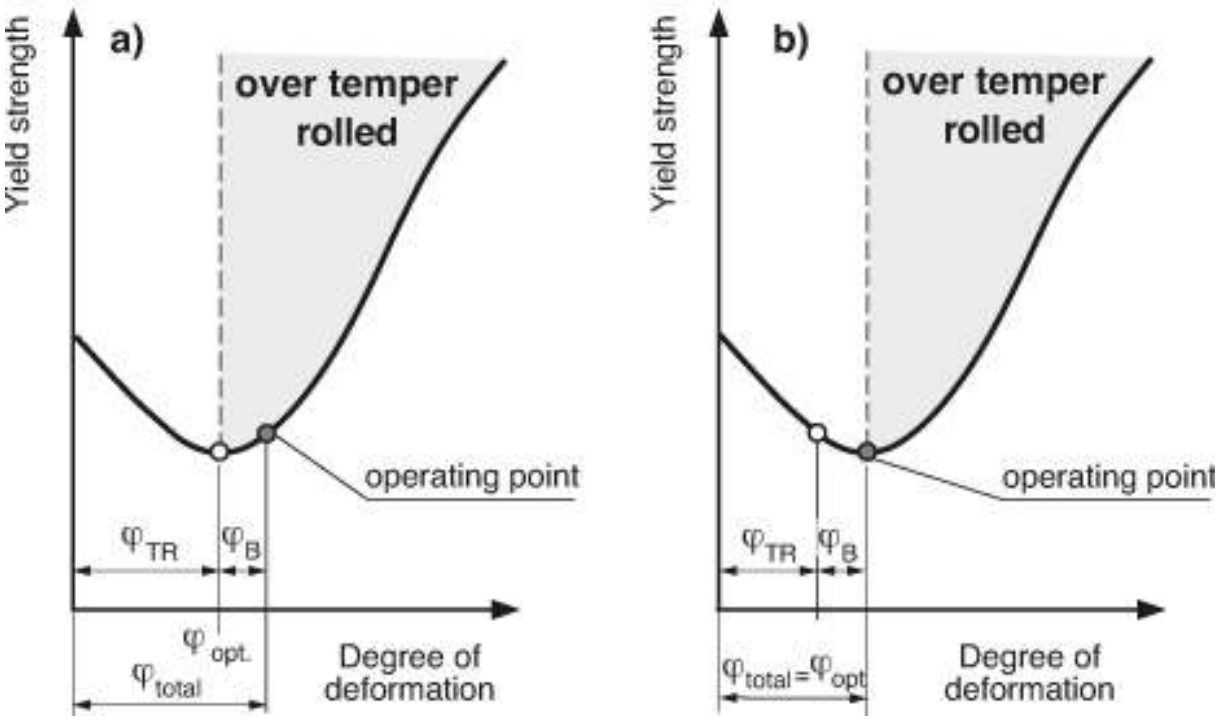

Figure 14: Position of the operating point in temper rolling, without a) and with consideration of bending deformation b)

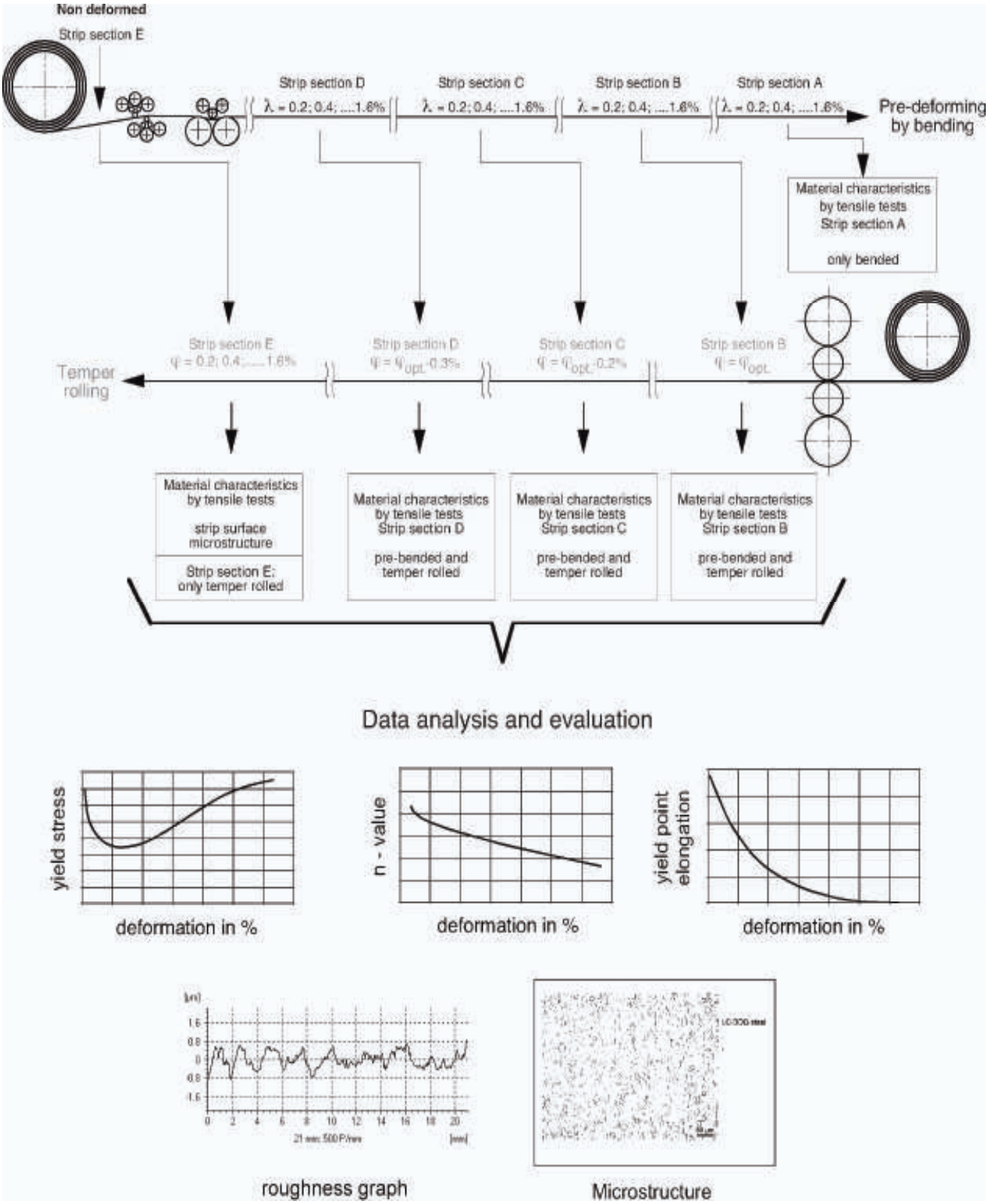

Figure 15: Schedule of selected bending and temper rolling trials as well as their combination

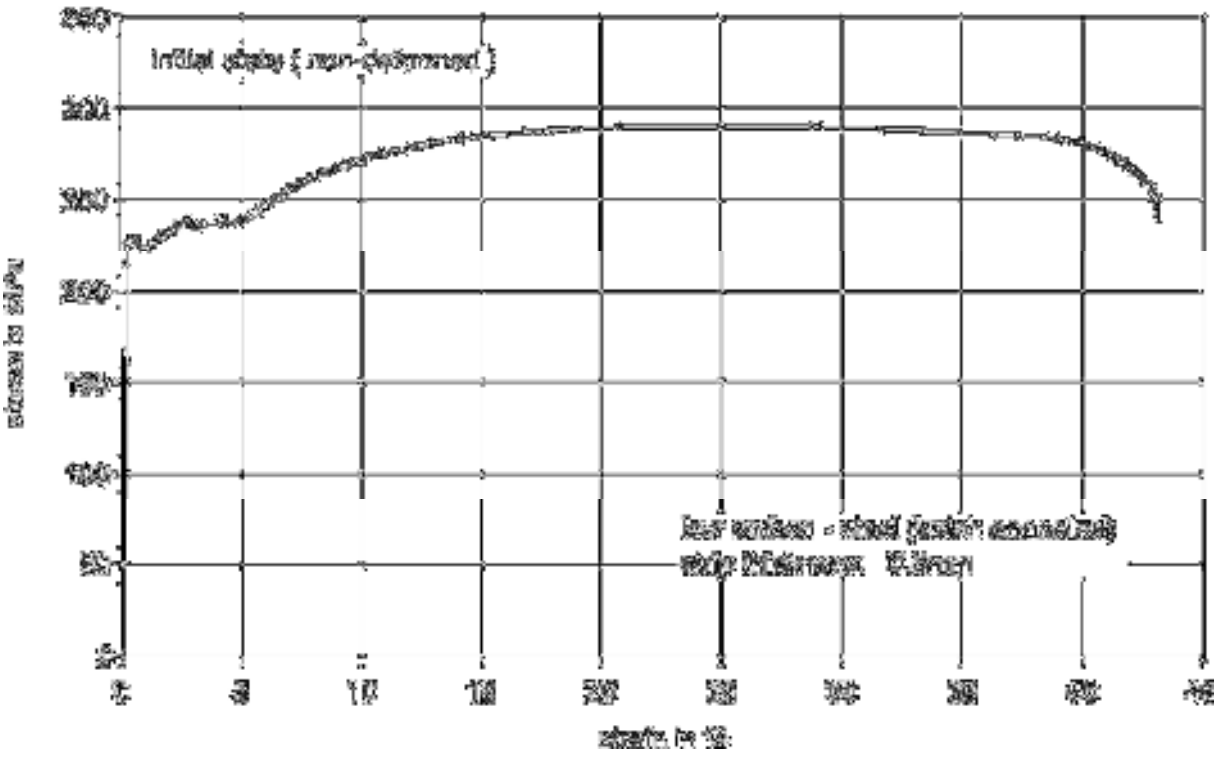

Figure 16: Stress-strain curves of the investigated strip demonstrating the initial state (batch annealed, non-deformed)

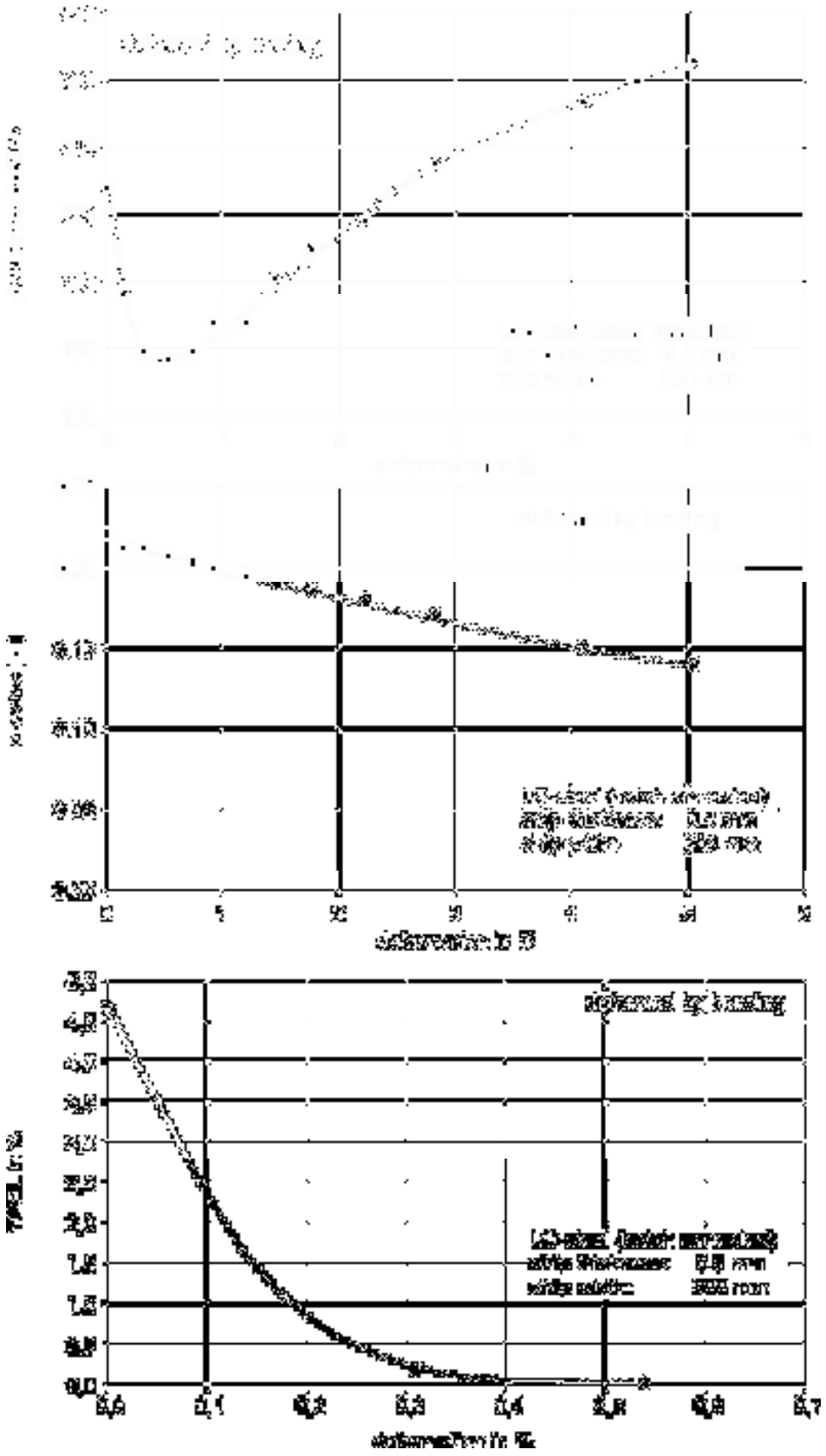

Figure 17: Influence of bending deformation on material characteristics of a batch annealed LC-steel

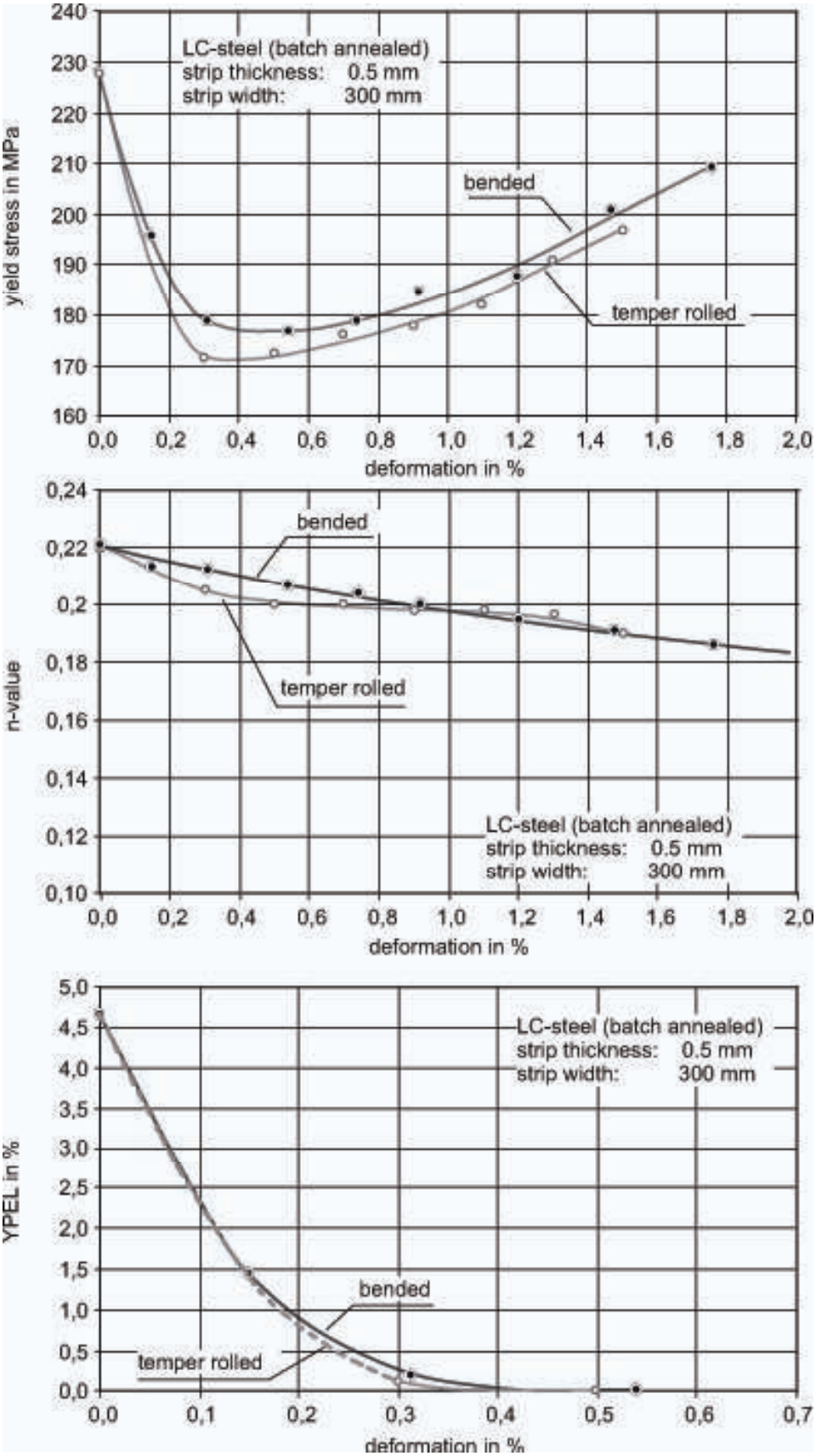

Figure 18: Influence of bending deformation on material characteristics of a batch annealed LC-steel compared to temper rolling

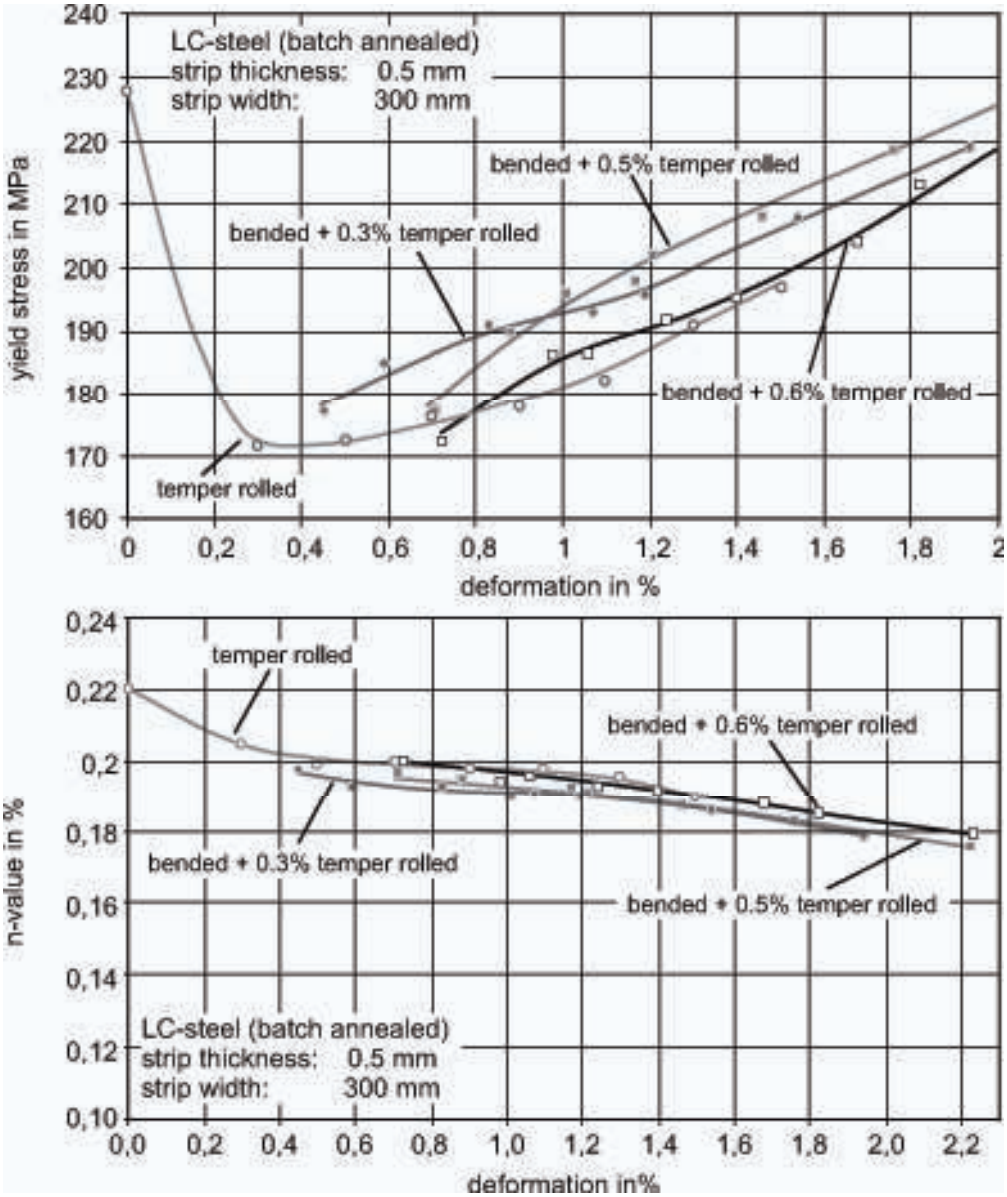

Figure 19: Influence of a superimposed bending and temper rolling deformation on material characteristics of a batch annealed LC-steel compared to temper rolling

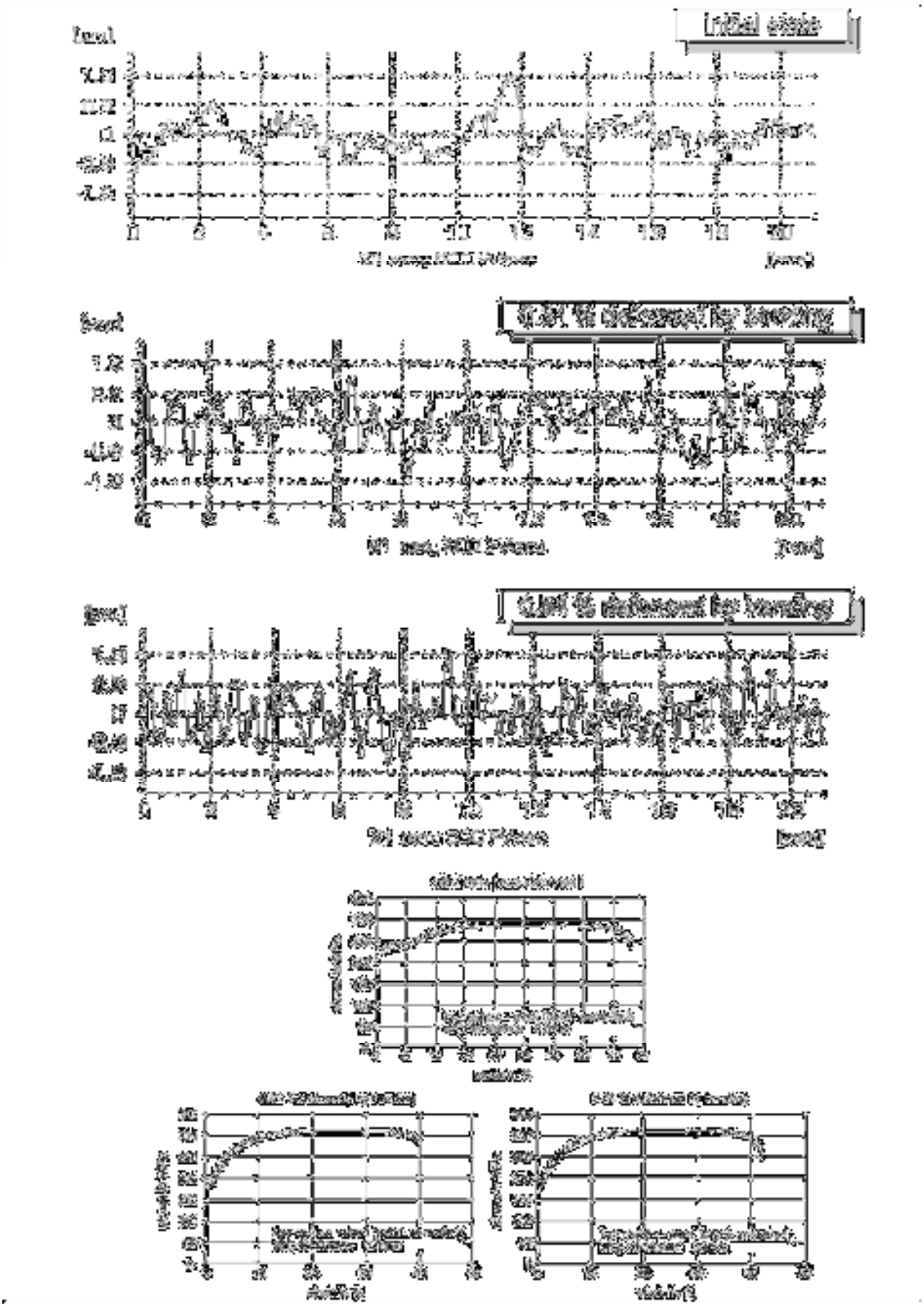

Figure 20: Height profiles of strip surface structure and stress- strain diagrams for different degrees of bending deformation

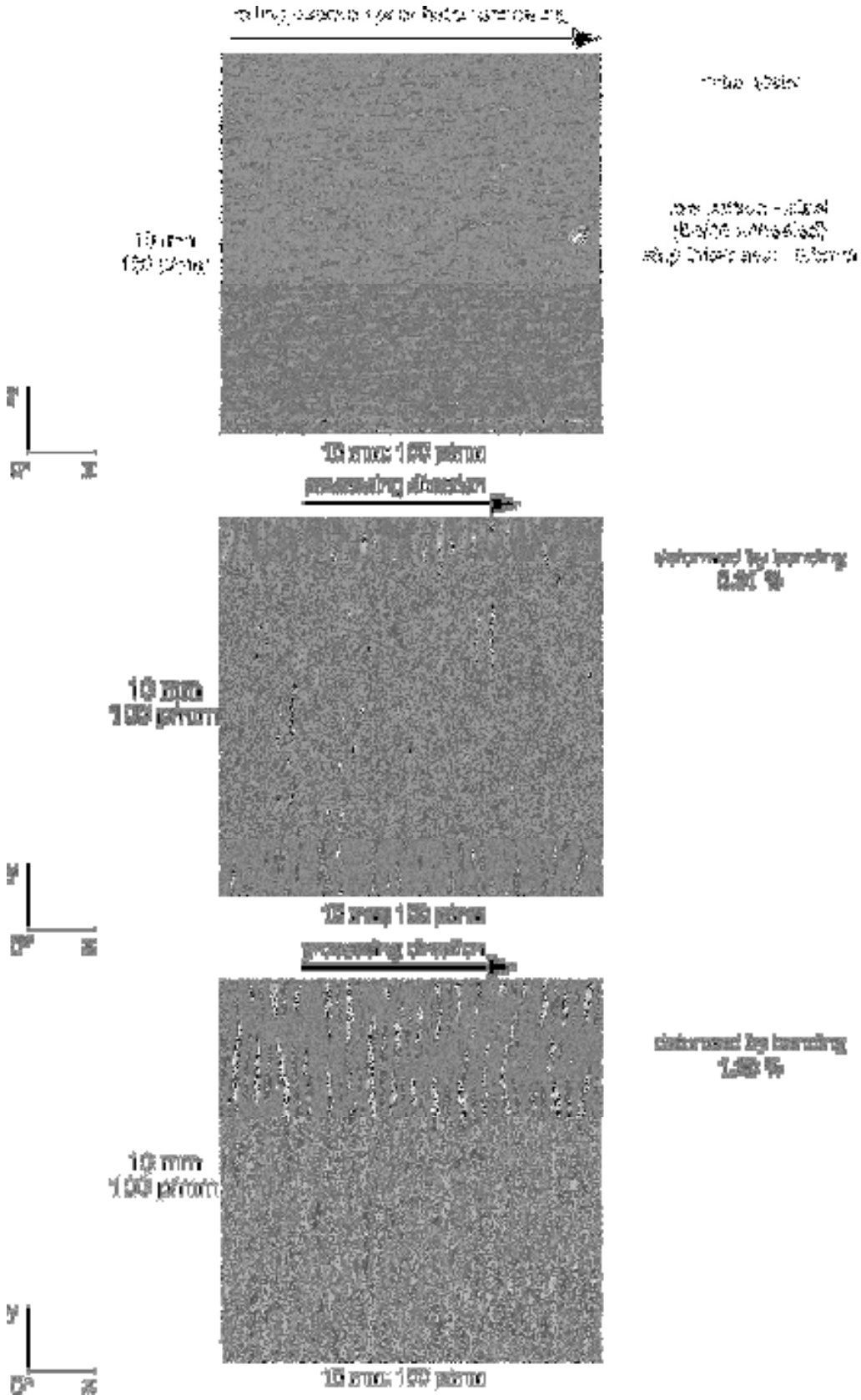

Figure 21: Strip surface topography for different degrees of bending deformation

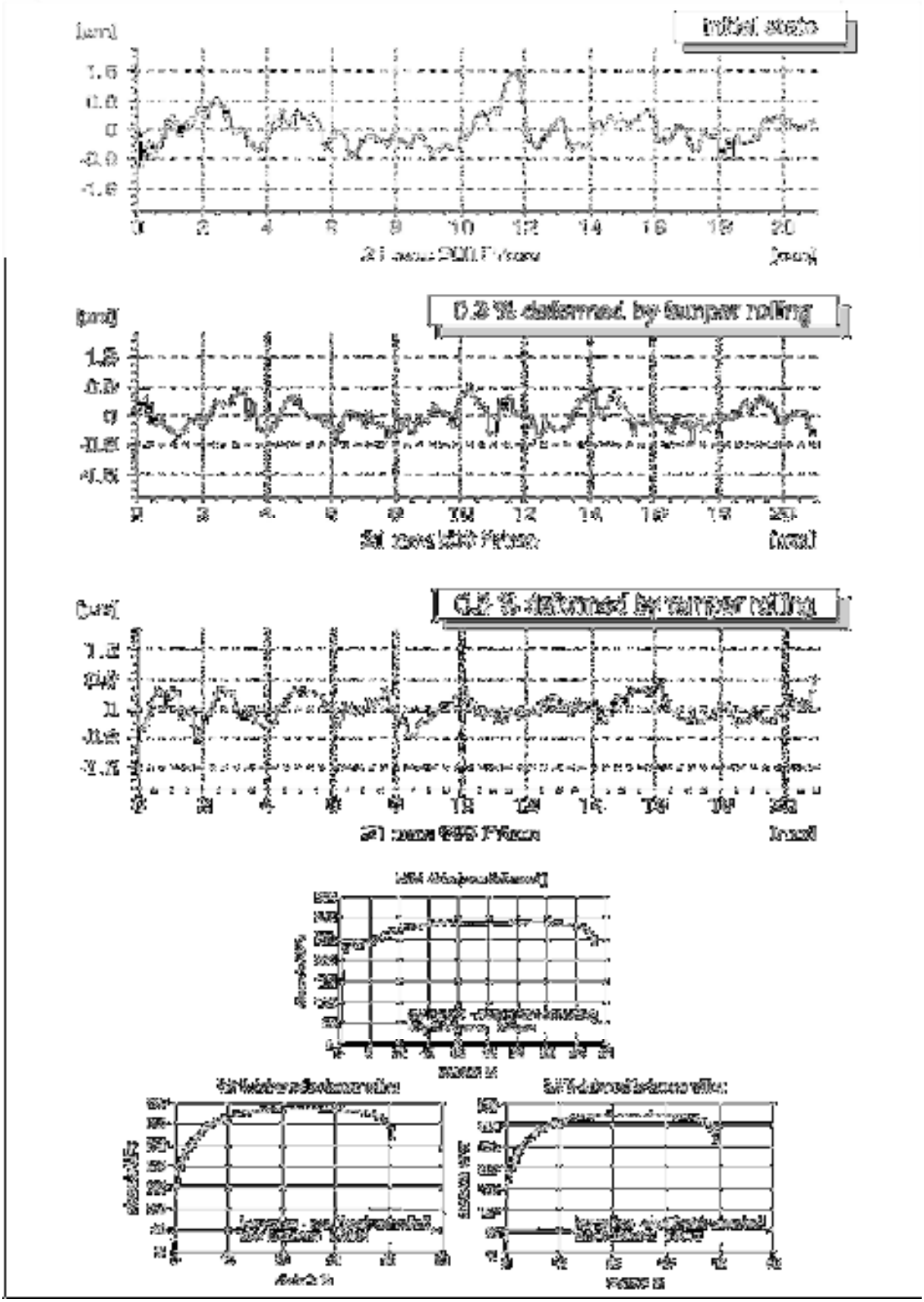

Figure 22: Height profiles of strip surface structure and stress- strain diagrams for different degrees of temper rolling

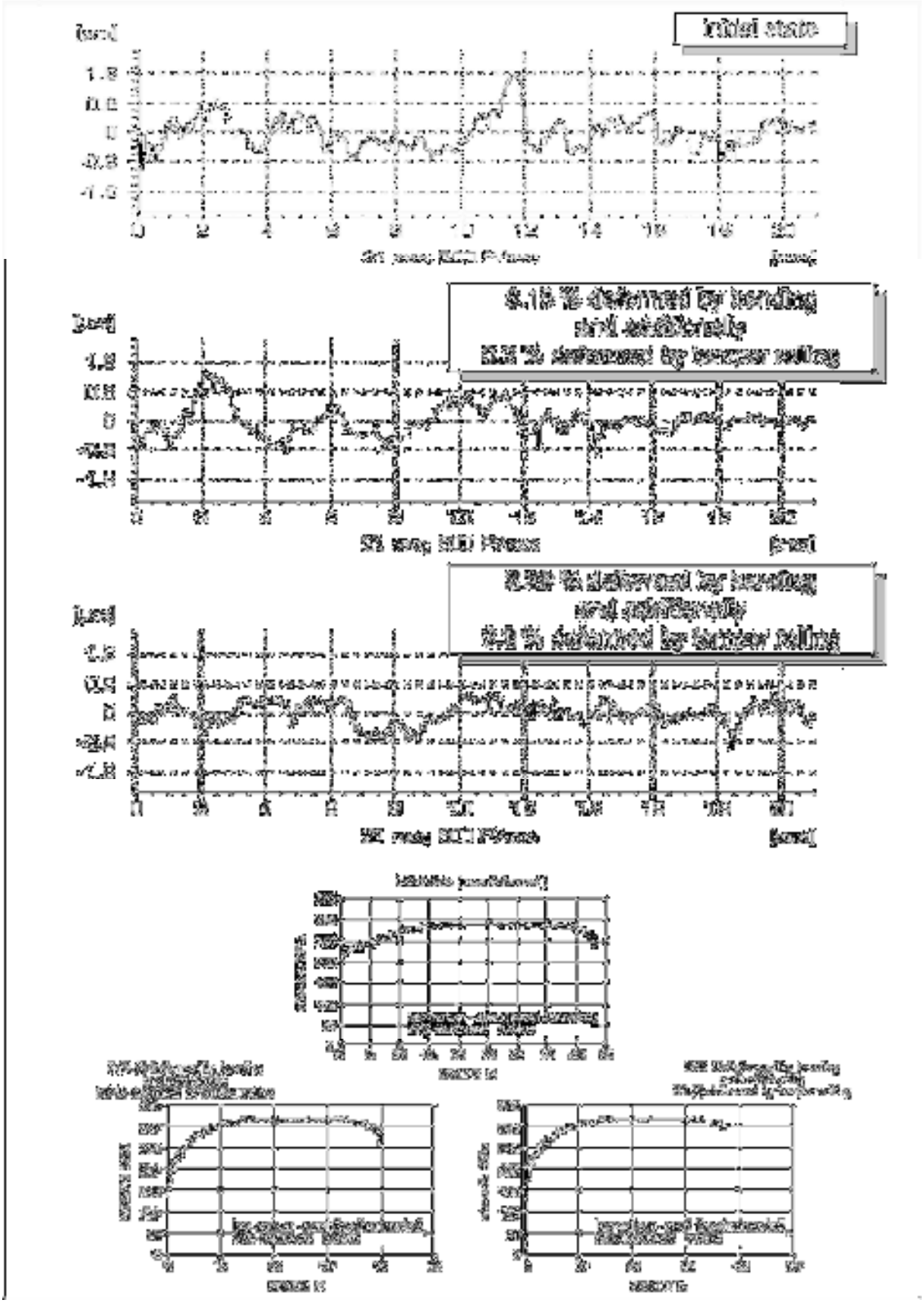

Figure 23: Height profiles of strip surface structure and stress-strain diagrams for different degrees of deformation in case of superimposing bending and temper rolling

FEM simulation studies : part 3 (Skin-Passing process)

List of tables and figures :

Nomenclature :

ε_e	Engineering strain defined as $(L-L_0)/L_0$
ε_L , ε	True strain defined as $ln(1+\varepsilon_e)$, local strain in FEM
σ	Local stress in FEM
σ_u , UYS	Upper yield stress
σ_b	Lower yield stress
ε_u	Uniform strain
R_{p02}	Engineering stress at equivalent plastic strain=0.2%
R_{eL}	R_{p02} falling within extended yield plateau
R_m	Tensile stress defined as total force divided by initial area
TS	Tensile Stress at uniform strain defined as total force divided by current area
CH	Continuous Hardening
LDH	Local Deformation Hardening
ε_o	offset strain in the constitutive models
σ_o	offset stress in the constitutive models
ε_b	Softening/hardening transition strain
SGLS	Scaled Gauge Length Segment
r	Skin pass elongation in %
SR	Strain rate in s-1

1/ INTRODUCTION

This part of the project has been concentrated on understanding conditions resulting in generation of Lüders bands in ferritic stainless steels strips during their processing and consequently prevention of their defects on their end-use applications by further metal forming. The focus was on the influence of the final step process parameters on the local deformation of the strip aiming to the suppression of extended yield elongation (YPEL). The work has been carried out taking as reference Thyssen Krupp Acciai Speciali Terni industrial configuration, in which the skin pass reduction is accompanied by bending at gripping rolls.

The research has been carried along five interlinked ways: standard tensile testing to characterise the strip mechanical properties, physical simulation of skin pass elongation by tension, pilot mill rolling, industrial rolling and numerical simulation of both the strip processing and its subsequent tensile testing. Extensive validation of the predictions against experiments has been carried out..

The importance of yielding phenomena to undesirable marks in the strip has been recognised for a long time. Brindley et al. **[1]** states that temper rolling should not only be intended for YPEL elimination but also for reduction of the sharp stress difference between upper and lower yield point, this believed to be the cause of 'stretcher-strain markings' in subsequent forming of the strip.

Butler et al. considered **[2]** that the efficiency of temper rolling as a method of removing stretcher-strain markings arises from the inhomogeneous structure produced in the sheet during rolling. They state that after 1% rolling reduction the strip consists of blocks of alternate deformed and undeformed material that run across the rolling direction, so there is a substantial proportion (order 50%) of undeformed material remaining. They consider that the absence of markings during sheet forming operations is related to easy nucleation of numerous macroscopic band fronts at the interfaces between deformed and undeformed regions of the temper-rolling pattern. Hodgson et al. **[3]** showed that for recovery annealed low C and ULC steels, a tension levelling of 0.3% strain was enough to reduce the upper yield stress in 250 MPa.

While the predominant variable to reduce YPEL and overcome the upper/lower stress transition is straining, several authors suggest that strain rate also plays an important role **[1, 4-7].** Yoshida **[5]** proposed a viscoplastic numerical model that reproduces well most of the features of tensile testing, but predicts the increasing of YPEL with strain rate; very low strain rates were used in that work.

Microplasticity models for the very early stages of deformation had been proposed **[8**], which consider that the measured upper yield stress is a statistical outcome where a large number of individual grains are already deformed.

In a previous ECSC project **[9]** Tsukahara et al. introduced the local constitutive law concept proposed by Estrin [**10-11]** and investigated Lüders bands mechanisms in bending and tension deformation modes.

The work in **[9]** on batch annealed low carbon deep drawable strips (LC-DDQ steel) clearly showed that plastic bending deformations influence mechanical strip properties in a similar degree than skin pass rolling itself. Further work was necessary to quantify the exact weight of bending on the strip mechanical properties and consequently the current work extends this research to combined modes involving skin pass rolling with and without bending and tension.

Previous work **[12]** on an industrial temper mill equipped with an anti-sticking roll showed that for determining the relevant properties, bending deformations have to be taken into account, and they

could be as high as 30% of the skin pass degree. This figure appeared to be high for the particular TK-AST configuration examined in the current project.

Skin-pass procedures without bending for strips were developed and validated against plant data in a previous ECSC-funded project **[13].** This research showed the importance of considering the deformation of the rolls as the strip thickness decreases. A simplified set-up model for the control system of the skin pass was derived from this research **[14]** and successfully installed in ILVA Novi Ligure Works.

One of the major questions posed on the current research was why rolling in both industrial and pilot mills achieved YPEL suppression earlier than predicted by applying the data from the routine tensile testing of the annealed sheet, this shifted by the process strain value. The local constitutive model introduced in **[9]** reduced this gap, but the resulting YPEL value was till greater than industrial practice.

Tracking the evolution of strip properties by using samples collected at different stages of the final step process is an almost impossible task, because of the need to interrupt the continuous annealing line with its drastic consequences to production costs and discards. Moreover, practical accessibility problems prevent obtaining samples at all required stages. In such context, the FEM simulation provides an alternative analysis but still does not provide immediate response. This can be overcome by condensing the results for wide sets of process parameters in a simplified PC-portable model.

2/ EXPERIMENTAL WORK

The current work was carried out on AISI430 ferritic stainless steel strips produced by Thyssen Krupp Acciai Speciali Terni, the chemical compositions of which are shown in **Table 1**.

2.1 Tensile testing at routine low strain rate of strips skin passed in a pilot mill

Bright Annealed (B.A.) strips of thickness ranging from 0.4 to 1.5 mm have been cut from industrial production and rolled in a 180 mm diameter pilot mill at skin pass elongations of 0.2%, 0.4%, 0.6%, 0.8%, 1.0%, 1.2% and 1.4% in several passes. ISO80 tensile specimens were next cut from these strips and subsequently tested at $2x10^{-3}$ s^{-1}. **Figure 1** shows some results for a 0.6 mm thickness strip. Both the R_{p02} and σ_u stresses initially diminish with the percentage of skin pass elongation **(Figure 2).** There is reduction of both R_{p02} and σ_u up to rolling elongations around 0.6-0.8%, which accompanies the elimination of yield point elongation (YPEL). The yield stress next increases as a consequence of the rolling elongation having entered the strain hardening region. Hardening for this particular steel grade is not very sensitive to the skin pass elongation, as revealed by the contained variation of the n-value in **Table 2** and **Figure 20**.

Figure 3 shows that YPEL follows in general a quadratic dependence with the original strip thickness, with a minimum around 1.00 mm thickness for the lower skin pass elongations. The smaller YPEL values obtained at higher skin pass elongations are less sensitive to the initial thickness. The YPEL completely vanishes for skin pass elongations over 0.8%.

2.2 Tensile testing at skin pass strain rates

Tensile testing at higher strain rates were carried out using a MTS servo hydraulic machine according to the conditions given in **Table 2**. The monotonic loading results in **Figure 4** and **Table 2** show that an increase of strain rate raises the stress level with a minimal influence on the hardening rate and

diminishes the YPEL, this last result contrary to the predictions of the numerical model from Yoshida **[5].** These results are relevant because as shown by the FEM simulation in **§4** , skin pass rolling involves strain rates that are higher than in the routine testing used to determine tensile properties of the strip (this being of the order of 10^{-3} s^{-1}).

2.3 Tensile testing at routine low strain rate of specimens pre-deformed in tension at skin pass strain rates

Another set of tensile experiments was carried out simulating the skin pass rolling up to a fixed elongation at an associated strain rate determined from the FEM results **(Figure 13c),** followed by unloading of the specimen and a routine strain rate (order 10^{-3} s^{-1}) full testing. The experiments were carried out with a high speed acquisition at a rate of 3000 per second, using the load reading to stop the first deformation. The results were partially successful, given the inertia of the hydraulic system to completely stop after the trigger order was issued.

The results show that below 1.5% elongation at the first strain rate, some YPEL remains during subsequent tensile testing. As suggested by the results at the several strain rates used in the first deformation, full YPEL elimination occurs beyond 0.13 s^{-1} **(Figure 5a).** For the conditions of suppressed YPEL, there is almost no difference in the continuous hardening between the stress-strain curve of the stepped-2 strain rates (0.16 s^{-1} followed by $4x10^{-3}$ s^{-1}) and continuous low strain rate ($4x10^{-3}$ s^{-1}) testing **(Figure 5b).**

This physical simulation was aimed to be compatible with the FEM numerical simulation, where the only history parameter of the elastoplastic model applied to skin pass rolling and consecutive tension was the accumulated plastic strain. Such hypothesis does not include any further constitutive change resulting from either processing or delaying times introduced by the machining of the tensile specimens.

2.4 Tensile testing from industrial skin pass rolled strips

Samples of skin passed commercial strips were also taken from the Thyssen Krupp AST 440 mm diameter roll mill, the configuration of which is given in **Figure 11** and ISO80 tension testing performed. The results in all cases showed total elimination of YPEL at skin pass reductions of 0.70-0.85%.

3/ MODELING TENSILE TESTING OF BRIGHT ANNEALED (B.A.) STRIP

3.1 Material behaviour modelling

The several constitutive models and parameters used along the project are summarised in **Table 3**.

The experimental raw data from the ISO80 tensile tests of the B.A. 0.6 mm thickness strip were used to generate both Conventional (CH) and Localised Deformation (LDH) **[9-11**] Hardening elastoplastic models. The CH model uses raw data converted to stress-strain in a standard manner while the LDH model exhibits a softening prior to a continuous hardening with a transition at a strain ε_b (stress-strain curve in **Figure 6** and local models in **Figures 7-8**).

3.2 Sensitivity analysis to geometry, stress state and numerical modelling assumptions

Two geometries were used for the FEM simulation: the real ISO80 specimen and a 'Scaled Gauged Length Segment' (SGLS, of length 15.62 mm), this thought to be cut from the rolled strip later in the

research. Both 2D (Plane Stress) and 3D modelling were carried out using the elements types CPS4 and C3D8I respectively with the commercial code Abaqus **[15].**

Simulation results for the macroscopic stress-strain measures, as defined in the experimental testing are shown in **Figure 7**. The initial fitting effort was aimed at the yield region and to the upper range of uniform deformation, which gave some small mismatching at the start of the continuous hardening, this later improved in the version LDH3 of the constitutive model. The simplest 2D Plane Stress results are acceptable for yield predictions, but it is clear their deterioration at bigger strains.

Other important issue guiding the LDH model calibration was the matching of the local stress-strain (Von Mises stress and equivalent plastic strain) monitored at sampling points against the corresponding macroscopic values true strain-true stress, as computed in the real test practice **(Figure 8).**

3.3 Sensitivity analysis to constitutive model parameters

A sensitivity analysis of the effects of the LDH model parameters upon the tensile testing predictions of as-annealed strip showed **(Table 4)** :

(a) Yielding region:

- Increasing the ε_b value in the local model produces in the test simulation an extension of YPEL, initially raising the R_{p02} level but this value next stabilises.
- Lowering the lower yield stress σ_b in the local model produces in the test simulation an increase in YPEL and lowers the R_{p02}.
- Increasing the upper yield stress σ_u in the local model produces in the test simulation an increase in YPEL and raises the R_{p02}.

(b) Continuous hardening region :

The 3-parameters LDH1 and LDH2 models found difficulties in reproducing well the experimental data in the continuous hardening region. Consequently, a 4-parameters LDH3 model was investigated **(Table 3). Figure 20a** compares the tensile new LDH3 simulation results against experiments; the R_{p02} and YPEL experimental data are well reproduced and while LDH2 overestimated the early continuous hardening, this is improved in the predictions of the LDH3 model.

3.4 Final results for B.A. strip

The final simulation results show that both the CH and LDH constitutive models can validate well the macroscopic engineering tensile test results **(Figure 6),** in particular the development of the Lüders plateau. The amount of material undergoing continuous hardening predicted by the two models, however, is radically different. For the CH model, hardening of the as-annealed strip starts at about YPEL=0.025 when all the specimen has been swept by an homogeneous-evolving deformation **(Figure 9).**

For the LDH model, continuous hardening starts at the much lower strain ε_b=0.012 **(Figure 6),** and develops expanding bands that cross the whole specimen section with associated plastic strains higher than the measured percentage total elongation **(Figure 10).** This figure also shows that extensometers placed in the central area of the specimen and on small gauge length will not necessarily register a meaningful local deformation, if the banding starts outside the gauging extremes.

4/ SKIN PASS MODELING

4.1 Industrial configuration and modeling hypotheses

Figure 11 shows the industrial configuration of the last step under study and **Table 5** its base processing parameters and the perturbations on them examined during the project. The roll diameters are 440 mm for the skin pass and 250 mm for the neighbouring gripping rolls.

The strip was modelled using the elastoplastic constitutive model LDH for the as-annealed material discussed above, with the parameters in **Table 3**. A process modelling of a strip length covering the whole span of the final step, however, would demand a large mesh discretisation effort. This is unjustifiable, given the localisation of deformation in very small areas of the strip being processed. Consequently, the distance between the skin pass and gripping rolls were scaled down, maintaining the angles as in **Figure 11**.

Linear, quadratic and special linear FEM elements were tried for the deforming strip, in both 2D-Plane Strain and fully 3D versions. It is well known that FEM traditional linear elements do not perform numerically well in the presence of bending, situation which is aggravated in the skin pass because both bending strains are of the same order than deformation components and unless a very fine discretisation is used, the element length is of the same order than the element's wall thickness **[15].** When submitted to bending, these elements develop spurious stiffness that alters the response in terms of stress and strain, introducing shear strains that do not really exist, the so-called parasitic shear. The problem is eliminated with the use of special elements having additional degrees of freedom (CPE4I in Abaqus **[15, 18]).** As the best 2D results were obtained by using these last type of element, the 3D simulations were carried with the equivalent element Abaqus type C3D8I.

The rolls were modelled using two hypotheses: as rigid surfaces and as fully elastic bodies and both results compared.

Contact was found to be the major difficulty in the FEM skin pass simulation. Due to the very small deformations underwent by the strip, the speed and convergence of the numerical solution becomes driven by the contact algorithm. Three main options were explored:

(a) Use of quadratic elements, which did not result in a significant gain respect to the special linear elements CPE4I and C3D8I.

(b) Two contact options allowing some minimal modelling interference to cope with the different curvature radius of strip and deforming rolls, which gave also marginal gains. They were: (b1) a 'hard contact' maximum roll-strip interference of 4.9×10^{-4} mm, (b2) a 'soft contact' with an exponential law for the contact pressure giving zero at 10^{-5} mm distance outside the roll surface, 10 MPa at contact and increasing at the rate 1000 MPa/mm into the roll.

(c) increasing the number of elements contacting the rolls, which was the most successful change for 2D-Plane Strain solutions but become impracticable to model realistic strip widths because the large number of elements demanded to cope with FEM aspect ratio constraints.

4.2 Modeling results

4.2.1 2D-Plane Strain simulations

Figure 12a shows the evolution of the strip geometry and its plastic strain during the final step. The through-thickness plastic strain distribution is shown in **Figure 12b**. It can be seen that the first bending roll only introduces a minor plastic strain concentrated at the strip upper layers, while the second roll is effective to reduce the uneven through-thickness plastic strain profile delivered by the asymmetric skin pass but also raises the strain level **(Figure 12b),** thus favoring Lüders bands suppression.

The implications of the use of the local LDH model, where hardening takes place earlier than suggested by the CH model, as discussed for tensile testing above **(Figures 6 and 9-10),** to skin pass rolling is paramount. To eliminate the YPEL, the CH model requires a skin pass macro-elongation of about 2.5%, in disagreement with all industrial practice. The LDH model, instead, requires only a fraction of this deformation to enter into continuous hardening and develops bands of higher strain **(Figure 10)** that sweep the deformed area. **Figures 12a and 12b** show that a skin pass macro-elongation of 1.08% on exiting the asymmetric rolling configuration defined by the gripping rolls is more than enough to induce Plasticity exceeding the limit ε_b =0.012 across the whole strip thickness.

The through-thickness plastic strain is very sensitive to the tension and bending angles. **Figure 12c** compares the findings obtained for the 440 mm roll industrial configuration for two cases: no-tension no-bending and bending with tension. At equal effective thickness reduction, in the last case the strain at the strip surfaces is about 25% higher than in the horizontal configuration. Both cases in the figure report the equivalent strain, which is always positive in contrast with some of its individual components (shear, bending) that can develop reversal. The horizontal configuration gives a symmetric plastic strain profile, which is not the case for the industrial configuration. In all cases, the macroscopic, engineering skin pass elongation (0.0073) is lower than the local plastic strain (average 0.0085) that also contains shear strain components.

Through-thickness maximum shear strain and elongational strain rate FEM results are shown in **Figures 13a and 13b** respectively. At equal roll diameter (440 mm) and roll speed (3.6 rad/s), the strain rate follows a quasi linear trend with the skin pass elongation **(Figure 13c).** This last result was used to programme the skin pass simulation by tensile testing described above in **§2**.

The results in **Figure 14a** give a quantification of the roll flattening for the case of the pilot mill geometry. The through-thickness plastic strain developed during no-bending skin pass is in general slightly higher towards the strip core, with minimal differences between the predictions for rigid and deformable rolls. **(Figure 14b)**

4.2.2 Full 3D simulations

Figure 15a displays the results obtained with a 3D-simulation of the last step. To cut down computing speed, only a tenth of the actual strip width, a symmetry plane at mid-width and rigid rolls were used. The upper roll has been removed from the picture to show the lateral spread representing a breakdown of the Plane Strain condition assumed in the 2D-model.

The results at the strip border show that the gripping rolls tend to narrow the strip, while the rolling pass generates a lateral spread of lower magnitude. Although these displacements are minimal, it has to be assessed whether they play any role in the levelling/development of residual tensions influencing the strip flatness. In spite of these lateral displacements, the plastic strain across the strip width is uniform as shown in **Figure 15b**, together with the position of the SGLS later isolated to perform the virtual tensile testing. The rolling results were produced with a mesh of 800 C3D8I elements in the rolling direction, 4 in thickness and 6 in width. Even this coarse discretisation at a 1/20 of the real width dimension proved to be extremely slow in convergence, due to the elsewhere mentioned problems with contact.

The major handicap of this modelling is the large computing turnaround time consumed by each simulation. Because of intrinsic numerical constrains on the maximum allowed width and length to thickness ratios of the element, enlarging the simulation to real strip width is prohibitive given the large amount of 3D elements that this would involve.

5/ INTEGRATED SIMULATION: SKIN PAS ROLLING -TENSILE TESTING

5.1 2D-Plane Strain no-bending no-tension rolling and 2D-Plane Strain tensile test

This part of the work was exploratory, focused on the yielding region, was carried out with the parameters of the early LDH1 model, and reflects the stopping point limitations then found by a full 3D simulation. Taking advantage of symmetries, the skin pass without bending configuration was modelled using a single roll and a half thickness strip with its midplane having the normal displacements constrained to zero.

The Plane Strain hypothesis constitutes a handicap to a subsequent tensile testing simulation, because it is not possible within the same FEM analysis to switch to a Plane Stress hypothesis (which within the 2D limitations represents better the early yielding, **Figure 7)** and also the specimen width contraction cannot be modelled. In spite of its oversimplification, simulations under plane strain conditions throughout the analysis were carried out for two main reasons. The first one was to obtain an estimation of the departure of its prediction from the experiments, should a conversion factor could be used to scale down the stress level as in **[9]** and simultaneously recover the yielding region experimental results. The second reason was to test and improve the 2D procedure releasing the SGLS segment common to both the skin pass rolling and the tensile testing, in view of its application in more accurate but drastically slower 3D-modelling (**section §4.2.2).** The procedure is outlined in **Figure 16a** and follows the steps :

(I) 2D-Plane Strain simulation of the skin pass using CPE4I elements.

(II) Decoupling a length of rolled mesh (SGLS) from the whole model, as in the real cutting from the strip, maintaining the original symmetric boundary conditions on the strip mid-plane. One extreme of the specimen remains clamped and eventual residual tensions are released as in the real case.

(III) Virtual tensile testing of the SGLS, recording the distance between two reference nodes P_0 and P_1, the rise of the reaction forces on the clamped nodes and the middle gauge length half thickness. To maintain proportions with the ISO80 testing, the initial gauge length L_0 is 2/3 of the total SGLS length. The true stress is computed as the total reaction force at the clamping end divided by the current thickness at the middle gauge length and the current elongation from the change in the separation between P_0 and P_1.

Figure 16b compares simulation and experimental results in terms of the macroscopic engineering stress-strain. **Table 6** shows the yielding region parameters obtained from this 2D-FEM simulation for different degrees of rolling elongation on a 0.6 mm strip. In overall, the 2D simulations overestimate the stress in about 14.2%, with a 12.3% excess for the upper yield stress, and 14% for the lower yield stress. The results show that a factor 1.16 could be used to scale down the stress simulation values to match the experiments, if such simplistic approach is chosen. The simulation reproduced the reduction of YPEL with the degree of skin pass elongation, but while YPEL suppression in the experiments was achieved with 0.4-0.6% skin pass elongation, in the 2D plane strain modelling that came only after

0.8%. This finding forced to review the LDH models parameters, with the outcome detailed in sections **§5.3** and **Figure 20** for the 4-parameters LDH3 model (**Table 2**).

One of the problems of this simplified modelling is its inability to represent the narrowing of the tensile specimen because the width dimension does not enter into the simulation.

5.2 3D rolling and 3D tensile test

Based on the good results obtained with the 3D simulation of as-annealed strip tensile testing in **§3**, combined fully-3D skin pass rolling followed by SGLS tensile testing simulations were performed on a 0.6 mm initial thickness strip rolled at different elongation ratios.

Figure 15b shows the Strip Gauged Length Segment (SGLS) to be cut away from a region where that strain is uniform and lateral spread is negligible, in order to perform the virtual tensile testing. Its initial dimensions in mm are: length L_0 = 15.625, width W_0= 6.0, thickness t_0=0.6 . The 3D virtual tensile testing follows the (I)-(III) steps described for the 2D model above, uses C3D8I elements and now the current width W separating two nodes at mid-gauge length is also monitored to compute the current area and therefore improve true stress prediction. Virtual tensile testing results for 2D and 3D SGLS segments skin passed at thickness reductions ranging from 0% to 0.9% are compared with experimental results in **Figure 17**. The improvement in stress matching against experiments achieved by the 3D simulation is clear, particularly in the continuous hardening regime. Both experimental trends: reduction of YPEL and raise of stress level with the degree of skin pass elongation are well reproduced. The model then used (LDH1), however, did not fully cancel the YPEL as in the experiments. These last results forced to review the LDH model parameters and consequently the simulations for the as-annealed strip in section **§2** above and skin passed in sections **§3.3** and **§4** reflect the change to the new LDH3 model constants. Yielding region parameters obtained from the 3D-FEM tensile testing simulations are shown in **Table 7**. Respect to the 2D predictions in **Table 6**, the new 3D results show a marginal increase in the amount of skin pass reduction necessary to remove the Lüders plateau.

Figure 18 shows the evolution of the total accumulated plastic strain at several stages of the 3D-SGLS virtual tensile testing, on a 0.45% skin passed, 0.6 mm initial thickness strip, with images sampled every 5 increments. The generation of higher local deformation, Lüders bands is clear. They start initially as one branch band crossing the specimen width at diagonal near the pulling end and progress developing two branches with a V-shaped front that sweeps the whole specimen length advancing towards the clamped end.

5.3 2D-Plane Strain skin pass rolling and 3D tensile test

To overcome the slow turnaround of the full 3D analysis described above, a drastic improvement was necessary, which was achieved in the form of a procedure that maps skin pass rolling results into the tension specimen geometry. It takes advantages of the fast 2D Plane Strain simulation of skin pass and makes no simplification either on the evolution of the stress or strain state or on the magnitude of deformation during subsequent tension. The last conditions allows to examine not only yielding but also tensile properties at larger strains. Also, because the second part is a full 3D analysis, the specimen's width and thickness contractions are available to obtain true stress values. The connection between the process and test FEM analyses is the mapping procedure summarised in **Figure 19** that transfers the skin pass exit strain state as initial conditions to the tensile testing. The geometry of the specimen in the second simulation can be the full ISO80 or the faster but less accurate SGLS.

The material model LDH3 (**Table 2**), calibrated for the annealed strip as detailed in section **§3**, was used in the simulations. **Figure 20** shows a comparison of predicted and experimental tensile true stress for skin passed strip having elongations ranging from 0 to 1.%. For comparative purposes, the

engineering stress in terms of the initial specimen area and its derivative respect to the logarithmic strain, which defines the uniform strain limit, have also been plotted. The results show an improved matching of tensile properties of skin passed strip against experiments in the upper range of uniform strains. As in all previous simulations, this model also predicts shortening of the YPEL with the degree of skin pass reduction.
The comparison of the LDH3 model simulation and experimental results in **Table 8** shows good agreement with bounded errors of ε_u at 3.4%, Rm at 2.4% and TS at 2.2%. at large strains. In the yielding region, however, the results show big scatter resulting from the uncertainty of the experimental measurement at 0.4 elongation, but giving the message that LDH3 still fails in giving an accurate YPEL prediction as skin pass elongation increases.

Figure 21 compares the performance of the two types of tensile specimen geometries when simulating tensile testing. The ISO80 specimen delivers a better defined YPEL and only marginally higher hardening than the faster turnaround SGLS geometry.
Even though a 3D simulation would have provided more information on the width dimension as lateral spread and flatness, the experience with both the simplest 2D simulation here and the previous 3D simulation with scaled down width in **§4.2.2**, advised that a 3D extension was going to be an unjustifiable effort to the prediction of mechanical properties. The breakthrough achieved with the mapping procedure summarised in **Figure 19** when applied to pilot mill rolling paved the way to analyse the industrial configuration and consequently several case studies have been examined using bending angles and tensions that were unavailable in the pilot mill.

6/ FINAL WORK ON NUMERICAL SIMULATIONS OF THE FINISHING CONFIGURATION WITH LOCAL LAW, WITH AND WITHOUT SUPERIMPOSED TENSION AND BENDING.

6.1 Tensile properties sensitivity to process parameters as predicted by the LDH model

A comparison of simulation results for the pilot and industrial configurations under the common hypotheses of no-bending and no-tension shows the absence of any influence of the working rolls diameter (**Figure 22a**) on tensile properties.

A reduction of the strip tensions applied during skin pass to 1/10 and 1/50 of their nominal values did not introduce any difference in subsequent tensile properties (**Figure 22b**). As tensions alter the rolled thickness, these simulation results were produced at equal effective skin pass reduction achieved by modifying the skin pass roll gap setup.

A steady state picture of the accumulated thickness reduction r undergone by the strip during the last processing step is shown in **Figure 23** for the case study B000 in **Table 5** . Even though the main contribution to strip thinning is given during the skin pass, the total plastic deformation due to the two gripping rolls also introduces a small total reduction of the order of 0.03% that represents a 4% of the total reduction in the step. The grey region in **Figure 23** corresponds to the effective reduction obtained after releasing a strip segment in order to perform the ISO80 tensile testing simulation with the mapping procedure described in **§5.3**.

The results in **Figure 21** show that a double 15° bending introduced by gripping rolls raises only marginally the tensile curve at the start of the continuous hardening, respect to the corresponding results for the no-bending configuration. The difference in stresses is reduced with the increase of the tensile testing strain. It can also be seen that bending, in spite of raising the average through thickness strain (**Figure 12c**), is effective in reducing the YPEL only in a small percentage (0.07% and 0.09% for skin pass elongation ratios 0.8% and 1% respectively) and is not as effective as the rolling reduction (**Figure 24a**).

Figure 24 shows the effects of the most sensitive parameters to tensile properties and the matching correlations found to construct a simplified model for off-line use.

6.2 Overall discussion and validations

The simulation results for the as-annealed strip in **Figures 6, 9 and 10** discussed in section **§3.1** show that while the CH model needs a YPEL=0.025 strain to enter into the continuous hardening region, the LDH model starts hardening at only a fraction ε_b =0.012 of that strain and matches well the experimental data up to the uniform strain limit. This study was carried out at low strain rate (order 10^{-3} s^{-1}) as in the industrial characterisation practice.

For skin passed strip, the results of the combined numerical simulations no-bending pilot rolling followed by routine tension testing in **§5.3** above validated up to uniform strain the elastoplastic LDH3 model against the corresponding experiments (**Figure 20**) at the low strain rate as in industrial characterisation practice, with a minor discrepancy on YPEL. This is not a problem for austenitic steels that do not exhibit extended yield elongation and for which a CH model will suffice.

At an earlier stage of the project, it was considered whether through-thickness strip non-uniformity or rate effects developing during skin pass were responsible for accelerating YPEL elimination in some strip layers with the net result of a lower YPEL in the macroscopic response of the whole thickness strip. Two possible hypotheses related to effects of subscale microstructural changes were considered :

- Formation of cell-block boundaries induced by crystal rotations **[16],** these being associated to shear strain components. Even though these strains are very small in skin pass rolling, they still might trigger incipient cell formation, thus reducing the dislocation mean free path. If the amount of cells is significant, they will anticipate continuous hardening at lower equivalent strains in the subsequent tension testing. The effect is bound to occur at selected bands centred about a quarter thickness from midplane, where the shear strain is higher (**Figure 13a**).

- Strain rate effects. The transition between the upper and lower yield point is associated to a negative strain rate dependence of the flow stress and induces dynamical ageing **[7],** which is not expected in this ferritic steel. Also, such a process would have recovered both YPEL and UYS, results which are not seen in the tensile experiments following skin pass rolling ((a), **Figure 25**). The magnitude of the strain rate, however, is worth to consider: in contrast with its normally low value in the characterising tensile test (order 10^{-3} s^{-1}), the strain rate during rolling raises and drops sharply under the roll gap with residence times in the industrial configuration of nearly 3 milliseconds. Although smaller respect to values reached in the hot and cold mills, the strain rate developing in the skin pass is still 10^{+2} to 10^{+4} times higher than the characterising tensile test, its height being smaller at the lowest reductions (**Figure 13b**) but in any case involving strain rate gradients of the order of 100000 to 250000 s^{-2}. Thus, the skin pass introduces an effect which is not detected if performing a routine low strain rate testing. As the dislocation density generation involved at skin pass rates is much higher than in the low strain rate purely tension characterizing test, continuous hardening and YPEL suppression at earlier strain in the process appears as a logical consequence.

Figure 25 summarises the YPEL findings of all experiments and numerical simulations. The following issues can be identified:

(1) The experimental combined skin pass pilot rolling followed by standard (order 10^{-3} s^{-1}) strain rate tension shows faster suppression of YPEL (curve (a), **Figure 25** from **§2.1**) than both the higher strain rate continuous (curve (b) from **§2.2**) and the stepped skin pass physical simulation followed by tensile testing (curve (c) from **§2.3**).

(2) At equal processing strain, YPEL results from experimental skin passed strip (curve (a)) are lower than both the CH (curve (e), **Figure 25**, which is coincident with the annealed strip raw data) and its improved LDH predictions (curves (f)) for the industrial base configuration. Given the low influence of both roll diameters (**Figure 22a**) and bending angles (**Figure 24b**), such disagreement can be attributed to two possible causes: larger strain rate in skin pass rolling ((a), **Figure 25**) than in the B.A. characterising tests ((e), **Figure 25**) and experimental fragmentation of the pilot skin pass rolling of (a) into several passes to achieve the nominal reductions reported in **§2.1**. This last condition contrasts with both the numerical (curves (e), (f)) and physical (curve (c)) simulations, as well as with the industrial conditions ((d) in **Figure 25**), because in all these four cases the skin pass reduction occurs in only one stroke.

(3) The stepped 2-strain rates experiments results (curve (c), **Figure 25**) point to a threshold strain rate (**Figure 5a**), above which the elongation to suppress YPEL is significantly lower than for the annealed stress-strain data (this given by curve (e) **Figure 25**, coincident with CH0). As this occurred in a pure tensile state, the hypothesis of shear strain effects (**Figure 13a**) induced during skin pass has to be discarded. It does, however, show that after a critical strain rate, which for the AISI430 0.6 mm strip is about 0.13 s^{-1} (**Figure 5a**), the YPEL elimination accelerates.

(4) Although the physical simulation results in (c) **Figure 25** appear as the most appropriate experimental reference for validation, they requires around 1.5% skin pass elongation to fully suppress YPEL and this value is still high respect to the industrial data (0.7-0.8% (d) in **Figure 25** and **Table 2**). Moreover, the (c) results are of the 'CH' type, this meaning YPEL is the direct reading from the experiment, which can be halved by the local LDH model (as shown by comparison of curves (e) and (f)). Therefore, an equivalent improvement on curve (c) will result in a LDH model as curve (g) that will fall well into the industrial data range (d). Proper quantification of these behaviour requires to introduce rate effects into the FEM constitutive model and obtaining further experimental data at several strain rates. As these results come late in the project, the correction was made only at the simplified model level.

Figure 26 shows the R_{p02} predicted by the several numerical, pilot and industrial mill measurements. It can be seen that the LDH model gives a good agreement respect to industrial measurements and also shows the scatter from the purely tensile experiments.

Both the results in **Figure 20** and in **Table 8** show that predictions in the uniform elongation region are very good, with maximum errors respect to experiments of 3.4% in strain and 2.4% in stresses.

6.3 Simplified model and its application to industrial plant optimization

An off-line simplified model based on the main correlations found by the FEM combined skin pass rolling-tensile testing simulations shown in **Figure 24** has been constructed. Due to the difficulties found in obtaining robust FEM solutions before the breakthrough detailed in **§5.3**, only the 0.6 mm strip thickness has been fully investigated. **Figure 27** shows the general layout of the model. It requires as input the strip thickness and its as-annealed stress strain curve, the bending angles a_1 to a_4, the differential tension between front and back, the amount of skin pass elongation and the output are the tensile properties. In order to consider the effects discussed in **(§6.2**) above, the experimental results (g) of **Figure 25** are applied.

The application of the model to TK-AST line data revealed a configuration fairly optimised with marginal gains for the AISI430 steel studied. The potential application of the model to other grades with minimum investment in testing, however, is relatively immediate and requires reduced effort: the stress-strain curve of the annealed steel grade considered for each given strip thickness gives already a

good prediction. For steels that exhibit a Lüders plateau, strain rate effects need to be considered and this requires a few more tensile testing with the physical simulation procedure detailed in **§2.3**.

7/ CONCLUSIONS

The main conclusions are :

Experiments :

- Routine strain rate tensile testing on B.A. annealed AISI430 steel strip showed that the strain to fully eliminate YPEL is 2.5%. At equal processing strain, the predictions from CH0 tensile testing require a much higher elongation than found in the pilot mill experiments.

- YPEL of B.A. strip depends on the strip thickness, with a minimum around 1.0 mm.

- The strain to suppress YPEL decreases with the increase of strain rate. The YPEL elimination strain determined from the CH0 low SR tension on B.A. strip is larger than from the higher strain rate physical simulation of the rolling step.

- No significant difference in hardening rate and uniform elongation was observed between the as-annealed and skin passed AISI430 strips examined.

- The difference in processing strain to suppress YPEL found between the pilot mill real rolling (0.6-0.8%) and its physical simulation (1.5%) is attributed to the nominal elongation being achieved in several passes in the first case. The physical simulation conditions are therefore closer to the one stroke elongation taking place in the industrial mill and they should be used to construct a local LDH model which starts hardening before the macro measure YPEL.

Numerical modeling :

- A Continuous Hardening CH constitutive model based on equivalent strain as the only history parameter is enough for predictions of tensile properties of steels that do not develop extended yield elongation. A more general and refined description requires a Local Deformation Hardening LDH model. The LDH model eliminates YPEL with a fraction of the macroscopic strain required by the CH model and develops bands of higher deformation that sweep the tensile specimen during its testing.
- The plastic strain predicted by the skin pass rolling model is about 16% higher than the engineering elongational strain, as the result of shear strain components in the process. The base industrial configuration develops local strains that are in average 25% higher than a no-bending case.

- No substantial differences were found by modelling the working rolls as rigid or elastically deformable.
- Strain rates during skin pass reaches values 2-3 orders of magnitude higher than the routine characterising test.

- The main difficulty found in the project was the FEM simulation of the skin pass rolling. Due to the small plastic deformation involved, the solution becomes controlled by contact algorithm. Of the several option examined: soft contact allowing some virtual roll/strip interference to

accommodate the different curvature ratios, use of quadratic elements and mesh refinements, only the last option was successful. However, the small thickness of the elements in the strip and their maximum allowed aspect ratios imposed a large discretisation effort which severely penalised the solution turnaround time. A simulation for the real 3D width was unthinkable with these constraints.

- A technique that maps 2-dimensional Plane Strain rolling deformation results upon either a SGLS segment or a full ISO80 specimen was developed with a successful outcome. It combines the fastest turnaround of the rolling model with the accurate tensile predictions of a full 3D model. It has been applied to both pilot mill and industrial configuration and results validated.

Overall conclusions :

- Good agreement in all tensile properties up to uniform strain can be obtained from a LDH model constructed from a single tensile test of the annealed material. The predicted YPEL is however overevaluated by this simulation for the higher strain rates corresponding to the bigger skin pass reductions. An improvement can be obtained from data obtained by a skin pass physical simulation followed by standard tensile testing, and these used to construct a model of the LDH type that has shown to perform best.

- An off-line simple model for plant use has been developed, which needs to be feed by the processing parameters and annealed material properties.

- The application of the model to TK-AST line data revealed a configuration fairly optimised, with marginal gains for the AISI430 steel studied. The potential application of the model to other grades however, is relatively immediate and requires limited mechanical testing effort.

- The most important conclusion of the Project is that YPEL elimination does not depend only on the accumulated strain, but on a combination of this with strain rate. For the 0.6 mm thickness AISI430 strip a threshold strain rate (order 0.13 s^{-1}) was identified, above which YPEL vanishes in subsequent tension earlier than predicted by the continuous testing at the routinely low strain rate of the characterising test (10^{-3} s^{-1}). This result from a physical simulation by tension, which involves a deformation mode very different than rolling with or without bending and tension, suggests that skin pass is not a requisite to eliminate YPEL and this could be achieved even by purely bending provided that the strain rate is high enough (0.13 s^{-1}). Such value is still reachable in industrial configurations, but not necessarily in lower speed pilot mills, where also maintaining the strip at a steady tension longitudinal differential that is uniformly distributed across width is not as difficult as for the industrial strip width (1200 mm).

List of references :

1 B. J. Brindley and P. J. Worthington, 'Yield-point phenomena in substitutional alloys', Metallurgical Reviews, 145, The Metals and Metallurgy Trust.

2 R. D. Butler and D. V. Wilson, 'The mechanical behaviour of temper rolled steel sheets, J. Iron and Steel Inst., 1963, 201,16

3 E. J. Hoggan, R. I. Scott, M. ZR. Barnett, P.D. Hodgson, 'Mechanical properties of tension levelled and skin passed steels', J. Mat. Proc. Tech., 125-126 (2002) 155-163.

4 M. Verduzco and N. H. Polakowski, 'Control of Lüders markings on mild steel strip by roller-flexing under tension', J. of The Iron and Steel Institute, October 1996, 1027-1033.

5 F. Garofalo, The effect of grain size and cross head velocity on the lower yield strength during inhomogeneous discontinuous yielding, Met. Trans. A, 4, 1973, 1557-1561

6 F. Yoshida, 'A model of cyclic viscoplasticity with special reference to yield-point phenomena', XXI ICTAM, 15-21 August 2004, Warsaw, Poland.

7 J. D. Baird, 'The effects of strain ageing due to interstitial solutes on the mechanical properties of metals' Metallurgical Reviews, 149, The Metals and Metallurgy Trust, 1971

8 N. Brown and K. F. Lukens, 'Microstrain in polycristalline metals', Act. Metall.,9 (2), 1961,106-111

9 D. Grandemange, H. Tsukahara, E. Vasseur, J.C. Herman, D. Pütz 'Control of the yielding and ageing behaviour in temper rolling ', ECSC 7210-PR/035, Technical Steel Research series, Final Report EUR 20214 EN, ISBN: 92-894-3366-3, Office for Official Publications of the EU, Luxembourg, 2002, 108 pgs.

10 Y. Estrin, Spatial coupling and propagative plastic instabilities in Continuum Models for materials with microstructures. John Wiley and sons Ltd, 1995, 395-450

11 Estrin Y. And Kubin L. P., 'Plastic instabilities: phenomenology and theory', Materials Sci and Eng., A137 (1991) 125-134.

12 D. Pütz, E. Neuschütz, M. Scherer, Investigation of Procedures for Optimizing Skin Pass Rolling, ECSC 7210-EA/143, CECA 7210-EA/144, Final Report, 1998

13 M. Lubrano, J. H. Bianchi, P. Pütz , H. Mennicken, M. Scherer. 'Development and testing of procedures for optimising the degree of strip reduction during skin-pass rolling', Technical Steel Research series, Final Report EUR 18917 EN, ISBN 92-828-7169-X, Office for Official Publications of the EU, Luxembourg, 1999, 118 pgs.

14 M. Lubrano, J. H. Bianchi , ' A simple model for on-line control of skin pass from FEM analysis of rolling deformation',2nd Int. Conference on Modelling of Metal Rolling Processes, The IOM, London, Dec. 1996.

15 Hibbitt, Karlson and Sorensen, ABAQUS ® Standard, User's Manual

16 B. Peeters , M. Seefeldt, C. Teodosiu, S. Kalidindi, P. Van Houtte, E. Aernoudt 'Work-hardening/softening behaviour of polycrystals during changing strain paths: I. An integrated model based on substructure and texture evolution, and its prediction of the stress-strain behaviour of an IF steel during two-stage strain paths', Act. Mater., 49 (2001), 1607-1619.

17 Y. Estrin and L. Kubin,'Local strain hardening and nonuniformity of plastic deformation', Acta Metall., 34, 12, 1986, 2455-2464

18 J. Simo, F. Armero, 'Geometrically nonlinear enhanced strain mixed methods and the method of incompatible modes', International Journal for Numerical Methods in Engineering, 110, 1993, 359–386.

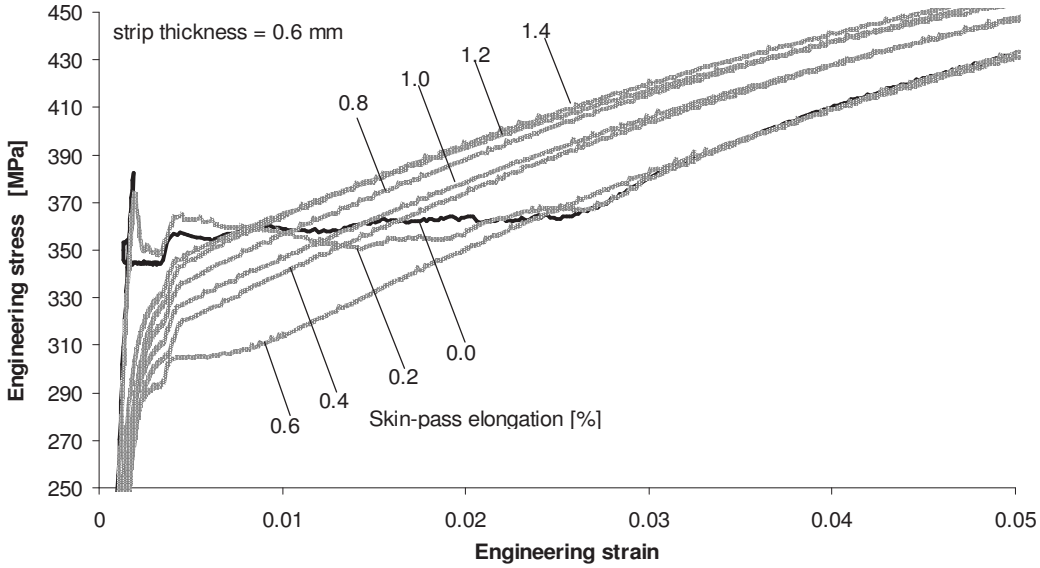

Figure 1 - Tensile testing results for strips of 0.6 mm thickness, skin pass rolled at different percentage elongations. Strain rate=$2x10^{-3}$ s^{-1}.

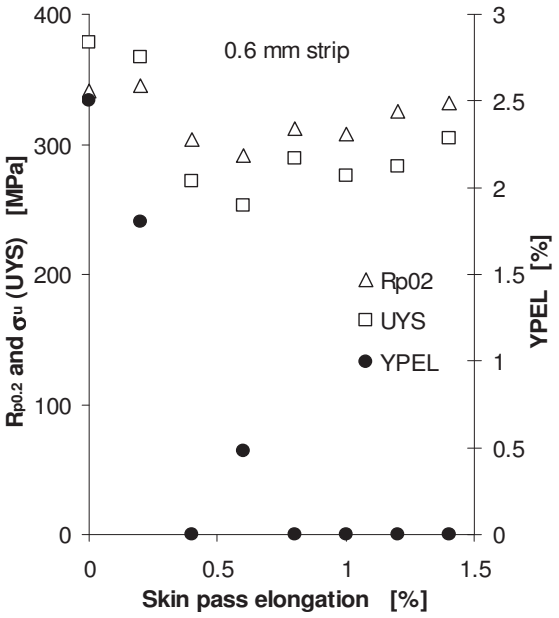

Figure 2 - Effects of percentage of skin pass elongation on yield stresses and on extension of the yield point elongation; initial thickness = 0.6 mm, strain rate=$2x10^{-3}s^{-1}$.

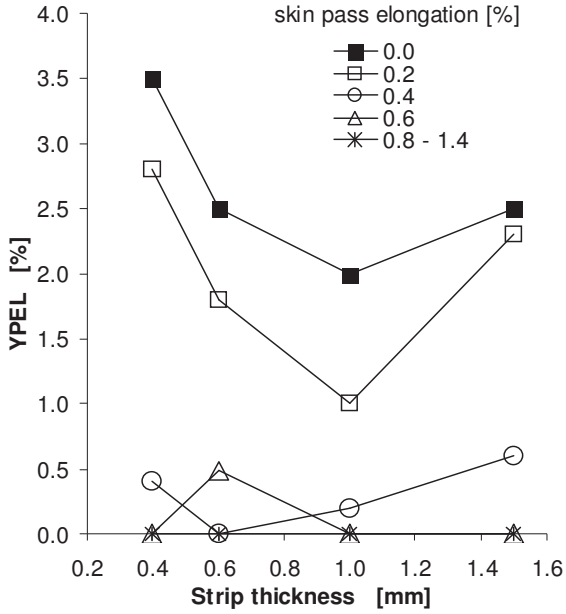

Figure 3 - Experimental tensile testing of the studied ferritic stainless steel strip: variation of YPEL with the degree of skin pass elongation for initial thickness ranging from 0.4 to 1.5 mm. Routine strain rate=$2x10^{-3}$ s^{-1}.

ID	cast ID	Thickness (mm)	Chemical composition [%]										
			C	Si	S	Nb	Mn	Cr	Ni	Mo	Cu	N	V
848732	553833	1.0	0.044	0.52	0.001	0.01	0.36	16.12	0.21	0.015	0.16	0.032	0.068
848736	553833	1.5	0.044	0.52	0.001	0.01	0.36	16.12	0.21	0.015	0.16	0.032	0.068
855414	467867	0.6	0.039	0.31	0.001	0.01	0.33	16.19	0.19	0.015	0.16	0.037	0.072
855024	554007	0.4	0.036	0.24	0.001	0.01	0.31	16.03	0.17	0.015	0.12	0.035	0.072

Table 1 - Chemical composition of the studied steel.

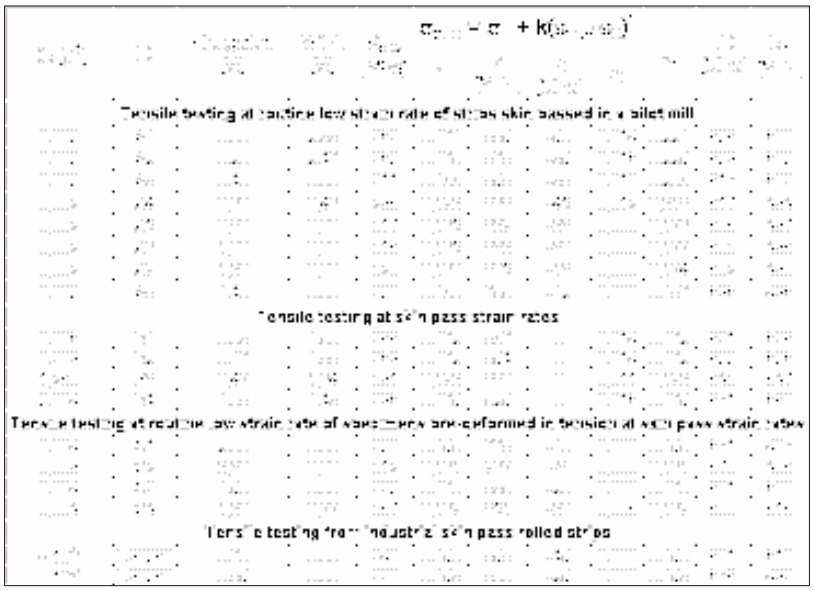

Table 2 – Conditions and main experimental results for tensile testing of 0.6 mm initial thickness, AISI430 strip.

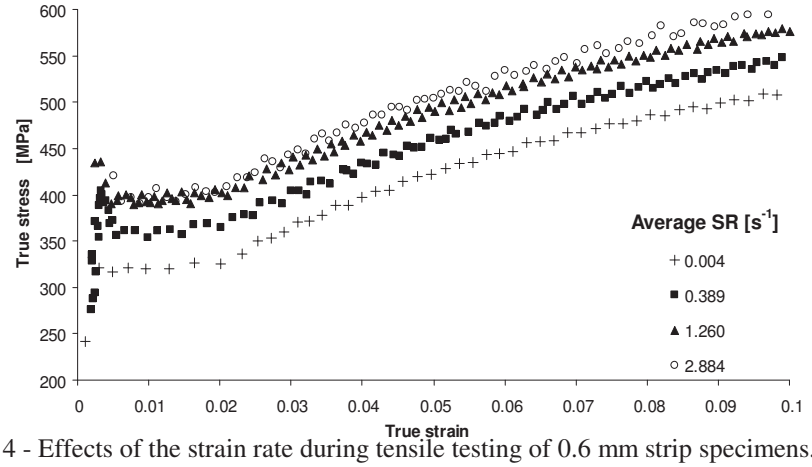

Figure 4 - Effects of the strain rate during tensile testing of 0.6 mm strip specimens.

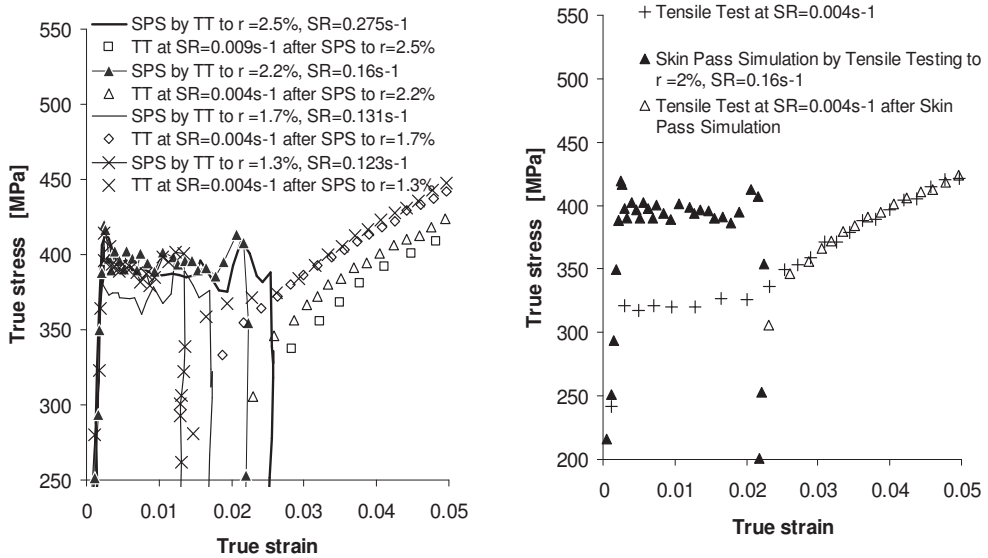

Figure 5 – Simulation of skin pass rolling by tension testing followed by tensile testing at routine low strain rate: (a) results for different elongations; (b) comparison of tensile testing at routine strain rate with and without prestraining at higher strain rate. SPS=Skin Pass Simulation, TT=Tensile Test, SR=strain rate.

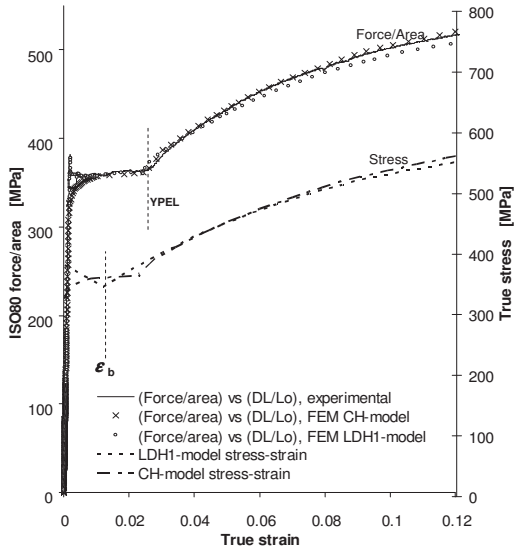

Figure 6 - ISO80 tensile testing of a B.A., 0.6 mm thickness ferritic stainless steel strip. Comparison of stress-strain results from experiments and 3D-FEM simulation.

Model ID	σ, σ_u, σ_b, ε_b, ε $a = \sigma_u$, $b = (\sigma_u - \sigma_b)/\varepsilon_b$	Parameters for as-annealed strip steel
CH	$\varepsilon \le \varepsilon_b : \sigma = a - b\varepsilon$ $\varepsilon > \varepsilon_b : \sigma = k\varepsilon^n$	$\varepsilon_b = 0.023$ $a = 365MPa, b = 0MPa$ $k = 865MPa, n = 0.214$
LDH1	$\varepsilon \le \varepsilon_b : \sigma = a - b\varepsilon$ $\varepsilon > \varepsilon_b : \sigma = k\varepsilon^n$	$\varepsilon_b = 0.012$ $a = 382MPa, b = 3055MPa$ $k = 865MPa, n = 0.214$
LDH2	$\varepsilon \le \varepsilon_b : \sigma = a - b\varepsilon$ $\varepsilon > \varepsilon_b : \sigma = k(\varepsilon - \varepsilon_0)^n$	$\varepsilon_b = 0.016$ $a = 383MPa, b = 3676MPa$ $k = 795MPa, \varepsilon_0 = 0.014, n = 0.16$
LDH3	$\varepsilon \le \varepsilon_b : \sigma = a - b\varepsilon$ $\varepsilon > \varepsilon_b : \sigma = \sigma_0 + k(\varepsilon - \varepsilon_0)^n$	$\varepsilon_b = 0.016$ $a = 383MPa, b = 3676MPa$ $\sigma_0 = -150MPa, k = 1015MPa$ $\varepsilon_0 = 0.0045, n = 0.17$

Table 3 - Summary of the constitute models used.

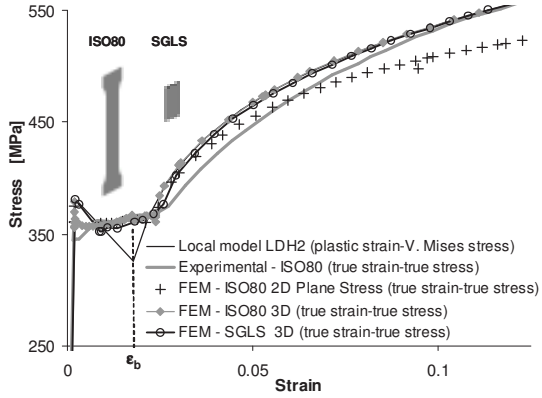

Figure 7 - Comparison of experimental and both 2D-Plane Stress and 3D-FEM simulation results of true stress vs. macroscopic logarithmic strain for the tensile testing. The LDH2 local model used in the simulations is also shown; 0.6 mm thickness strip, as-annealed ferritic stainless steel AISI430.

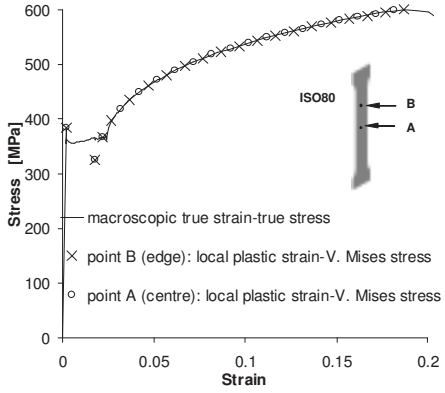

Figure 8 - Comparison of macroscopic and local strain-stress results from LDH2 FEM simulations of ISO80-3D cut from a 0.6 mm thickness strip, as-annealed ferritic stainless steel AISI430.

LDH1 model base parameters $\varepsilon_b = 0.012$, $\sigma_b = 346$ MPa, $\sigma_u = 382$ MPa, $n = 0.214$, $\varepsilon_o = 0$, $k = 865$ MPa			
All other parameters as BASE above	Variable parameter	YPEL	R_{p02} [MPa]
	ε_b =0.003	0.0097	356
	ε_b =0.012	0.0208	367
	ε_b =0.021	0.0258	367
	σ_b =326	0.0228	350
	σ_b =346	0.0208	364
	σ_b =366	0.0189	371
	σ_u =362	0.0164	354
	σ_u =382	0.0208	364
	σ_u =402	0.0235	374

Table 4 - Simulation results for tensile testing of as-annealed strip. Sensitivity analysis on the effect of the LDH1 model constants on the main tensile testing parameters.

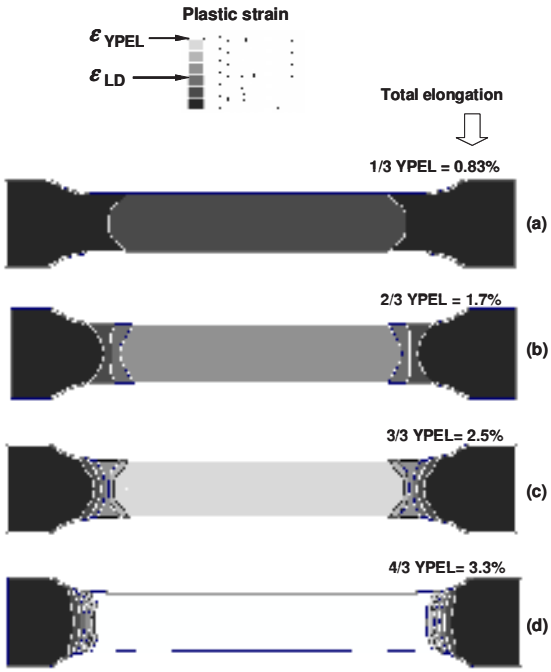

Figure 9 - Comparison of the percentage total elongation and the local strain during ISO80 tensile testing, 3D-FEM simulation with the CH model, B.A., 0.6 mm thickness ferritic stainless steel strip.

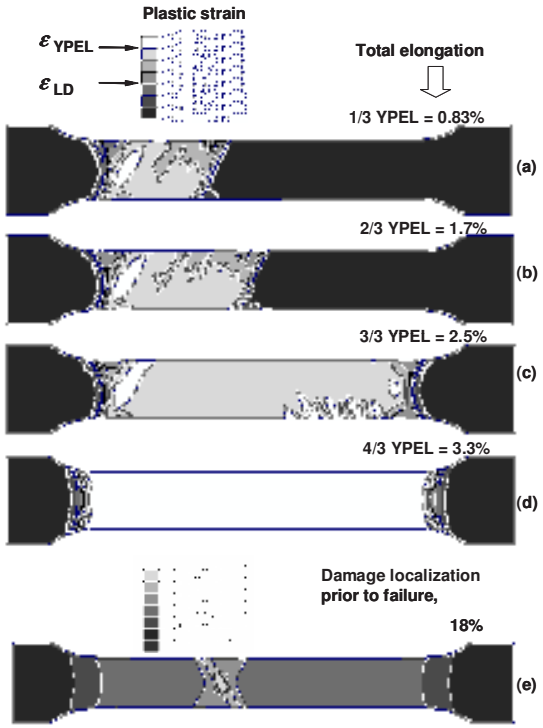

Figure 10 - Comparison of the percentage total elongation and the local strain during ISO80 tensile testing, 3D-FEM simulation with the LDH1 model, B.A., 0.6 mm ferritic thickness stainless steel strip.

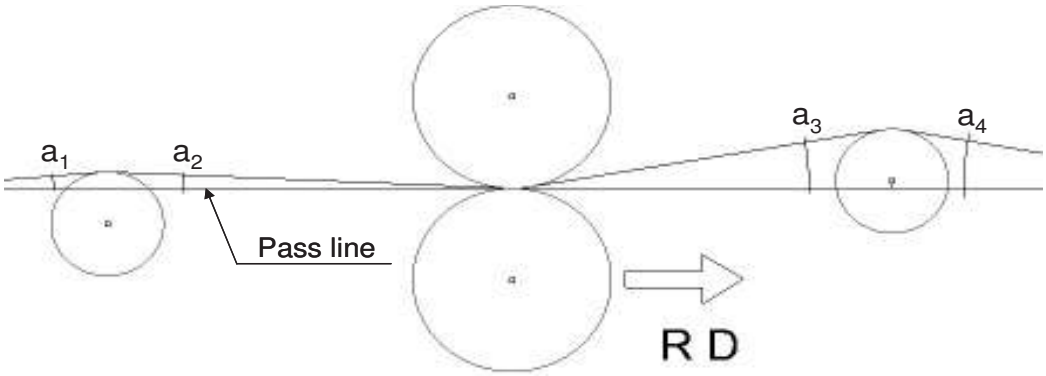

Figure 11 - Geometry of the final process step industrial configuration.

(a)

Strip initial thickness [mm]	Width [mm]	Backward tension [tonn]	Forward tension [tonn]	Elongation
0.6	1270	7.2	7.2	0.7%

(b)

	ID	a_1	a_2	a_3	a_4	Thickness reduction [%]	Forward tension increase [%]
Incoming strip angle effect	B030	10.83°	10.96°	9.96°	10.30°	0.74	0.0
	B020	7.57°	6.08°	9.96°	10.30°	0.74	"
	B010	5.6°	3.44°	9.96°	10.30°	0.74	"
Base	B000	4.9°	2.56°	9.96°	10.30°	0.73	"
Thickness reduction effect	B100	4.9°	2.56°	9.96°	10.30°	0.17	"
	B200	4.9°	2.56°	9.96°	10.30°	0.29	"
	B300	4.9°	2.56°	9.96°	10.30°	0.38	"
	B400	4.9°	2.56°	9.96°	10.30°	0.59	"
	B500	4.9°	2.56°	9.96°	10.30°	0.82	"
	B600	4.9°	2.56°	9.96°	10.30°	1.01	"
	B700	4.9°	2.56°	9.96°	10.30°	1.19	"
	B800	4.9°	2.56°	9.96°	10.30°	1.42	"
Forward tension effect	B001	4.9°	2.56°	9.96°	10.30°	0.74	10
	B002	4.9°	2.56°	9.96°	10.30°	0.75	20
	B003	4.9°	2.56°	9.96°	10.30°	0.76	30
Magnitudo of tension	C001	0	15	15	0	1	BT=5.6tons, FT=6.8tons
	C002	0	15	15	0	1	BT = 0.56tons, FT = 0.68tons
	C003	0	15	15	0	1	BT = 0.112tons, FT = 0.136tons

Table 5 - Industrial configuration studied: (a) base parameters; (b) varying parameters considered. BT=Backwards Tension, FT=Forward Tension.

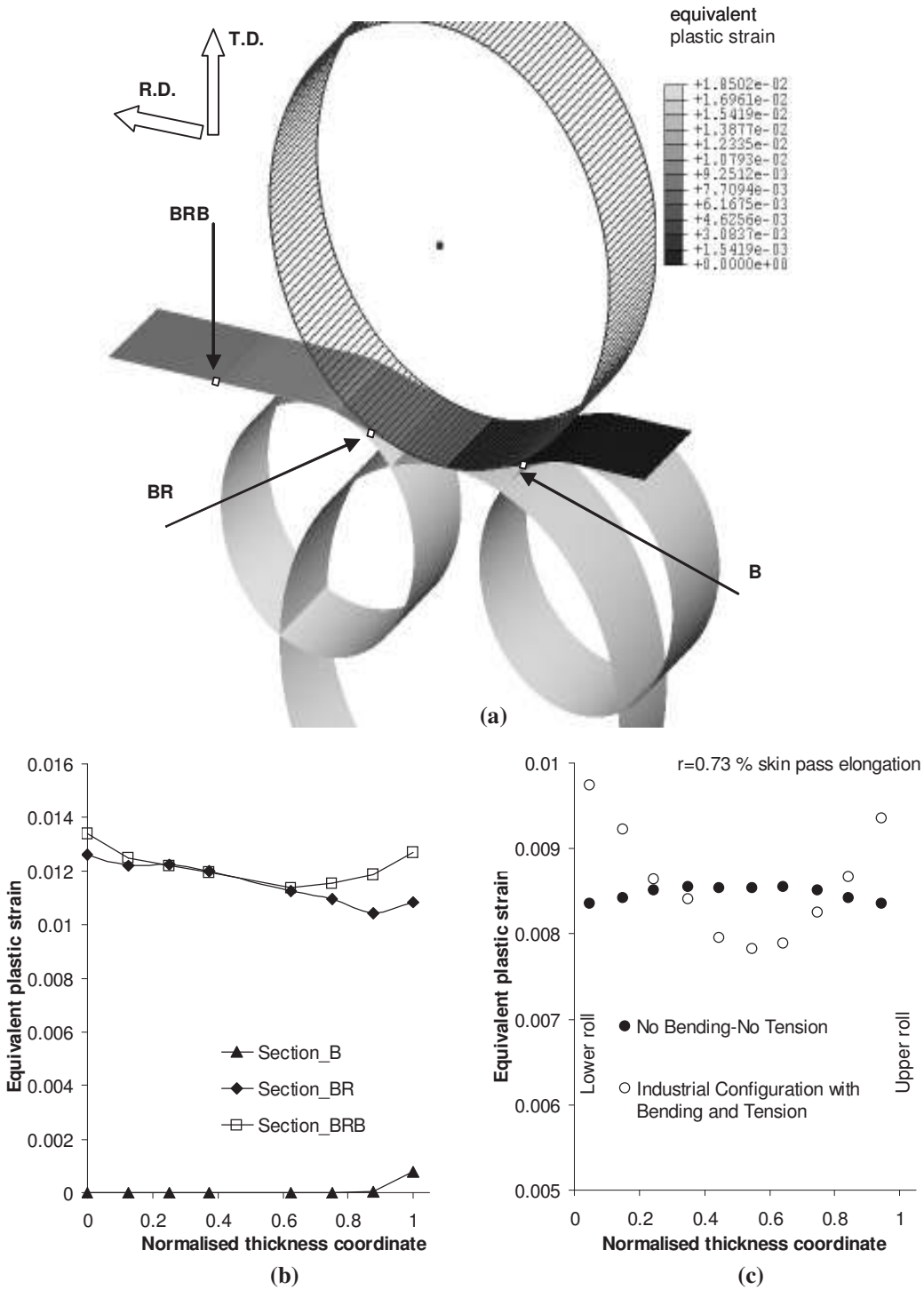

Figure 12 - (a) Evolution of plastic strain as predicted by a 2D Plane Strain simulation with LDH3 model, 0.6 mm initial strip thickness, industrial configuration with 440 mm roll diameter, 0.1 Coulomb friction; (b) effects of the antigripping, skin pass and gripping rolls on the evolving through-thickness plastic strain for angles $a_2=a_3=15°$, $a_1=a_4=0°$ and skin pass elongation 1.08%; (c) comparison at 0.73% common skin pass elongation of through-thickness strain between no-tension no-bending ($a_1=a_2=a_3=a_4=0°$) and $a_1=9.96°$, $a_2=4.90°$, $a_3=2.56°$, $a_4=10.30°$, 7.2 tons backward and forward tensions.

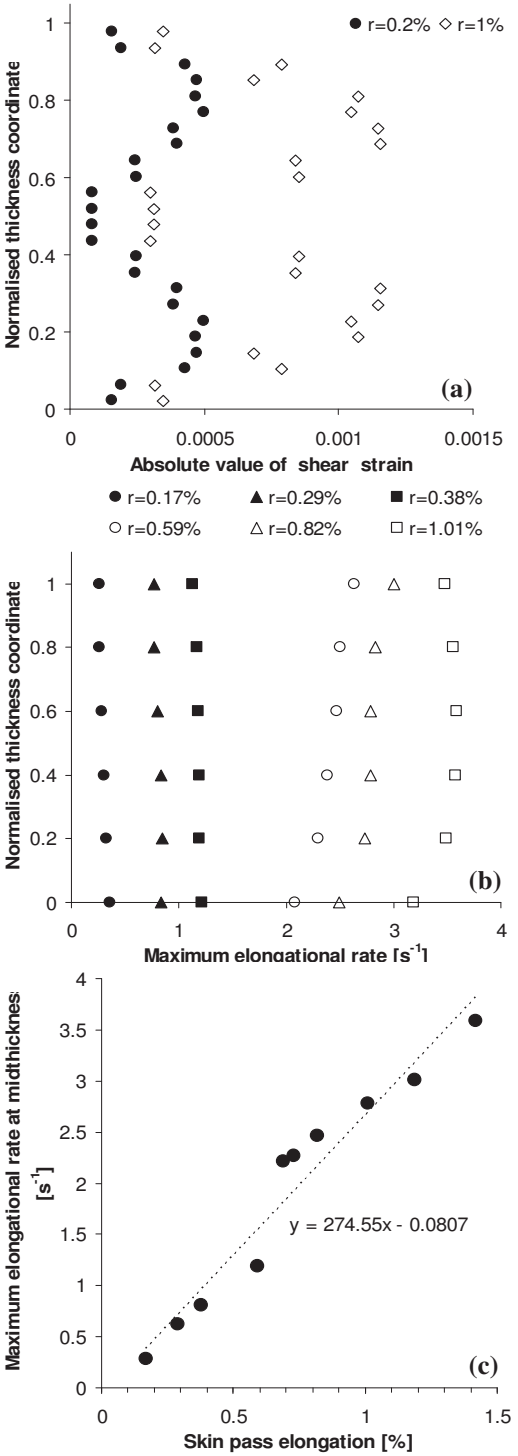

Figure 13 - Skin pass rolling simulation, LDH3 constitutive model, 0.1 Coulomb friction, 0.6 mm initial strip thickness, several skin pass elongations r [%]: (a) through-thickness maximum shear strain for no-bending conditions, pilot mill; (b) through-thickness maximum elongational rate for industrial configuration (serie Bx00, Table 5); (c) dependency of the maximum elongational rate at the strip midplane with the percentage of skin pass elongation for industrial configuration (serie Bx00).

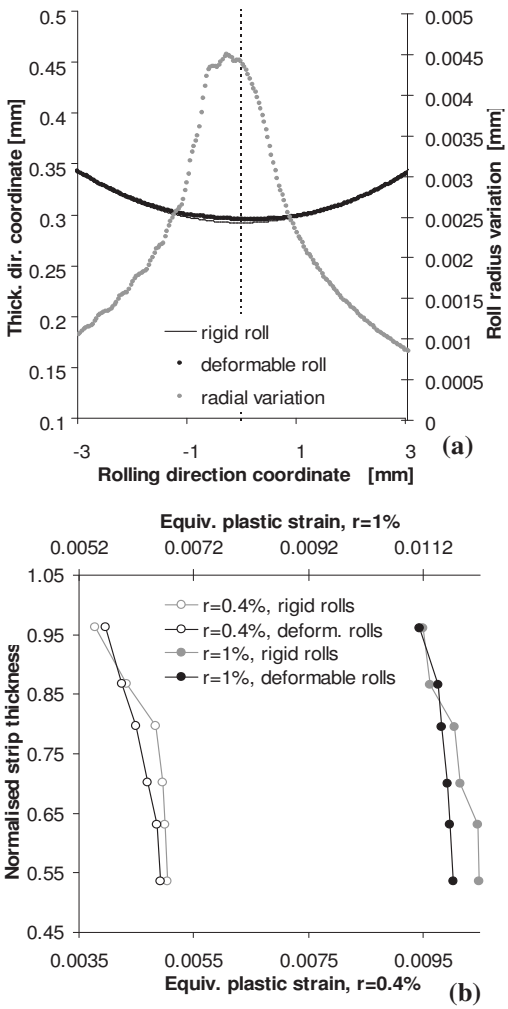

Figure 14 - Comparison of skin pass simulations results obtained by applying the rigid and deformable rolls assumptions: (a) roll flattening effects; (b) effect of the roll hypothesis on the resulting through-thickness strain profile for two reductions. Plane Strain 2D simulations, 180 mm roll diameter, 0.6 mm initial strip thickness, 0.1 Coulomb friction, no-tension, no-bending.

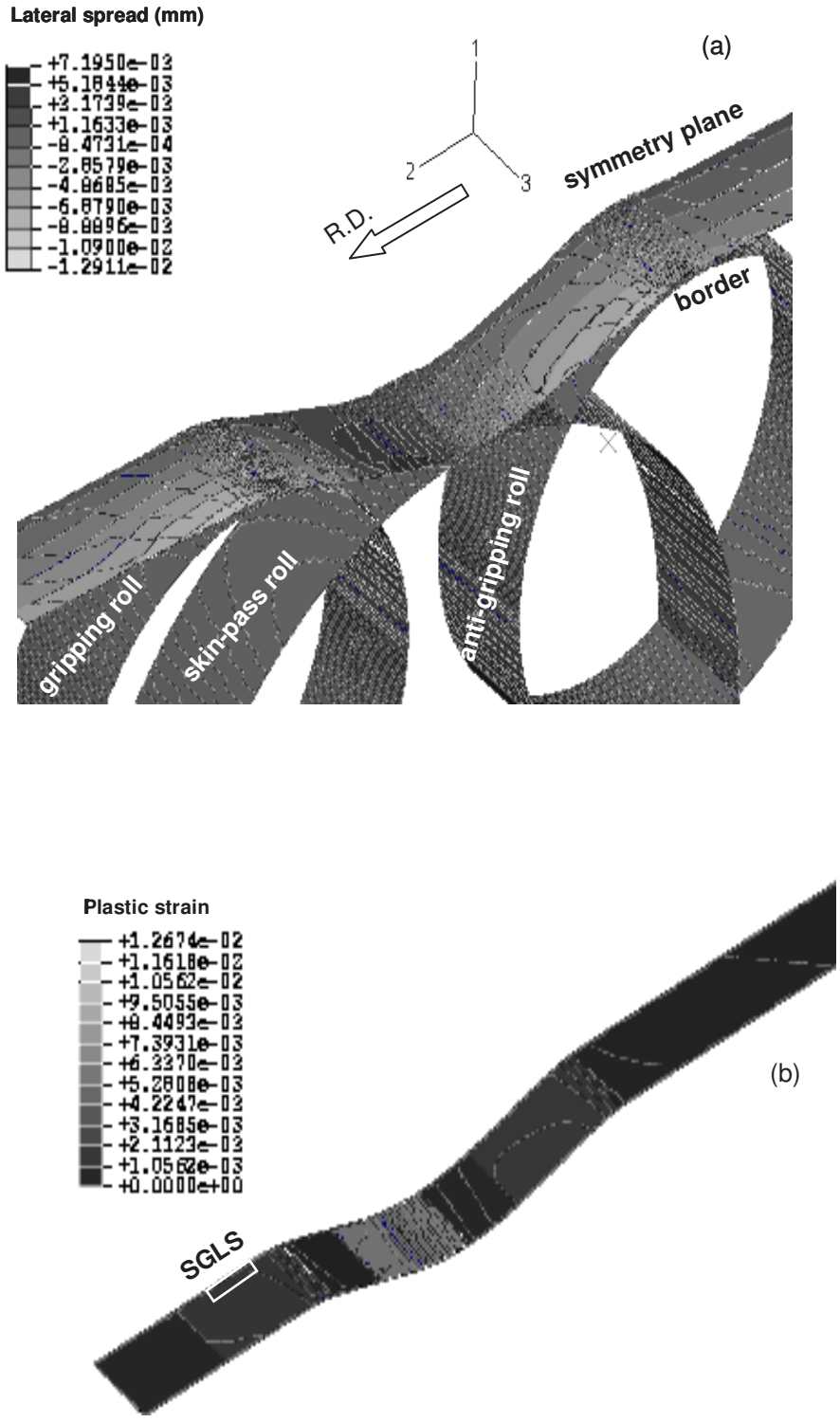

Figure 15 - 3D simulation of the last step configuration, 0.6 mm initial thickness, 1.08% elongation: (a) detail of lateral displacements (parallel to roll axis); (b) resulting plastic strain. SGLS=segment to be isolated for tensile testing.

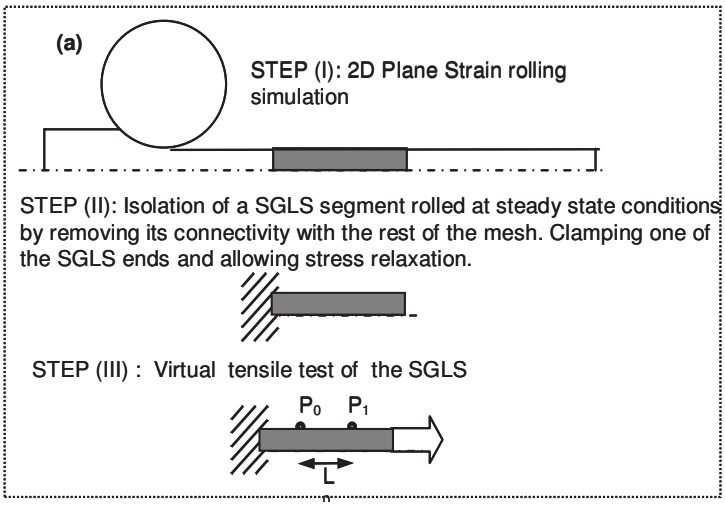

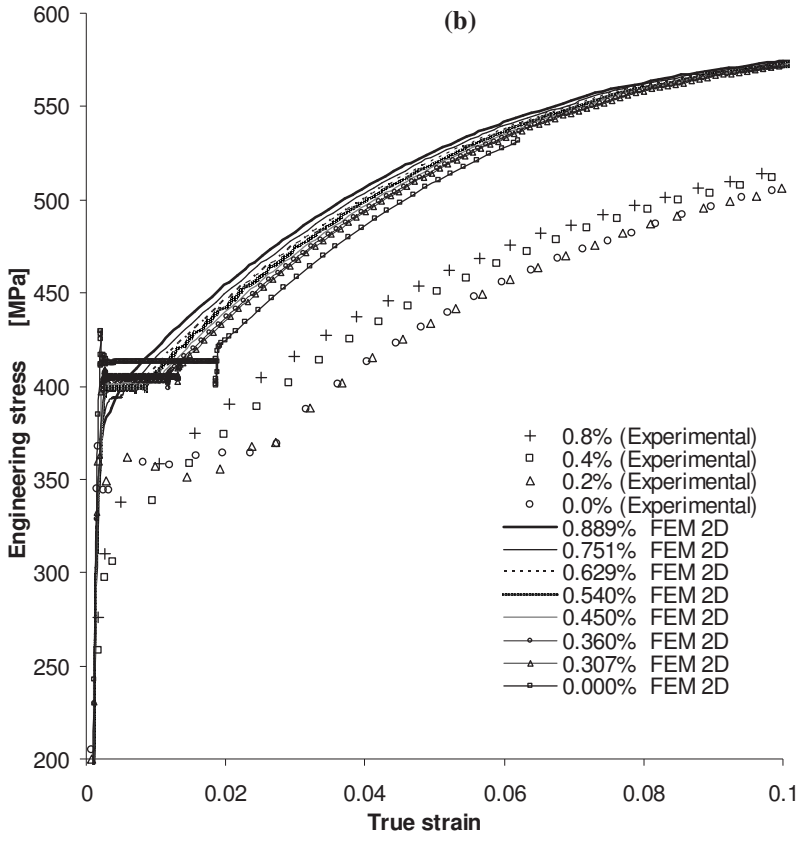

Figure 16 - Combined 2D-FEM skin pass pilot mill rolling and 2D-SGLS tensile test simulations: (a) procedure to decouple the SGLS segment used to perform the tensile test; (b) comparison of experimental and Plane Strain 2D-FEM simulations after skin pass elongations in the range 0% to 0.89%.

Thickness reduction	Lüders plateau	YPEL [%]	Upper Yield Stress [MPa]	Lower Yield Stress [MPa]
0.000%	Yes	1.8	429.0	410.74
0.307%	Yes	1.3	408.8	404.80
0.360%	Yes	1.1	407.2	402.80
0.450%	Yes	1.04	404.6	400.80
0.540%	Yes	0.85	401.2	398.84
0.629%	Yes	0.7	398.3	397.00
0.716%	Yes	0.54	395.3	394.58
0.751%	Yes	0.49	393.8	393.80
0.803%	No	0	=	=
0.889%	No	0	=	=
0.975%	No	0	=	=

Table 6 – Tension testing parameters results from a 2D-SGLS simulation following a 2D Plane Strain skin pass rolling simulation.

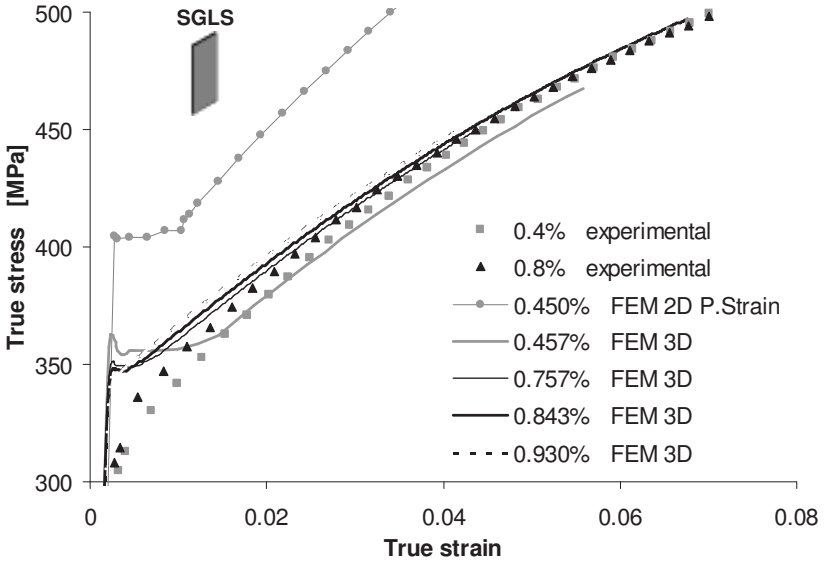

Figure 17 - Comparison of experimental vs. 3D tensile test simulation results for skin pass elongations ranging from 0% to 0.93%. Plane Strain 2D results for a 0.4% skin passed strip are also shown.

Thickness reduction	Lüders plateau	YPEL [%]	Upper Yield Stress [MPa]	Lower Yield Stress [MPa]
0.000%	Yes	2.03	380.7	357.5
0.191%	Yes	1.64	372.1	354.6
0.457%	Yes	1.19	360.6	351.4
0.671%	Yes	0.70	351.9	347.7
0.757%	Yes	0.54	348.1	345.7
0.843%	Yes	0.41	344.6	343.8
0.930%	No	0.30	341.5	341.5

Table 7 – Tension testing parameters results from a 3D-SGLS simulation following a 3D skin pass rolling simulation.

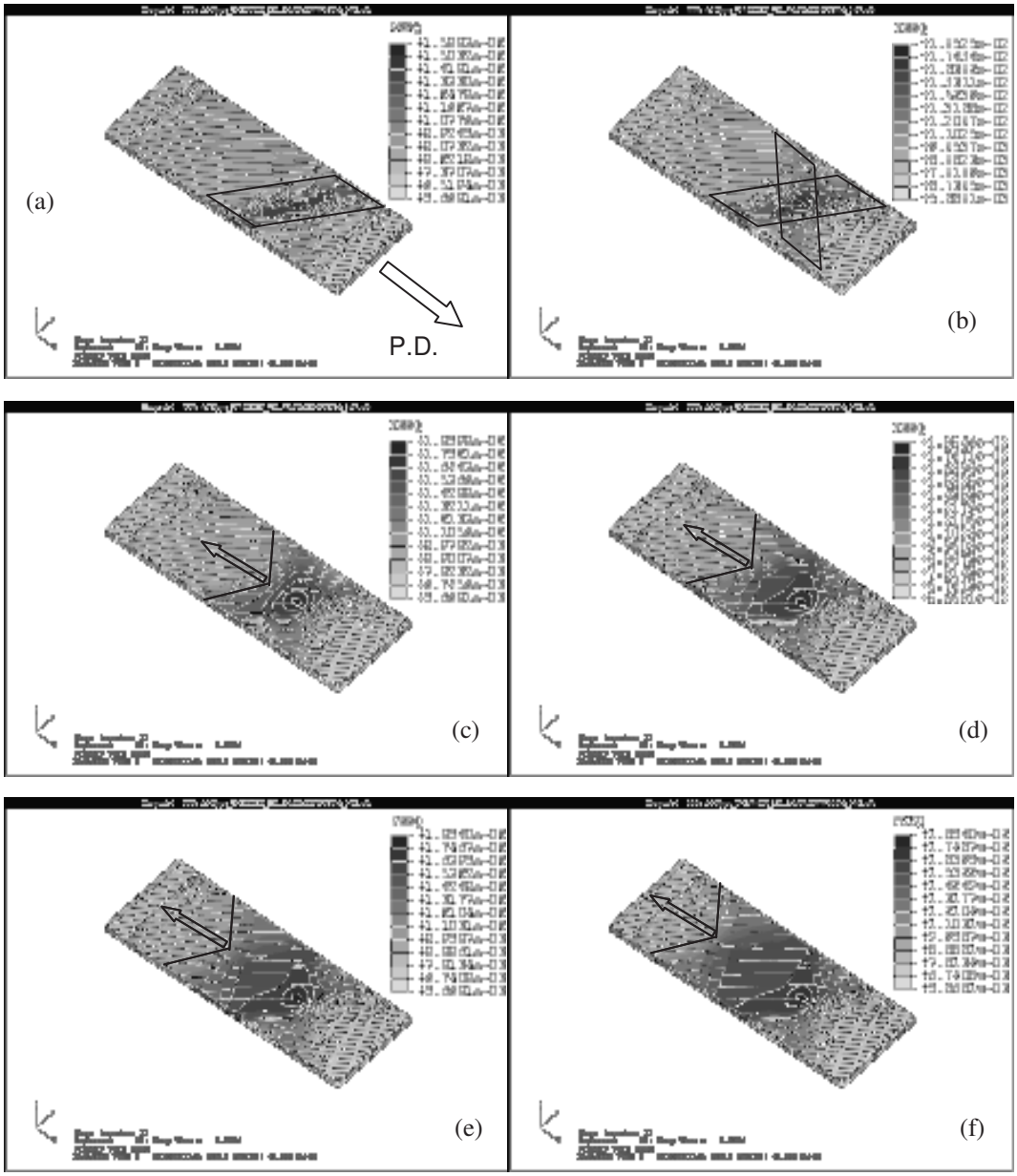

Figure 18 - Generation and propagation of Lüders bands during tensile testing; PD=Pulling Direction≡Rolling Direction. Images are sampled every 5 increments. Virtual tensile testing on a 3D-SGLS, skin pass elongation 0.457%, initial strip thickness=0.6 mm.

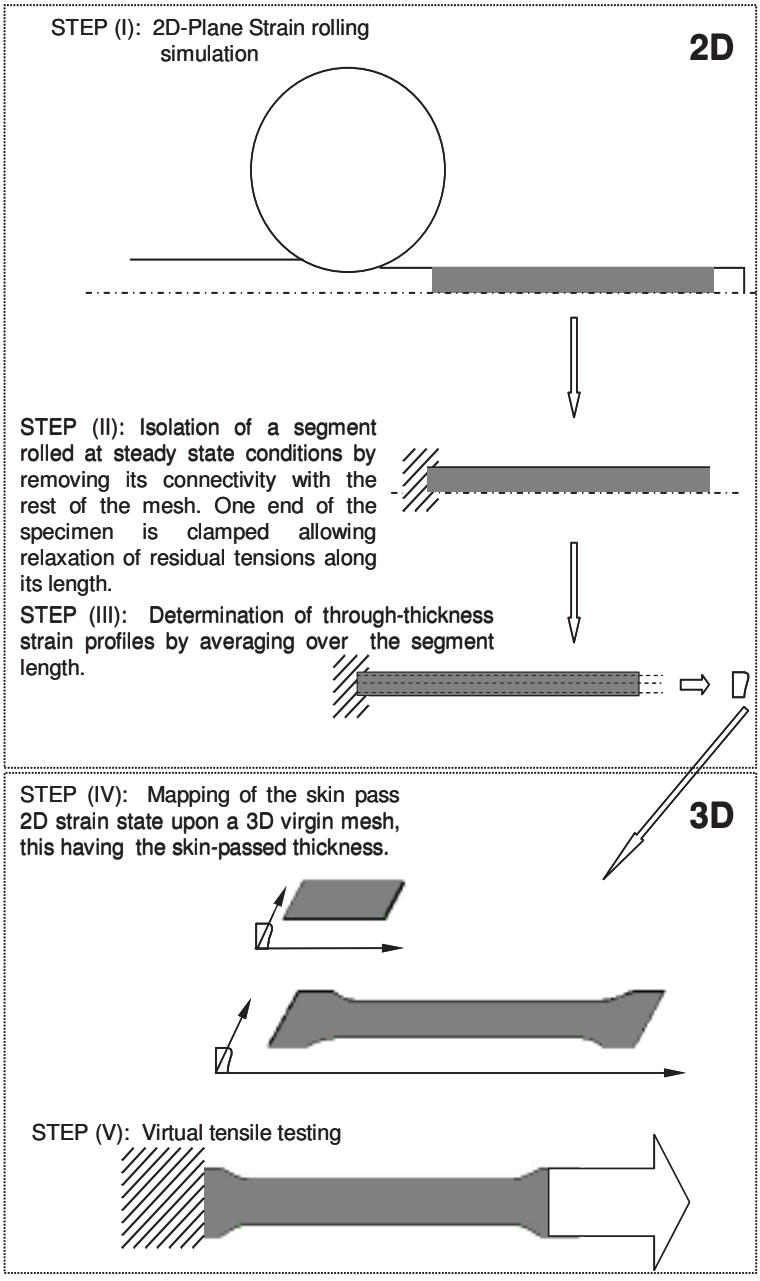

Figure 19 - Details of the procedure used to transfer the skin pass 2D-Plane Strain state to a 3D-specimen for ISO80 virtual tensile testing.

Skinpass elong. [%]	YPEL			$R_{p0.2}$ [MPa]			ε_u			R_m [MPa]			TS [Mpa]		
	exp.	FEM	diff. %	exp.	FEM	diff. %	exp.	FEM	diff. %	exp.	FEM	diff. %	exp.	FEM	diff. %
0.0	0.023	0.023	-1.8	359	352	-1.9	0.170	0.175	3.4	500	504	0.8	592	595	0.5
0.2	0.017	0.018	3.2	353	351	-0.6	0.175	0.172	-1.8	502	503	0.1	598	598	-0.1
0.4	0.000	0.015	-	275	344	24.9	0.165	0.170	2.6	502	503	0.1	593	592	-0.1
0.6	0.003	0.012	337	280	341	21.9	0.168	0.167	-0.4	495	504	2.0	585	596	1.8
0.8	0.000	0.009	-	296	336	13.4	0.165	0.164	-0.8	496	505	1.7	585	594	1.6
1.0	0.000	0.006	-	286	332	16.0	0.165	0.163	-1.7	496	507	2.4	585	598	2.2

Table 8 – Comparison of experimental and 2D Plane Strain rolling + 3D ISO80 tensile simulation results using the LDH3 model.

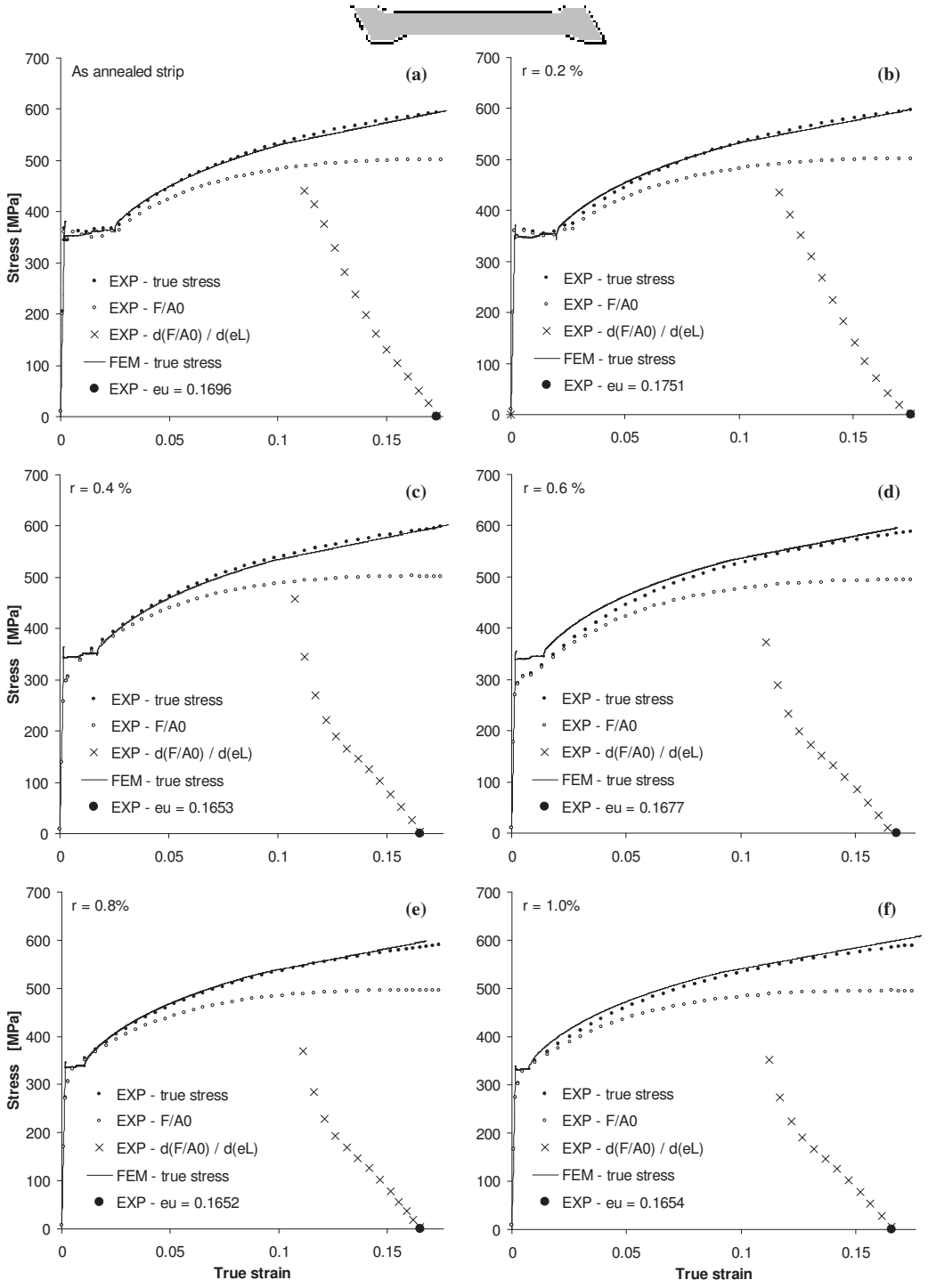

Figure 20 - Comparison of tensile testing experimental and 2DPS+3D ISO80 simulation results of skin passed strip at different elongations; 0.6 mm thickness strip, ferritic AISI430 steel, LDH3 constitutive model.

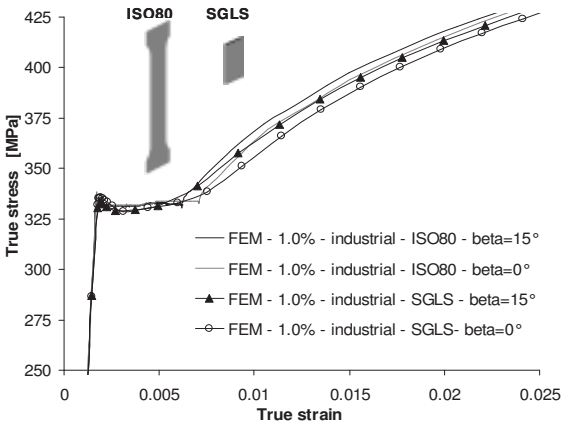

Figure 21 - Effect of the tensile specimen geometry: comparison in the yielding region of predictions obtained from mapping 2D skin pass results upon both ISO80 and SGLS specimens and performing virtual tensile testing on them; a_2=a_3=beta, backward tension=5.6 tons, forward tension=6.8 tons, initial strip thickness=0.6 mm, skin pass elongation=0.8%.

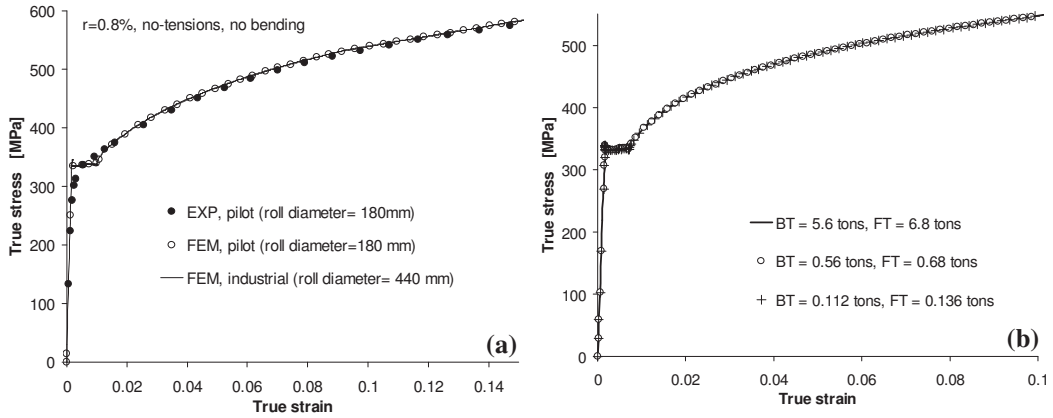

Figure 22 - (a) Effect of the skin pass roll diameter on tensile properties, LDH3 model predictions. Comparison under no-tensions no-bending conditions, initial strip thickness=0.6 mm, skin pass elongation=0.8%. (b) Effect of strip tensions at equal effective skin pass elongation=1% on tensile properties. Industrial configuration, 0.6 mm initial thickness strip. BT=Backwards Tension, FT=Forward Tension.

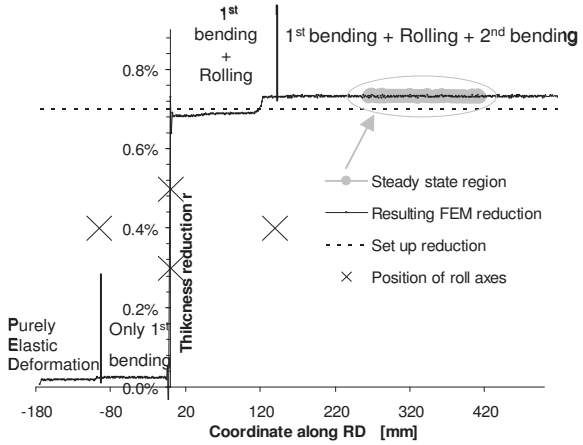

Figure 23 - Strip thinning at different positions of the last processing step.

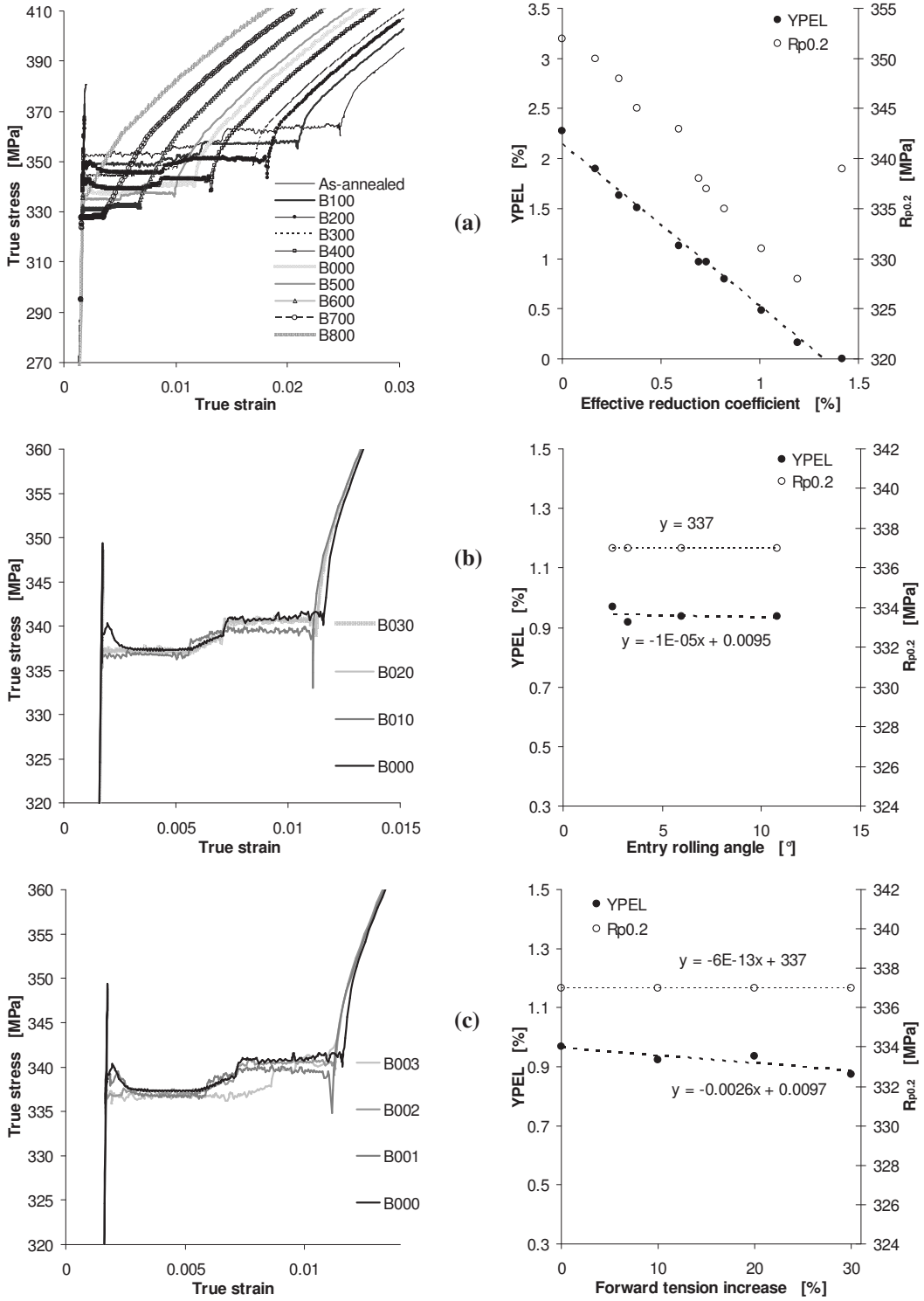

Figure 24 - Effect on tensile properties of changes in industrial parameters: (a) skin pass reduction; (b) entry angle a_2; (c) forward tension. Results from combined skin pass rolling – tensile testing FEM simulations, 0.6 mm initial thickness strip, LDH3 model.

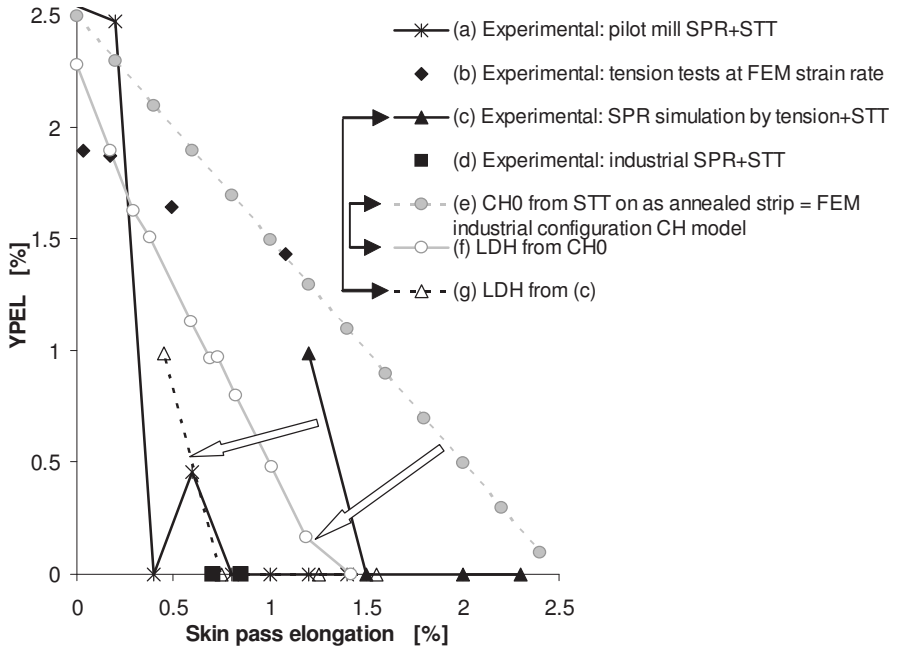

Figure 25 - Summary of YPEL measurements and predictions. SPR=Skin Pass Rolling; STT=Standard Tensile Test at strain rate of order 10^{-3} s^{-1}.

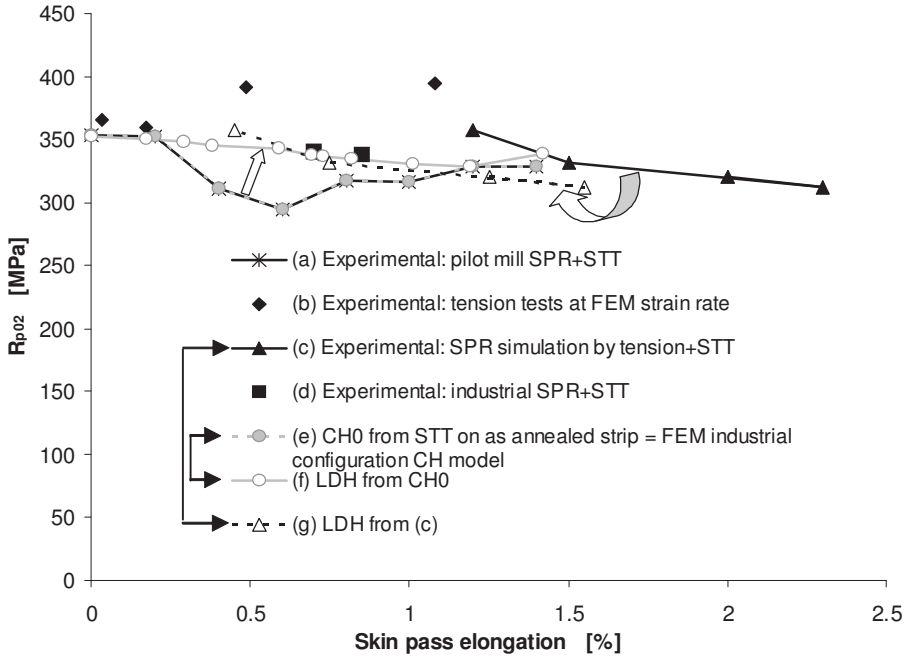

Figure 26 - Summary of R_{p02} measurements and predictions. SPR=Skin Pass Rolling; STT=Standard Tensile Test at strain rate of order 10^{-3} s^{-1}.

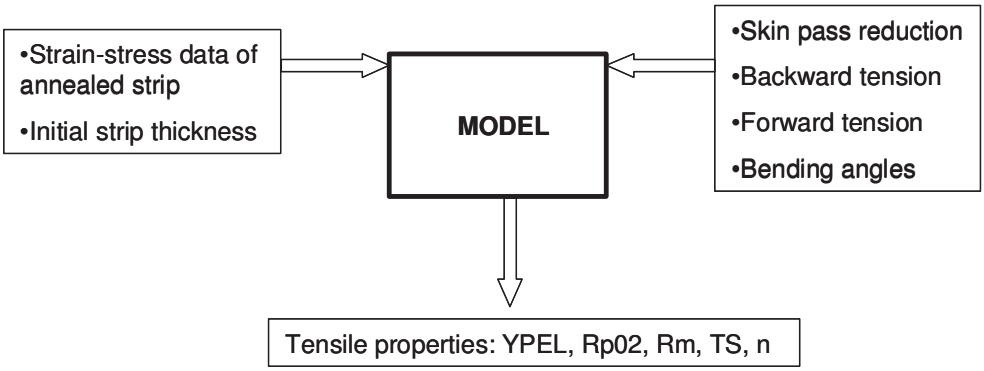

Figure 27 -Layout of the simplified model

FEM simulation studies : part 4 (Bending process)

List of tables and figures :

1/ INTRODUCTION

The Piobert-Lüders behaviour is a plastic instability that occurs in steels containing interstitial elements in solid solution such as carbon or nitrogen. These elements may segregate to dislocations during ageing and lock them. Under a subsequent tensile test, the specimen thus exhibits a strain localisation oriented at approximately 50° from the tensile direction, growing from one head of the specimen to the other. During this localisation propagation, the specimen response, force, is constant thus leading to what is called the yield point elongation.

This phenomenon is of prime importance for finishing lines such as temper rolling process, of which one of the main aims is to suppress the yield point elongation (YPEL) before steel sheet delivery to customers.

Dealing with the problem of sheet surface defects in finishing lines, this project is somehow the continuity of a previous ECSC project **(1)** in the field of Piobert-Lüders behaviour where it has been successfully shown that the Lüders phenomenom, which is at the heart of our project, can be satisfactorily modeled both in an uniaxial tensile test and during temper rolling process by means of a numerical procedure based upon finite element method.
The aim was to precise the temper rolling conditions necessary to suppress the YPEL as a function of the initial yielding behaviour of steel **(1, 2, 3)**

Because of the more than encouraging results gathered, ARCELOR RESEARCH SA has decided to go on using this modeling method but focused this time in the **course of bending (single or alternative) deformations, with or without surimposed tension**, that occur on deflecting rolls before or/and after the temper rolling process (one of the main final strip production steps).

These bending test simulations are considered as a crucial step towards the entire modeling of tension leveling process and industrial skin-pass lines including deflecting rolls.

2/ DESCRIPTION OF THE METHOD

The finite element codes are currently robust enough to carry out simulations of materials with a softening behaviour as in the case of the Lüders phenomenom. Once the strong interstitial pinning due to the Cottrell atmosphere is overcome, there is either an activation of dislocation sources or a release of the pinned dislocations, finally leading to a softening at the very area of the material.

The Lüders behaviour is the result of firstly, an increase in yield stress due to the dislocation pinning and secondly, a softening attributed to dislocations unpinning or multiplication. Given a local behaviour as simple as the dashed line in **Figure 1**, one should raise σ_0, the yield stress before ageing, of $\Delta\sigma$, in order to take into account the dislocation pinning.
During the tensile test, when the stress is locally high enough to overcome $\sigma_0 + \Delta\sigma$, i.e. high enough to unpin or activate new dislocations sources, the material softens on a certain strain increment ($\Delta\varepsilon$) before reaching its actual hardening behaviour. $\Delta\varepsilon$ is related to the easiness of the band propagation, which in turn is linked to the number of obstacles encountered by a band front during its movement. These obstacles are mainly grain boundaries. It has been suggested a direct proportional relationship between grain size and Lüders band velocity, which is also proportional to the strain rate.

3/ FEM LÜDERS MODELING OF BENDING DEFORMATION PROCESS

3-1 Preliminary qualitative aspects

The above paragraph has established the physical basis of our modeling, which is mainly the description of the local constitutive behaviour of a Lüders material.

We then modeled a simple three-roll system 2D bending deformation test using the finite element code ABAQUS.

The parts assembly consists in :

- a 3mm thick, 1m long material with 5 mesh elements through the thickness to start with.
- 3 Φ 60mm rigid body rolls : 1 upper imbrication roll and 2 lower fixed rolls (inter axis 70mm)

We directly got ourselves inspired by the previous ECSC contract (B) to chose both the mesh element type (namely CPS4R : four nodes linear plain stress elements with reduced integration in ABAQUS words) and the local constitutive behaviours (with and without the Lüders phenomenom) these later being illustrated in **Figure 2**.

Contact between the sheet and rolls is of the **softened type** and **no surimposed tensions** are applied.

The sketch of the whole system is in **Figure 3**.

Nota : the choice for dimensioning such a system is typical of a leveling process. The ratio between rolls diameters and inter-axis ≈ 1,15 ensures plastic deformation in the material thickness, depending of course on the degree of intermesh performed.

3-1-1 FEM numerical simulation results :

Proof is made that the introduction of a local constitutive behaviour taking into account the Lüders phenomenom, still allows us to simulate the appearance of Lüders bands.
To do so, we applied on the mobile upper roll successive and increasing downwards displacements stepped from 1mm to 7mm followed by a 150mm longitudinal strip displacement (levelling step without tension).

Figures 4 and 5 show the resulting iso-contour plots of the plastic equivalent strain (PEEQ) for a 3mm downwards displacement using two local constitutive behaviors, the former with a classic strain hardening law (monotonic) and the later taking into account the Lüders phenomenom.

It is noticeable that, compared with a classic strain hardening behaviour where no localization phenomenom is observed apart from well separated plastic and yielded zones in the material thickness, it appears that the Lüders phenemenom law is clearly responsible for the particular strain patterns exhibited, this, strongly suggesting that we are facing the appearance of Lüders bands.

This result means that, in the course of bending deformation process, Lüders band defect can be successfully simulated with the help of a local constitutive behaviour that takes into account the Lüders phenomenom and this is has to be proved for our subsequent tasks.

As an exemple, **Figure 6** shows the evolution of the material strain localization and propagation with increasing intermesh steps when passing all along the 3 rolls system.

It is also shown that when intermesh level increases the inter-Lüders band spacing decreases until almost complete disappearance at the exit of the "simulated bending unit".

3-2 Further qualitative investigations : FEM Optimisation

Encouraging results obtained through the preliminary FEM investigation led us to introduce a tension parameter in our further simulations in order to assess the effect of combined bending and tensioning deformations on the Lüders bands defect evolution.

Nevertheless, in the course of this preliminary FEM study, we had to face many numerical calculation troubles (converging problems) mainly due the choice of softened contact (supposing to ease numerical solutions but not adapted to account for reality), an unoptimised mesh density and moreover an unconventional Lüders local constituve behaviour leading to unstable contact algorithm resulting in cut-backs of the automatic time stepping leading to unpredictable halts of solutions.
Too much a calculation time-spending with this way of simulating an entire tension levelling process (~3 weeks for a single numerical test without knowing whether it will end satisfactorily or not !), convinced us before going any further, to find an optimized FEM simulation strategy.

3-2-1 Optimisation of FEM simulation of bending process

The optimised calculation strategy used to overcome numerical solutions troubles is defined as :

- keeping the same 2D, 3 rolls bending system and tested steel product **(figure 3)** and the local constitutive behaviours both with and without Lüders phenomenom **(figure 2).**

- using "hard contact " which is more realistic than the softened contact used so far.

- choosing the appropriate type of Abaqus mesh element (plane stress or plane strain hypothesis ?)

- optimising the mesh density in the sheet thickness : from 5 (initially tested) to 25 squared elements (4 nodes linear plain stress = CPS4R or plane strain =CPE4R elements with reduced integration

3-2-2 FEM numerical simulation results

3-2-2-1 Type of FEM element : (plane stress or plane strain hypothesis ?)

With Abaqus FEM code, to simulate our mechanical 3 rolls bending system, it is necessary for calculations to choose the appropriate input hypothesis in terms of plane stress or plane strain.
To know how much different are the results given by a calculation performed with one or the other 2D hypothesis, numerical simulations have been tested with 2 different kinds of elements using both a classic (monotonic) strain hardening behaviour and a Lüders work hardening behaviour

The namely elements tested in Abaqus FEM code are :

- CPS4R = plane stress hypothesis (4 nodes linear plane stress element with reduced integration)

- CPE4R = plane strain hypothesis (4 nodes linear plane strain element with reduced integration)

The results in terms of PEEQ (Equivalent Plastic strain) iso-contours obtained at the end of a 3 mm imbrication are exhibited in **figure 7** (classic constitutive law) and **figure 8** (Lüders constitutive law).

The analysis shows that in the case of a classic "monotonic" law (no Lüders phenomenom), apart from a light difference in the PEEQ values, the iso-contours are very much alike whether we use a CPS4R or a CPE4R element.

On the contrary, in the case of a Lüders kind behaviour, both PEEQ values and iso-contours are quite different. The choice of a CPS4R element leads to a finer description of what we should expect from a Lüders bands pattern generation point of view.

Referring to these results, the most appropriate choice (especially when using a Lüders local constitutive law) is a plane stress 2D hypothesis that is a namely CPS4R element in Abaqus FEM code.
All further numerical simulations will from now on be based on that hypothesis .

3-2-2-2 Mesh density in the steel thickness :

To study the influence of this important parameter, five different mesh densities have been tested in Abaqus calculations : from 5 to 25 CPS4R squared elements in the 3 mm steel thickness, each case using both the 2 local constitutive laws (classis and Lüders behaviours) to compare with.

The results in terms of PEEQ (Equivalent Plastic Strain) iso-contours obtained after an imbrication of 3mm and a ~100mm longitudinal displacement (complete exit from the 3 rolls bending system) are presented in **figure 9** (classic strain hardening law) and **figure 10** (Lüders kind behaviour).

The results show that the finer the mesh density, the better it is to describe phenomena in the course of bending deformation modelling.

A few remarks though :

We notice that in the case of a classical monotonic law (no Lüders yield elongation point), 15 squared elements through the material thickness are sufficient enough to reach and acceptable precision (asymptote) : no need for more elements in the sheet thickness.

The strain distribution in the through thickness corresponds to what is usually observed with monotonic strain hardening steel, where homogeneous well separated longitudinal plastic zones (upper and lower edges of sheet thickness) and a yielded zone (middle of sheet thickness : neutral fibre) are observed.

The above general trend is deeply modified when using a Lüders local constitutive law which exhibits more complex phenomena.

The asymptotic PEEQ values are reached from 15 squared elements in the material thickness where a Lüders bands pattern is partly appearing (which is not the case with a lower mesh density !) and mainly in the tension zone. Nevertheless, at least 25 elements are necessary to obtain a sufficiently precise description of the whole Lüders band patterning (strain localisations in compression and tension zones) in both longitudinal and through thickness directions.
It is also observed that the finer the mesh density the more serrated the inter-band spacing is !

One additional remarkable fact to be underlined is that the strain localisations are orientated at ~ 45° from the levelling direction (such a pattern has been reported in the past by a few authors regarding tensile testing, bending or temper-rolling processes). In the preliminary study (**§ 3-1-1**), these strain localisations were normal to the sheet surface probably due to the use of a "softened contact" in the Abaqus FEM code.

Summing-up these results on the effect of the mesh density on the strain pattern and <u>if one wants to account for a fully precise real Lüders band patterning</u> we can retained the main conspicuous fact :

The mesh size is a key parameter : modelling the bending process using a Lüders local constitutive law involves complex phenomena and requires a sufficiently fine mesh density. This mesh density also directly affect the inter-band spacing meaning that there is a scale factor that will surely lead us to set up an appropriate meshing calibration when tackling the quantitative aspect of this project (numerical simulation versus experimental or industrial results).

3-2-2-3 Effect of local constitutive behaviours :

Two local laws have been compared : a classic "monotonic" work hardening behaviour and a Lüders work hardening behaviour.

Along with these calculations, all other parameters were kept identical, that is :

- CPS4R element (plane stress hypothesis),
- 25 squared elements in the sheet through thickness
- downwards displacement of the upper mobile roll (intermesh) = 3 mm
- longitudinal displacement of sheet ~100 mm (complete exit of the bending system)

From the resulting PEEQ (Equivalent Plastic Strain) iso-contours presented in **figure 11**, it clearly appears that the Lüders kind behaviour is responsible for the particular strain pattern observed. Remarkably, we are facing a complete Lüders band network both in the tension and the compression zones. Plastic and yielded bands alternate with an orientation around 45° from the free surfaces as reported by a few authors.

This aspect is most encouraging for our subsequent tasks because though still being on a qualitative basis, we can expect that, in the course of bending deformation, the Lüders band defect will be satisfactorily simulated when using this specific Lüders strain work hardening law.

3-2-2-4 Effect of intermesh level (no tension applied) :

From a Lüders pattern point of view, the evolution of the strain localisation with an intermesh = 3 mm have been compared with two other intermesh levels, 1 and 2 mm, keeping the same data described at the previous chapter above.

From the resulting PEEQ iso-contours shown on **figure 12**, it is noticed that with the lower intermesh (1 mm), Lüders bands start appearing (orientated at ~45°) but only from the bottom surface of the sheet thickness which is in a tension state with the contacting bending roll. With increasing imbrications, the Lüders bands network is getting more and more pronounced included in the compression zone. The intermesh of 3 mm finally leads to a total spreading of the strain localisation through the whole thickness of the tested material.

When exiting the bending system, the sheet thickness exhibits two distinct zones : a complete plastic zone on the upper and lower parts and a central zone (neutral fiber) composed of Lüders bands, both in tension and compression directions. This described morphology could suggest that the Yield point elongation has been totally eliminated. This point has been verified later in the course of this project by means of "virtual" tensile tests extracted from calculations results.

3-2-2-5 Combined effect of bending deformation and tensioning on the appearance of Lüders bands

Figures 13, 14 and 15 represent the iso-contour plots related to the Equivalent Plastic Strain (PEEQ) for 3 intermesh studied levels (1, 2 and 3 mm). On each of these figures, a comparison is made between calculation performed with and without applied tension

The results obtained clearly exhibit quite a remarkable influence of tensioning compared to cases where no tension is applied. This is particularly obvious in the tested case with a 1 mm intermesh level (**figure 13**). Without tension, the Lüders bands hardly appear at the surface of the sheet whereas, when applying tension, a Lüders bands network is spreading all over the through-thickness.
With increasing intermesh levels, this fact is emphasized (**figures 14 and 15**).

This means that in the course of processes involving combined bending deformation and tensioning, the tension level adjustment deeply eases the occurrence of Lüders bands defect and is to be set with care depending on whether this defect is suitable as in the case of anti-coil break roller system or should be avoided along a process pass-line where many types of rolls, if not correctly dimensioned may create such an undesirable surface defect.

3-3 Quantitative aspects of FEM Lüders modeling of bending process

In previous chapters, we have demonstrated that the Lüders phenomenom can be successfully modeled in bending test condition under tension. The simulation mainly uses the Abaqus finite element code for the mechanical part of the problem, and a local constitutive behaviour that is based on the physics underlying the Lüders effect.. The qualitative study consisted in optimising the Abaqus simulation parameters such as mesh refinement, finite element type, choice of contact…).

The quantitative study is focused on the aspect of the Lüders phenomena simulation in the course of bending process in order to assess the ability of the Abaqus finite element code to correctly account for reality.

To do so, experimental trials have been performed on the BFI tension bridle pilot with bending unit with the collaboration of the CRM and BFI.
FEM 2D Abaqus simulations have been simulated on this basis in order to compare the results in terms of Lüders bands defect evolution (inter-spacing) in the tested product through thickness and Yield Point Elongation (YPEL) evolution with respect to bending elongation by means of virtual tensile tests machining after the simulated bending processes.

3-3-1 Experimental tests conditions

Experimental bending trials on batch annealed ELC steel grade provided by CRM have been performed on the BFI tension bridle with bending unit pilot equipment where 3 different parameters have been studied :

- elongation obtained by bending (□) from 0.4 to 2.3% (through tension adjustment),
- Intermesh level : 4 and 8 mm
- strip speed from 0.6 to 6 m/min.

(To ease the Abaqus FEM 2D simulations in terms of contact conditions and to shorten calculation time, the cross-bow unit was not activated on the BFI pilot !)

The bending trials matrix is presented in **table 1**.

The relation between these parameters, the appearance and morphology of Lüders band defects (including the inter bands spacing) and the mechanical properties have been investigated by CRM.

The details of the experimental testing conditions and results going with are presented in the course of the CRM contribution (cf. & 3).

3-3-2 Bending process Abaqus FEM 2D numerical simulations

Numerical simulations carried out are related to the following experimental conditions :
table 1, samples 1 to 7.

The objective is to assess the FEM Abaqus code ability to correctly account for reality not only in term of simulating the appearance of Lüders bands but also to check and to compare the experimental surface defect characteristics and in particular the inter band spacings and Yield Point Elongation (YPEL) evolutions.

3-3-3 2D FEM Abaqus modelling of the local plastic constitutive law.

Referring to the steel grade used for the experimental trials performed (cf. CRM contribution, chapter III), the first stage consisted in identifying the local experimental constitutive flow behaviour to be introduced in our calculations by means of a virtual uniaxial tensile test

The numerical conditions of a 2D FEM virtual tensile test modelling test have been already presented in a previous ECSC project **(1).**
Figure 16 just recalls the specimen geometry and meshing used.

The identification of the local constitutive law parameters to be used in the calculations is made using the plane stress hypothesis (CPS4R element) that is more representative of real tensile test conditions on flat specimens.
Figure 17 presents the results from 2D FEM calculations in term of true stress-true strain curve. The comparison between the experimental tensile test and the Abaqus virtual tensile test produced under the plane stress hypothesis and the identified local constitutive law shows a very good agreement. This identified local constitutive law has then been injected in all the Abaqus FEM simulations so performed.

This once again emphasizes the fact that the modelling pattern of the local constitutive law is efficient enough to reproduce any experimental tensile test.

3-3-4 Conditions of the Abaqus 2D FEM simulations of experimental trials

According to the qualitative work already done to optimise the Abaqus simulations parameters in the course of a bending process where Lüders bands are likely to appear, all numerical calculations have been carried out using the following parameters :

- hard contact between bending rolls and strip,
- plane stress hypothesis (CPS4R element in Abaqus words),

- a sufficiently refined meshing (at least 6 squared elements through the 0.62mm tested product thickness) for simulation time spending matter,

- 8 mm intermesh,

- bending elongations from 0 to more than 5% through back tension adjustment in a range from 30 to 150 MPa.

3-3-5 FEM simulations results

3-3-5-1 Lüders bands appearance and inter-band spacings

The calculations results obtained after modelling the experimental trials are expressed in terms of Lüders bands occurrence and inter-bands spacing in the steel strip through thickness (2D).
Table 2 exhibits the comparison between these simulations and the experimental results.
Figure 18 presents the results in terms of surface aspect and inter- bands spacing of the defects.

Figures 19 to 22 show the Plastic Equivalent Strain (PEEQ) iso contours calculated in the through thickness of the deformed strip after the simulated bending process and corresponding to samples 1, 2 ,3 and 7 respectively.

According to these simulations results, when compared to the experimental ones, it appears the main following facts :

The calculated and experimental tendencies are very similar in terms of :

- Increasing both deformation by bending and intermesh level lead to an increase of the Lüders bands defect (higher surface defect density), The Lüders bands inter-spacing become more and more serrated

- The calculated bands inter-spacing are in a very good agreement with the experimental ones but only for the higher intermesh level (8mm) as shown in **figures 19, 20 et 21**.

- Regarding results issued from the lower intermesh level (4mm), whereas Lüders bands are observed on the strip surface of experimental trials, the simulations do not exhibit any Lüders bands occurrence with deformations less than 1% (samples 5 and 6). The defect starts appearing for higher bending deformations (increasing tensions) but the inter- bands spacing seems shorter (sample 7). It is suspected that such discrepancy is due to an insufficient mesh refinement.

3-3-6 Numerical simulation of a tensile test after simulated bending process

This numerical machining method has been already developed in the course of a previous ECSC project (B). It consists of extracting a 10mm long rectangular specimen from the sheet through thickness after bending process simulation. Simulations of the tensile tests are conducted using the plane stress hypothesis (CPS4R elements in Abaqus words).

3-3-6-1 Simulated cases and results

To account for a continuous and complete description of the influence of the bending process elongation on the resultant yielding behaviour, simulations of bending processes and subsequent tensile tests have been performed according to the following parameters :

- plane stress hypotheses (CPS4R elements) for both bending processes and tensile tests. These hypotheses correspond to a correct description of such processes. Anyhow, Abaqus does not allow switching from plane strain to plane stress,

- the local plastic constitutive law (Lüders law) is the one as described in chapter 3-3-3 **fig 17,**

- 6 and 24 squared elements in the 0,62mm tested sheet thickness (effect of meshing),

- the intermesh level is set to 8mm corresponding to the experimental one (samples 1 to 3) ,

- bending process elongations from 0 to 5% through back tension adjustments from 30 to 150 MPa)

A) The results of simulations expressing the evolution of the Yield Point Elongation (YPEL) for 2 types of meshing refinements versus the corresponding bending process elongations and comparison with experimental results are presented in **figure 23**.

Comparisons between numerical simulations and experiments lead to the main following relevant facts:

- the FEM 2D simulated evolution of the Yield Point Elongation (YPEL) versus bending process elongation exhibits a similar tendency : decrease until suppression of the YPEL with an increasing bending process elongation.
A very good agreement is found with the finer meshing*.

- for a given bending process elongation, FEM 2D simulations tend to under-estimate the corresponding Yield Point Elongation (YPEL),

- the calculated decrease of the YPEL (Lüders plateau) is under-estimated. A simulated 4,5% (meshing = 6) and 3,5% meshing = 24) elongations are respectively necessary to completely suppress the Lüders plateau whereas 3% is experimentally required.

** Remarks : The accuracy of results highly depends on the meshing refinement !*
The drawback is that the finer the meshing and the much more longer the calculation time.
As an example, for a meshing of 24 squared elements it takes two full months of calculations to obtain the complete curve whereas two weeks are just necessary for a meshing of 6 squared elements (ratio 4/1).
This might lead to an unrealistic FEM modelling towards industrial applications due to a lack of actual computer/station power. In the future, this obstacle will surely be overcome.

B) Extracted from the simulations with a meshing of 24 squared elements in the strip thickness , the results of simulations of FEM 2D virtual tensile test machining expressing both the comparison of experimental and calculated stress-strain curves and the evolution of the Yield Stress (YS) versus the corresponding bending process elongations are presented in **figures 24 and 25** respectively.

Comparisons between numerical simulations and experiments lead to the main following relevant facts:

- in term of tendency, a rather good agreement between bending unit pilot experiments and calculations is found in terms of evolution of the Yield Stress (YS) and bending process elongation levels (**figure 25**).

- Nevertheless, the calculated drop in yield stress is lower than the measured one. It is worth noting that in the yield stress versus bending process diagramm, the experimental elongation (3%) leading to the minimum yield stress is lower than the one leading to the yield point suppression (3,5%).

4/ CONCLUSIONS

It has been demonstrated that a finite element method associated to a physically based description of the constitutive behaviour of steel allows to simulate the bending process and to predict the elongation necessary to suppress the yield point elongation.

The main following conclusions can be drawn from the work performed by ARCELOR RESEARCH SA :

- Numerical simulations of tensile test and bending test have been designed. In all cases, rather good agreement is found between Lüders bands pattern observed experimentally and simulated numerically.

- Regarding tensile test simulations, it was demonstrated that the local constitutive behaviour must present an initial stress drop to simulate satisfyingly the experimental force-displacement response of the steel.

- A numerical machining procedure of flat tensile specimens in bended steel sheet has been developed. It allows to determine the force-displacement curve after bending process and thus to study the influence of the bending conditions on subsequent yielding behaviour.

- Provided the local flow behaviour of the non bended material is determined, good agreement between experimental and calculated evolution of YPEL as a function of the bending process elongation is found. It is worth noting that systematically, the bending elongation leading to the minimum yield stress of the bended steel is lower than the one leading to the suppression of the Lüders plateau.

5/ LIST OF REFERENCES

1 IRSID, D. Grandemange, H. Tsukahara, E. Vasseur, CRM, J.- C. Herman, BFI, P.- D. Pütz
Control of the yielding and ageing behaviour in temper rolling, (Draft Final Report), CECA 7210-PR/035, 2001

2 S. Ribau, ENSPM – Etude numérique et expérimentale du phénomène de Piobert-Lüders-MPM 98/1718 : August 1998

3 D. Grandemange, E. Vasseur, H. Tsukahara IRSID -Contrôle du phénomène de Lüders et du vieillissement au skin-pass- CMC/01/2961

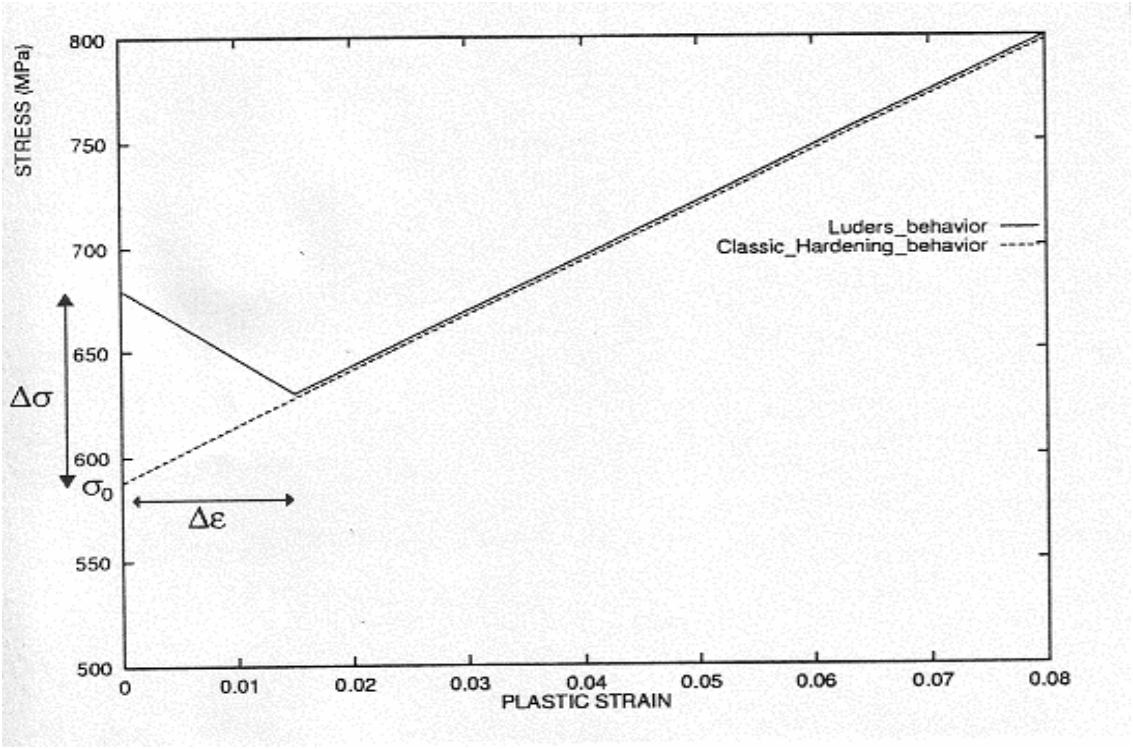

Figure 1
Local constitutive behaviours.

- the dashed line represents a classic strain hardening behaviour taken as a straight line for simplicity.
- the plain line is the local constitutive behaviour used to take into account the Lüders phenomenom.

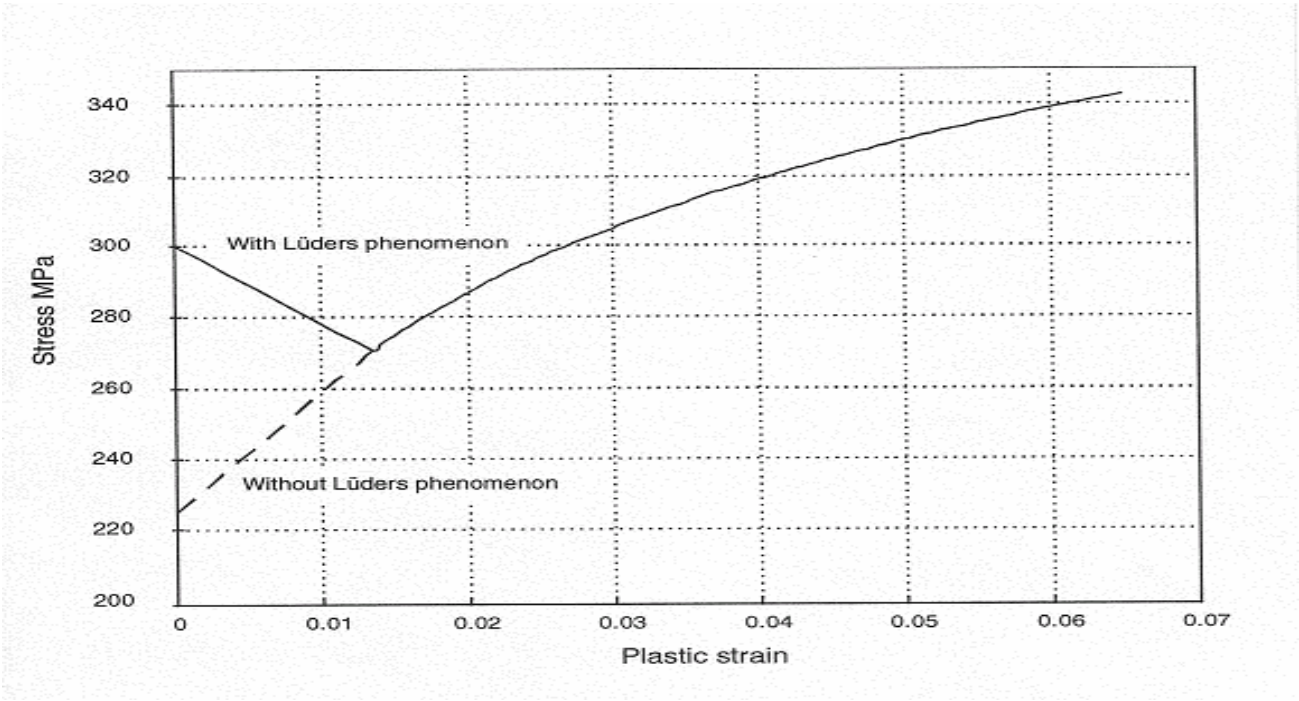

Figure 2
Local constitutive behaviours used in the bending deformation simulations

- the dashed line represents a classic strain hardening behaviour (without Lüders phenomenom).
- the plain line is the local constitutive behaviour used to take into account the Lüders phenomenom.

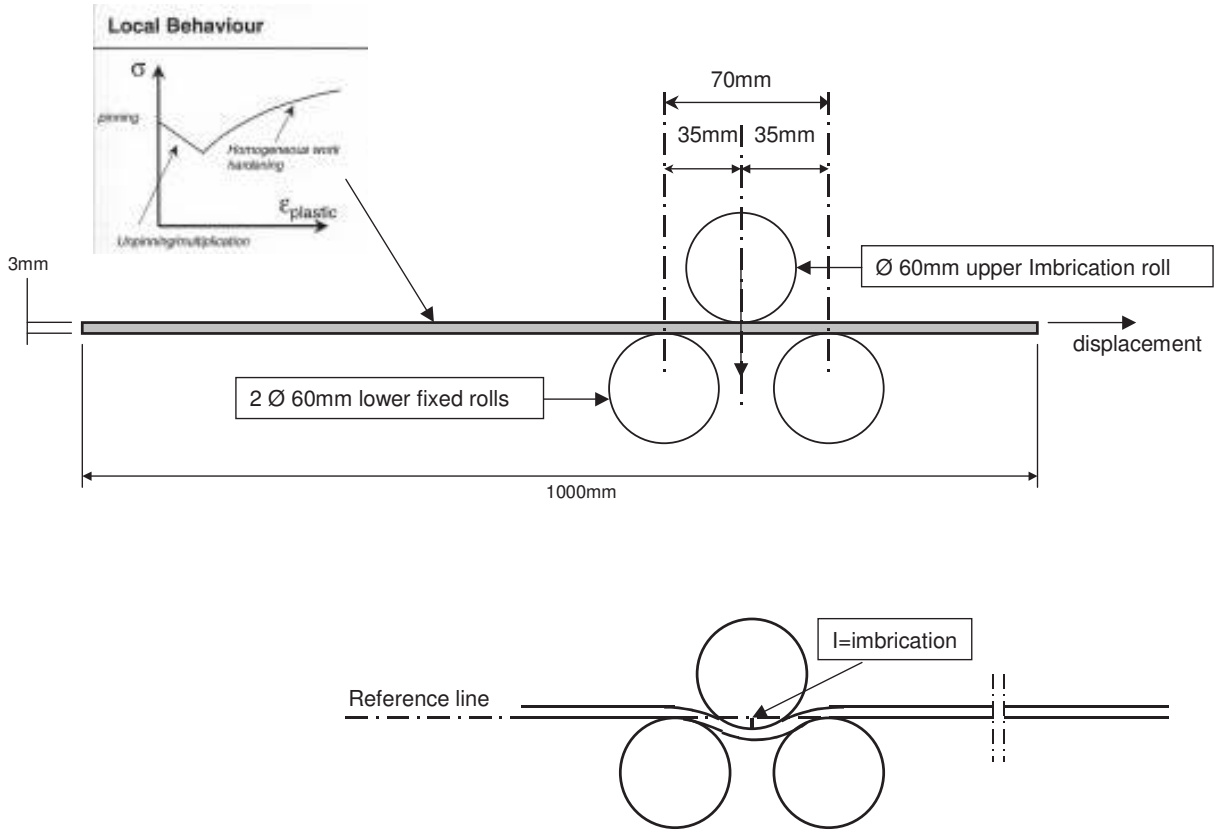

Figure 3

Sketch of the parts assembly used for bending deformation test with ABAQUS FE code

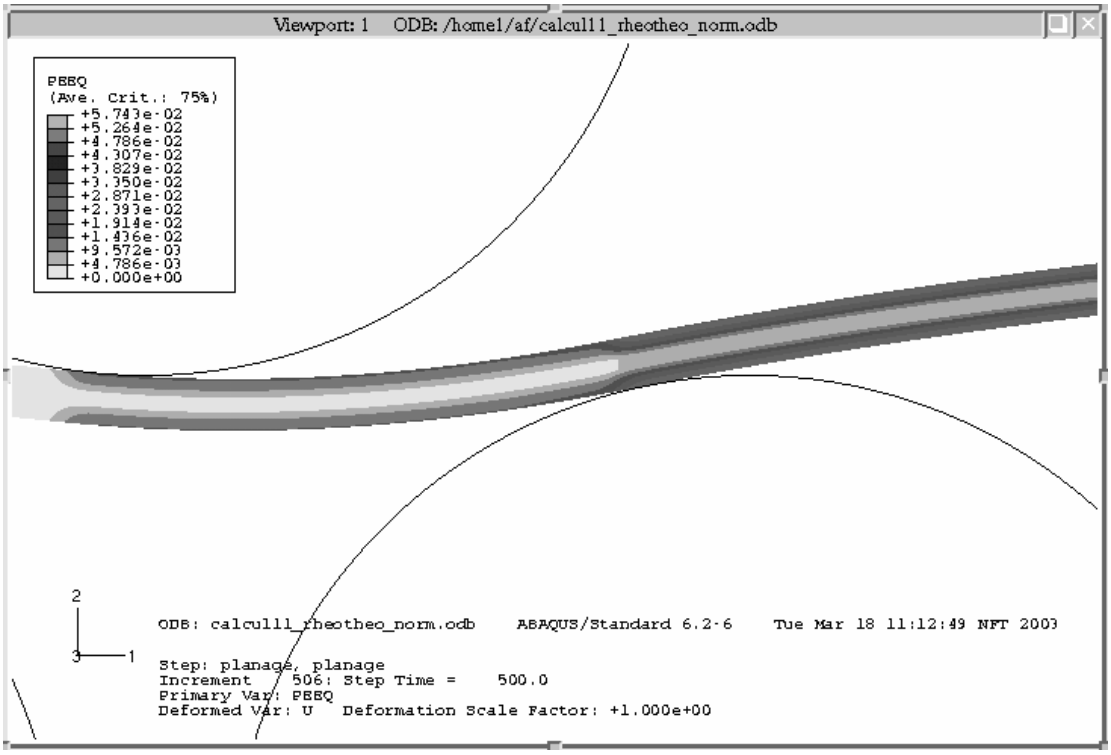

Figure 4
Iso-contour plot for PEEQ (plastic equivalent strain) with a classic strain hardening behaviour (without Lüders phenomenom)

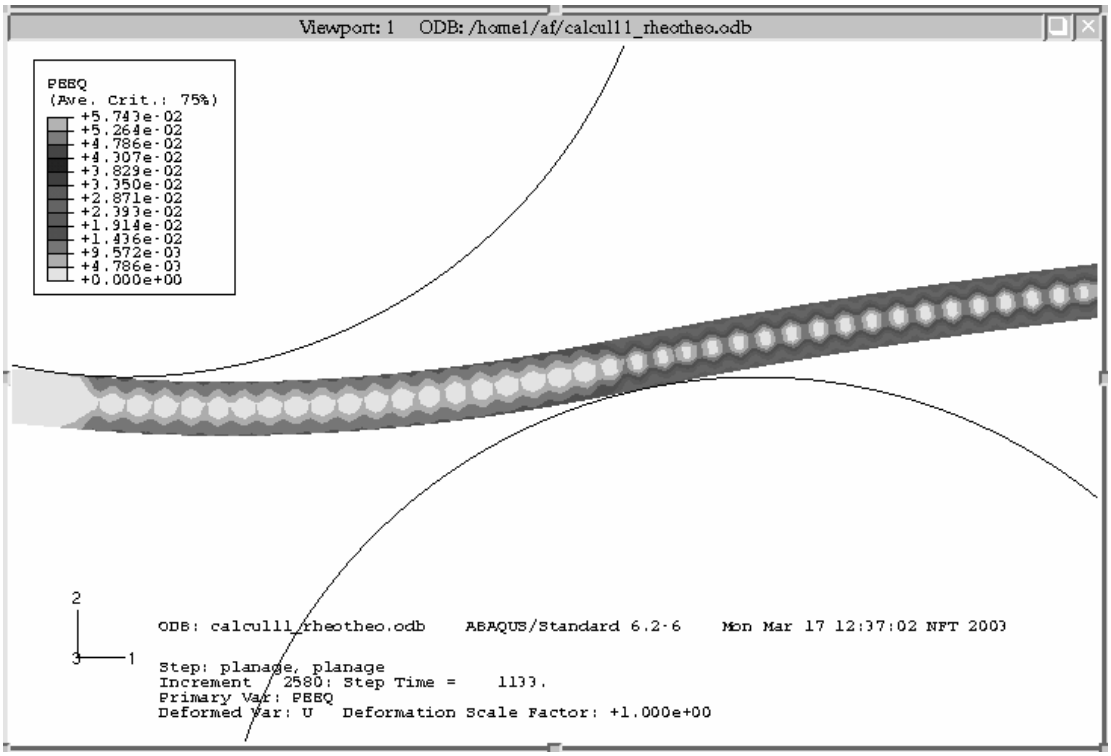

Figure 5

Iso-contour plot for PEEQ (plastic equivalent strain) with the local constitutive behaviour used to take into account the Lüders phenomenom

intermesh = 2 mmm

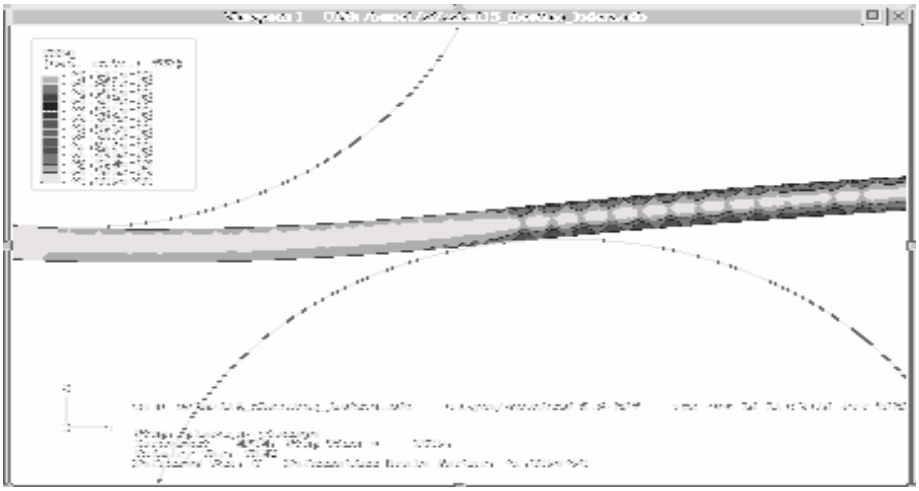

intermesh = 5 mm

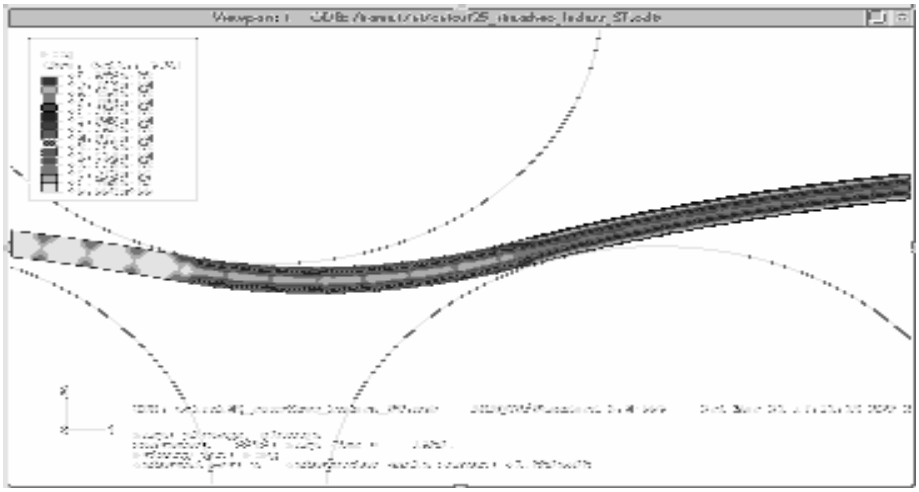

intermesh = 7 mm

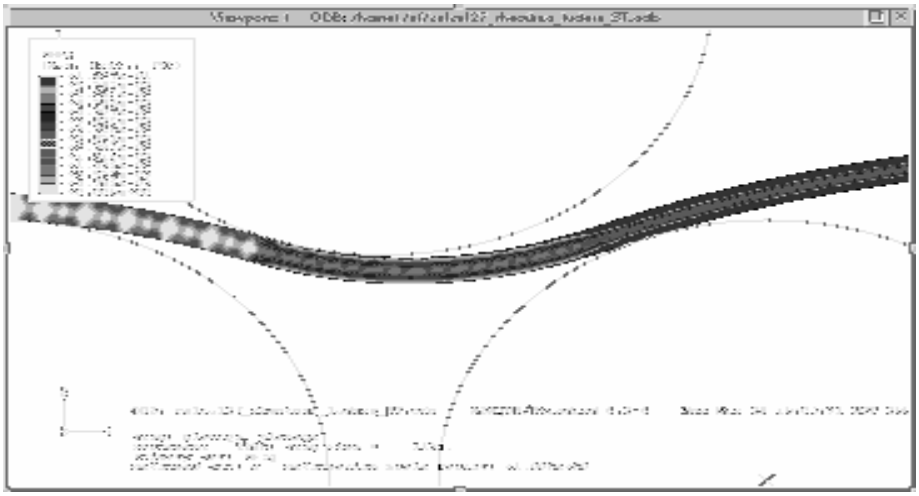

Figure 6

Iso-contour plots for PEEQ (plastic equivalent strain) with the local constitutive behaviour and increasing imbrications

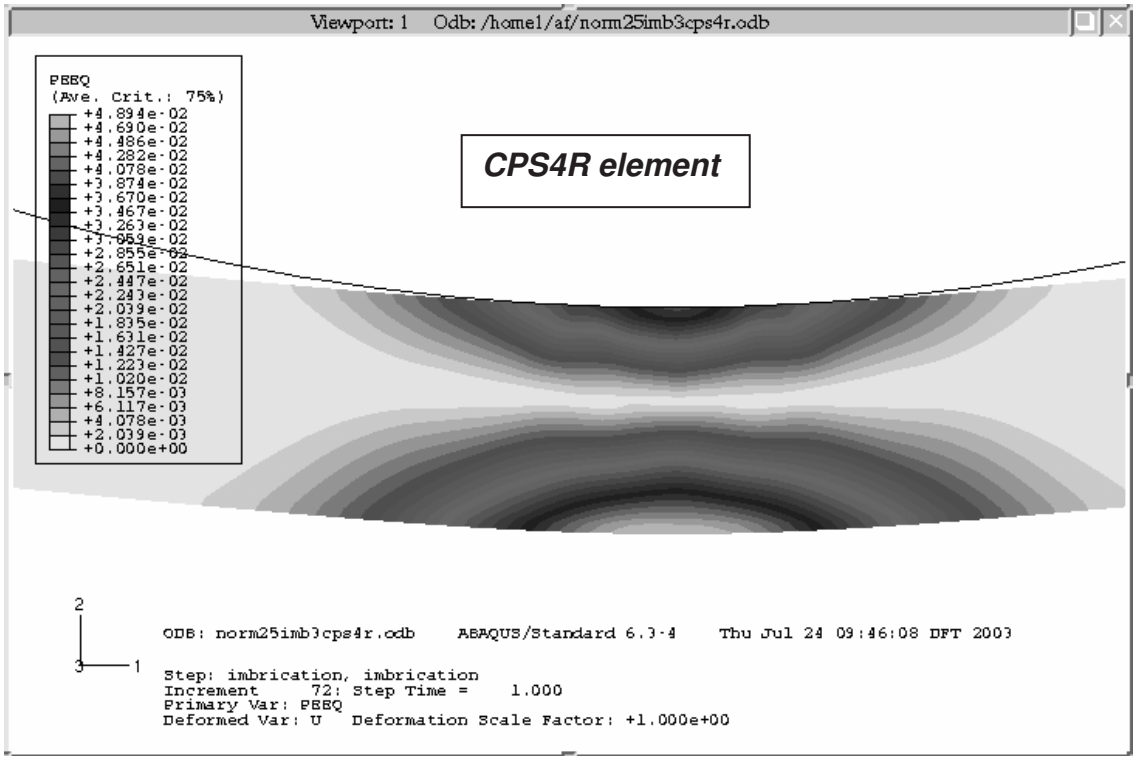

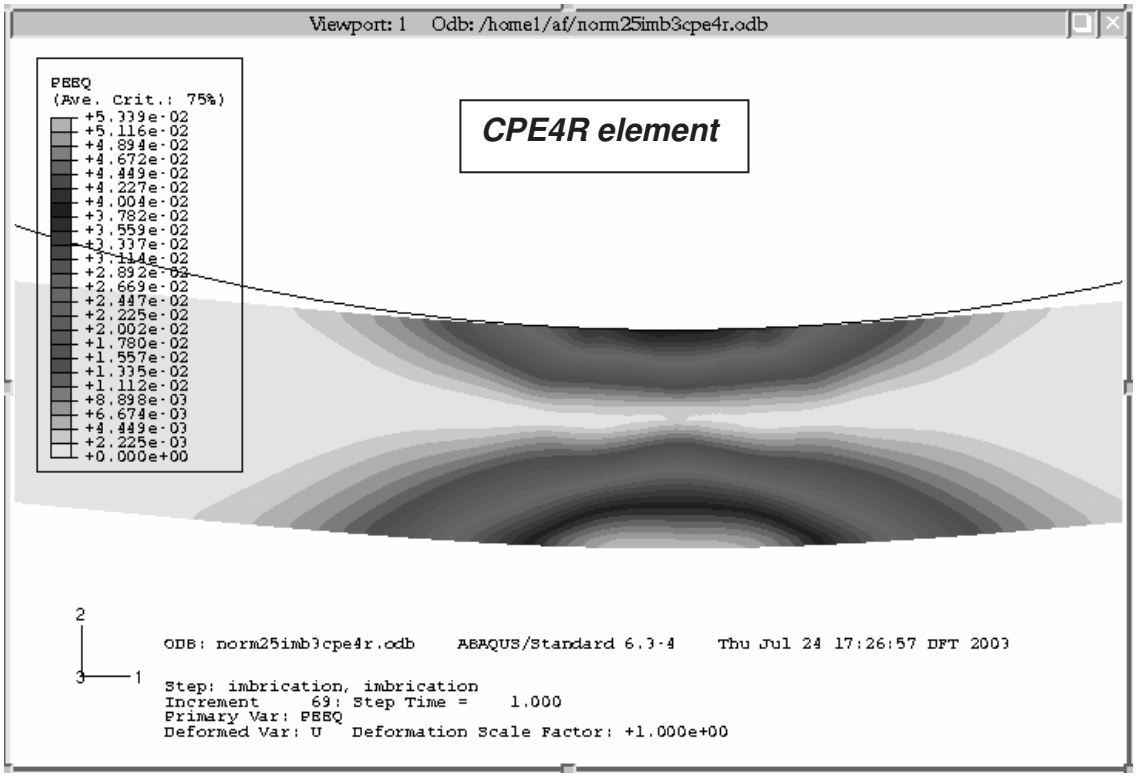

Figure 7
Iso-contour plots for PEEQ (Equivalent Plastic Strain) for two types of Abaqus elements and a classic strain hardening behaviour (no Lüders phenomenom)
upper picture : CPS4R = plane stress hypothesis lower picture : CPE4R = plane strain hypothesis

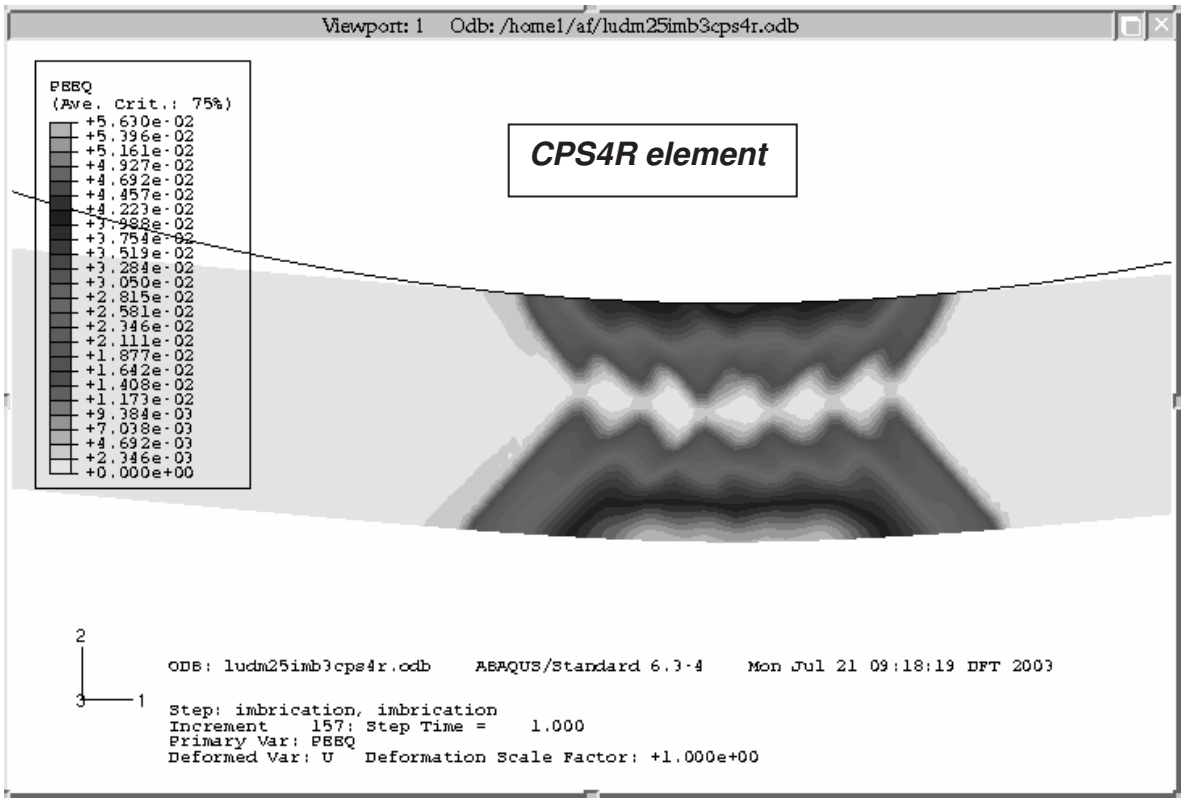

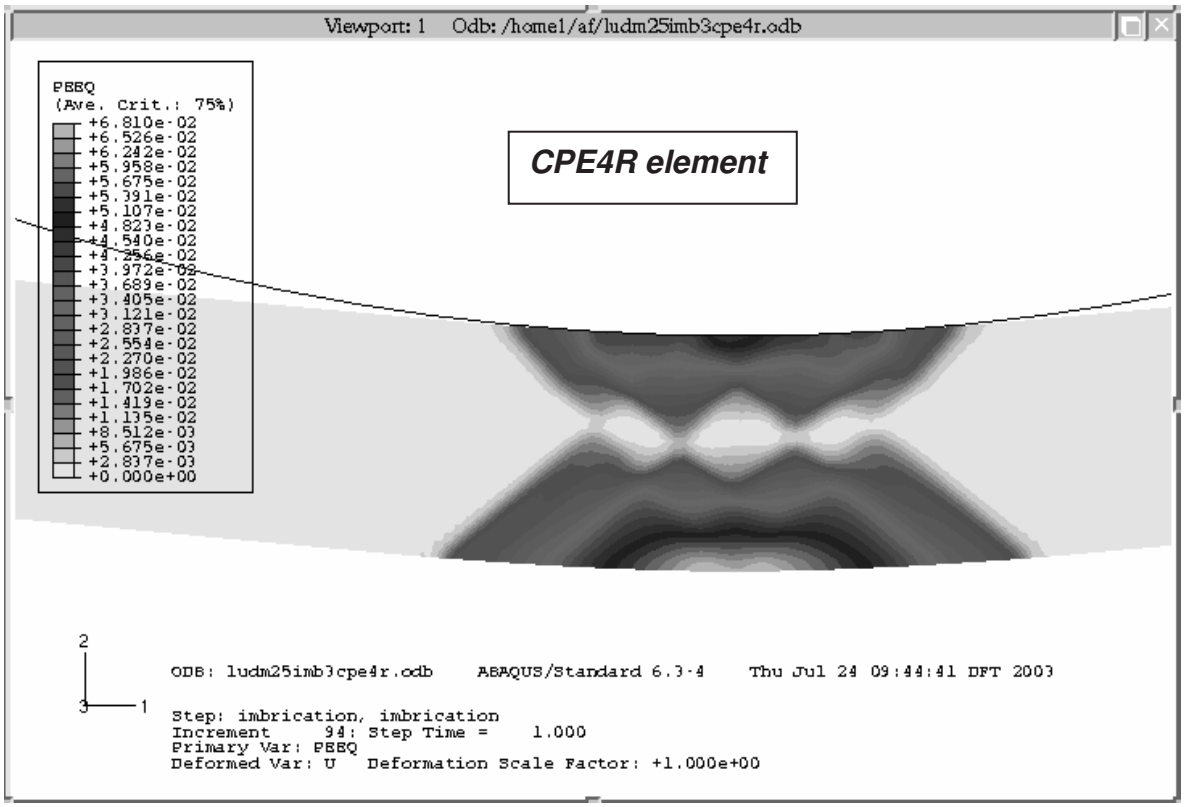

Figure 8

Iso-contour plots for PEEQ (Equivalent Plastic Strain) for two types of Abaqus elements and a Lüders strain hardening behaviour (taking into account the Lüders phenomenom)
upper picture : CPS4R = plane stress hypothesis lower picture : CPE4R = plane strain hypothesis

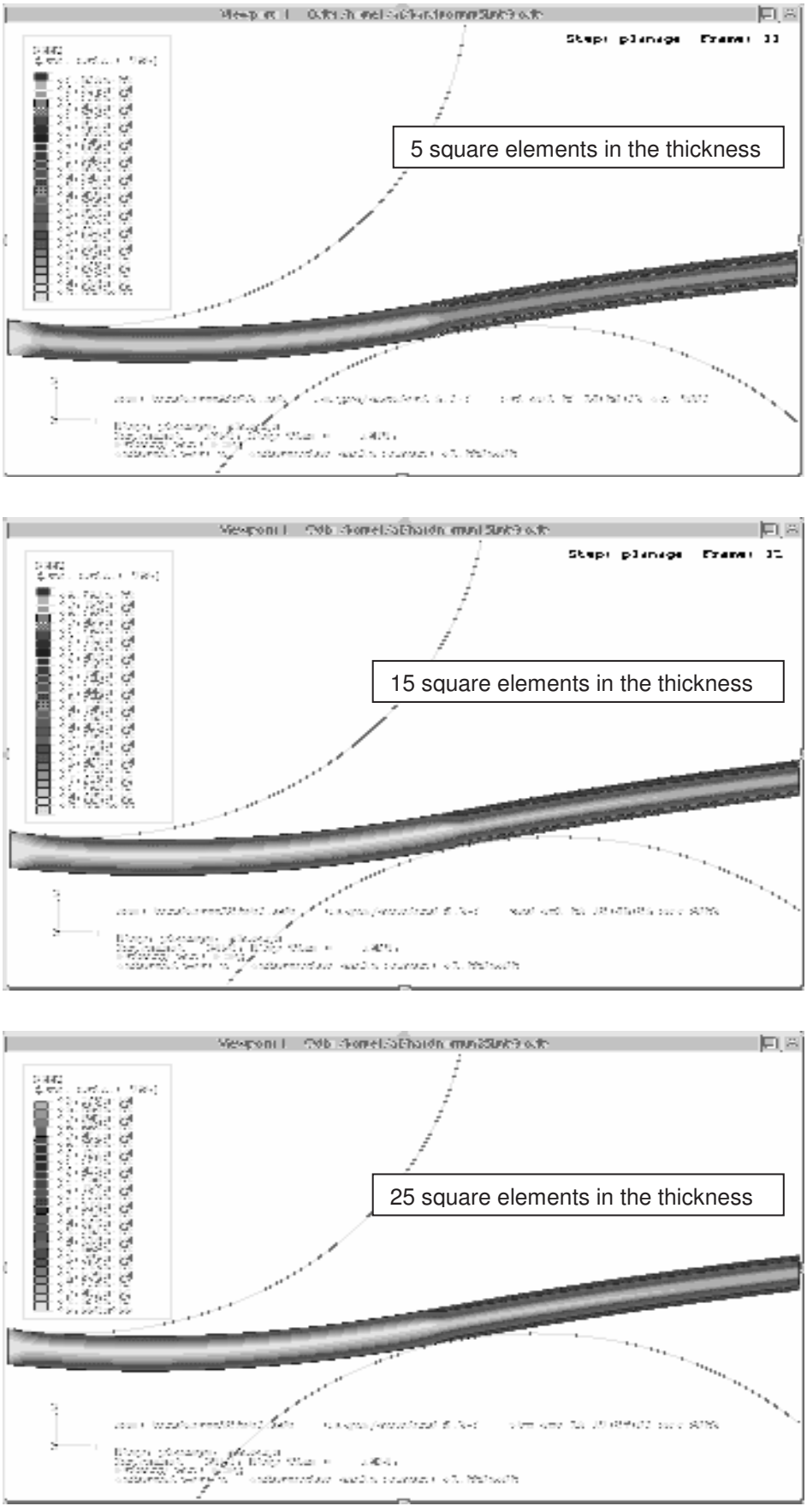

Figure 9
Iso-contour plots for PEEQ (Equivalent Plastic Strain) with a classic strain hardening behaviour (no Lüders phenomenom) and increasing mesh density

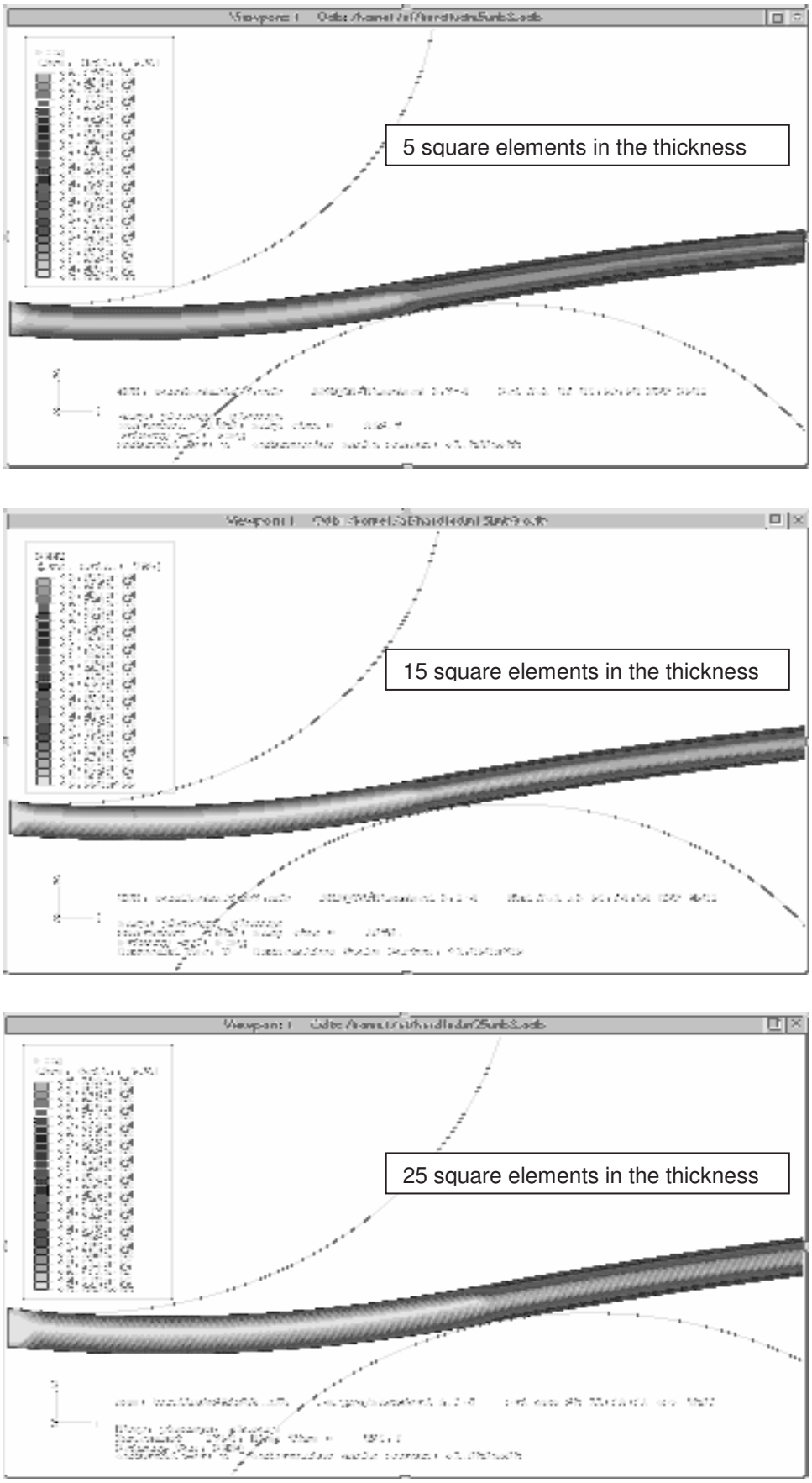

Figure 10
Iso-contour plots for PEEQ (Equivalent Plastic Strain) with a Lüders strain hardening behaviour (taking into account the Lüders phenomenom) and increasing mesh density

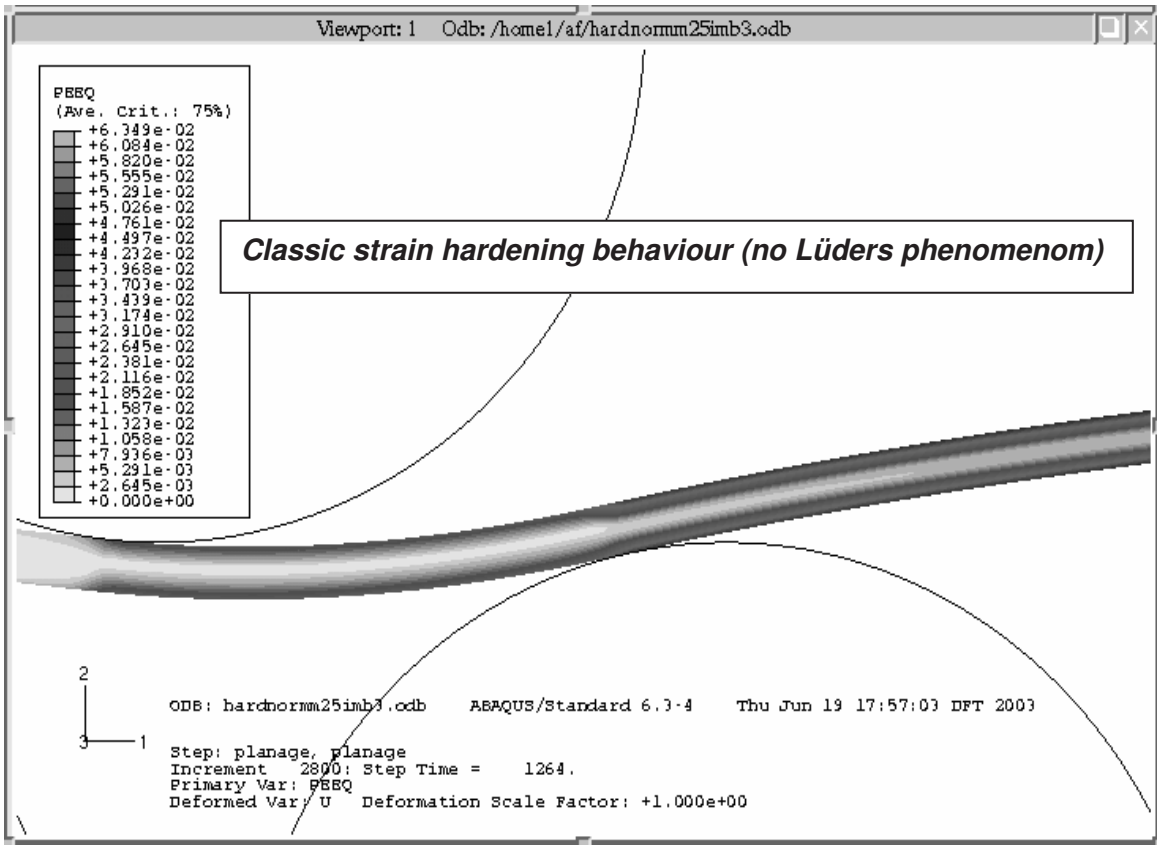

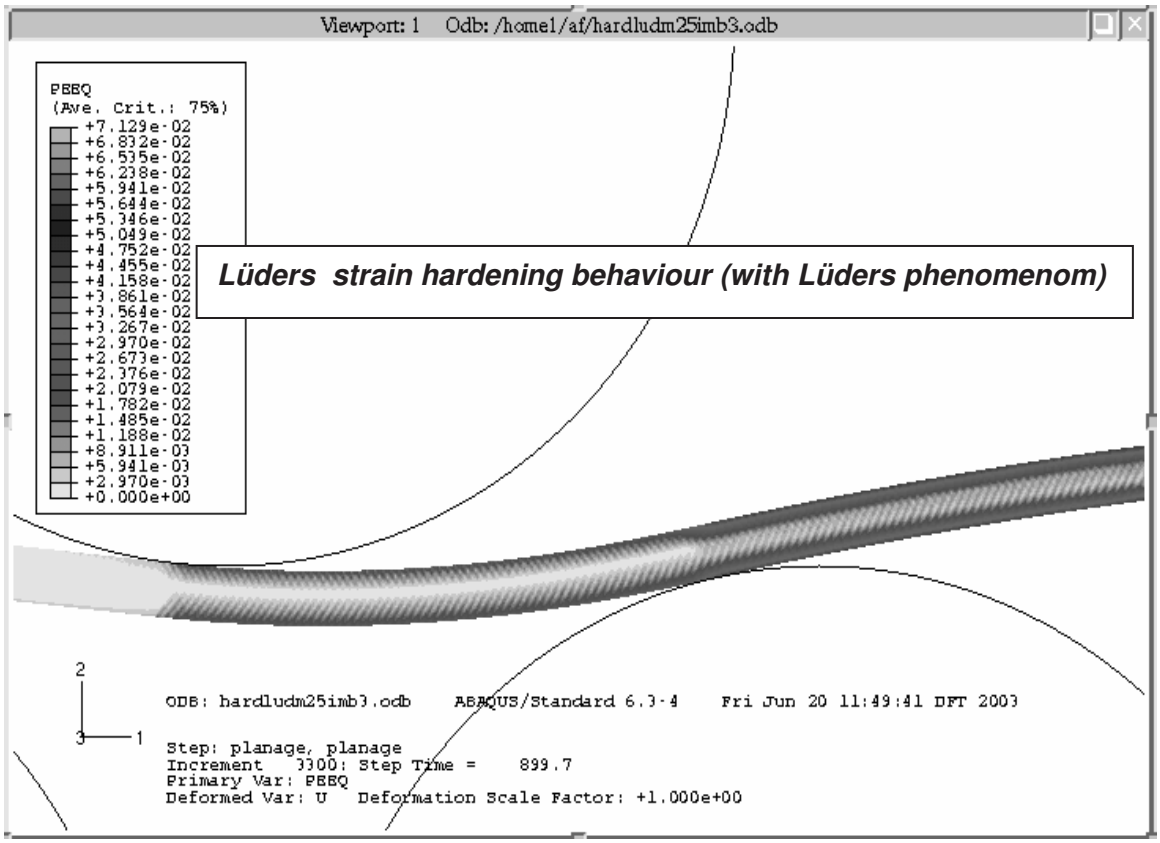

Figure 11

Iso-contour plots for PEEQ (Equivalent Plastic Strain) for two local constitutive behaviours :
Classic work hardening behaviour (upper picture) Lüders hardening behaviour (lower picture

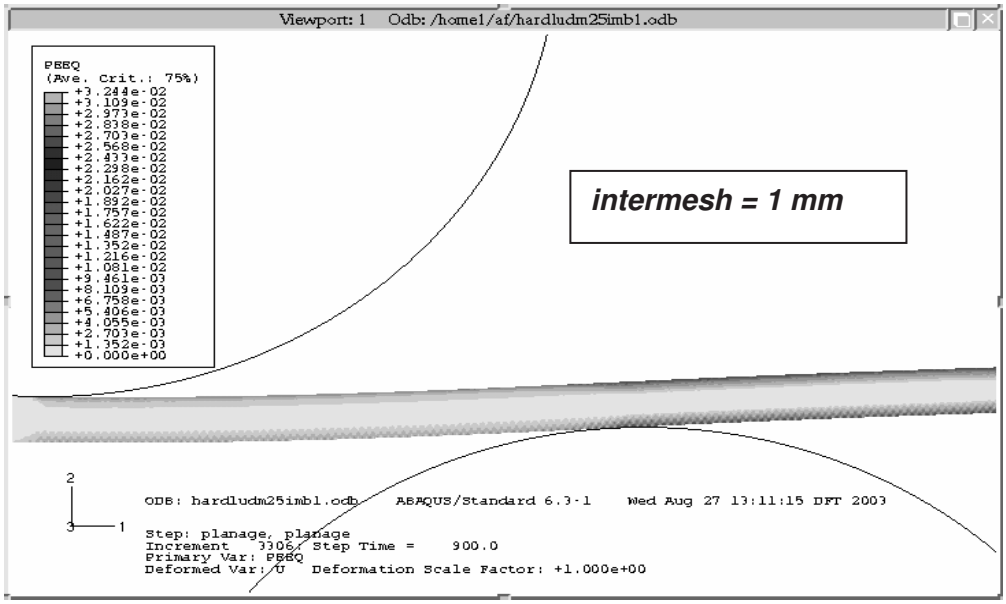

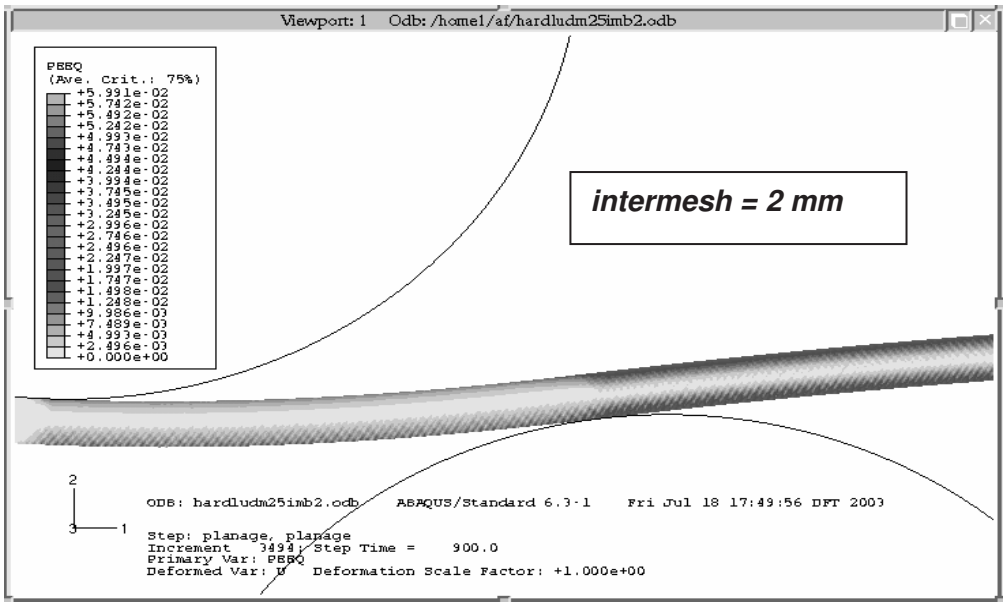

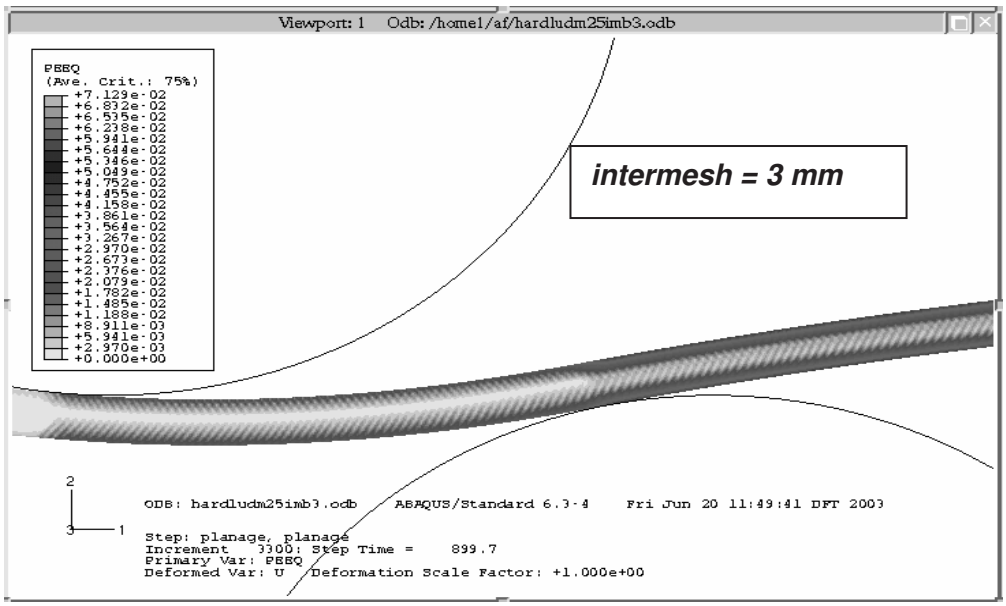

Figure 12

iso-contour plots for PEEQ (Equivalent Plastic Strain) with a Lüders strain hardening behaviour (with Lüders phenomenom) and increasing intermesh levels

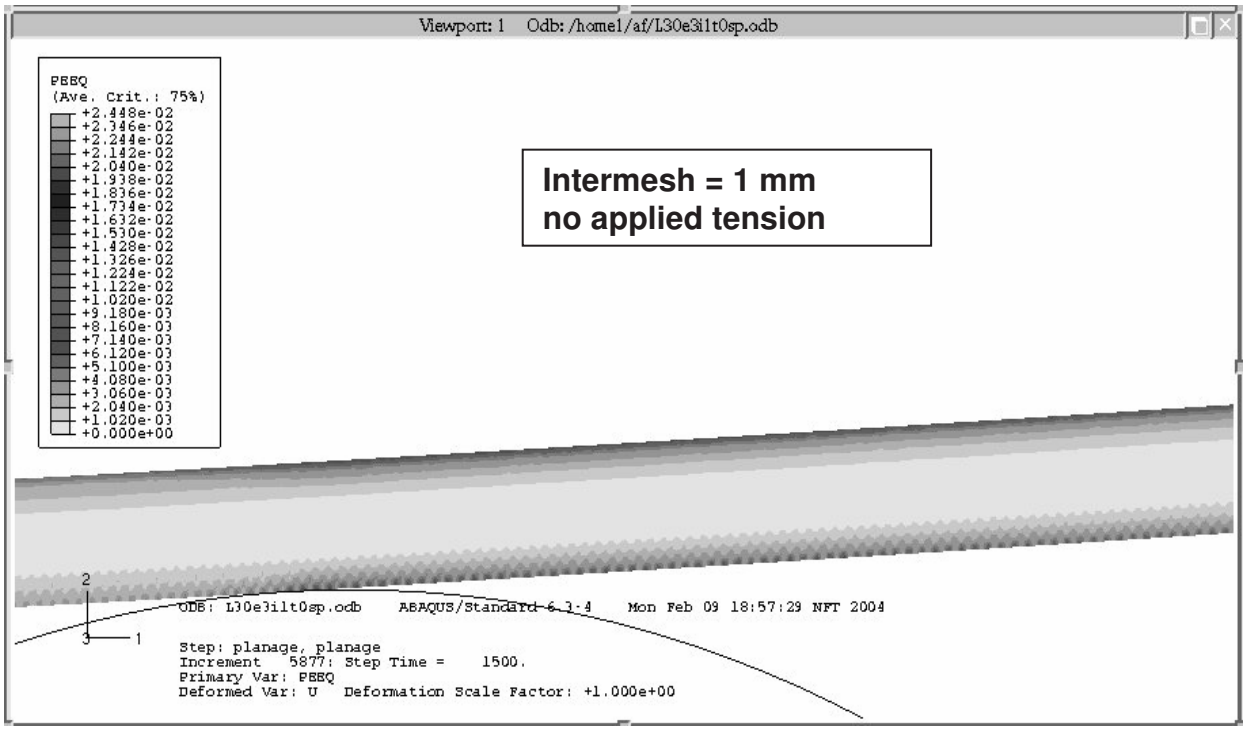

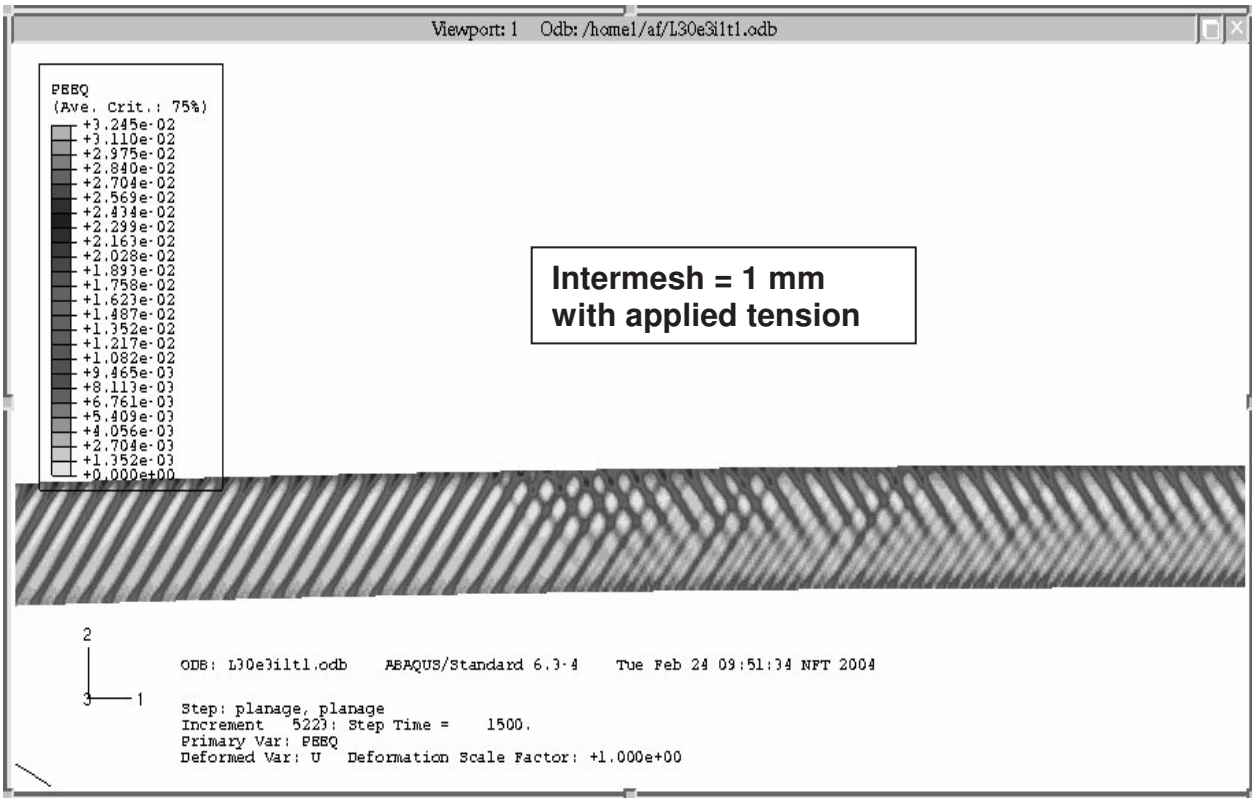

Figure 13
Iso-contour plots for PEEQ (Equivalent Plastic Strain) with Lüders work hardening behaviour : Effect of combined bending deformation and tension with a 1 mm intermesh level

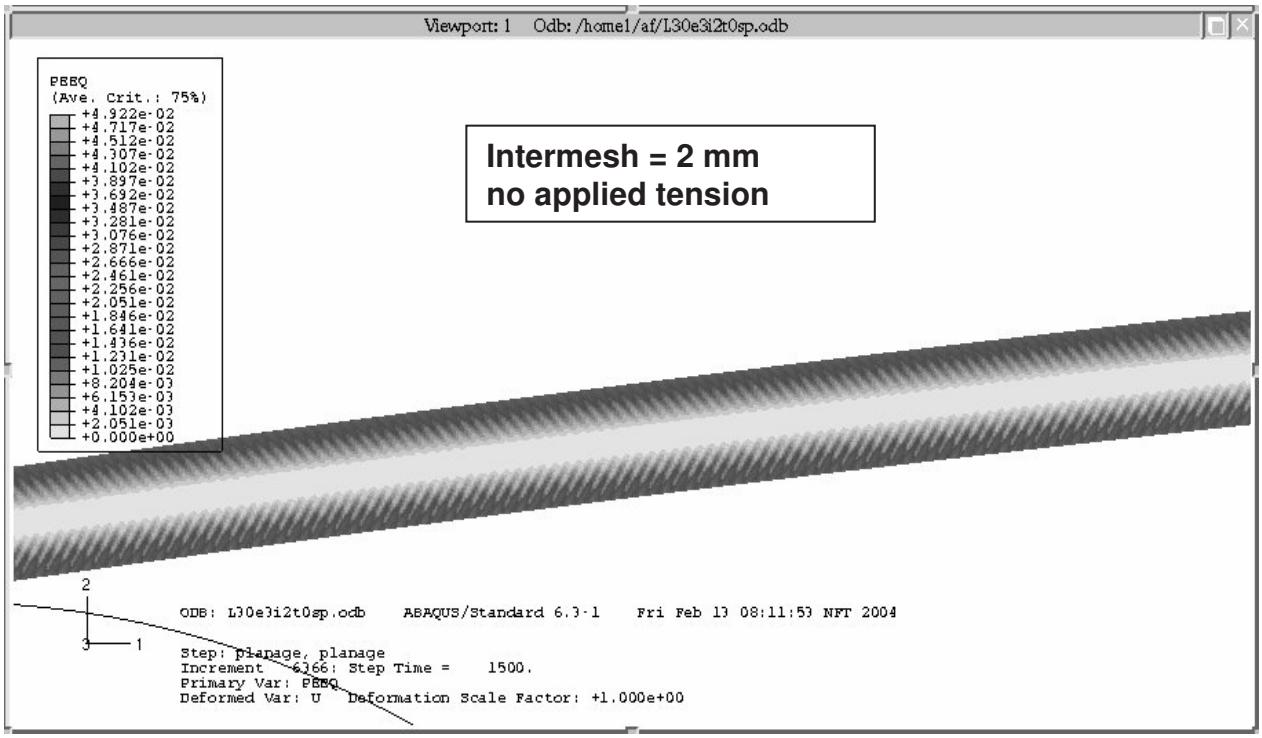

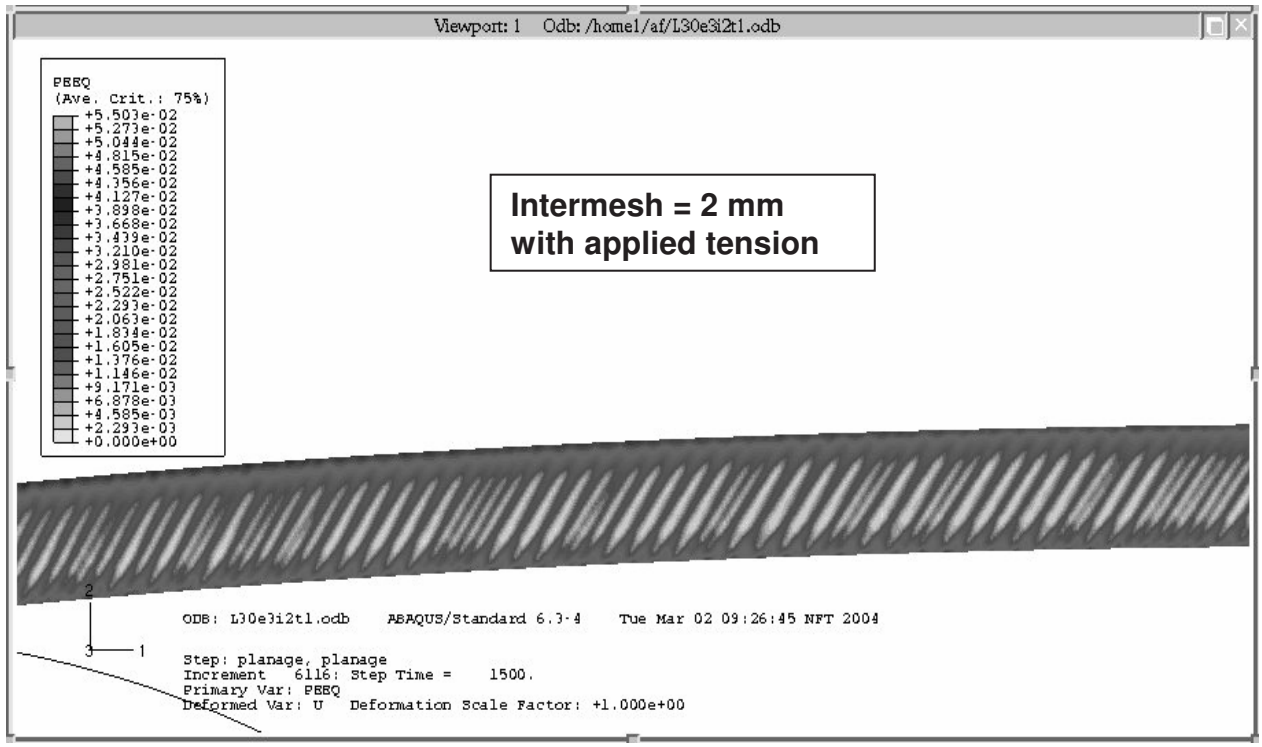

Figure 14

Iso-contour plots for PEEQ (Equivalent Plastic Strain) with Lüders work hardening behaviour : Effect of combined bending deformation and tension with a 2 mm intermesh level

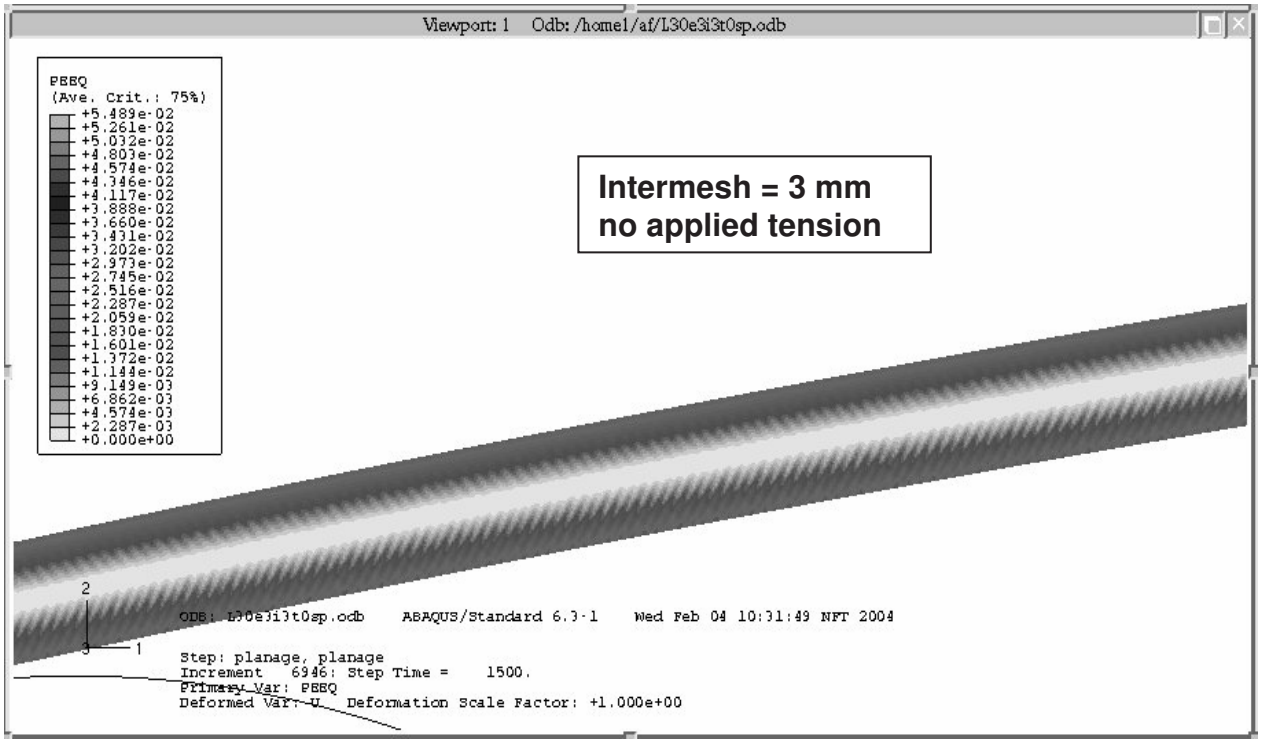

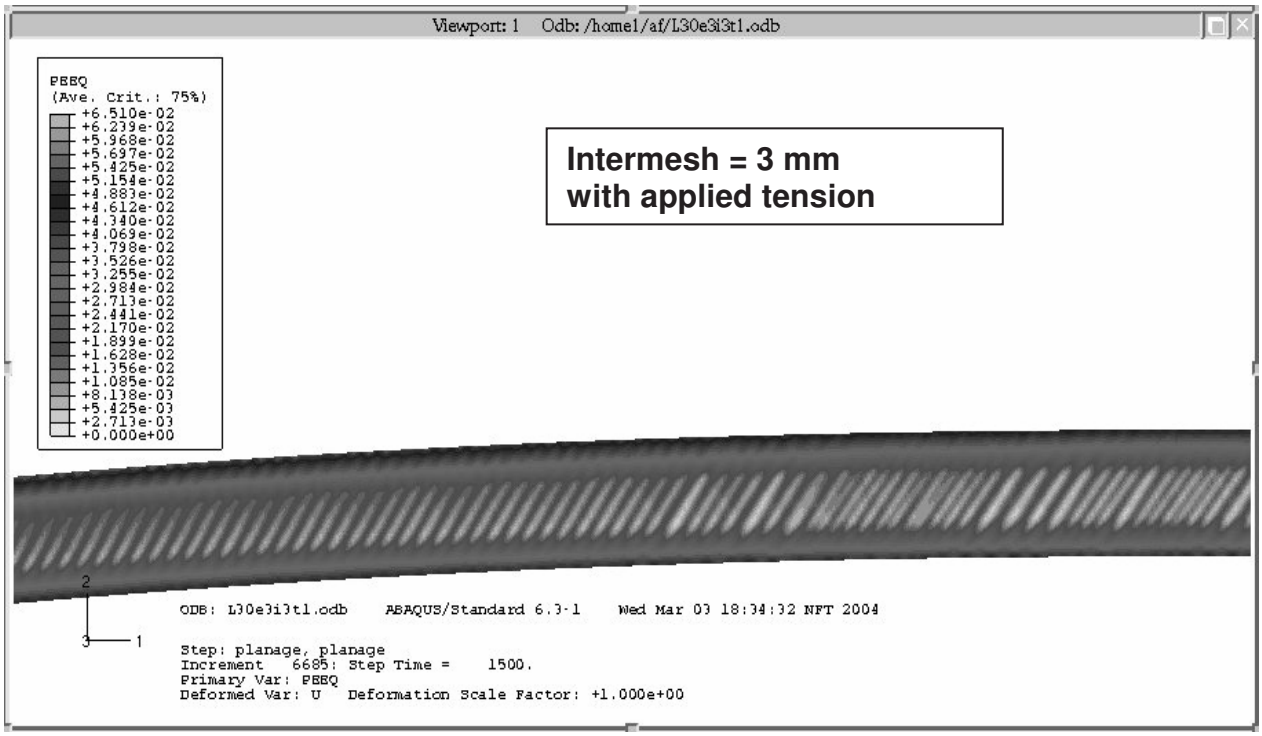

Figure 15

Iso-contour plots for PEEQ (Equivalent Plastic Strain) with Lüders work hardening behaviour : Effect of combined bending deformation and tension with a 3 mm intermesh level

Sample	intermesh mm	v m/min	λ %
1	8	2.6	0.90
2	8	2.6	0.60
3	8	2.6	2.30
5	4	2.6	0.80
6	4	2.6	0.40
7	4	2.6	1.10
8	8	0.6	1.00
9	8	6	0.70

Table 1

Experimental bending trials matrix performed on theBFI bending unit

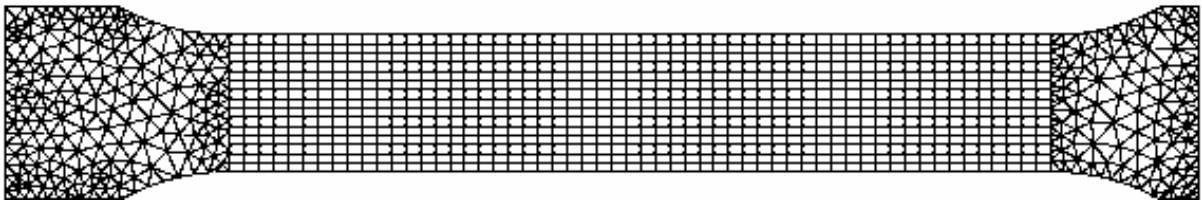

Figure 16

Specimen geometry and mesh used for the calculation with ABAQUS. CPS3 linear elements type have been used for the heads and CPS4R (plane stress) elements type for the gage length

(The gage length is 7.5 cm and the gage width is 1.25 cm)

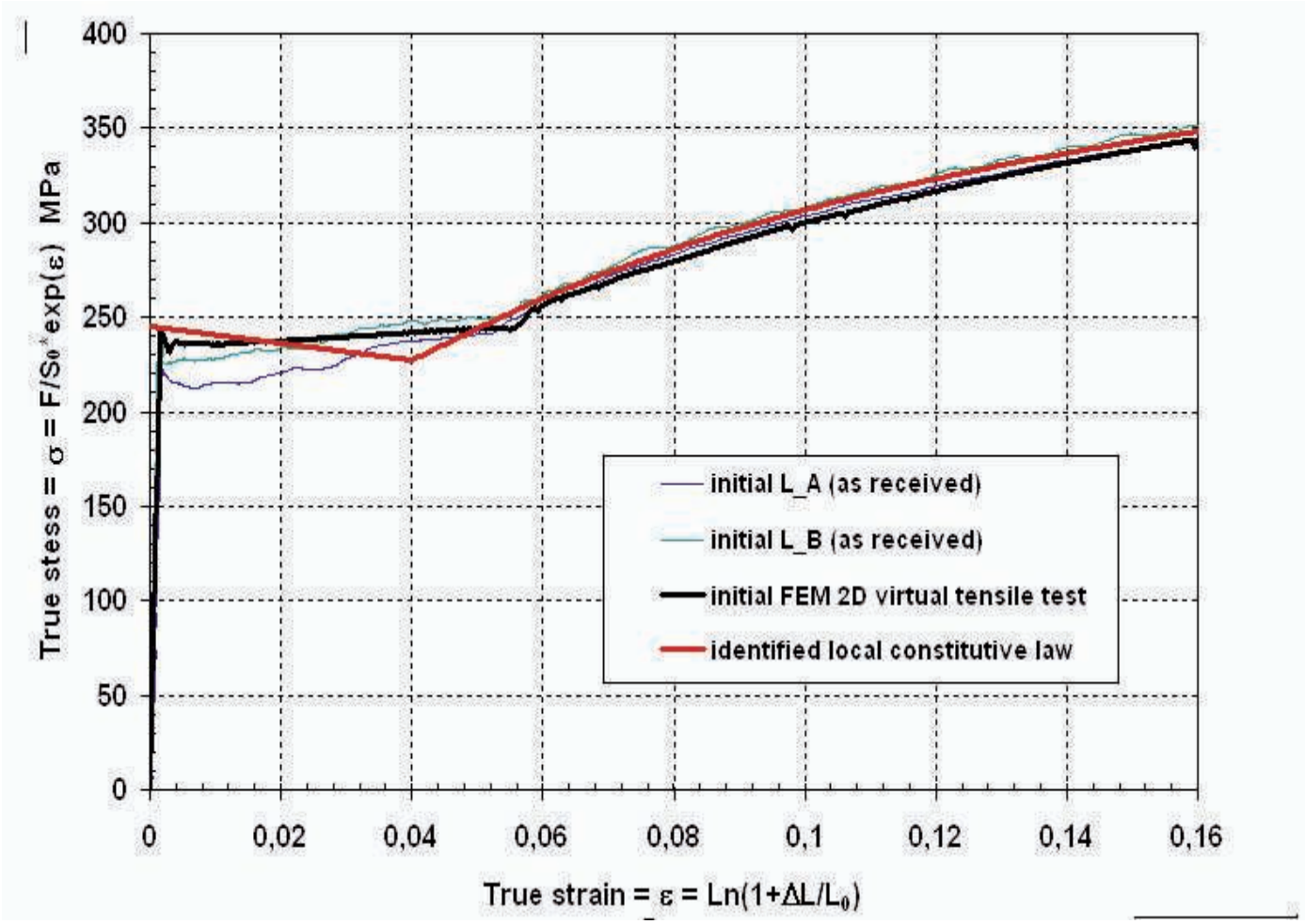

Figure 17

Identification of the local constitutive law to be used in calculations.
Comparison of the engineering true stress--true stain results between experiment and plane stress 2D

Experimental conditions					CRM results	FEM Abaqus results
sample n° n°	applied intermesh level *mm*	measured strip tension *Mpa*	achieved strip elongation *%*	strip speed *m/min*	mean measured inter bands spacing *mm*	mean calculated inter bands spacing *mm*
1	8	56,4	0,9	2,6	**1,6**	**1,57**
2	8	39,4	0,6	2,6	**2,7**	**2,4**
3	8	68,8	2,3	2,6	**1,5**	**1,4**
5	4	88,9	0,8	2,6	**2,7**	**no Lüders bands**
6	4	74,4	0,4	2,6	**3,3**	**no Lüders bands**
7	4	103,2	1,1	2,6	**2,7**	**2,2**
8	8	51,8	1	0,6	**1,7**	**not simulated**
9	8	51	0,7	6	**1,7**	**not simulated**

Table 2
Comparison between simulations and experimental results in terms of Lüders bands occurrence and mean inter-bands spacing

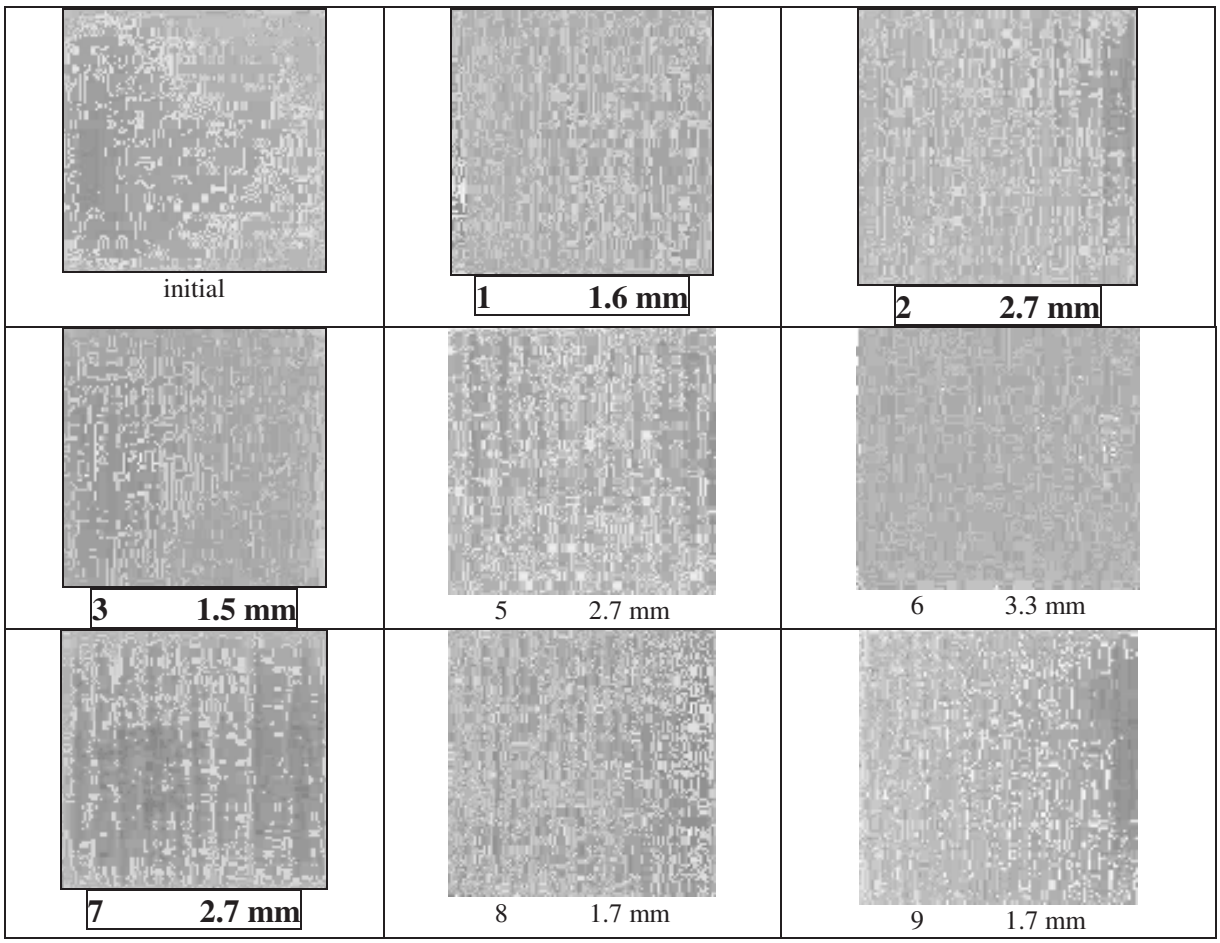

Figure 18

Results obtained after experimental bending trials in terms of aspect and spacing of the defects

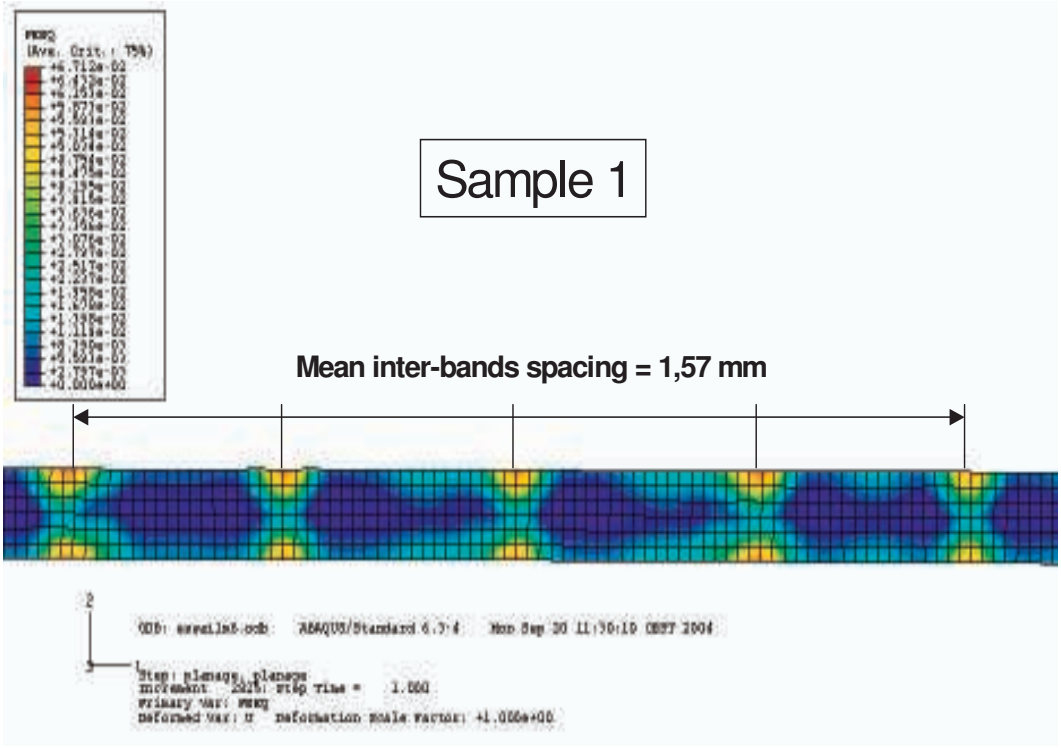

Figure 19

Plastic Equivalent Strain (PEEQ) iso contour plot obtained in material thickness for trial n°1

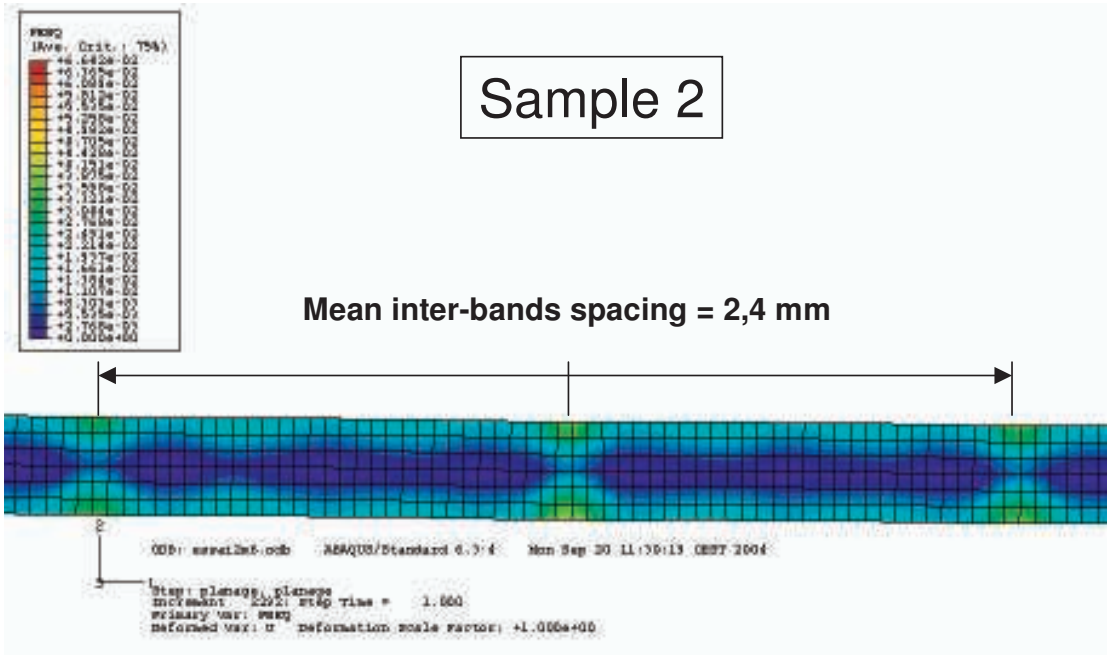

Figure 20

Plastic Equivalent Strain (PEEQ) iso contour plot obtained in material thickness for trial n°2

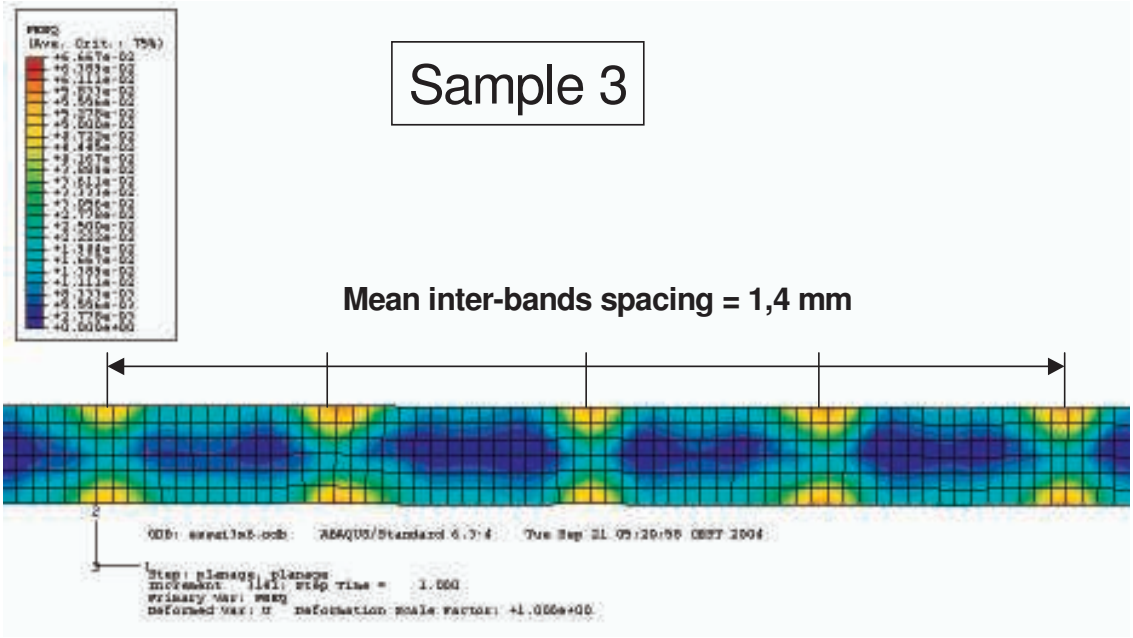

Figure 21

Plastic Equivalent Strain (PEEQ) iso contour plot obtained in material thickness for trial n°3

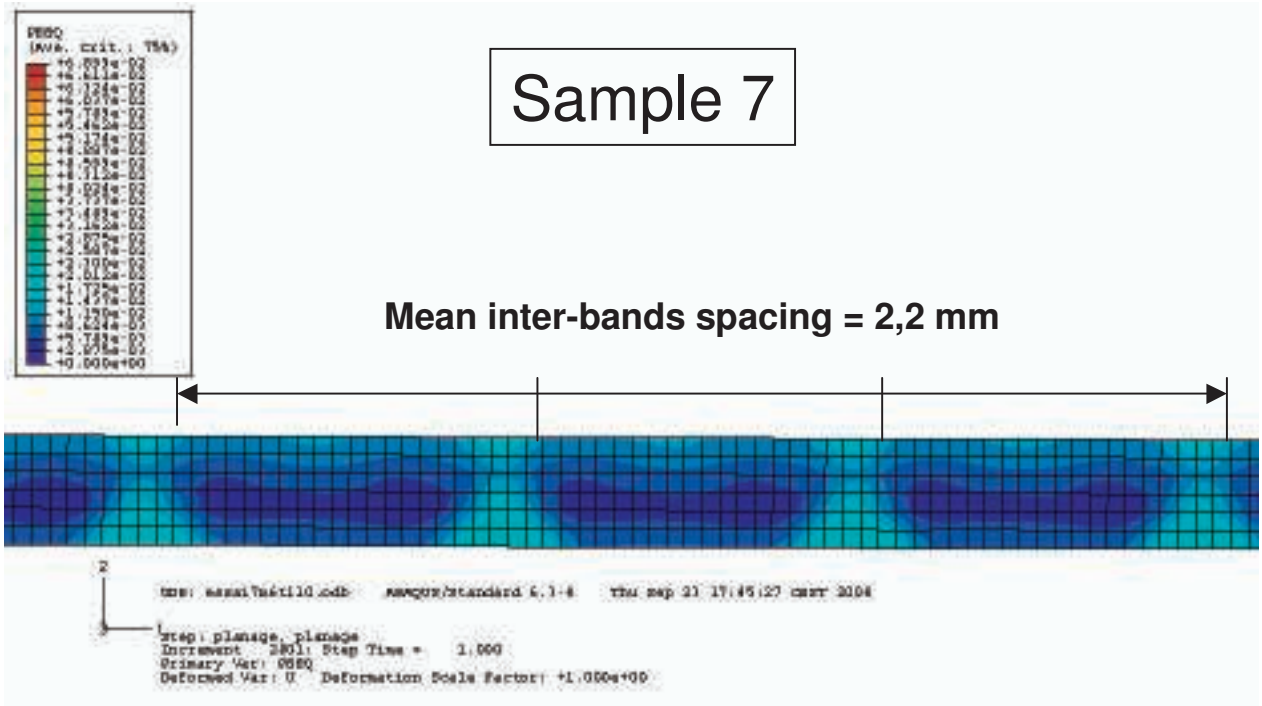

Figure 22

Plastic Equivalent Strain (PEEQ) iso contour plot obtained in material thickness for trial n°7

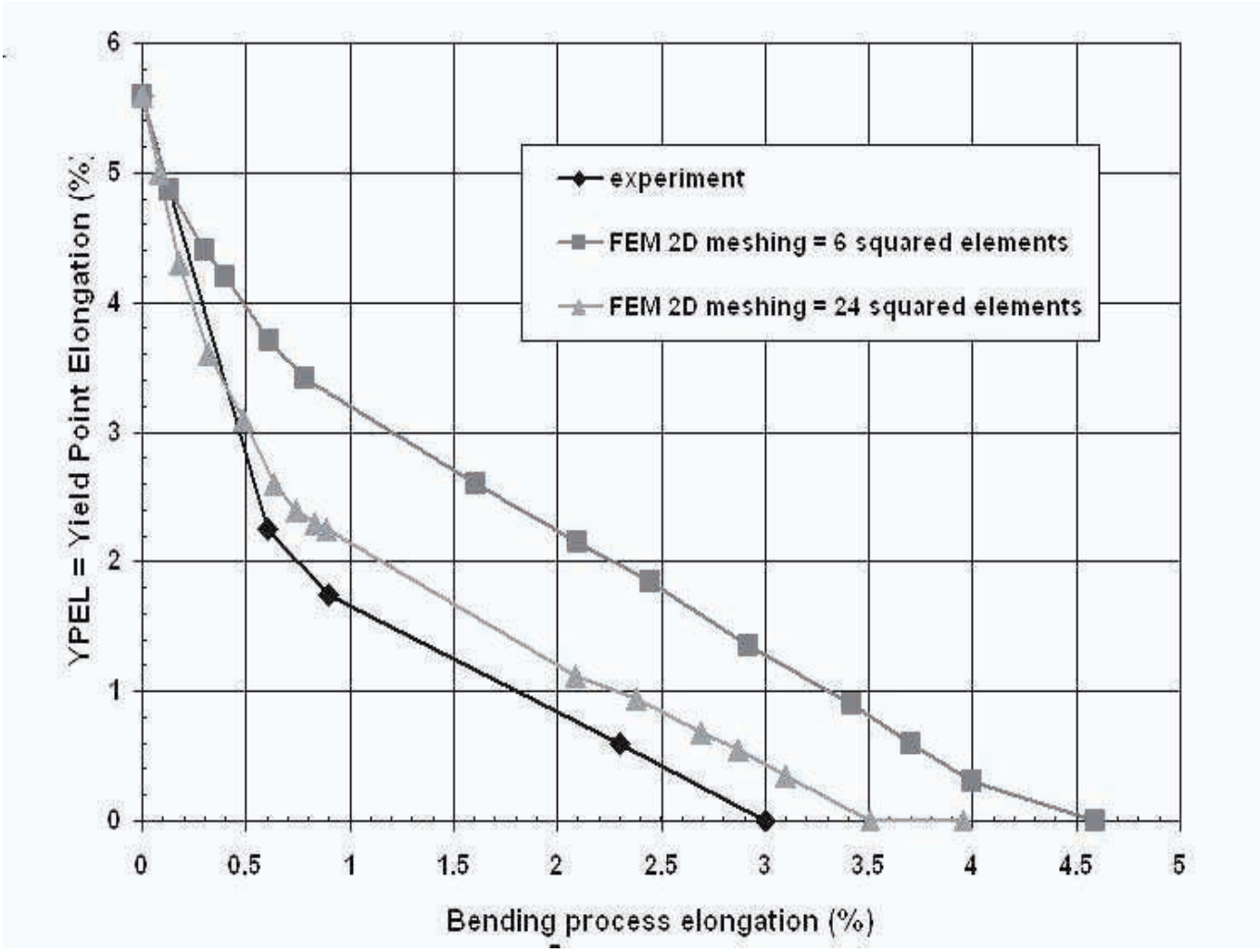

Figure 23

Evolution of Yield Point Elongation (YPEL) versus bending process elongation
Comparison between experimental results and FEM 2D numerical results with 2 types of meshing

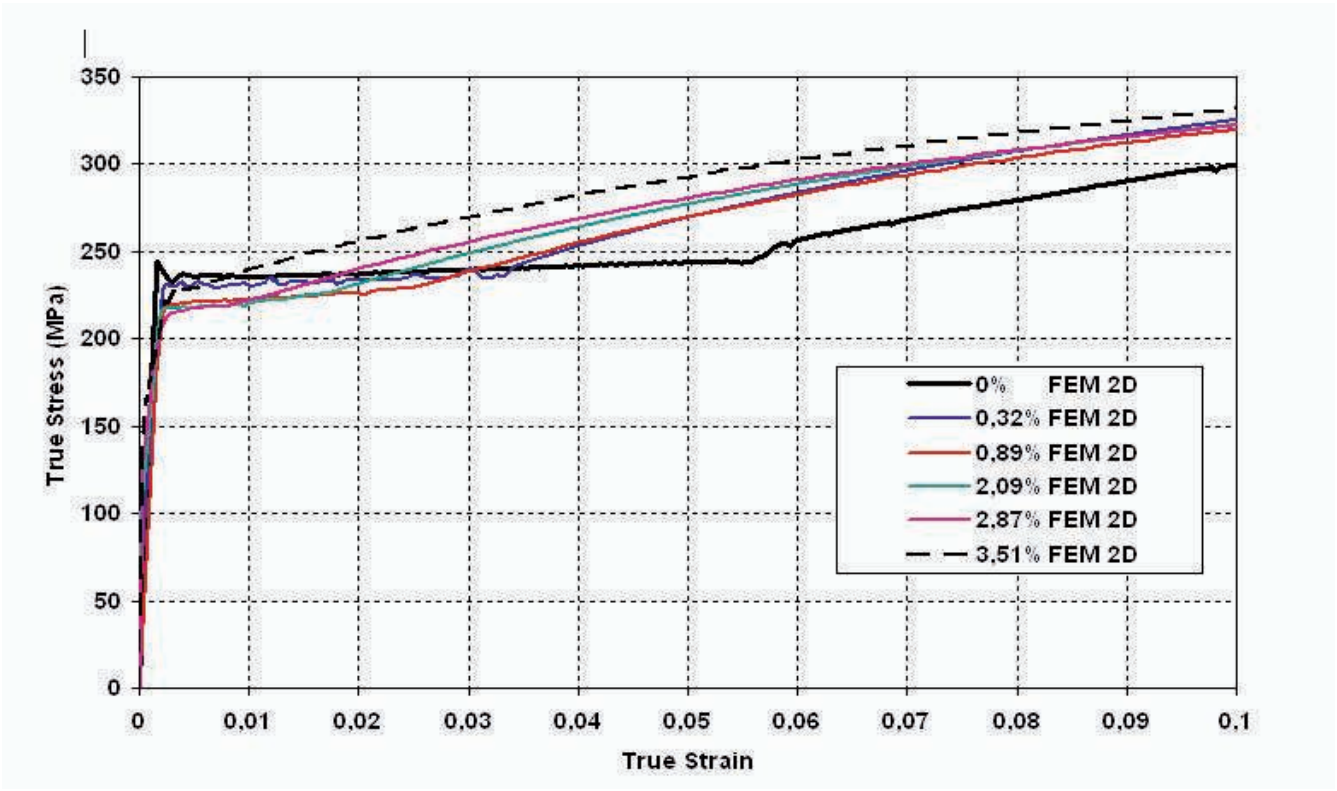

Figure 24

Evolution of FEM 2D calculated True stress versus True Strain post bending process

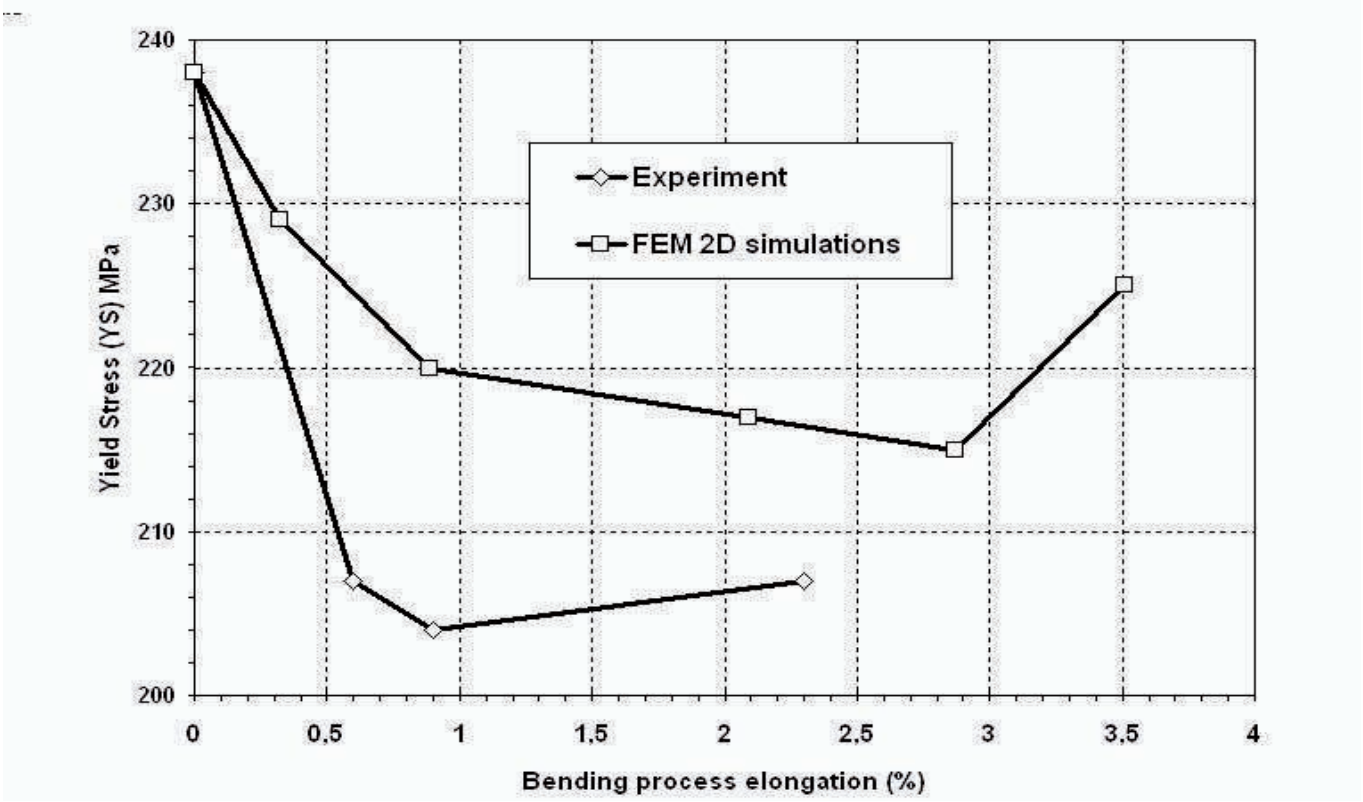

Figure 25

Evolution of FEM 2D calculated Yield Stress versus Bending process elongation.
Comparison with experiments

OVERALL CONCLUSIONS OF THE PROJECT

This project has been conducted in three main directions dealing with the yielding and ageing behaviour in temper rolling process related to the surface aspect in terms of Lüders bands appearance and evolution of mechanical characteristics, mainly Yield stress (YS) and Yield point Elongation (YPEL).

- CRM focused on the ageing behaviour of steel as a function of metallurgical and processing conditions during annealing and temper rolling,

- BFI studied the influence of pre-deformation by bending on the subsequent yielding behaviour of steel,

- ARCELOR RESEARCH and CSM developed a new method for the simulation of bending and temper rolling processes, using finite elements method based on a physical description of the Piobert-Lüders phenomenon in steel .

The main following conclusions can be drawn from this work.

During skin pass rolling the strip receives additional plastic deformations by bending at rollers or roll systems which are part of the process. As the tests carried out at BFI have shown, these deformations influence the mechanical properties of the strips in a similar way as the process of skin pass rolling itself. From the investigation, it can be concluded that it is necessary to conduct the process of skin pass rolling in such a way that those deformations caused by plastic bending have to be taken into account when the optimum degree of temper rolling is specified. This makes it possible to achieve the most favourable mechanical strip properties.

The bending deformation caused by the rollers (coiler, anti-sticking roll, and deflection roll) depends on the effective bending radius, material yield strength, and the strip tension. Whereas the bending deformations induced by the coilers change along the strip length due to the varying coil radius, the deformations caused by the anti-sticking roll are constant along the coil length at a stable wrap angle. The result of the sum of all deformations occurring in the process is a non-unified degree of deformation along the coil length. Subjects of future research should be the development of algorithms, which allows setting the roll gap in such a way that the same degree of deformation is applied to the complete strip length.
This creates the possibility to set the most favourable and uniform mechanical material properties along the coil length and also from coil to coil.

ARCELOR RESEARCH SA and CSM have demonstrated that a finite element method associated to a physically based description of the constitutive behaviour of steel allows to simulate both bending and temper rolling processes and to predict the skin-pass elongation necessary to suppress the yield point elongation. The local constitutive behaviour must present an initial stress drop to simulate satisfyingly the experimental force-displacement response of the steel.

A numerical machining procedure of flat tensile specimens in numerically temper rolled steel sheet has been developed. It allows to determine the force-displacement curve after bending and temper rolling and thus to study the influence of the temper rolling conditions on subsequent yielding behaviour.
Good agreement between experimental and calculated evolution of YPEL as a function of the the bending process elongation and the temper rolling reduction is found. It is worth noting that systematically, the bending process elongation and the skin-pass reduction leading to the minimum yield stress is lower than the one leading to the suppression of the Lüders plateau. This numerical result is confirmed by experimental results obtained by all partners.
Moreover, it is found that in the range of variation tested nor the roll diameter, neither the initial sheet thickness influence the yielding behaviour after temper rolling. As demonstrated experimentally by BFI, a simple pre-deformation by bending, contributes to the suppression of the YPEL.

Some improvements of this numerical procedure could be necessary in order to be still more representative of industrial temper rolling conditions.

We think that such a numerical procedure can efficiently replace exhaustive and expensive experimental work at the laboratory scale in order to determine the skin pass reduction required for suppressing the Lüders plateau taking into account deflecting rolls and potential subsequent plastic bending deformations going with. A simple tensile test before temper rolling is necessary to determine the local constitutive behaviour to input in the finite element calculations.
This method could also be useful to build master charts giving the critical temper rolling reduction to apply in order to suppress the yield point elongation.

Regarding CRM contribution, Special attention has been devoted to relate both the defect appearance to the microstructure and to the mechanical properties (sensitivity study) and ageing properties in relation with the deformation modes (skin-pass and bending) and the processing parameters used for the suppression of YELP.

a) In term of relation between stress-strain curve and microstructure, a short literature review has been performed (effect of the grain size, Csol content, alloying elements, temperature and strain rate) and has been followed by the observation of Lüders defects on industrial and laboratory samples.
All these parameters have been tested at the laboratory scale : ELC steels have been annealed following several thermal cycles to produce the aimed microstructures. The evolution of mechanical properties (YS, TEl, YPEl) have been studied. Results observed in the literature study are globally confirmed.

A finer grain size will induce the apparition of more numerous Lüders bands.

A higher C_{sol} content leads to the formation of more numerous but finer Lüders defect.

At the same grain size, the Lüders strain is reduced by a P addition. The effect of Sn addition on the Lüders strain of low-carbon steel is quite similar to that of phosphorus.

An increase of the tensile temperature implies a lower YS and a shorter YPEl, whereas a higher tensile strain rate, implies a higher YS and a longer YPEl.

b) In term of relation between the deformation mode (tensile, bending, skin pass) and the appearance of surface defects is concerned, the main results show that :

The SKP deformation is the most efficient mode to remove the YPEL.

In bending deformation it is noticed that even when the YPEl is suppressed, the YS values remains high in comparison with SKP deformation.

The deformation by tensile has only a low influence on the YPEl and YS behaviour.

Concerning the ageing behaviour, SKP and bending deformation modes do not seem to be affected by a laboratory ageing treatment (1 hour at 100°C) : YS and YPEL remain unchanged.

For the tensile deformation mode, it can be noticed that YS slightly increases after ageing while the YPEL values keep the same level

All this work could be also useful for hot rolled sheet steels that are not temper rolled but processed through pickling and/or levelling lines. Such processing lines also induced deformation that can trigger Piobert-Lüders phenomenon resulting in the appearance of surface defects and/or change in the subsequent ageing behaviour of steel. As depicted by CRM, it seems also important to study in more details the ageing behaviour as a function of the deformation mode (tension, compression, bending).

PUBLICATIONS AND PATENTS

The results of the project could be submitted for a publication in the " Technical Steel Research" series and/or for a communication during the next ATS December 2006 meeting.

KEYWORDS

- Finishing line
- Temper rolling
- Skin-pass
- Optimum temper rolling degree
- Mechanical properties
- Bending deformation
- Yielding
- Stress-Strain
- Strain hardening
- Lüders bands
- Suppression of the Yield point elongation
- Modeling
- Mechanical behavior
- Finite element simulation
- Ageing behavior
- Deflecting rolls

COPY OF TECHNICAL ANNEX

Contract n° : 7210-PA/PB/PC/PD/338
Reference n° : 02-D2.02a,b,c,d
Project n° : P4508

TITLE :

Control of sheet surface defects and deep drawing properties in final strip production steps

Short summary

The main objectives of the research work are

(1) to understand and to get under control sheet surface defects coming from Lüders' bands in finishing lines, so to guarantee the strip quality by optimising process parameters.

(2) to develop and validate industrial procedures to set the optimum temper rolling degree in such a way that plastic bending deformations induced by participating rolls and by bending caused by coiling are compensated. These procedures should finally create the possibility to set the most favourable and uniform mechanical strip properties along the total strip length and also from coil to coil.

Long summary

The first objectives of this research is to understand formation mechanisms of Lüders' band and to determine product parameters (composition, thickness…) and process parameters (bending and tensile deformation, temperature, speed…) in order to get under control sheet surface defects. So, we will be able to determine the real influence of anti-coil break rolls, levelling with or without tensile stress (pure stretch levelling) on Lüders' bands and to foresee the size and the morphology of Lüders' bands in function of product and type (level) of applied deformation. The understanding of Lüders' formation in finishing lines will help us to define product state after skin pass and strip performance in end-user applications.
Besides strip flatness and strip surface the mechanical properties of cold rolled strip depend to a high extent on the temper rolling conditions.
Subsequent process stages of skin passed strip, e.g. by deep drawing or stretching processes, usually require the use of temper rolled metal sheet, Lüders' free on its full range of deformability. To be able to produce such strip, it is necessary to control the skin passing process in such a way that the total strip deformation will come as close as possible to the optimum skin pass degree.
Rolls and roll systems like deflecting rolls, anti-sticking rolls and coilers which are participating at the temper rolling process, induce bending deformations into the strip, which extend the yield strength of the rolled material and thus lead to additional plastic deformations of the strip. These additional deformations may exceed up to 30% of the pass reduction with the consequence of non-uniform deformation along the strip length. Furthermore, rolls that introduce levelling of the strip (as in the case of AST configuration) produce non-symmetric rolling conditions in the skin-pass and this affects the through thickness strain distribution in the strip. Current industrial setting procedures of optimum temper rolling degree and therefore the resulting mechanical strip properties, do not include the plastic bending.

The most favourable mechanical strip properties however are achieved when the total deformation (bending plus rolling deformation) leads to such a constant minimum deformation along the total strip length which guarantees a complete suppression of the yield point elongation (concerning e.g. LC-DDQ-steels) and a minimum of yield strength including a high strain hardening exponent.
One objective of the research work is to develop and validate industrial procedures to set the optimum temper rolling degree in such a way that plastic bending deformations induced by rolls and by coiling are compensated. These measures should finally create the possibility to set the most favourable and uniform mechanical strip properties along the coil length and also from coil to coil.

Objectives

The first objectives of this research is to understand formation mechanisms of Lüders' band and to determine product parameters (composition, thickness…) and process parameters (bending and tensile deformation, temperature, speed…) in order to get under control sheet surface defects. So, we will be able to determine the real influence of anti-coil break rolls, levelling with or without tensile stress (pure stretch levelling) on Lüders' bands and to foresee the size and the morphology of Lüders' bands in function of product and type (level) of applied deformation. The understanding of Lüders' formation in finishing lines will help us to define product state after skin pass.
The mechanical properties of cold rolled strip which is finally passed to subsequent process stages like deep drawing or stretch forming depend to a high degree on the temper rolling conditions set at the cold finishing line.

The results of an ECSC finished project/1,2/ indicated that the final mechanical strip properties depend to a high extent on the global deformation resulting from work roll deformation of the skin pass mill and bending deformation by guiding the strip around roller bodies and by coiling during the temper rolling process. The two types of deformation can be mutually interlinked: rolls producing a bending prior to entry with a degree of levelling of the strip (as in AST plant) introduce non-symmetric rolling conditions in the skin-pass and this alters the contacting arc and consequently the through thickness strain distribution in the strip. This needs to be corrected by the rollers placed past the skin pass. The most favourable mechanical strip properties are then achieved when the total deformation leads to such a minimum deformation which guarantees a complete suppression of the yield point elongation (elimination of the Lüders' elongation) and a minimum of yield strength including a high strain hardening exponent.
One target of the research work is to develop algorithms which allow to set the temper rolling degree in such way that plastic bending deformations are compensated. The control strategy must take into account that varying bending radii (e.g. coiler, changing wrap angles of deflecting rolls) along the coil length lead to varying degrees of deformation to be set in the temper mill's roll gap for compensating the different bending deformations. These measures should finally create the possibility to set the most favourable and uniform mechanical strip properties along the strip length and also from coil to coil.*

State of the art

A deep knowledge on the Lüders' bands mechanisms and their consequences on subsequent cold forming came from previous study /2/. H. Tsukahara had made some numerical simulation with local law in order to find the characteristic behaviour law in presence of Lüders' band in bending and tension deformation mode.

Temper rolling of cold rolled strip is marked by the demand to offer an optimum product to subsequent process stages (deep drawing, stretch forming etc.), e.g. referring to properties such as:
- strip flatness
- surface quality, and
- deformability

The deformability of the skin passed strip, e.g. in deep drawing, is essentially favoured by a high r-value for anisotropy, a high exponent n of strain hardening, corresponding to a great uniformity of elongation, as well as a minimum yield stress. The two last mentioned nominal values will be set most favourably if the optimum skin pass degree is adjusted on skin passing. This will be the case if the strip is rolled with a degree of deformation corresponding to the minimum of the yield stress curve. Pass reductions below the optimum skin pass degree should absolutely be avoided (under-skin-passed) to eliminate the appearance of Lüders´ lines in subsequent processing stages, e.g. on materials with upper and lower yield point. So, light over-skin-passing, connected with a small increase of the yield strength and a small reduction of uniformity of elongation, will be tolerated.

Processing of steel strip by deep drawing or stretching processes, usually requires the use of skin passed metal sheet, Lüders' free on its full range of deformability. To be able to produce this strip demanded by the market, it is necessary to control the skin passing process in such a way that total strip deformation will come as close as possible to the optimum skin pass degree.

Temper rolling plants are equipped with measuring and control systems to conduct the skin pass rolling process in such a way that the target plastic deformation to be set by the roll adjustment is safely achieved.
Rolls and roll systems like deflecting rolls, anti-sticking rolls and coilers which are integrated into the pass line of temper rolling plants, induce bending deformations into the strip, which extend the yield strength of the rolled material and thus lead to plastic deformations of the strip. The presence of bending and levelling can introduce non-symmetric rolling conditions that alter the skin-pass contacting arc and therefore the through thickness strain distribution in the strip. When setting the optimum temper rolling degree and thus the resulting mechanical strip properties, these plastic bending deformations have not been taken into account so far.
Prior trials /1/ on an industrial temper mill equipped with an anti-sticking roll showed that for determining the relevant deformation all plastic strip deformations have to be taken into account, that means not only the pass reduction by rolling but also the plastic bending deformation caused by the anti-sticking roll was very relevant. The bending deformation has proved to accept values up to 30% of the target value of the skin pass degree. Comparing the yield stress - curves evaluated for the temper rolling conditions - rolled without and with acting anti-sticking roll – it can be deduced that in case of pre-deformation by bending the setting of the temper rolling degree has to be compensated by the amount of the pre-deformation in order to achieve a standardisation of the optimum skin pass degree.
Recent investigations carried out within the scope of a ECSC project /2/ dealt with the effect of plastic bending deformations on the mechanical strip properties, namely
- Stress-strain behaviour
- Yielding behaviour
- Strain hardening behaviour and
- Lüders' behaviour

The trials were carried out with batch annealed low carbon deep drawable strips (LC-DDQ steel). The test results showed, that plastic bending deformations influence mechanical strip properties in a similar degree than skin pass rolling itself.
Regarding the behaviour of yield stress, the minimum of yield strength, especially for thicker strips, is shifted to higher degrees of deformation than compared to temper rolling. The work hardening, which takes place after the minimum of yield stress, is accompanied by a significantly lower gradient of the yield stress curve than the compression strain caused by skin pass rolling The thinner the strip thickness, this effect is stronger.
The dependency of the hardening exponent on the degree of deformation shows the same trend for both bending and rolling deformation.
Independently from being bending or a rolling deformation, the resulting gradients of the work hardening exponent lead to the same values.
From the investigation, it can be concluded that it is necessary to conduct the process of skin pass rolling in such a way that those deformations caused by plastic bending have to be taken into account when the optimum degree of temper rolling is specified. This makes it possible to achieve the most favourable mechanical strip properties.

Skin-pass procedures without bending for strips were developed and validated against plant data in a previous ECSC funded project /4/. This research showed the importance of considering the deformation of the rolls as the strip thickness decreases. A simplified set-up model for the control system of the skin pass was derived from this research /5/ and successfully installed in AST Terni. A new project on improving formability of low carbon steels by controlling the ageing in the finishing line is starting this year /3/.

Innovative contents

Roll systems introduce bending deformation that can lead to plastic deformation on the strip. In the previous project /2/, the effect of plastic bending deformations on the mechanical strip properties was investigated at the laboratory scale. The use of bending deformations in order to get under control sheet surface defects in finishing lines has been never done before at the industrial scale.
In temper rolling plastic bending deformations have not been taken into consideration so far.
The results obtained in /1,2/ demonstrate the necessity that both deformation modes, rolling deformation as well as bending deformation, have to be taken into account when the optimum degree of skin pass rolling as target value is specified.
The algorithms and industrial procedures to be derived for a control strategy of the optimum degree of deformation will take into account for the first time the interacting effects by rolling and bending. Thus these new process strategies will improve the process of skin pass rolling under the aspect of setting most favourable and uniform mechanical strip properties over the strip length and from coil to coil.

Ways and means

For BFI's experimental studies a tension bridle with bending unit is available. Temper rolling trials can be carried out on the laboratory-reversing mill.

Two aspects will be studied by CRM.
A) The relation between the stress-strain curve and the microstructure
CRM is equipped with a high-speed (usually 5 m/s but possible up to 8 m/s) tensile machine working in the range (-180 °C --> +600 °C). This equipment allows the study of the temperature / strain rate sensitivity of various initial materials in the range 0-5% of total deformation including the study of the YPEl. Tensile tests will be performed on large specimens (150-mm width).
B) The relation between the deformation mode (tensile or bending) and the appearance of surface defects.

At IRSID, machines and material involved in the project:
FE codes for deformation: ABAQUS and LAM3
Industrial pilots
Tensile, bending machine
Tests on industrial scale will be done.

CSM work will be focused on ferritic stainless steel strip at the finishing line past the bright annealing furnace of Acciai Speciali Terni plant. The configuration consists of bending rolls, a levelling roll , the skin pass rolling and a coiler. The strip will be mechanically characterised before and on exiting the configuration by tensile testing. A combined process+tensile testing model will be developed using the FEM code ABAQUS which will be validated against the experimental testing and industrial data. The validated model will be used as a generator of a database of results from which a simplified model will be produced. This model will be used in the plant as a fast alternative to current trial and error procedures to predict the effect of changing process parameters (front and rear tension on the skin pass, strip thickness and levelling/bending degree) on the strip mechanical properties and for optimization of the processing route.

Work programme and distribution of tasks

ARCELOR RESEARCH SA's task description

The investigations can be subdivided into the following main tasks :

- Characterisation of sheet surface defects on industrial samples
- Measurements of Lüders' elongation at different step of finish line using tensile tests
- Numerical simulations with local law for bending with or not superimposed tension: numerical simulation of BFI's experimental studies on the influence of bending deformations and numerical simulations of industrials samples
- Definition of criterion on Lüders' band generation and morphology
- Comparison with industrial trials and BFI's experimental studies.
- Study of the good dimension of anti coil break rolls at the entry of cut to length line or descaling line to avoid eye appearance of Lüders' band before and after painting
- Optimisation (size,pre-setting) of the finish line tools (anti coil break roll, straightener, leveller, tension leveller, pure stretch leveller) in order to avoid or limit visible (perceptible) surface defects.
- Calculation of plastic bending deformations for a process and a product to compare with BFI's measurements and algorithm results.

BFI's Task description

BFI's investigations can be subdivided into the following main tasks :
- Experimental studies on BFI's laboratory plant to improve the knowledge about the influence of bending deformations upon the mechanical strip properties (stress-strain behaviour, yielding behaviour, strain hardening behaviour and Lüders' behaviour)
Incorporation of the results obtained into a combination of bending and temper rolling deformation
Deriving algorithms to set the target degree of temper rolling in order to achieve optimum and uniform mechanical strip properties along the strip length and from coil to coil
Experimental tests of the derived algorithms on the laboratory reversing mill

Influence of bending deformations on the mechanical strip properties

Based on the results of a recently terminated ECSC-project /2/ the influence of bending deformations upon the mechanical strip properties:
stress-strain behaviour
yielding behaviour
strain hardening behaviour and
Lüders' behaviour
will be investigated on BFI's tension bridle plant with integrated bending unit. For the deformation range investigated the yielding behaviour of strips does not illustrate complete conformity when different strip thickness are compared. That's why two different thickness will be tested as well as two different steel grades:
Strip thickness: 0,5; 0,8 mm
Steel grade: two LC-DDQ steels, (batch annealed)
The characteristic values describing the mechanical properties will be delivered by tensile tests of strip specimen.

Combining of bending and temper rolling deformation

Based on the results obtained the influence of the two deformation modes rolling and bending will be joined together under the aspect of setting the degree of deformation of the temper mill in such a way that the optimum and uniform mechanical strip properties along the strip length will be obtained.

Algorithms for the target degree of temper rolling

From the knowledge of the interacting effects by the rolling and bending deformation mode upon the mechanical strip properties there will be derived strategies how to conduct an optimum temper rolling process. Bending characteristics like actual coil diameter, constant or varying wrap angle of deflecting- and anti-sticking rolls, strip thickness as well as tensile stress of the strip must be taken into consideration for the control algorithm (comparison with IRSID calculation of plastic bending deformations for a process and a product).

Experimental tests of the derived algorithm
The algorithm will be applied to the laboratory rolling plant. Rolling tests will be carried out to adapt the model to the plant and strip characteristics and finally to optimise and examine and tuning the model‘s validity. The following parameters are to be considered:
geometrical bending conditions of the participating rolls
strip thickness
entry and exit strip tension
steel grade (like 3.1.1)

CRM’s task description

The main CRM objective is to relate the defect appearance to the microstructure and to the mechanical properties (sensitivity study).

CRM help partners to select of industrial grades sensitive to surface defects generated by the presence of Lüders’ bands (Hot strips before pickling, annealed and galvanised sheets before the final skin pass).

The microstructure is characterised by the following parameters:
- grain size,
- texture,
- solute C and/or N (eventually after and overageing treatment in annealing line) or after pickling of hot strips,
- the substructure.

The mechanical properties are characterised by:
- the lower yield strength level (flow stress),
- the YPEL,
- the strain rate sensitivity.

In a first step, ELC, LC and IF steel grades will be considered. Starting from industrial materials, the microstructures will be changed by laboratory thermal treatments (mainly annealing treatments followed by quench with or without overageing, slow cooling).

Additionally, different initial microstructures will be analysed.
1) UFC treated hot strips with a well-developed sub-structure induced by fast cooling.
2) Ferritic hot rolled strips with a (100) texture.
3) Effect of initial grain size and solute carbon content.

CSM’s task description

CSM work will be focused on ferritic stainless steel strips of thickness 0.4 to 1mm produced at the Acciai Speciali Terni (AST SpA) plant.

The research programme consists of the following tasks:

- Tensile test characterisation of the stainless steel strip at the exit of AST bright annealing furnace.
- Development of a FEM model for skin pass rolling with deforming rolls, deflecting, levelling and anti-gripping rolls and coilers. Development of a FEM-based tensile testing simulation of the finished strip. The combined models will use the material characteristics determined by the testing above and are aimed to predict, after proper validation, the effect of each stage of the finishing line on the yield point elongation.

- Experimental characterisation of the industrial finished strip and validation against the numerical predictions.

- Development of a simplified, PC-portable model for the finishing line formed by the skin pass and guiding rolls. Study to determine the optimal degree of bending and rolling deformation for typical thickness in terms of skin pass reduction, position of the different auxiliary rollers and front/rear tensions.

- Industrial trials of the optimised configuration/process parameters and conclusions

Partnership and management

France: ARCELOR RESEARCH SA

Belgium: CRM

Germany: BFI/VDEh

Italy: CSM

ARCELOR RESEARCH S.A. as coordinator will be in charge of the overall management of the project.

Industrial, technical, economic, social, environmental benefits

The realisation of a strategy to conduct the temper rolling process in such a way that the bending deformations induced into the strip are taken into account by setting the optimum temper rolling degree leads to an improvement of quality of the skin passed strip. The mechanical strip properties which are to be set in temper rolling as the final forming stage before subsequent strip processes like deep drawing and stretch forming will thus achieve most favoured values, equalised along the strip length and from coil to coil.

Many European companies are interested by the problem of Luders' lines or coil breaks, either on soft hot strips or on galvanised sheets.
Different aspects should be considered:

-Understanding of the formation of the Luders' lines. (analysing the effects of the steel composition or steel strength, of the strip or sheet thickness, of the processing parameters, of the final texture and microstructure, of the solute C-content, ...).

-Thin hot strips for direct application (eventually with adherent scale or after pickling). In some case, the SKP operation can be omitted. The problem can occur when decoiling by the customers or in finishing lines.

-Galvanised sheets: the defects can be visible in the production line. (at the exit of the galvanisation section at ~470 °C) but is probably induced in the reheating / soaking / cooling sections. (as discussed by phone, this is outside the present proposal).

-Appearance of surface defects in service centre due to Lüders' bands for numerous products.
-After traction levelling in pickling lines, temper milled thin hot strips could present the problem.
-Temper milled ferritic stainless steel is sensitive to Lüders' band.
-Dimension of anti coil break rolls at the entry.

So, to get under control sheet surface defects will reduce scrap wastes at finishing lines. And finally, this project could give us the way to control process to produce some sensitive product. So, the competitiveness of European steel producers in the international market will be increased.

References

/1/ P. D. Pütz, E. Neuschütz, M. Scherer, Investigation of Procedures for Optimizing Skin Pass Rolling, CECA 7210-EA/143, CECA 7210-EA/144, 1998

/2/ IRSID, D. Grandemange, H. Tsukahara, E. Vasseur
CRM, J.- C. Herman
BFI, P.- D. Pütz
Control of the yielding and ageing behaviour in temper rolling, (Draft Final Report), CECA 7210-PR/035, 2001

/3/ CSM-MAGONA, SOLLAC, CRM, 'Improvement of formability of continuously organic coated coils by controlling ageing of low carbon steel substrates', Proposal4389 (F4) ECSC2001, approved, to start July 2001.

/4/ Lubrano M., Bianchi J.H., Pütz P., Mennicken H., Scherer M. 'Development and testing of procedures for optimising the degree of strip reduction during skin-pass rolling', EUR 18917 EN,1999.

/5/ Lubrano M., Bianchi J.H., ' A simple model for on-line control of skin pass from FEM analysis of rolling deformation',2nd Int. Conference on Modelling of Metal Rolling Processes, The IOM, London, Dec. 1996.

Keywords

- Finishing line
- Temper rolling
- Skin pass
- Optimum temper rolling degree
- Mechanical properties
- Bending
- Yielding
- Stress-strain
- Strain hardening
- Lüders'

Results

The results of the project will be subject of a publication in the "Technical Steel Research" series.

The research described above will be placed in the area by the Executive Committee D2, "Rolling – Flat Products.

European Commission

EUR 22566 — Hot and cold rolling processes
Control of sheet surface defects and deep drawing properties in final strip production steps

A. Fouratier, A. Lucas, J. H. Bianchi, P. Vescovo, F. Dionisi, P. D. Pütz

Luxembourg: Office for Official Publications of the European Communities

2007 — 161 pp. — 21 × 29.7 cm

Technical steel research series

ISBN 92-79-05018-3

ISSN 1018-5593

Price (excluding VAT) in Luxembourg: EUR 25